



**UNIVERSIDADE DE LISBOA  
INSTITUTO SUPERIOR TÉCNICO**

**Bioprocess development for scalable generation of functional  
liver micro-tissues/organoids from human pluripotent stem cells**

**Saeed Abbasalizadeh**

**Supervisors: Doctor Joaquim Manuel Sampaio Cabral  
Doctor Hossein Baharvand**

**Thesis approved in public session to obtain the PhD Degree in  
Bioengineering**

**Jury Final Classification: Pass with Distinction**

**2021**

**UNIVERSIDADE DE LISBOA**  
**INSTITUTO SUPERIOR TÉCNICO**

**Bioprocess development for scalable generation of functional  
liver micro-tissues/organoids from human pluripotent stem cells**

Saeed Abbasalizadeh

**Supervisor:** Doctor Joaquim Manuel Sampaio Cabral  
Doctor Hossein Baharvand

**Thesis approved in public session to obtain the PhD Degree in  
Bioengineering**

**Jury Final Classification: Pass with Distinction**

**Jury:**

**Chairperson :** Doctor Duarte Miguel de França Teixeira dos Prazeres, Instituto Superior Técnico, Universidade de Lisboa

**Members of the Committee:**

**Doctor** Joaquim Manuel Sampaio Cabral, Instituto Superior Técnico, Universidade de Lisboa

**Doctor** Lino da Silva Ferreira, Faculdade de Medicina, Universidade de Coimbra

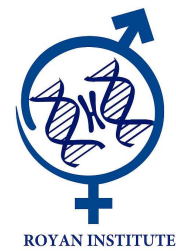
**Doctor** Maria Margarida de Carvalho Negrão Serra, IBET - Instituto de Biologia Experimental e Tecnológica

**Doctor** Maria Margarida Fonseca Rodrigues Diogo, Instituto Superior Técnico, Universidade de Lisboa

**Doctor** Tiago Paulo Gonçalves Fernandes, Instituto Superior Técnico, Universidade de Lisboa



This PhD thesis project has been done as collaborative sandwich program between University of Lisbon (Instituto Superior Técnico, IST), Royan Institute, and Prof. Robert Langer Lab at Koch Institute for Integrative Cancer Research, Massachusetts institute of technology



**MIT Langer Lab**

MIT Department of Chemical Engineering



**“Just follow your heart. Pick something you think you are going to love.  
Create things that could change the world and make it a better place”**

*Robert S. Langer*



## Resumo

As doenças hepáticas crônicas ainda são consideradas um problema de saúde globalmente negligenciado, uma vez que o transplante de fígado é apenas uma opção disponível para tratamento e altamente limitado, devido à escassez de fígados transplantáveis disponíveis e ao aumento da taxa de prevalência de insuficiência hepática. Para abordar este desafio, tem havido um esforço científico e tecnológico global de modo a desenvolver terapias alternativas e regenerativas para responder a essa necessidade médica atualmente negligenciada. Uma das tecnologias regenerativas mais promissoras é a "a medicina de organóides" e a obtenção escalonável de organóides hepáticos funcionais / vascularizados a partir de fontes celulares disponíveis, como células estaminais pluripotentes humanas, para potencial transplante e aplicação terapêutica. No entanto, a maioria dos protocolos estabelecidos para a obtenção funcional de organóides hepáticos tem sido em pequena escala ou com problemas de escalabilidade para produção em larga escala e ampla aplicação clínica. Nesta tese, desenvolvemos um protocolo robusto e um processo a montante para produção escalonável de organóides hepáticos funcionais do tipo fetal a partir de células estaminais pluripotentes humanas em biorreatores agitados, que incluem hepatócitos e glóbulos vermelhos, otimizando os principais parâmetros do bioprocessamento durante o processo de diferenciação hepática integrado. Os organóides gerados expressam genes marcadores específicos do fígado, pré-formando as principais funções metabólicas do fígado (ou seja, secreção de albumina, produção de uréia, captação de indocianina verde (ICG) e LDL e armazenamento de glicogênio) e alta atividade do citocromo P450 induzível

Paralelamente, para produzir organóides hepáticos complexos e altamente funcionais de maneira escalável, estabelecemos também, uma plataforma escalável para obtenção de endoderme hepática, células estaminais mesenquimais e células endoteliais a partir de células estaminais pluripotentes humanas, como fontes celulares necessárias para a geração escalonável de gomos hepáticos vascularizados funcionais através de cultura e auto-organização. Um sistema microfluídico escalável foi também estabelecido para a geração contínua de gomos no fígado em gotículas biodegradáveis 4-armPEG-MMP degradável peptídeo e PGA. Os organóides hepatobiliares vascularizados auto-organizados foram gerados após a otimização das condições de co-cultura e a transferência de organóides para a cultura em suspensão dinâmica 3D para uma maior maturação. Os organóides hepatobiliares vascularizados apresentaram funções essenciais do fígado, como a expressão de genes marcadores específicos do fígado, a pré-formação das principais funções metabólicas do fígado e o metabolismo induzido por medicamentos próximo ao fígado adulto. Assim, estas plataformas podem ser úteis para a produção em larga escala de organóides do fígado humano e uma fonte valiosa e ilimitada para triagem de medicamentos e desenvolvimento *in vitro* de tecidos / órgão do fígado.

Palavras-chave: Doença hepática crônica, organóides hepáticos, produção escalonável, microfluídica, núcleo degradável e cápsulas.

## Abstract

Chronic liver diseases are still considered as an unmet medical need and a globally neglected health problem since liver transplantation is only available option for treatment, but highly limited due to shortages of available transplantable livers and increasing prevalence rate of liver failure. To cope with this challenge, there is a global scientific and technological effort to develop alternative and regenerative therapies to address this currently unmet medical need. One the most promising regenerative technologies is “Organoid medicine” and scalable generation of functional/vascularized liver organoids from readily available cell sources such as human pluripotent stem cells for potential transplantation and therapeutic application. However, most of the established protocols for functional liver organoid generation have conducted in small scale or suffering scalability issues for large scale production and widespread clinical application. Here, we have developed a robust protocol and upstream process for scalable production of functional fetal-like liver organoids from hPSCs in stirred suspension bioreactors comprising hepatocytes and red blood cells by optimizing key bioprocess parameters during integrated hepatic differentiation process. Generated organoids expressed liver-specific marker genes, performing main liver metabolic functions (i.e. albumin secretion, urea production, Indocyanine green (ICG) and LDL uptake, and glycogen storage), and high inducible cytochrome P450 activity.

In parallel and to produce complex and highly functional liver organoids in scalable manner, we also established a scalable platform for generation of hepatic endoderm, mesenchymal stem cells and endothelial cells from hPSCs as required cell ingredients for scalable generation of functional vascularized liver buds through co-culture and self-organization. A scalable microfluidic system has also established for continuous generation of liver organoids in biodegradable 4-armPEG-MMP degradable peptide or PGA fabricated core and shell microcapsules. Self-organized vascularized hepatobiliary organoids have been generated after optimizing co-culture condition and transferring organoids to 3D dynamic suspension culture for further maturation. The vascularized hepatobiliary organoids after 7 days of maturation showed key functional of liver such as expressing liver-specific marker genes, performing main liver metabolic functions and induced drug metabolism close to adult liver. The established platforms might be useful for mass production human liver organoids and provide a valuable and unlimited source for drug screening, organoid medicine, and *in vitro* development of liver tissues/organ.

**Keywords:** Chronic liver disease, Liver organoids, Scalable production, Microfluidics, Degradable core -shell microcapsules

## Acknowledgements

First, I would like to acknowledge my lovely wife Mana for her endless love, support and taking care of our cute boys Danial and Daian during the lab work and made whatever I accomplish possible. Also, I want to thank my kind Mom, Dad, and Brother Omid for their kindness, pure love, and support during this journey. I also acknowledge some of the people that were part of my experience and really contributed to this thesis. The first person I must acknowledge is Prof. Baharvand that introduced this unique PhD program to me as well as Claudia Labato from IST that introduced this PhD program to Prof. Baharvand.

I started the program in Lisbon, one the most beautiful cities visited in my life with friendly and smiling peoples, nice weather, delicious food, and amazing chocolates and cookies. I had a unique experience and learned a lot during attending courses at IST, other distinguished research centres and hospitals including IBET, Hospital de Santa Maria, and IMM. I highly appreciated all kind, welcoming, and supporting people at IST including Claudia Lobato, Margarida Diogo, Tiago Fernandes, and my smart and friendly classmates Joao, Teresa, Diogo, Susana and others that made my stay at Lisbon unforgettable. I would also like to highly appreciate Prof. Cabral for his kind help and support during this journey and supervising the thesis project and Rosa for her kindness and administrative help.

I came back to Royan Institute after finishing courses at IST and started the PhD project in Royan institute stem cells science technology department under Prof. Baharvand supervision. I would like to appreciate all stem cells department members and GI and liver research group members of Royan for their sincere cooperation and providing this opportunity with especial thank to Dr. farzaneh and Ms. Mazidi for their collaboration and great assistance in this project. I was also get involved in establishment of a sophisticated cell and gene therapy manufacturing process development facility in Royan institute (Royan ATMP technology development centre) for translating lab scale protocols to robust manufacturing process of ATMP products that was also a unique experience for me.

After 3 years, I moved from Royan institute to Prof. Langer lab at MIT for one-year appointment to develop the scalable microfluidic platform for continuous production of vascularized liver organoids as last part of project. I gained invaluable experience in Langer Lab as one the most reputable and biggest labs in bioengineering and Koch Institute for Integrative Cancer Research as distinguished center for multidisciplinary research populated by talented biologists, MDs, bioengineers, and biomedical engineers.

I would like to convey my appreciation to Prof. Langer and Dr. Giovanni Traverso for their interest in my project and accepting me as a visiting scholar in the world-class Langer lab and their great help, support, advise, and mentoring during stay in the lab.

I would also like to thank to Sahab, Yichao, Johanna, Vance, Jake, Tiffany and Declan for being great lab mates, by helping me in the lab for all required device fabrications task, supplying required materials, equipment's and tools for set up experiments. A huge thanks to the Koch institute and Langer lab friendly peoples available for help 24h/day with always a smile on face. Special thank to Ilda Thomson and Idulia Lavato for their great assistance during one-year appointment and sending multiple letters to US embassy to accept my Visa. I also convey my heartfelt appreciate to Prof. Langer and Dr. Giovanni Traverso for their financial support and sincere cooperation for health insurance and 4-month accommodation cost to continue the project when I encountered significant problem for money transfer due to US and Iran tensions.

Finally, I want to thank Prof. Baharvand for everything that he taught me, from the most basic concept design of project, analyzing data, planning experiments, interpreting results and, above all, to look at the results from a different perspective. I would like to appreciate and convey my heartfelt wishes to all peoples not named here that shared great moments with me in Tehran, Lisbon, and Boston that I will keep them in heart for lifetime. I hope that could continue this project to translate into clinical application and improve patient life quality and save their lives as my main mission, passion, and dream as a bioengineer.

# Index

RESUMO.....	I
ABSTRACT .....	II
ACKNOWLEDGEMENTS .....	III
INDEX.....	V
LIST OF FIGURES .....	VII
LIST OF ABBREVIATIONS.....	XI
LIST OF PUBLICATIONS .....	XIV
<b>CHAPTER 1. THEORETICAL BACKGROUND .....</b>	<b>16</b>
CHRONIC LIVER DISEASES AND LIVER CIRRHOSIS .....	17
<i>Etiology and prevalence of CLDs .....</i>	<i>19</i>
<i>Liver cirrhosis as an unmet medical need.....</i>	<i>19</i>
CURRENT TREATMENTS FOR ACUTE LIVER FAILURE.....	21
<i>Cell-based liver assistive devices and regenerative therapies for cirrhosis and acute liver failure treatment .....</i>	<i>21</i>
<i>Liver buds and organoids .....</i>	<i>33</i>
<i>Liver cells, hepatocyte like cells and stromal cells.....</i>	<i>42</i>
COMPARING THE TRANSLATIONAL POTENTIAL OF THERAPEUTIC COMPONENTS AND ESTABLISHED PLATFORMS FOR TREATING LIVER CIRRHOSIS AND THEIR WIDESPREAD CLINICAL APPLICATION.....	52
CURRENT CHALLENGES IN SCALABLE GENERATION AND CLINICAL APPLICATION OF VASCULARIZED LIVER BUDS/ORGANOIDS .....	55
<i>Production scalability issue .....</i>	<i>55</i>
<i>Organoids functionality issue .....</i>	<i>56</i>
<i>Challenges in transplanting liver organoids.....</i>	<i>56</i>
SCALABLE TECHNIQUES FOR GENERATION OF LIVER BUD'S/ORGANOIDS .....	56
REFERENCES.....	60
<b>II. CHAPTER 2. SCALABLE PRODUCTION OF HEPATIC ORGANOIDS BY INTEGRATED DIFFERENTIATION OF HPSCS UNDER FULLY CONTROLLED CULTURE CONDITION.....</b>	<b>68</b>
<i>Introduction.....</i>	<i>71</i>
<i>Material and Methods .....</i>	<i>73</i>
<i>Results .....</i>	<i>79</i>
<i>Discussion.....</i>	<i>96</i>
<i>Conclusions.....</i>	<i>101</i>
<i>Acknowledgments.....</i>	<i>103</i>
<i>References.....</i>	<i>103</i>
<i>Supplementary Material .....</i>	<i>107</i>
<b>III. CHAPTER 3. SCALABLE PRODUCTION OF HEPATIC ENDODERM, ENDOTHELIAL PROGENITORS, AND MESENCHYMAL STROMAL CELL DERIVED FROM HPSCS FOR SCALABLE VASCULARIZED LIVER BUD/ORGANOID GENERATION.....</b>	<b>112</b>
<i>Chapter Introduction.....</i>	<i>113</i>
SCALABLE PRODUCTION OF DEFINITIVE AND HEPATIC ENDODERM CELLS AS 3D AGGREGATES.....	114
<i>Introduction.....</i>	<i>114</i>
<i>Material and Methods .....</i>	<i>116</i>
RESULTS.....	119
SCALABLE PRODUCTION OF PROGENITORS AND MATURE ENDOTHELIAL CELLS FORM HPSCS .....	125
<i>Introduction.....</i>	<i>125</i>
<i>Materials and Methods.....</i>	<i>128</i>
<i>Integrated differentiation of hPSCs to endothelial cells as 3D aggregates.....</i>	<i>128</i>
RESULTS.....	133
<i>Integrated endothelial differentiation of hPSCs as 3D aggregates.....</i>	<i>133</i>
<i>Integrated endothelial differentiation of hPSCs on microcarriers.....</i>	<i>134</i>

<i>Integrated maturation of endothelial progenitor cells towards mature endothelial cells on collagen coated microcarriers</i> .....	136
SCALABLE AND GMP-COMPATIBLE PRODUCTION OF HMSCs DERIVED FROM HUMAN PLURIPOTENT STEM CELLS .....	140
<i>Introduction</i> .....	140
<i>Materials and Methods</i> .....	141
<i>Results</i> .....	145
<b>IV. CHAPTER 4. LARGE SCALE AND CONTINUOUS PRODUCTION OF VASCULARIZED LIVER ORGANIDS USING SCALABLE MICROFLUIDIC TECHNOLOGY</b> .....	<b>148</b>
<i>Introduction</i> .....	149
<i>Materials and Methods</i> .....	152
<i>Results</i> .....	163
<i>Discussion</i> .....	187
REFERENCES.....	201
<i>Supplementary information</i> .....	215
<b>VI. CHAPTER 5. CONCLUSIONS AND FUTURE DIRECTIONS</b> .....	<b>220</b>
<i>Future perspective</i> .....	221

## List of figures

Figure I-1 Chronic liver injuries potential causes and the progression form normal liver to cirrhosis and hepatocellular carcinoma <sup>4</sup> .....	17
Figure I-2 Major causes of fibrosis and CLDs.....	18
Figure I-3 Most important Liver assistive systems and regenerative medicine components for potential treatment of CLDs and cirrhosis .....	22
Figure I-4 General concept and steps for the generation of bioengineered liver tissue.....	25
Figure I-5. Main pros (green boxes) and cons (red boxes) of the principal liver bioengineering approaches. ECM: extracellular matrix <sup>47</sup> .....	27
Figure I-6. Construction of human liver seed grafts. (A) Human hepatic aggregates containing human primary hepatocytes and NHDFs were created using pyramidal microwells. (B) Hepatic aggregates (red) were then combined with geometrically patterned human endothelial cell cords (green) in a fibrin hydrogel to create “liver tissue seeds” that were then implanted ectopically into FNRG mice. Right: Blue-gloved finger demonstrates macroscopic scale of human liver tissue seeds <sup>22</sup> .....	31
Figure I-7. Human iPS-HLC sheet transplantation have significantly increased survival rate for CCL <sub>4</sub> -induced mice through HGF secretion <sup>77</sup> .....	33
Figure I-8. Generating liver organoids from human liver. Liver-resident progenitor cells are isolated from a liver biopsy or liver resection. The bipotent progenitor cells are selected by sorting and embedded into Matrigel, soaked with culture medium rich in growth factors. They proliferate and self-organize into 3D structures, reforming into their original patterning. Organoids derived from proliferative hepatocytes form clusters of cells (Hep-Org), where gutters between cells (yellow lines) connect them as a “canalicular” structure. Organoids derived from EpCAM+ cells form spheroids with a central hollow area (Chol-Org). Notably, the organoids derived from liver-resident progenitor cells contain epithelial cells only <sup>92</sup> .....	36
Figure I-9. Liver organoids can also be generated from pluripotent stem cells (iPSCs and ESCs), usually by a three-stage differentiation process that recapitulates the signaling programs active during development. iPSCs/ESCs are first directed towards an endodermal fate by exposure to Act A and Wnt. These endoderm cells then progress to a hepatic fate following induction of HGF and FGF signaling. These hepatic progenitors are hepatoblast-like cells. The hepatic progenitors can form hepatocyte-like cells in response to OSM signaling. Conversely, by placing the hepatic progenitors in ECM and modulating FGF, EGF and Act A signaling, ductal organoids can be generated. Act A, Activin A; BMP, bone morphogenetic protein; ECM, extracellular matrix; EGF, epidermal growth factor; ESCs, embryonic stem cells; FGF, fibroblast growth factor; FSK, forskolin; HGF, hepatocyte growth factor; ICM, inner cell mass; iPSCs, induced pluripotent stem cells; OSM, Oncostatin M; TGF $\beta$ i, transforming growth factor beta inhibitor; TNF $\alpha$ , tumor necrosis factor-alpha <sup>92</sup> .....	38
Figure I-10. Progress in vascularized liver bud technology by Takebe group.....	40
Figure I-11. Approaches to generate hepatocyte progenitors in vitro. Current approaches to generate in vitro-expandable hepatocytes include differentiation of human pluripotent stem cells, reprogramming of fibroblasts and cells of a similar developmental origin, identification of liver progenitor cells, and reprogramming of mature hepatocytes. In vitro-expandable	

hepatocytes are required as a therapeutic alternative to liver transplantation and for drug development <sup>94</sup> .....	45
Figure I-12. Generation of ProlIHs liver progenitor cells that can mature following in vitro differentiation or transplantation <sup>113</sup> , an overview of the protocol used for generation of human hepatocytes-derived liver progenitor-like cells (HepLPCs) in vitro <sup>114</sup> .....	46
Figure I-13. Derivation and applications of human hepatocyte-like cells. A: Directed differentiation process of human pluripotent stem cells (hPSCs)-derived hepatocyte-like cells (HLCs) in vitro includes endoderm development, endoderm hepatic specification, and hepatic maturation stages; B: Applications of human HLCs. HPSC-derived HLCs can be used to generate disease models to study rare or common genetic variants. These cellular models can be applied in pathophysiological research, drug screening, and toxicity testing. Cohorts of HLCs provide in vitro cell models for genome-wide association studies and potentially pharmacogenomics in dishes. HLCs also offer a potential cell source for bioartificial livers or liver transplantation. HLCs: Hepatocyte-like cells; hPSCs: Human pluripotent stem cells <sup>115</sup> .....	48
Fig I-13. Thesis project outline for scalable generation of vascularized liver organoids. ...	59
Figure II-1 Integrated hepatic differentiation of hPSC 3D spheroids (hPSpheres) into hepatic organoids in a stirred tank bioreactor under fully controlled conditions .....	80
Figure II-2 The effect of controlled DO on differentiation to endodermal cells. ....	82
Figure II-3 The effect of controlled DO on hepatoblast differentiation. ....	84
Figure II-4 The effect of controlled DO on differentiation to hepatocyte-like cells. ....	86
Figure II-5 The gene and protein expression of the hepatic organoids.....	89
Figure II-6 The functional activity of hepatic organoids. ....	92
Figure II-7 Validation of the developed integrated hepatic differentiation protocol at 30% DO concentration.....	95
Figure II-8 Employing fully controlled dissolved oxygen (DO) at physiologically relevant concentration level similar to liver tissue and pH during integrated differentiation process led to regulating the fate of human pluripotent stem cell (hPSC) aggregates and generation of fetal-like hepatic organoids including red blood cells (RBCs). ....	102
Supplementary Figure II-1.....	110
Supplementary Figure II-2. Flow cytometry analysis. Upper panel shows the isotype control population. Lower panel shows the representative dot plots and percent of SOX17-positive cells in endospheres derived under different dissolved oxygen (DO) conditions. ....	110
Supplementary Figure II-3. The quantification of western blot data. The expression of hepatospecific markers at day 9 (A) and day 20 (B) of differentiation procedure under different DO conditions in compared to uncontrolled condition (as dotted line). Data (mean±SD) were analyzed with ANOVA and Tukey's post hoc test. n=3. *: $p < 0.05$ ; **: $p < 0.01$ .....	111
Figure III-1. Integrated differentiation protocol for scalable generation of liver progenitors form hPSCs as 3D aggregates under dynamic suspension culture condition.....	115

Figure III-2. Integrated differentiation of hPSCs (H9, and Episomal hiPSC) using two different protocols for scalable generation of DE endospheres .....	119
Figure III.3 Schematic design of the protocol optimization for generation of endospheres from hPSCs under dynamic suspension culture condition.....	121
Figure III-4 Schematic design of the protocol optimization for generation of hepatic endoderm aggregates form endospheres under dynamic suspension culture condition ..	123
Figure III-5. Comparing currently established protocols for scalable production of functional endothelial cells from hPSCs.....	126
Figure III-6 Scalable endothelial differentiation strategy under dynamic culture using small molecule or growth factor-based differentiation strategy as well as culture mode (3D aggregate vs. micro-carrier culture approach).....	127
Figure III-7 Integrated differentiation of hPSCs to endothelial progenitors .....	135
Fig III-8 Schematic design of integrated endothelial differentiation of hPSCs under 3D dynamic suspension culture .....	137
Figure III-9 Tube formation assay of H9 derived endothelial cells.....	138
Figure IV-1. Schematic design of 3D flow focusing chip and scalable microfluidic platform for generation of liver organoids. Concept of droplet microfluidic chip including information about different streams including core, shell, shielding oil or crosslinking oil compositions (A). PC-controlled scalable microfluidic droplet generation platform using pressure-based remote pumps and vessels for aseptic production of microcapsules and vascularized liver organoids, and their further maturation under dynamic suspension culture condition (B).	155
Figure IV-2. Optimizing cell ratio and cell density co-culture condition for efficient self-condensation of hPSCs derived tHE, EC, and MSC for generation of liver bud like structure. Hepatic endoderm cells, KDR+/CD31+ endothelial cells and hPSCs-derived mesenchymal stromal cells were resuspended at different ratio 10:8:5, 10:8:2, 10:5:5, 10:5:2, 10:2:2 in co-culture medium transferred to Corning® 384-well Round Bottom Ultra-Low Attachment Spheroid Microplate and monitored by light microscopy after 24h (A). Explored the transitional hepatic endoderm cells differentiation day (Day 9-12) and total cell mix density (20,40, and 60 million cells/ml) on self-condensation efficacy and liver organoid generation (B). Delayed aggregate formation after using combination of 2% Mebiol® Gel PNIPAAm-PEG 3D and 1g/L dextran sulfate addition to co-culture media compared to control group (C). Dynamic suspension co-culture of tHE, EC, and MSC for generation of liver bud like structure (D).	166
Figure IV-3. Synthesis of biodegradable 4arm-PEG-MMP sensitive peptide as shell material. Conjugation of fast degradable MMP1 sensitive peptide to 4-arm-10/40 PEG-MAL for generation of biodegradable hydrogel (A), Adding maleimide group to 4-arm-10/40 PEG-PEPTIDE using Sulfo-MBS (B). Synthesized 4-arm-10K PEG-PEPTIDE and 4-arm-40K PEG-PEPTIDE (C) Crosslinking concept of 4-arm-10/40 PEG-PEPTIDE for generation of biodegradable shell microcapsule (D). Mass-spectrometry characterization of 4-arm-10K PEG-PEPTIDE (E), Mass-spectrometry characterization of 4-arm-10K PEG-PEPTIDE-MAL (F) and its NMR (G).	168
Figure IV-4. 3D flow focusing chip design and fabrication. Different channel junction configuration 45° and 90° junction design (A). Channels depth configuration at 90° (B). Core and shell flow and droplet formation (C). 3D printed 3D flow focusing chip using VeroClear material (D) Polycarbonate based 3d flow focusing chip (E). PGA based	

microcapsules (F) 4-arm 10k PEG-PEPTIDE based microcapsules (G). Effect of shell flow rate on overall dimension (OD) of PGA and 4-arm 10K PEG-PEPTIDE microcapsules diameter (OD) (G), Effect of PGA concentration on shell thickness of microcapsules (H) Effect of 4-arm 10K PEG-PEPTIDE concentration on shell thickness of microcapsules (I) Release of 75kDa rhodamine-dextran (red) from capsules of 2% PGA, 8% 4-arm 10K PEG, and 8% 4-arm 10K PEG-PEPTIDE. Fluorescein-labeled PEG (green) is used to visualize shell B) Fluorescence intensity of capsules over time. Dotted lines represent  $\pm$  SD from measured numbers of capsules (n=10).....171

Figure IV-5 Scalable and continuous production of liquid core and shell microcapsules using microfluidic platform. Microfluidic set-up for continuous production of microcapsules including liver organoids under aseptic culture condition (A). 50 ml cell mixing spinner in 400ml pressure chamber for introducing core solution to the droplet generation chip (B). Droplet generation chip generating 4-arm 10K PEG-PEPTIDE microcapsule with uniform size at optimal flow rates (C). Jacketed/temperature-controlled spinner flask for collecting generated microcapsules (D). Microcapsules generated with different co-culture densities in core solution including  $1 \times 10^6$  cells/ml,  $20 \times 10^6$  cells/ml, and  $40 \times 10^6$  cells/ml. Immunostaining of albumin (tHE) and CD31+ (Endothelial cells) inside microcapsules (F). Microcapsules generation process comprising generated microcapsules at  $40 \times 10^6$  cells/ml density (G), dynamic suspension culture of microcapsules in spinner flask and AirWheel bioreactors for self- condensation of 3 cell types tHE, EC, MSC (H), Dynamic suspension culture of vascularized liver buds/organoids released form microcapsules for further integrated differentiation/maturation (I). Self-condensation of 3 cell types tHE, EC, MSC in microcapsules after 48h and release after 4 days including viability of cells in generated vascularized organoid (J). Phase-contrast images of self-organized organoids after 7 days culture under dynamic suspension condition including immunostaining of organoids after 6- and 7-days culture for ALB<sup>+</sup> and CD31<sup>+</sup> cells (K).....175

Figure IV-6 Generation of highly functional and vascularized hepatobiliary organoids.....178

Figure IV-7 Vascularized structure of generated hepatobiliary organoids and their CYP expression.....180

Figure IV-8 Metabolic activity properties of VHOs and their key genes and protein expression.....182

Figure IV-9 Western blot analysis and VHOs total DNA content.....186

Fig IV. 10. Comparing the structure on vascularized hepatobiliary organoid generated in this study to other similar studies.....199

## List of Abbreviations

2D	Two-dimensional
3D	Three-dimensional
ANOVA	Analysis of variance
ATMP	Advanced therapy medicinal products
bFGF	Basic fibroblast growth factor
BM	Bone marrow
BMP	Bone morphogenic protein
CHO	Chinese hamster ovary
CLDs	Chronic liver diseases
CM	Conditioned medium
CQA	Critical quality attributes
DCM	Dichloromethane
DMEM	Dulbecco's modified eagle's medium
DMSO	Dimethyl sulfoxide
DNA	Deoxyribonucleic acid
DO	Dissolved oxygen
EBM	Endothelial basal medium
EC	Endothelial cells
ECM	Extracellular matrix
EGF	Epidermal growth factor
EGM	Endothelial growth medium
ELISA	Enzyme-linked immunosorbent assay
EPC	Endothelial progenitor cells
ESC	Embryonic stem cells
EV	Extracellular vesicles
FBS	Fetal bovine serum
FC	Flow cytometry
FDA	Food and drug administration
FI	Fold increase
GAPDH	Glyceraldehyde 3-phosphate dehydrogenase
GATA6	GATA binding protein 6
GelMa	Gelatin methacrylate
GMP	Good manufacturing practices
HCM	Hepatocyte culture medium
HGF	Hepatocyte growth factor

HIF-1	Hypoxia-inducible factor-1-alpha
hiPSC	Human induced pluripotent stem cells
HUVEC	Human umbilical vein endothelial cells
hPL	Human platelet lysate
HSC	Hematopoietic stem cells
HUVEC	Human umbilical vein endothelial cells
ID	Inner Diameter
ISF	Integrated shear factor
MMP	Matrix Metalloproteinases
MSC	Mesenchymal stem/stromal cells
MWCO	Molecular weight cut-off
OD	Outer Diameter
PAS	Periodic Acid-Schiff
PBS	Phosphate buffered saline
PCL	Polycaprolactone
PD	Population doublings
PDGF	Platelet-derived growth factor
PDMS	Polydimethylsiloxane
PEG	Polyethylene Glycol
PFA	Paraformaldehyde
PGA	Polyglycolic acid
PMMA	Polymethyl methacrylate
PRP	Platelet-rich plasma
PSC	Pluripotent stem cells
ROS	Reactive oxygen species
RT	Room temperature
RT-PCR	Real-time, reverse transcription polymerase chain reaction
S/XF	Serum-/xenogeneic-free
SD	Standard deviation
SEM	Standard error of mean
SFM	Serum-free medium
SMC	Smooth muscle cells
ST	Shell thickness
STR	Stirred tank reactor
TCEP	Tri(2-carboxyethyl) phosphine hydrochloride
TEA	Triethanolamine

TMFC	Thermal mass flow controller
VCAM	Vascular cell adhesion molecule
VEGF	Vascular Endothelial Growth Factor
VHO	Vascularized hepatobiliary organoid
VVM	Volume per volume per minute
VW	Vertical-Wheel™
vWF	von Willebrand factor
XF	Xenogeneic-free

## List of publications

This thesis project conducted a sub project of a main project in GI and liver group of Royan institute entitled “Developing regenerative therapies for acute liver failure”

### Manuscripts:

J1. **Abbasalizadeh, S.**, Pakzad, M., Cabral, J. M. et al. Allogeneic cell therapy manufacturing: process development technologies and facility design options. *Expert Opinion on Biological Therapy* 17, 1201-1219 (2017).

J2. Farzaneh, Z., Najarasl, M., **Abbasalizadeh, S.**, Vosough, M. & Baharvand, H. Developing a cost-effective and scalable production of human hepatic competent endoderm from size-controlled pluripotent stem cell aggregates. *Stem cells and development* 27, 262-274 (2018).

J3. Farzaneh, Z., **Abassalizadeh, S.**, Asghari-Vostikolaee, M. H. *et al.* Dissolved oxygen concentration regulates human hepatic organoid formation from pluripotent stem cells in a fully controlled bioreactor. *Biotechnology and Bioengineering* (2020).

J4. **Saeed Abbasalizadeh**, Sahab Babaei, Yichao Shi, Zahra Mazidi, Jake Weiner, Reza Kowsari, Arnab Radua, Joaquim Cabral, Giovanni Traverso, Hossein Baharvand. Continuous production of vascularized hepatobiliary organoids from human pluripotent systems using a High-throughput and scalable microfluidic system-under preparation. Under review by Prof. baharvand and Dr. Teraverso

“Authors preferred to not publish the main materials and methods including results of VHO production as poster or presenting in conference before filing the Patent”

(this page intentionally left blank)

## Chapter 1. Theoretical Background

---

## Chronic liver diseases and liver cirrhosis

The liver is the largest solid vital organ and the largest gland in the human body. It carries out over 500 metabolic functions such as protein, carbohydrate, and lipid metabolism, detoxification of xenobiotics, storage of glycogen and vital biomolecules, production and excretion of bile and cholesterol compounds, synthesis of albumin and clotting factors, ammonia detoxification and more<sup>1</sup>. Because of the importance of the liver and its unique functions, evolution has ensured that it can regenerate and regrow rapidly as long as it is kept healthy. This ability is seen in all vertebrates from fish to humans<sup>2</sup>. However, chronic liver diseases (CLDs) that are result of gradual damage to the liver over long periods of time can lead to chronic inflammation, parenchymal cell death, angiogenesis, and significant decrease in ability of the liver to hepatic function and repair itself (e.g. hepatocellular carcinoma, hepatic encephalopathy, gastrointestinal hemorrhage, infections, and renal failure). The end result for most untreated chronic liver diseasesd is the development of cirrhosis, hepatocellular carcinoma, or acute liver failure, characterized by fatal and resource intensive complications including irreversible distortion of the liver structure and architecture, and significant loss of critical metabolic functions, and aberrant hepatocyte regeneration (Fig I-1)<sup>3,4</sup>.

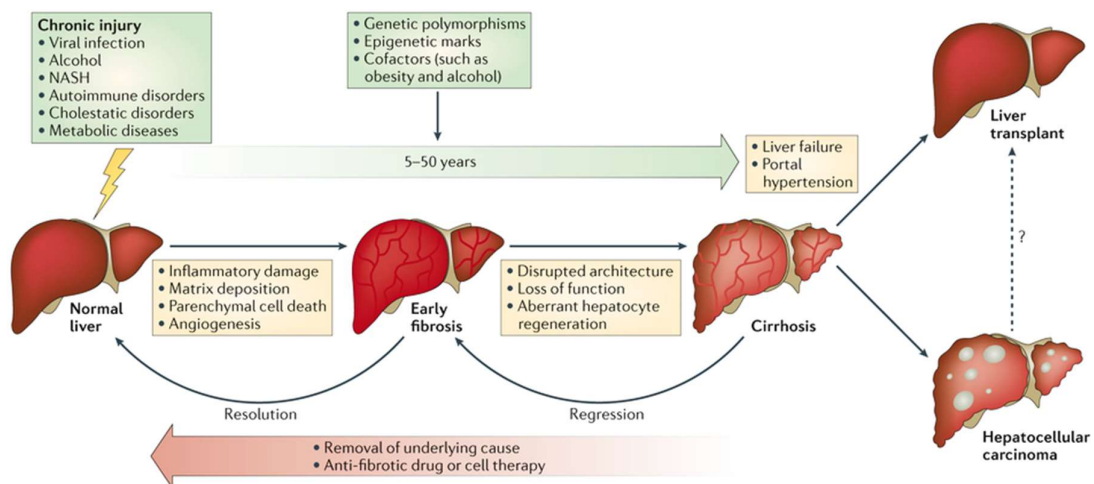
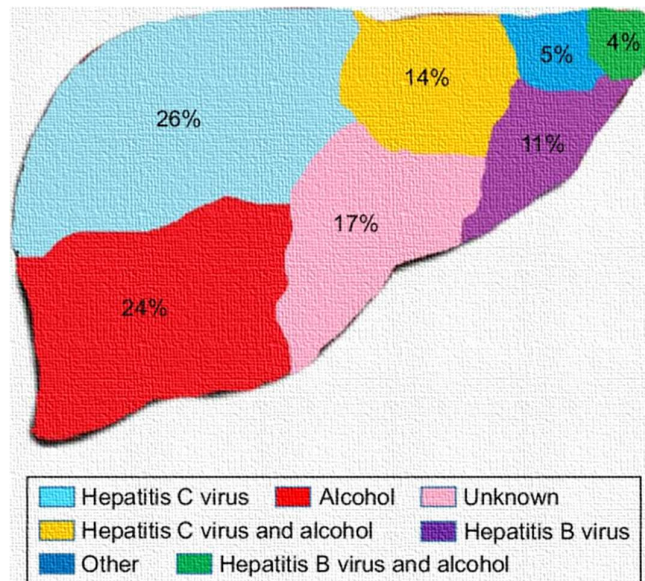


Figure I-1 Chronic liver injuries potential causes and the progression form normal liver to cirrhosis and hepatocellular carcinoma<sup>4</sup>

Alcohol abuse, hepatitis viral infections, genetic abnormalities, steatohepatitis, autoimmunity and other non-infectious diseases like fatty liver contribute to development of chronic liver diseases that are given in Figure I-2. Although most of the liver cirrhosis causes are quite complex and multifactorial, there are some important pathological characteristics that are pretty common in all cases of liver cirrhosis, including degeneration and necrosis of hepatocytes and regenerative nodules, replacement of liver parenchyma by fibrotic tissues, scar formation, and loss of liver function. Fibrosis as a precursor of cirrhosis is a pivotal pathological process in the evolution of all CLDs to cirrhosis.



**Figure I-2 Major causes of fibrosis and CLDs.**

Progressive liver dysfunction and complications of portal hypertension are also the most potential outcomes of the cirrhosis that can lead to acute liver failure and high short-term mortality <sup>5,6</sup>. In spite of extensive research in the field, the exact mechanisms involved in developing liver cirrhosis is still not completely defined and conducting extensive research for better understanding of the pathogenesis of liver cirrhosis is in progress to facilitate the development of more effective treatment options.

### **Etiology and prevalence of CLDs**

It has been demonstrated that etiology of CLDs and cirrhosis varies geographically. For instance, alcoholism, chronic hepatitis C virus infection, and non-alcoholic fatty liver disease (NAFLD) are the most common causes in western countries, whereas chronic hepatitis B is the primary cause of liver cirrhosis in the Asia-Pacific region. Inherited diseases such as hemochromatosis and Wilson's disease, primary biliary cirrhosis, primary sclerosing cholangitis, and autoimmune hepatitis are considered as other causes for developing liver cirrhosis. However, NAFLD has become a leading cause of chronic liver disease in United States and European union, with a prevalence of as high as 30% in the general population. Thus, NAFLD has attracted increasingly extensive attention during recent years as an important cause of chronic liver diseases and liver cirrhosis <sup>7,8</sup>.

Unfortunately, the liver cirrhosis prevalence is experiencing an increasing trend. For instance, prevalence of cirrhosis has been compounded by a doubling in the USA during last decade. Although hepatitis C virus that is considered as a major cause of cirrhosis, could be eradicated and treated given the recent advent of widely available and highly effective antiviral therapy, this trend is likely to continue and deaths due to cirrhosis are expected to triple by 2030 <sup>9,10</sup>. It has been reported that CLDs induce cirrhosis in 633,000 patients per year with a prevalence of 4.5% to 9% worldwide. However, the reported prevalence of cirrhosis is probably underestimated as most patients remain asymptomatic and undiagnosed and a number of clinicians suggested to include liver inflammation and fibrosis biomarkers in routine blood tests <sup>11</sup>.

### **Liver cirrhosis as an unmet medical need**

Recent studies in CLDs have highlighted that these diseases still represent an important and certainly underestimated global public health problem. As mentioned before, CLDs are highly prevalent and silent related to different and mainly associated causes. So, there is an

urgent need for effective global actions including education, prevention and early diagnosis to manage and treat CLDs and subsequently preventing cirrhosis-related morbidity and mortality <sup>11</sup>.

Liver disease accounts for approximately 2 million deaths per year worldwide, more than 1 million comes from complications of cirrhosis and 1 million due to viral hepatitis and hepatocellular carcinoma. Recent reports indicating that 844 million people have CLDs Worldwide and cirrhosis currently causes 1.16 million deaths together with liver cancer 788,000 deaths. This making them as the 11th and 16th most common causes of death, respectively, each year <sup>12</sup>. The mortality rate of CLDs can be compared with other major public health problems related to chronic diseases such as diabetes (422 million, 1.6 million deaths), pulmonary (650 million, 6.17 million deaths) and cardiovascular diseases (540 million, 17.7 million deaths) that indicating its high importance. Despite high prevalence and mortality rate of CLDs and cirrhosis, effective strategies to treat liver cirrhosis are still lacking, partially because of a poor understanding of the molecular mechanisms leading to cirrhosis <sup>11</sup>. Many patients have CLDs for several years with no significant symptoms but get diagnosed when reaching to end-stage liver cirrhosis or acute liver failure, have limited time frame (few weeks to few month) to receive treatment while with no treatment option except receiving a liver transplant. Liver transplants is highly limited while 15%-80% of patients die without receiving liver transplant based on their geographical location. Moreover, for every 100 people who receive a liver transplant for any reason, about 70 will live for five years and 30 will die within five years <sup>12</sup>. Therefore, treating liver cirrhosis and acute liver failure is an unmet medical need that need to be addressed by establishing global and local prevention and diagnosis programs as well as developing innovative and effective treatment technologies. These technologies may also provide a bridge to surgery supporting liver function and, potentially, reducing the waitlist mortality rate for patients.

### **Current treatments for acute liver failure**

Although liver transplantation is a highly successful treatment for chronic liver diseases, but it is the only available option and increasingly numbers of patients die every day or experiencing health conditions deteriorate while waiting on liver transplantation lists. This happens because of the local and worldwide critical shortage of available transplantable liver donors (approximately 25000 liver transplants are available worldwide per year) <sup>13,14</sup>. Even those who receive a successful transplantation often experience complications associated with physical and emotional suffering and in some cases, premature mortality <sup>5</sup>. Scarcity of donor, high cost of treatment, lifelong immunosuppression, and surgical complications are the major issues associated with liver transplantation <sup>15</sup>.

To cope with this unmet medical need, different research groups and companies have been focused in developing promising regenerative medicine technologies using different cell types as starting material (e.g. hPSCs, adult derived progenitors, and induced hepatocyte-like (iHep) cells from somatic cells) to manufacture external liver supports or generate functional hepatocyte-like cells, liver organoids, or tissue constructs <sup>16</sup> as therapeutic components for transplantation.

### **Cell-based liver assistive devices and regenerative therapies for cirrhosis and acute liver failure treatment**

During recent years, different research groups and companies have developed promising assistive and regenerative medicine technologies to treat acute liver failures such as external liver support systems/liver assistive devices to help to recover patient liver inherent regeneration capacity and extend their survival to receive a transplant <sup>17</sup>. Scalable production of human functional hepatocyte like cells generated from human pluripotent stem cells <sup>18</sup>, inducing human adult cells *In vitro* generation of a recellularized whole liver organ <sup>19</sup>, generation of liver organoids from adult human liver and high-throughput generation of

vascularized human liver buds from human pluripotent stem cells (hPSCs) for organoid medicine application <sup>20,21</sup>, development of *in situ* expandable liver tissue <sup>22</sup> are some the most promising regenerative technologies. New approaches based on extracellular vesicles/exosomes are also being investigated as cell-free alternative. It has been reported that extracellular vesicles can modulate liver regeneration and restore hepatic function through the transfer of bioactive molecules (Fig I-3) <sup>23</sup>.

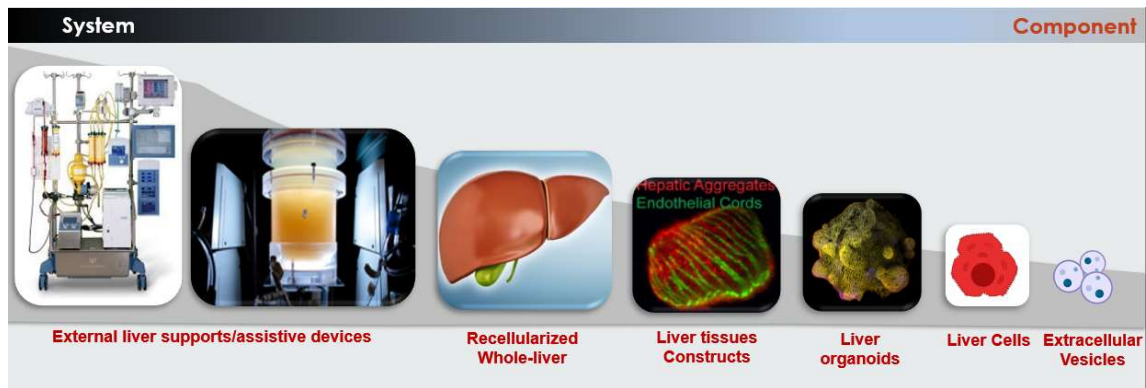


**Figure I-3 Most important Liver assistive systems and regenerative medicine components for potential treatment of CLDs and cirrhosis**

### Liver-assistive devices and external supports

For more than 65 years, researchers and companies from all over the world tried to develop a promising liver assist device (e.g. Extracorporeal Liver Assist Device (ELAD) <sup>24</sup>, HepatAssist <sup>25</sup>, Bioartificial Liver Support System <sup>26</sup>, The Academic Medical Center-Bioartificial Liver (AMC-BAL) <sup>27</sup>, Modular Extracorporeal Liver Support Device (MELS) <sup>28</sup>) to support those patients suffering liver failure, a really dramatic condition that result in unacceptably high mortality rate <sup>29</sup>. Numerous techniques of extracorporeal support have been established to fill this role; however, only few trials reported promising outcomes and extracorporeal support technology remained an unproven therapy in liver disease with mainly unsatisfactory results <sup>30</sup>. These outcomes are not surprising, considering the complexity of liver functions and the heterogeneity of patients to be treated. Despite of the clinical study, development, cost-effectiveness, and technical challenges, research continues in this field because of a shortage

of available liver transplants and increasing recognition of the liver's unique ability to regenerate in the setting of an acute failure. There are currently two main approaches being pursued: (1) an artificial liver support system, using or adapting pre-existing renal replacement technology with adsorbent or detoxifying capacity, and (2) a bioartificial support system with the integration of living hepatocytes into an extracorporeal circuit, with provision of metabolism and synthetic function, 3) addressing the issue of specific cytokine removal or endotoxin clearance, two pathophysiologic mechanisms involved in liver failure and its consequences 4) developing an ideal cell line for use in liver bioreactors representing full functionality of adult human hepatocytes, unlimited lifespan, potentials for in vitro proliferative capacity, no risk for metastatic tumor formation, nor zoonosis transmission or immunogenicity, 5) developing a efficient bioreactor for providing an in vivo like environment for optimal viability and functionality of hepatocytes <sup>30</sup>. Therefore, other methods to support the failing liver are under development including developing other approaches such as cell therapy and regenerative medicine technologies that has gained increasingly attention during recent years to establish more viable and effective therapeutic strategies.

### ***Bioengineered whole human liver***

The human liver as a very complex organ with specific zonation and diverse metabolic properties essentially requires continuous perfusion for the delivery of nutrients and oxygen and the removal of metabolites and wastes in order to survive and maintain a proper function. Thus, re-creating such a big, complex, and highly vascularized structure by combining proper cells and biomaterials and employing established sophisticated fabrication techniques such as 3D bioprinting is still very hard and challenging. One of the new approaches to liver regenerative medicine involves re-creating 3D organs with a decellularized, native scaffold that can be repopulated with parenchymal and non-parenchymal cells in laboratory settings <sup>31</sup>. The organ native ECM has a complex composition and topography, serving as a customised native structure for cell-ECM adhesion, interaction, and polarity that can regulate

cell morphology, homing, proliferation, differentiation, maturation, function, and cell-cell interactions after reseeding <sup>32</sup>. Therefore, an efficient decellularization/recellularization strategy is one of the promising approaches aiming at the possibility of producing a fully functional organ with in vitro-developed construction for clinical applications to replace failed livers (Fig. I-4). Organ/tissue decellularization techniques were gained increasingly attention in the 1980s <sup>33</sup>, and the concept of whole-organ decellularization was employed later by Ott and colleagues to develop a mouse heart <sup>34</sup> as well as humanized rat heart <sup>35</sup>. Advances in developing efficient protocols for whole solid and vascularized organs decellularization in parallel with efficient isolation, generation, and scalable production of required various cell types (e.g. stem cells or progenitor cells with stem cells, somatic cells or adult allogeneic human tissue origin) for recellularization and developing improved recellularization techniques have raised new hopes to regrow organs in the lab. Several other solid organs have been generated using this platform such as, Kidney <sup>36</sup>, Lung <sup>37</sup>. This technique was later adapted for liver engineering purposes with the preservation of the chemical composition and structure of the ECM with structurally intact vessels, and bile ducts <sup>38,39</sup>. Practically, donor livers unsuitable for transplantation are used to create whole-liver scaffolds which are subsequently reseeded with different cell type of liver (e.g. hepatocytes and endothelial cells) to create transplantable grafts and organ. The recellularized graft transplanted in vivo and perfused ex vivo demonstrated mature liver functions and then adapted to human liver. In a study, the decellularized human liver has been repopulated using hepatic stellate cells (LX2), hepatocellular carcinoma (Sk-Hep-1) and hepatoblastoma cells (HepG2). Ex-vivo preservation was prolonged for up to 21 days, with excellent cell viability, motility and proliferation and remodeling of the extracellular matrix <sup>38</sup>. Another study created a humanized porcine liver by using human fetal hepatocytes and stellate cells for recellularization of decellularized pig liver.

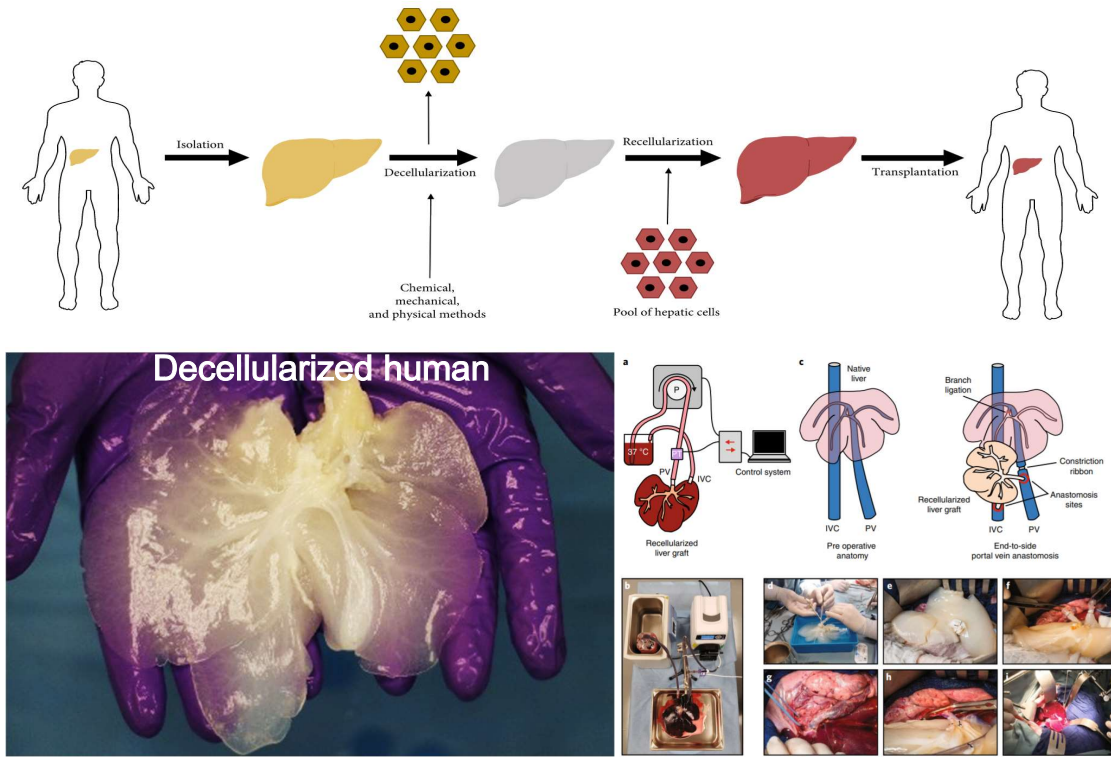


**Figure I-4 General concept and steps for the generation of bioengineered liver tissue.**

Organs that are nonviable for transplantation may serve as the basis for the generation of a scaffold that can then be repopulated with liver cells for subsequent transplantation in patients with liver disease 40. A diagram (a) and photo (b) of the set-up of the in vitro blood circuit used to evaluate rBEL patency. The circuit perfuses a rBEL with warm, heparinized whole porcine blood and is driven by a peristaltic pump controlled by a pressure-based custom control system. c, an illustration of an in vivo heterotopic liver implant model where the rBEL is anastomosed via the PV and IVC to the native PV and IVC. Partial flow was given to both the rBEL and the native liver by restricting flow to the native liver. d–i, Representative images of the heterotopic liver implant depicting rBEL preparation (d), positioning in the abdominal cavity (e), positioning of rBEL vessels prior to anastomosis (f), constriction of the native PV (g), anastomosis of rBEL vessels with native PV and IVC (h), and rBEL reperfusion (i) 41.

This study demonstrated that the acellularized matrix could support and induce phenotypic maturation of engrafted human fetal hepatocytes in a continuously perfused system 42. The feasibility of established protocols was also demonstrated in larger animal models 43, and even in humans to translate the approach to clinical scale. Although these studies seem promising and hold great potential as a therapeutic approach but technical challenges associated with different steps of technology especially recellularization process are still critical and not resolved such as maintain required cells as single cells during perfusion process, very slow and tricky process due to vascular structure of tissue, inefficient recellularization, heterogenous repopulation of decellularized tissue due to potential formation of cell clumps in

small vessels, and poor function of recellularized organ. It has been shown that currently established techniques allow for the successful seeding and culture of hepatocytes, but colonization of the bile duct with functional cells (i.e. cholangiocytes) and the achievement of an intact vascular network by endothelial cells remain to be perfected. Another critical issue that should be addressed before using whole liver scaffolds in clinical practice is the lack of a suitable source of cells for the recellularization process. The limited availability and inability to expand primary hepatocytes has led researchers in the field to search for a new cell source such as fetal/progenitor liver cells, stem cells or iPSCs for generating hepatocytes, endothelial cells and cholangiocytes. However, the production of huge numbers of these cell types is still far beyond current technical capability. Thus, developing scalable production processes of required functional and/or proper cell materials (e.g. billion numbers of hepatocyte like cells, endothelial cells, or progenitors) for repopulation of a whole human liver is necessary. Another hurdle that should be promptly addressed is “sample to sample” variation due to the unique condition of each donor deriving from the use of discarded livers<sup>44</sup>. Finally, neo-bioengineered organ should be able to present some levels of functional maturation after creating in lab and demonstrate long-term survival after transplantation that has not yet been achieved and main goals of bioengineering research will be to solve these problems.

#### ***Liver tissue constructs and liver cell sheets***

Progress in the fields of biomaterial science, microfabrication, bioengineering, genetic engineering, and developmental biology have enabled novel *in vitro* platforms and implantable tissues that recapitulate the structural complexity and functional axes of the liver<sup>45</sup>. Liver tissue constructs and liver patches are therapeutic components typically smaller than the whole-liver organ that aims to create organic or polymeric constructs that mimic the liver ECM and replicate functional characteristics such as cell adhesion, viability, growth, proliferation, differentiation, maturation, and function. In addition, even if it is possible to grow liver tissue *in vitro*, the main challenges remain after surgery. For instance, the bioengineered tissue mass

should have approximately 30% of patient liver mass or be expandable to demonstrate the therapeutic outcome. It is essential to demonstrate that bioengineered livers are clinically safe, the vasculature network is intact to allow a functional vascularization, and the organ has regenerative capacities <sup>46</sup>.

The principal strategies and main component of scaffolds for clinical applications are mainly based on biomaterials such as decellularized liver tissue as ECM which discussed before, natural, synthetic or their combination based polymeric 3D constructs, and bio-printed 3D constructs and scaffolds. Below we provide an overview of such bioengineering approaches, and Figure I-5 shows the main pros and cons of each of them.

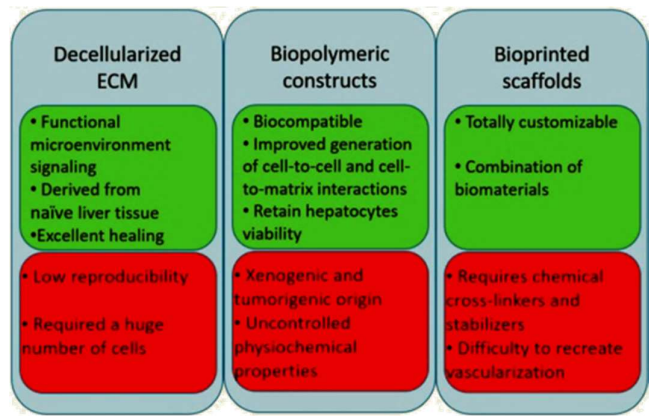


Figure I-5. Main pros (green boxes) and cons (red boxes) of the principal liver bioengineering approaches. ECM: extracellular matrix <sup>47</sup>.

***Polymeric scaffolds***

Several studies explored different biomaterials and polymers to create scaffolds that mimic the natural liver tissue ECM for clinical or drug discovery/toxicity applications. The most main components of these scaffolds are collagen and hyaluronic acid and its derivatives as well as polysaccharides (e.g. alginate, chitin/chitosan), proteins (e.g. Gelatin, Fibrin, elastin, laminin silk, Matrigel®), synthetic polymers (e.g. Polylactic acid (PLA), Polyglycolic acid (PGA), Poly(ε-caprolactone) (PCL)) or a blends of different types of materials <sup>48,49</sup>. Among these materials, hyaluronic acid derivatives demonstrated more robust support for cell attachment, proliferation, differentiation, growth, and migration for hepatocytes and can retain hepatocyte

viability for 4 weeks <sup>50</sup>. Generally, natural biomaterials such as alginate and Matrigel<sup>®</sup> that were used in numerous studies to culture hepatocytes and induce the hepatic differentiation of stem cells, forming biocompatible hydrogels and can largely improve the generation of cell-to-cell and cell-to-matrix interactions to generate a functional bioengineered tissue <sup>51,52</sup>. However, these natural biomaterials have some important limits that prevent their clinical application including their uncontrollable physicochemical properties, degradability, lack of regenerative ability, and inconsistent mechanical properties. Moreover, due to the xenogeneic and tumorigenic origin of Matrigel, it is not an optimal support for clinical applications in liver bioengineering <sup>53</sup>. On the other hand, synthetic materials offer a wide range of physicochemical properties and a better control over them to create a customised and spatiotemporal tunable scaffold. Scaffolds containing biodegradable polymers such as PLA, PGA, PCA polyanhydrides, polyfumarates, polyorthoesters, polycaprolactones, and polycarbonates demonstrated facilitate cell regeneration, transplantation, and degradation with tunable properties <sup>49</sup>. The biocompatibility and surface properties of bioengineered matrices and scaffold adhesion properties could also be improved by chemically modifying these polymers (e.g., by incorporating proteins and special bioactive domains), stimulating cell attachment and migration, and thereby facilitating liver tissue repair <sup>54</sup>. However, currently established biomaterials and constructs still fail to perfectly reproduce the microenvironment of the liver, an essential criterion to reach a functional liver cell activity. For this reason, their therapeutic potential is still limited while extensive research is in progress to overcome current hurdles.

### ***Bio-printed Scaffolds and tissue constructs***

Although the use of biomaterials for creating 3D culture and creating combination of 3D scaffold and cells for generating tissue constructs has improved the settings for liver tissue engineering, it has some limitations such as technical issues for creating complex and vascularised biological and tissue mimicking structures and designs due to size, material,

compositional, and inefficient cells attachment and proliferation constraints. 3D printing technology is an innovative solution to these problems through providing complex printed scaffolds, tissue-mimicking constructs using biocompatible materials (i.e., bio-inks) that can be combined with printing proper cell type for creating a customised tissue construct <sup>55</sup>. Advances in 3D printing technology have enabled the creation of more complex 3D structures such as hepatic lobules with different cell types incorporation during biomaterials printing using 3D bioprinting technology <sup>56,57</sup>. 3D bioprinting technology can offer totally customized printing procedure that also guarantees the complete personalization of the final product according to intended applications. Extrusion, inkjet, and laser-assisted bioprinting are the most common bioprinting modalities <sup>58</sup>. However, extrusion bioprinting that offer a strong degree of customization with few restrictions on the cells printing is the most often used bioprinting technology in bioengineering and biomedical research <sup>56</sup>. Nevertheless, the choice of proper biomaterials or a blend of them for 3D printing a tissue is more restrictive, as they should be either easy to print and biocompatible for the cell type to be printed, but typically finding an optimal choice for both is not possible <sup>59</sup>. The ideal characteristics of bio-inks for extrusion bioprinting are viscosity to enable printing at RT and cell culture temperature condition, associated with an adequate elasticity to maintain the intended structure, while also provide high biocompatibility to maintain cell viability and support its function <sup>60</sup>.

To date, collagen, alginate, polyethylene glycol (PEG), hyaluronic acid, fibrin, gelatin, or polycaprolactone are the most common biomaterials that were used for 3D bioprinting for tissue constructs <sup>55</sup>. Except for collagen that can form hydrogels and 3D scaffold with simple temperature or pH transition, other biomaterials need the addition of a mainly chemical and toxic cross-linker that could adversely affect the cells viability and proliferation during construct fabrication process. Thus, the combination of biomaterials need to be appropriately balanced to guarantee the best biocompatibility of the bio-ink being used <sup>55</sup>. Although collagen offering very unique environment and biocompatibility properties, it is a poor bioprinting material since require a time- and temperature-sensitive cross-linking <sup>61</sup>. A multi-component hybrid bio-ink is

therefore a potential and viable solution to tune the physicochemical achieving ideal physiological relevance and bio-printability. Unfortunately, durable 3D construct fabrication requires the incorporation of chemical stabilizers, such as polycaprolactone, showing the limitations of bio-inking technologies in mimicking both the biochemical composition and the complex 3D structure of the liver. Another important challenge in 3D bioprinting is developing innovative approaches to fabricate and mimic cellular microenvironments from molecular to macroscopic scales for generating whole functional and vascularised liver with zonation and proper metabolic activity properties suitable for transplantation. The main, but some important issues, such as vascularization, should be addressed before this methodology can really be implemented.

To address some of these issues, Stevens et al. bio-printed constructs of sacrificial lattices of carbohydrate glass using a custom-built three-dimensional printer containing a heated nozzle and then embedded it within a fibrin hydrogel and dissolved using phosphate-buffered saline (PBS) to leave open channels. Afterwards, channels were filled by pipetting a slurry containing HUVECs and neutralized collagen as well as aggregates of co-cultured primary hepatocytes with human dermal fibroblast one by one channel in parallel (Fig 1-6). Interestingly, the transplanted bioengineered tissue showed a 50-fold expansion in response to regenerative stimulus in fumarylacetoacetate hydrolase-deficient, nonobese diabetic, recombinae activating gene-deficient and IL-2 receptor  $\gamma$  chain-deficient mice. Necessarily, recombinae activating gene-deficient and IL-2 receptor  $\gamma$  chain-deficient mice treated with NTBC to avoid liver failure. It always has been shown that animals treated by cycles of NTBC withdrawal to cause liver injury and regenerative stimulus have larger hepatic grafts than the ones who remained under NTBC. Moreover, grafts were positive for proliferative markers and show a higher mRNA expression of genes known to induce hepatic proliferation. This work provided a proof of principle that engineered liver tissue can adopt hepatic regenerative properties in response to proliferative cues.

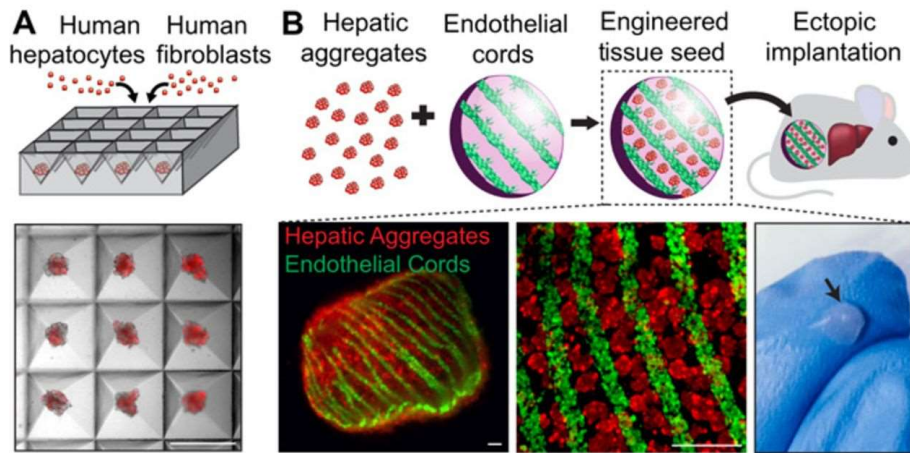


**Figure I-6. Construction of human liver seed grafts. (A) Human hepatic aggregates containing human primary hepatocytes and NHDFs were created using pyramidal microwells. (B) Hepatic aggregates (red) were then combined with geometrically patterned human endothelial cell cords (green) in a fibrin hydrogel to create “liver tissue seeds” that were then implanted ectopically into FNRG mice. Right: Blue-gloved finger demonstrates macroscopic scale of human liver tissue seeds <sup>22</sup>.**

Finally, scaffold-free bioprinting using a new technique that adapted for constructing a human mini-liver model involving printing hepatospheres on a needle array using Regeneron<sup>®</sup> apparatus and then perfusion culture of the construct in a perfusion chamber for merging spheroids, tubular mini liver tissue formation, and functionalization <sup>62</sup>. However, this technique is not scalable for construction large tissue construct for clinical application. Thus, despite the amazing breakthroughs in generating bioengineered liver constructs, there is much work left to do.

### ***Liver Cell Sheets/Patches***

Within the last two decades, sheets of various cell types have been used to regenerate several types of tissues and/or organs including (but not limited to) the heart, cartilage and tendons, meniscus, bone, cornea, skin, periodontal tissue, blood vessels, oral cavity, gastrointestinal tract, and bladder <sup>63</sup>. In 2012, Okano’s group has introduced the first generation of cell-sheet engineering approach for liver using primary murine hepatocyte sheets, created on special culture dishes coated with thermos- responsive polymer (PNIPAAm) that also offering hydrophilicity-hydrophobicity transition. The sheet structure supported hepatocyte

functionality after 48 h that providing a platform for drug testing applications <sup>64,65</sup>. Afterwards, different studies have engineered hepatic tissue sheets/patches composed of different hepatocytes, cell types, and ECM components (e.g. decellularized liver ECM) to the construction of small liver tissues *in vitro* and transplanted these constructions to subcutaneous vascularized spaces mainly in mice models <sup>66-69</sup>. Interestingly, some report demonstrated pre-vascularization of the subcutaneous space before transplantation, by basic fibroblast growth factor (bFGF)-releasing devices, allows the creation of 3D hepatic tissues by stacking multiple primary hepatocyte sheets that maintained the hepatic functions and morphology for longer than 200 day <sup>65</sup>. To overcome low primary hepatocyte proliferation and fragility of the engineered sheets issues observed in previous studies, innovative multilayered human primary fibroblast/hepatocyte cell-sheets with improved handling properties have been engineered while maintaining high levels of hepatic-specific functions (i.e. albumin and urea synthesis) and high potential for vascularization *in vitro* after subcutaneous transplantation <sup>70-72</sup>.

Advanced in assembly techniques such as a sandwich assembly approach combined with bioprinting technology resulted in generation of several layers of cell-sheets to fabricate 3D liver-like tissues with hepatic functions *in vitro* <sup>73</sup>. Okano's group have employed sandwich approach to combine a hepatocyte sheet layer between two endothelial sheets layers *in vitro* that resulted in creating triple-layered hepatic tissues with preserved hepatocytes specific cell polarity <sup>74</sup>. This approach has also adapted to creating human cells sheets by loading of cells sterically onto other cells previously coated with fibronectin and gelatin nanofilms generated via LbL assembly that showed superior albumin production ability than non-vascularized tissue or a hepatocyte suspension in the vascularized tissue. Recently, Eguchi's group developed a new strategy to use hepatic nonparenchymal cells (NPCs) sheets co-cultured with adipose-derived stem cells (ADSCs) <sup>75</sup>. Subcutaneous implantation of these sheets in mice showed to be able to form functioning bile canaliculi, store glycogen and survived for 4 weeks without pre-vascularization, probably due to the presence of signs of vascularization.

More recently, liver organoids generated from LGR5-positive bipotential human liver stem cells repopulated decellularized liver discs and formed liver-like tissue after transplantation while showing key liver metabolic functions <sup>76</sup>. While transplantation of hepatocyte or hepatocyte-like cell sheets, human iPSC-derived hepatocyte sheet (Fig I-7) <sup>77</sup>, and 3D patches appears to be considered as an innovative therapeutic strategy for liver injuries and consequently liver diseases in small animal models, the presented results justify the application of these cell-sheets to large animals and subsequently to clinical trials.

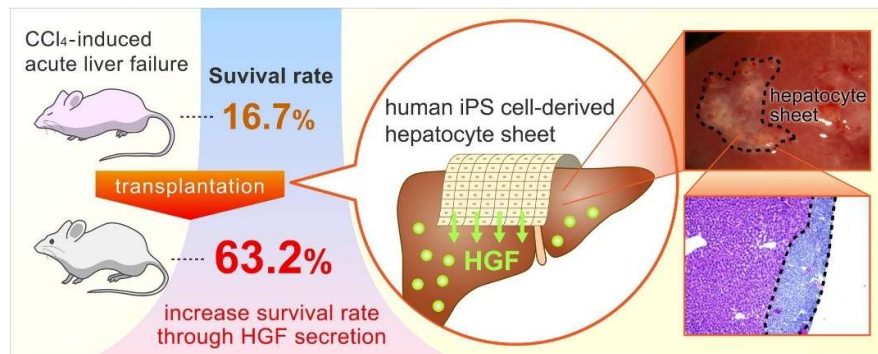


**Figure I-7. Human iPSC-HLC sheet transplantation have significantly increased survival rate for CCL4-induced mice through HGF secretion <sup>77</sup>.**

### Liver buds and organoids

The first organoid concept has been described about one century ago in 1907 by Henry Van Peters Wilson who reported self-reaggregation and reassembly of sponge cells after dissociation into a whole organism <sup>78</sup>. However, the organoid concept become an advanced and cutting-edge technology thanks to great progress in the understanding of morphogenesis and stem cell biology during the 20th century and transformed from a mere experimental tool to a sophisticated biological technology. Meanwhile, organoids have preliminary recognized as unique *in vitro model* systems hold the promise to generate organ-like tissues in a dish for

disease modeling, developmental studies, and drug discovery/toxicology<sup>79-81</sup>. With advances in organoids generation techniques and improving the robustness of protocols for scale-up production as well as their unique features including recapitulating native organ like structure and more importantly fetal to near organ-level functionality, they gained increasingly attention to be used as potential therapeutic component and reach to the point of emergence of “organoid medicine” in the next decade<sup>82</sup>.

Organoids are mainly defined as a 3D-multicellular cluster derived from stem/progenitor cells under *in vitro* culture condition, capable of self-renewal and self-organization, that recapitulates the function of the tissue from which it was derived<sup>83</sup>. Neural organoids was the first organoids that generated with advanced stem cells research techniques including self-organisation concept in 2008, and then different research groups have developed different organoid technologies to generate optic cup, pituitary gland, intestine, colon, stomach, pancreas, lung, kidney, and liver *in vitro*<sup>84</sup>. Liver organoids generated from different techniques have different properties and diverse phenotypes but generally they can be defined as three-dimensional (3D) structures that preserves the key physiological features of the liver<sup>85</sup>. In terms of scale, liver organoids are mainly in form a spherical monolayer of epithelium or dense/cystic spheres self-organizing and growing to the size of 100  $\mu\text{m}$  to 1 mm in diameter<sup>82</sup>. Thus, they can be considered as a bridge between using individual liver cells (e.g. HLCc or MSCs isolated form liver) for liver cell therapy that suffering from functionality/production scalability issues and 3D tissue constructs/whole liver bioengineering for transplantation that mainly suffering from technical and production scalability issue. To date, liver organoids has been generated employing different approaches including bioprinting<sup>86</sup>, isolation/expansion pf liver progenitors or expandable hepatocytes from adult liver tissue<sup>85,87</sup>, integrated differentiation of hPSCs<sup>88</sup> or their genetically engineered form<sup>89</sup>, and co-culturing as a three-dimensional (3D) structure<sup>90</sup> or through dynamic self-organization/ self-condensation driven by cell-cell interactions among co-differentiating cells<sup>21</sup>. Here, generation techniques and reports that demonstrated more potential for therapeutic application will be described further.

***Isolation/expansion of liver progenitors from adult liver tissue for liver organoid generation***

Isolation of primary cells mainly liver progenitors from fetal or adult livers under physiological or pathological conditions has emerged as a viable organoid generation technique from 2013. This novel technique has been first established by Hans Clevers's group, as pioneer in the liver organoid field, that isolated Lgr5 liver cells from mouse liver and expanded them as bipotent progenitor organoids *in vitro*, which showed the ability to differentiate into functional liver organoids (Fig. 1-8) <sup>85</sup>.

The protocol have been also adapted to human liver for generation of human liver organoids and they long term expansion for potential clinical application <sup>87</sup>. This innovative technique involved two methods to generate liver organoids: cholangiocyte-derived organoids (Chol-Orgs) or proliferative and expandable hepatocyte organoids (Hep-Orgs). Practically, the human liver tissues/biopsies are dissociated, and epithelial cell adhesion molecule (EpCAM+) cells (bipotent progenitor cells) are sorted and seeded into Matrigel (gel-forming extracellular matrix complex) for generation of Chol-Orgs.

Using a culture medium highly enriched with growth factors, the sorted cells proliferate and self-organize into spheres like shape and epithelial structure that can be differentiated into either a hepatocyte or cholangiocyte phenotype upon modification of growth stimuli. It has been demonstrated that Lgr5 expression in the liver is restricted to a unique subset of hepatocytes most adjacent to the central veins <sup>91</sup>. Recently, Has Cleavers group has also established a scalable approach for expansion of these bipotent stem cells under dynamic suspension culture to translate the technology for clinical application <sup>76</sup>.

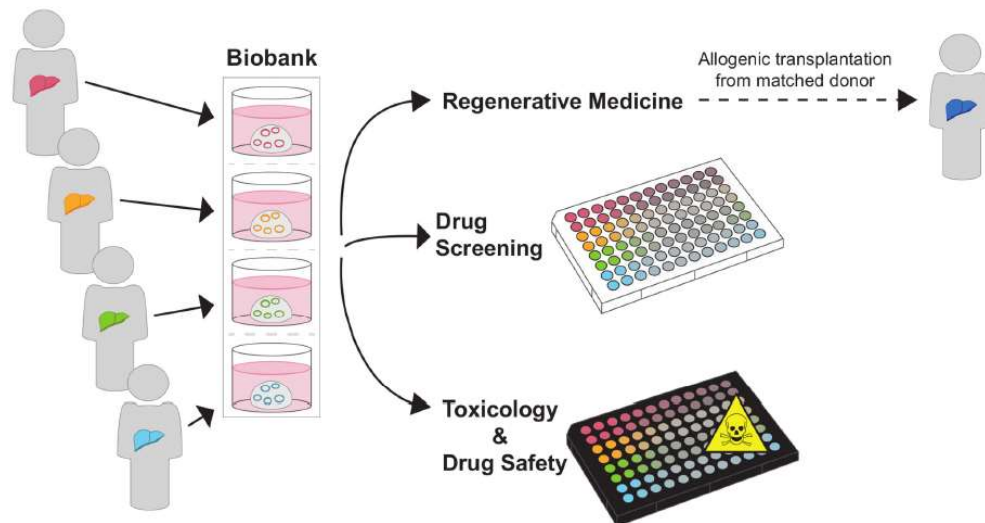
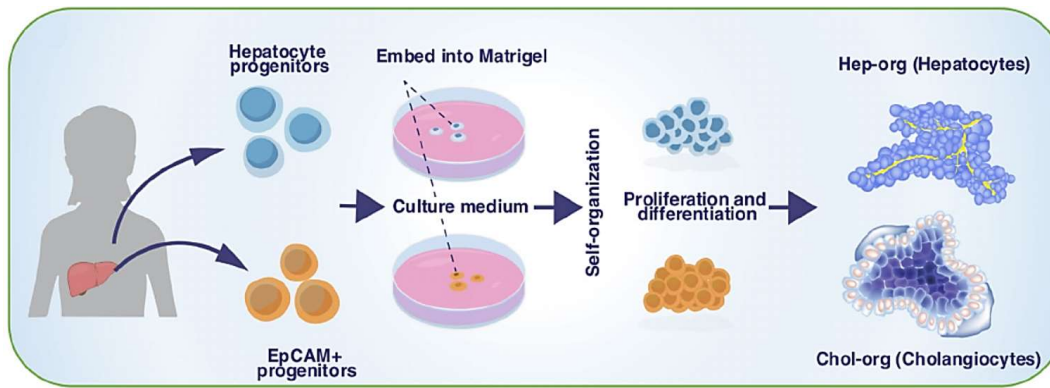


**Figure I-8. Generating liver organoids from human liver. Liver-resident progenitor cells are isolated from a liver biopsy or liver resection.** The bipotent progenitor cells are selected by sorting and embedded into Matrigel, soaked with culture medium rich in growth factors. They proliferate and self-organize into 3D structures, reforming into their original patterning. Organoids derived from proliferative hepatocytes form clusters of cells (Hep-Org), where gutters between cells (yellow lines) connect them as a “canalicular” structure. Organoids derived from EpCAM+ cells form spheroids with a central hollow area (Chol-Org). Notably, the organoids derived from liver-resident progenitor cells contain epithelial cells only <sup>92</sup>.

They reported an average 40-fold cell expansion for organoids after 2 weeks culture in spinner flask, compared with 6-fold expansion in static cultures. Moreover, the organoids repopulated decellularized liver discs and formed liver-like tissue after transplantation in after xenotransplantation in mice. However, the culture media used for scale-up culture was also

supplemented with xenogeneic Matrigel ECM that will limit the use of this protocol in commercial production and clinical settings.

Another novel method to generate liver organoids has recently been reported including isolation of proliferative hepatocytes from human fetal livers by Percoll gradient centrifugation and embedding isolated cells into the Matrigel/growth factors supplemented culture medium. Hepatic organoids exhibit hepatoblast-like features (AFP+: alphafetoprotein+) and interestingly bile canalicular structure in 3D <sup>93</sup>.

Generally, using fetal or adult liver tissues as a source of isolating proliferating liver progenitors or hepatocytes offers the advantages of genomic stability of cells in organoids and higher efficiency in their differentiation. Moreover, it can offer higher safety profile for potential clinical application due to the lack of genetic manipulations during the process. Because the adult stem cells are already committed to differentiate into hepatocytes or cholangiocytes, shorter time is required to mature in culture. However, most of the protocols depends on using Matrigel in culture system as key component for organoid generation/expansion that is not compatible for GMP manufacturing of cell based therapeutic products. Moreover, generated organoids are mainly compatible for autologous application and allogeneic application will require creating a large bank of HLA matched bank of organoids for patients with different genetic background.

#### ***Generation of liver organoids/buds from human pluripotent stem cells***

hPSCs including hESCs and hiPSCs can be considered a unique and readily available source of cells for generation of liver organoids/buds due to their self-renewality, pluripotency differentiate into multiple lineages, and amenability for scale-up culture including expansion and integrated differentiation to hepatocytes and/or liver organoids <sup>18,89,94,95</sup>. Several studies reported generation of liver organoids/buds from hPSCs using different approaches that will be discussed further (Fig. I-9).

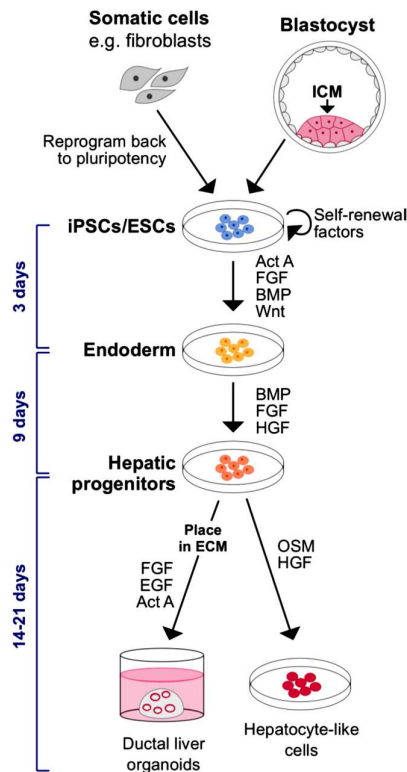


**Figure I-9. Liver organoids can also be generated from pluripotent stem cells (iPSCs and ESCs), usually by a three-stage differentiation process that recapitulates the signaling programs active during development.** iPSCs/ESCs are first directed towards an endodermal fate by exposure to Act A and Wnt. These endoderm cells then progress to a hepatic fate following induction of HGF and FGF signaling. These hepatic progenitors are hepatoblast-like cells. The hepatic progenitors can form hepatocyte-like cells in response to OSM signaling. Conversely, by placing the hepatic progenitors in ECM and modulating FGF, EGF and Act A signaling, ductal organoids can be generated. Act A, Activin A; BMP, bone morphogenetic protein; ECM, extracellular matrix; EGF, epidermal growth factor; ESCs, embryonic stem cells; FGF, fibroblast growth factor; FSK, forskolin; HGF, hepatocyte growth factor; ICM, inner cell mass; iPSCs, induced pluripotent stem cells; OSM, Oncostatin M; TGF $\beta$ i, transforming growth factor beta inhibitor; TNF $\alpha$ , tumor necrosis factor-alpha <sup>92</sup>.

### *Integrated differentiation of hPSCs*

Sgouda et. al. reported a scalable 3D suspension culture system for generation of liver organoids from hPSCs aggregates using integrated expansion and differentiation strategy. Generated liver organoids maintained for up to 3 weeks with stable gene expression profiles and metabolic features in a suspension culture system ranging from a 1.5 mL up to a 15 mL. Moreover, optimizing culture conditions has resulted in reproducible generation of homogenous size organoids with more hepatic functionality properties compared to hepatic PSC derivatives in 2D culture condition <sup>88</sup>. However, this study has not demonstrated any self-

organisation event or generating multiple liver cell types within generated organoids to meet organoids definition criteria.

### ***Engineered hPSCs for generating liver buds***

Guype et. al. developed a novel approach for generating and then co-differentiating hiPSC-derived progenitors employing a genetically engineered pulse of GATA-binding protein 6 (GATA6) expression during differentiation process <sup>89</sup>. Employing strategy resulted in rapid emergence of all three germ layers as a complex function of GATA6 expression levels and tissue context. A complex tissue recapitulates early developmental processes with liver bud-like phenotype, including haematopoietic and stromal cells as well as a neuronal niche obtained within 2 weeks of culture. Interestingly, this approach demonstrated a unique self-organisation event and derivation of complex tissues from hiPSCs using a single autologous hiPSCs as source and generated a range of stromal cells that co-develop with parenchymal cells to form tissues. This innovative approach provides a promising platform for generation of complex and functional liver organoids for potential therapeutic application. However, the protocol is suffering from necessity of genetic manipulation that is not preferable by regulatory authorities for clinical applications as well as necessity of a static seeding step of hPSCs that is limiting the scalability of protocol for large scale production of liver organoids.

### ***Vascularized liver bud generation from hPSCs***

Takebe group is pioneer in vascularised liver bud generation from hPSCs, they reported a novel method to generate liver buds from iPSCs by coculturing with vascular stem cells and mesenchymal stem cells by recapitulating the developmental stages of hepatogenesis <sup>20</sup>. They separately differentiated iPSCs into the endoderm, endothelial cells, and mesenchymal cells in 2D culture dish, followed by dissociation and co-culture with optimized ratio in a Matrigel drop. After 24-72 h of co-culture, the reconstituted cell mixture condensed and self-organized into spheres, which developed a liver bud-like structure with vascular network

inside. Gene expression profiles showed that liver buds gene expression is closer to human embryos than human iPSC-derived mature hepatocyte-like cells. Transplantation of the liver buds into different organs (liver, kidney, or brain) of immunodeficient mice resulted in fast integration (after 48h) to host and generation of multicellular liver organoids that were perfused by the host's blood because of its vascular structure and gained further hepatic maturation *in vivo*. Afterwards, the platform has been adapted for generation of organ buds from diverse tissues (e.g. brain, heart, kidney) and demonstrated the key role of mesenchymal stem cells for regulating self-condensation and organisation of buds from mixture of single cells <sup>96</sup>. Recently, same group scaled- up the liver bud generation protocol by developing an omni-well-array culture platform for mass producing homogeneous and miniaturized liver buds on a clinically relevant large scale ( $>10^8$ ) to translate the protocol for clinical application (Fig. I-10) <sup>21</sup>. This has been achieved by identifying three progenitor populations that could effectively generate liver buds in a highly reproducible manner: hepatic endoderm, endothelium, and septum mesenchyme.

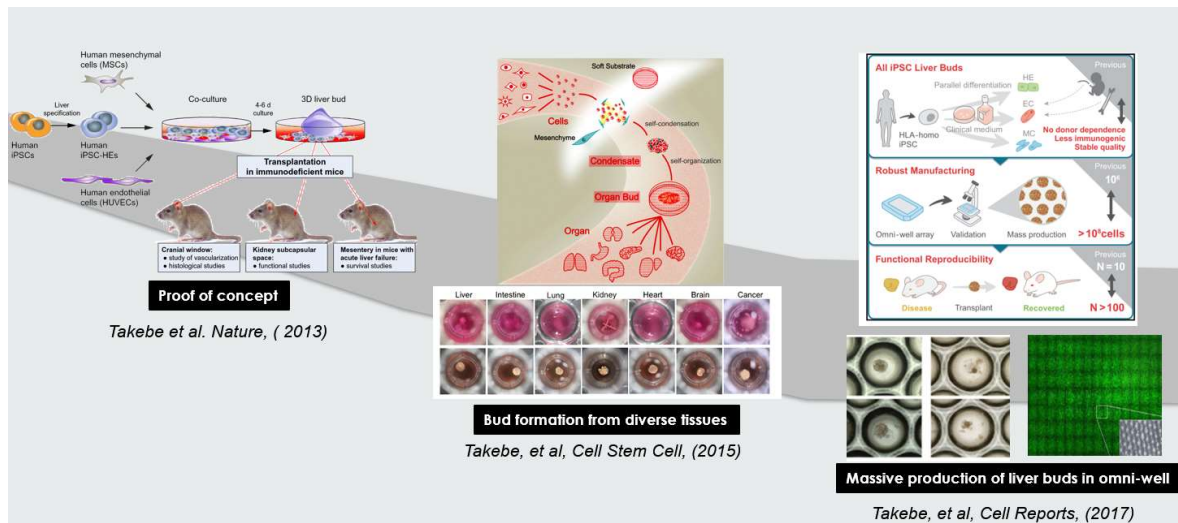


**Figure I-10. Progress in vascularized liver bud technology by Takebe group.**

However, the cell number that has been achieved by the established technology was enough for one pediatric patient that indicating the poor scalability of protocol. In another study, Ran-Ran Zhang and his colleagues cultured posterior gut endoderm cells (PGECs) derived from

hPSCs and co-cultured then with HUVEC and MSC to generate PGEC-LBs <sup>97</sup>. The immunohistochemistry showed positive detection of the CD31, CK19 and ALB, suggesting the mature function of human PGEC-LBs.

#### ***Co-culturing as a three-dimensional (3D) structure for generating liver buds and organoids***

3D organization of the cells is known to improve stem cells differentiation capacity and preserve their metabolic functions, compared to 2D cultures <sup>98</sup>. This strategy combined with co-culturing employed for development of different organoids including liver organoids. Mun et al. generated a self-renewal liver organoid based on human embryonic stem cells and induced pluripotent stem cells (PSCs) <sup>99</sup>. Co-culturing human induced pluripotent stem cells (hiPSCs) with Human Adipose Microvascular Endothelial Cells (HAMEC) using a 3D human embryoid bodies (hEBs) formation technology resulted in generation of fully functional and vascularised hepatocyte-like organoids with higher differentiation yield and notable improvements across a wide range of hepatic functions <sup>100</sup>. However, this strategy also suffering poor scalability due to employing static 3D hEBs formation technology.

#### ***Liver bud's generation from hMSCs***

In 2018, a study showed LBs was made up of single cell lineage. Jing Li et al. differentiated MSCs into three kinds of cells (hepatocytes, hepatic stellate cells (HSCs)-like cells, liver sinusoidal endothelial cells (LSECs) -like cells). And cocultured three kinds of cells with MSCs to generated functional MSCs-LBs after 72 h <sup>101</sup>.

#### ***Clinical application potential of liver organoids***

The liver organoid may prove to be an efficient strategy for hepatocellular transplantation because of its ability to stably proliferate. This proliferative ability will overcome the difficulty with current hepatocellular transplantation models, namely, the poor supply of human primary hepatocytes. The genomic stability of liver organoids derived from liver tissues will add the

benefit of safety.<sup>5</sup> Their superb scalability will make organoid-derived hepatocellular transplantation more feasible. CRISPR/Cas9 genome editing will also be possible to correct genetic mutations, and autologous organoid transplantation will be achievable. In addition, for liver organoids derived from iPSCs, because of their self-supporting ability (mesenchymal support and vascular integration), an ectopic organoid transplantation could become a better option as a “bridge” to liver transplantation. In transplant experiments in mice, it was proven that human iPSC-organoids were functional and sustainable relatively long term when implanted into the kidney capsules or the mesentery.<sup>19</sup> Transplanting liver organoids into the mesentery as a “second” liver to support a failing liver is an attractive approach. regarding the direct clinical application of organoid technology, there are many challenges. Malignant transformation of the stem cell-derived organoids is a major concern after transplantation, and extensive investigations in animal models are underway to address this concern. Another challenge is to determine the optimal method of organoid production. In the current methods of organoid culture, the use of bioengineered growth factors and extracellular matrix (Matrigel) is essential; these contain animal-derived materials (i.e., bovine serum). The carryover of these materials can contaminate the organoid products and may cause reactions in the human host. Also, the use of chemically undefined bioproducts (i.e., Matrigel) has a major negative impact on quality control; thus, further bioengineering is necessary to generate organoids via chemically defined methods.

### **Liver cells, hepatocyte like cells and stromal cells**

During the last ten years, cell therapy of liver has gained increasing attention due to advances in liver cells/ stem cells/ expandable progenitor cells isolation/ derivation and their directed/integrated differentiation from human pluripotent stem cells or adult/induced progenitor cells towards different cell lineages that mainly populated and exist in liver tissue such as hepatocytes <sup>12</sup>, macrophages <sup>102</sup>, and mesenchymal stem cells <sup>12</sup>. Hepatocytes,

macrophages and mesenchymal stem cells have been transplanted with varying degrees of success that will be described here. In the last two decades, a growing number of studies demonstrated that 3D cultures have several advantages over traditional two-dimensional (2D) cell cultures [110,111]. A physiologically 3D microenvironment is crucial to the development of *in vitro* tissue models, particularly for such complex tissues as the liver, in which the interaction between hepatocytes, hepatic stellate cells, and extracellular matrix (ECM) creates the microenvironment of the hepatic lobules <sup>103</sup>.

### ***Primary Hepatocytes***

Primary human hepatocytes that can be isolated from cadaveric livers for cell therapy applications and regenerate the liver tissue are main parenchymal and functional cell type in the liver tissue and make up 55-65% of the liver's mass. They can be considered as the chief functional units of liver that play a critical role in synthesis, metabolism, and detoxification processes. Thus, a critical mass of functioning hepatocytes is essential to meet the daily demands of homeostasis. This is ensured by unique inherent hepatic regenerative capacity, which enables replacement of lost hepatocytes through proliferation of healthy adult hepatocytes <sup>104</sup>. These cells can then move into the liver, replace damaged cells, and help support the organ after transplantation. The first primary hepatocyte transplantation in humans' dates to 1992 for the treatment of cirrhotic patients. However, the results of this first autologous transplantation were uncertain <sup>105</sup>. Later, cell therapy with primary hepatocytes as a treatment for CLDs has demonstrated promising results after splenic or portal vein infusions. It has been reported transplanting individual hepatocytes allows their rapid attachment to existing extracellular matrix *in vivo* and inducing modest reductions in ammonia levels and encephalopathy in both animal models and humans <sup>106</sup>. Since then, hepatocyte transplantation has been extended to other liver pathologies, including those induced by metabolic defects and demonstrated partial metabolic recovery, such as urea cycle disorder and Crigler–Najjar syndrome <sup>107</sup>, glycogen storage disease type 1a patient with partial

correction of metabolic abnormalities after transplantation that lasted beyond 9 months <sup>108</sup>, and hepatic failure induced by mushroom intoxication with Improvement in hepatic function results <sup>109</sup>.

However, primary hepatocytes transplantation facing critical issues for widespread clinical application including; 1) difficulty of isolating a sufficient quantity of high-quality and metabolically active cells and maintain their quantity and quality before transplantation, 2) High sensitivity of these cells to freeze-thaw process and losing viability and engraftment after cryopreservation and reviving, 3) loss of proliferative ability when cultured in vitro, and 4) shortage of their supply for widespread clinical application <sup>110</sup>, Thus, developing innovative technologies that can expand and maintain primary hepatocytes under in vitro culture condition is in progress such as generation of expandable progenitor population from these cells and then further differentiation to mature hepatocytes or cholangiocytes, generation of hepatocyte-like cells from human pluripotent stem cells, and exploring alternative sources of cells for liver cell therapy like mesenchymal stem cells .

### ***Expandable liver progenitor cells***

Recent studies proposed that hepatocytes are a source of expandable hepatic cells and isolated/generated expandable hepatic progenitor population from liver tissue or primary hepatocytes (Fig I-11). In 2008, Utoh et al. identified a small population (0.01–0.09% depending on donor age) of replicative hepatocytes, termed colony-forming parenchymal hepatocytes (CFPHs), in long-term cultures of human adult hepatocytes. When CFPHs were transplanted into uPA/SCID mice, they engrafted into the liver and grew for at least 10 weeks with maximum 27% repopulation rate that indicate their slow proliferation and re-populative capacity <sup>111</sup>. Another study generated more proliferative and functional cells called human chemically derived hepatic progenitors (hCdHs) from adult hepatocytes using HGF, A83-01 and CHIR99021 for chemical reprogramming. hCdHs proliferated for at least 10 passages without losing differentiation potential in vitro and engrafted and repopulated about 20% of the

diseased parenchyma within 3 weeks after transplantation into Alb-TRECK/SCID mice <sup>112</sup>. Fu et al. also developed a transition and expansion medium (EM), which can be used to convert human hepatocytes into hepatocyte-derived liver progenitor-like cells (HepLPCs) in vitro [16, 42]. When HepLPC-derived hepatocytes (HepLPC-Heps) were transplanted into F/R mice, human ALB-positive cells covered 7.2–16.1% of the liver parenchyma in surviving mice. Using a similar method, Zhang et al. generated proliferating human hepatocytes (ProlIHs) in human liver isolation medium containing the same supplements as EM and lacked R-spondin1, Noggin, and forskolin, and introduced Wnt3a as the key factor for generation of these cells. Following transplantation of ProlIHs, 11 of 14 FRG mice survived for more than 4 months, whereas all FRG mice not transplanted with hepatocytes died within 4 months. Interestingly, ProlIHs expressed phase I and II enzymes and transporters at levels comparable with those in primary human hepatocytes after transplantation (Fig I-12) <sup>113</sup>. While these studies reported relatively promising results in animal studies, potential clinical use of these cells need more extensive research including scale up trials for demonstrating their stability and then testing in larger animal models.

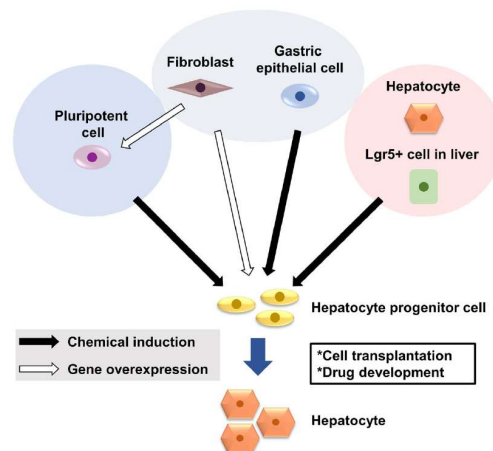


**Figure I-11. Approaches to generate hepatocyte progenitors in vitro.** Current approaches to generate in vitro-expandable hepatocytes include differentiation of human pluripotent stem cells, reprogramming of fibroblasts and cells of a similar developmental origin, identification of liver progenitor cells, and reprogramming of mature hepatocytes. In vitro-expandable hepatocytes are required as a therapeutic alternative to liver transplantation and for drug development <sup>94</sup>.

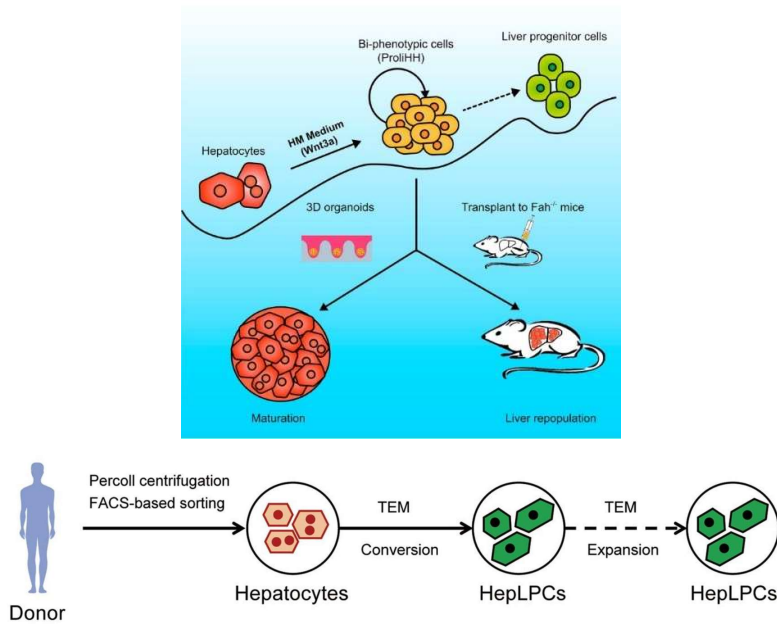


**Figure I-12. Generation of ProlIHs liver progenitor cells that can mature following in vitro differentiation or transplantation** <sup>113</sup>, an overview of the protocol used for generation of human hepatocytes-derived liver progenitor-like cells (HepLPCs) in vitro <sup>114</sup>.

***Hepatocyte-like cells derived from human Pluripotent Stem Cells***

As mentioned before, another highly promising cell types as alternative to primary hepatocytes are human hepatocyte-like cells (HLCs) derived from human pluripotent stem cells including human embryonic and induced pluripotent stem cells. These cells promise a valuable source of cells with human genetic background, physiologically relevant liver functions, and unlimited supply due to hPSCs amenability for scale-up culture including expansion and integrated differentiation to hepatocytes <sup>18,94</sup>. With over 12 years' efforts in this field of pluripotent stem cells technology, great achievements have been made including generation of HLCs that have been successfully derived and applied in disease modeling, toxicity testing and drug discovery (Fig I-13) <sup>115</sup>.

To date, several studies have established protocols for differentiation of ESCs into hepatocyte-like cells that express key hepatocyte-related genes and mimic some liver metabolic functions <sup>116-119</sup>. ESC-derived hepatocytes also have the typical morphology of mature hepatocytes and are able to colonize liver tissue after transplantation, promoting the injured liver's recovery via

cell replacement and stimulating endogenous regeneration <sup>119,120</sup>. Despite these promising results and the favorable characteristics of human ESCs, such as a good resistance to cryopreservation, practical and ethical barriers have always precluded their application in clinical practice.

The discovery made by Gurdon and Yamanaka that somatic cells from health individuals and patients can be reprogrammed to iPSCs has opened up the possibility to generate pluripotent stem cells from mature cells as well as patients for offering personalized medicine, disease modeling, and drug discovery <sup>121</sup>.

Therefore, human induced pluripotent stem cells (iPSCs) have emerged as a way of bypassing the ethical concerns associated with the use of ESCs and generating therapeutic derivatives for potential clinical applications. The iPSCs are mainly derived by reprogramming mature somatic cells induced by different transcription factors and their self-renewal and pluripotency properties make them as viable alternative for ESCs to generate different cell lineages including hepatocyte like cells <sup>122,123</sup>.

Protocols established to generate HLCs from human ESCs and human iPSCs are basically mimic the developmental pathway of the liver during embryogenesis and have vastly improved in recent years <sup>124</sup>. Nevertheless, there are several issues regarding the safety and reproducibility of iPSCs that still need to be addressed before their potential use for clinical application, including tumorigenicity and teratoma formation, the debate on their immunogenicity, long-term safety and efficacy, and the safe reprogramming techniques <sup>122,125,126</sup>.

Nonetheless, significant progress is being made in developing robust, safe and non-viral or integration-free reprogramming technologies (e.g. Small molecule based approach) to address translational challenged of iPSCs technology <sup>127</sup>.

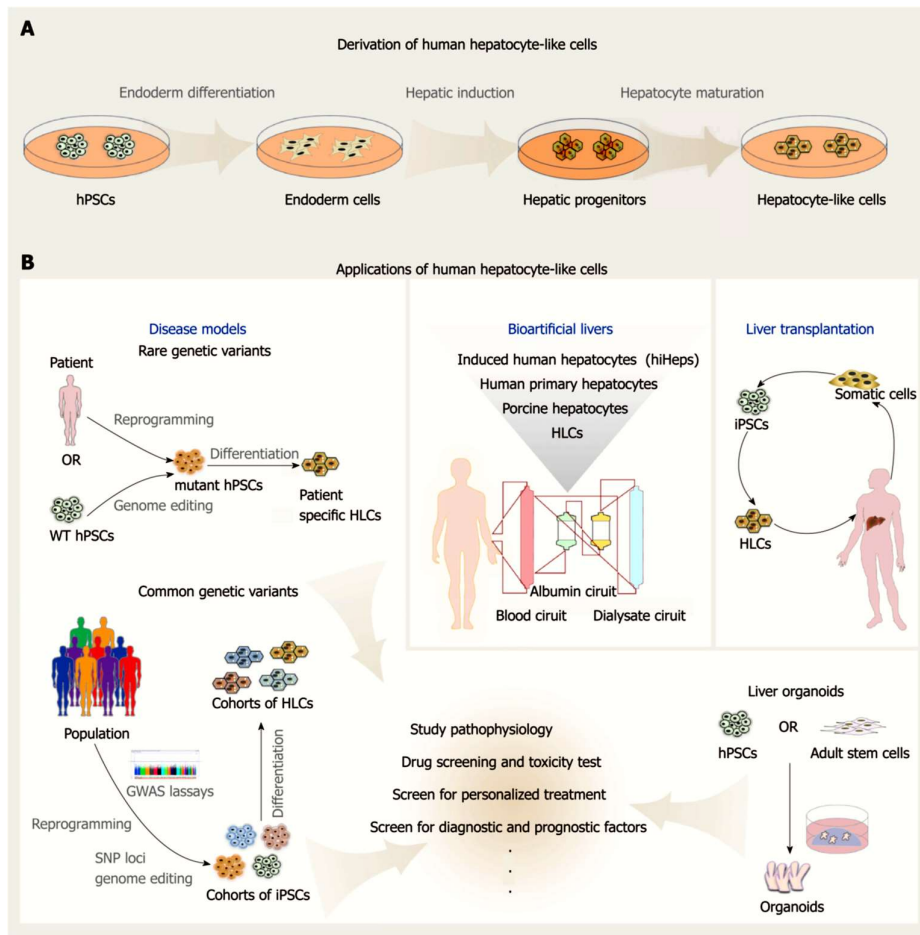


**Figure I-13. Derivation and applications of human hepatocyte-like cells.** A: Directed differentiation process of human pluripotent stem cells (hPSCs)-derived hepatocyte-like cells (HLCs) in vitro includes endoderm development, endoderm hepatic specification, and hepatic maturation stages; B: Applications of human HLCs. HPSC-derived HLCs can be used to generate disease models to study rare or common genetic variants. These cellular models can be applied in pathophysiological research, drug screening, and toxicity testing. Cohorts of HLCs provide in vitro cell models for genome-wide association studies and potentially pharmacogenomics in dishes. HLCs also offer a potential cell source for bioartificial livers or liver transplantation. HLCs: Hepatocyte-like cells; hPSCs: Human pluripotent stem cells <sup>115</sup>.

Despite the promising insight of hepatocyte derived from hPSCs and several reports claimed generation of functional hepatocytes from these stem cell, hepatocytes derived from stem cells often have incomplete function and mainly exhibit characteristics of fetal liver cells rather than mature hepatocytes. Thus, they are generally defined as hepatocyte-like cells (HLCs) <sup>128-130</sup>. On the other hand, most of studied generated HLCs in small and static culture system (e.g. culture dishes and multi-well plates) that are suffering from limited scalability and not

amenable for large scale production of cells as an essential prerequisite for conducting clinical trials and then commercial production (e.g. up to  $10^8$  cells produced using high-throughput micro-well culture system per batch which may be only enough for treating one pediatric patient) <sup>21,131</sup>. Therefore, one of the main and current bottleneck and technical issue in translating these technologies for clinical application is their limited scalability for production of sufficient therapeutic doses of hepatocytes cells for one adult patient ( $1-2 \times 10^9$  cells per patient) or few hundred billion cells for allogeneic liver cell therapy <sup>132</sup>.

To date, a limited number of protocols and reports published that aimed to develop scalable and integrated production process for generation of hepatocytes/liver organoids from hPSCs, but these methods suffer from critical technical challenges including scalability that preclude their potential use in clinical or commercial applications<sup>95,133,134</sup>. For instance, most of these studies have been performed under uncontrolled culture conditions in limited culture working volumes (1.5-50 ml) or used static cultures for generation of hepatocytes which offer poor scalability for commercial scale production <sup>95</sup>. Moreover, some other very important issues still need be addressed such as quality issues including low differentiation efficacy and functionality of hepatocytes (i.e., poor gene expression profiles and metabolic characteristics) compared to primary hepatocytes, as the most important quality criteria and also productivity issues such as cell yield, product homogeneity, and process reproducibility <sup>133</sup>. Thus, development of a robust, GMP (good manufacturing practice) compatible culture system and bioprocess for large scale production of human functional hepatocytes and hepatic organoids is a necessary step that should be taken before the clinical translation of currently developed regenerative medicine technologies.

### ***Macrophages***

It has been well-demonstrated that hepatic macrophages can reverse fibrosis process as the main regulator of dynamic fibrogenesis-fibrosis resolution paradigm [55,56]. It has been also suggested that the regulatory effect of macrophages in liver fibrosis is associated with balance

of profibrotic and restorative macrophages [57]. Therefore, A better understanding of the mechanisms controlling this process could yield novel monocyte/macrophage-based cell and regenerative therapies.

Monocytic populations can be produced via autologous propagation or derivation from human pluripotent stem cells. However, the technology is not still mature and monocyte/macrophage-based approach to damping liver fibrosis has already been attempted in animal models. For instance, intraportal administration of differentiated BM-derived macrophages (BMMs) improved liver fibrosis, regeneration, and function via a wide range of reparative pathways, with a therapeutic benefit. On the other hand, liver fibrosis was not significantly affected by the infusion of macrophage precursors, and it was interestingly even exacerbated by whole BM cells <sup>135</sup>. In another recent study, combination therapy using mesenchymal stem cells and colony-stimulating factor-1-induced bone marrow-derived macrophages (id-BMMs) reduced liver fibrosis (associated with increased matrix metalloproteinases expression), increased hepatocyte proliferation (associated with increased hepatocyte growth factor, vascular endothelial growth factor, and Oncostatin M in the liver), and reduced blood levels of liver enzymes, more effectively than MSCs or id-BMMs monotherapy in mice with CCl<sub>4</sub>-induced cirrhosis <sup>135</sup>. Therefore, macrophages can induce whole-organ changes and encouraging a translational perspective and suggesting a future clinical potential.

#### ***Adult Stem Cells and MSC-derived hepatocytes***

Adult Stem cells such as mesenchymal stem cells are also considered as an valid alternative sources for the treatment of liver diseases <sup>136</sup>. It has been suggested that the main function of these cells is modulating the liver's regenerative processes to reduce scarring in cirrhosis, and to down-regulate immune-mediated liver damage. Adult stem cells could also be differentiated into hepatocytes for cell therapy application <sup>136,137</sup>. Different types of adult stem cells have been tested over the years, including hematopoietic stem cells (HSCs), mesenchymal stem cells (MSCs), endothelial progenitor cells (EPCs), and hepatic progenitor

cells (HPCs) <sup>138-140</sup>. HSCs are populated in bone marrow and express the surface marker CD34. HSCs can easily be isolated in the bloodstream and differentiated to generate hepatocyte like cells. It has been demonstrated that hepatocyte-like cells derived from HSCs can support liver regeneration through novo-generation of hepatocytes via transdifferentiation or the genetic reprogramming of resident hepatocytes through cell fusion, as well as stimulating regeneration <sup>140-144</sup>.

Endothelial progenitor cells (EPCs) are another candidates for liver cell therapy that can be found in both peripheral blood vessels and bone marrow, and their main function is promoting neovascularization in damaged tissues. However, animal study in Rat model of fibrosis demonstrated that the transplantation of EPCs into fibrotic liver or in combination with hepatocyte stem cells led to a lessening of tissue fibrosis <sup>145,146</sup>. Promoting hepatocyte proliferation and increase matrix metalloproteinase activity through increased secretion of specific growth factors are other potential benefits of EPCs transplantation <sup>147</sup>.

It has been also demonstrated that mesenchymal stem cells (MSCs) that can be found in different tissues (e.g. bone marrow, adipose tissue, placenta, amniotic fluid, umbilical cord blood, and umbilical cord) can repair acute liver injury when systematically administered <sup>51,148</sup>. Different studies demonstrated that MSCs have the capacity to provide both metabolic and trophic support due to their potential for hepatocytic differentiation, and their secretion of anti-inflammatory, anti-apoptotic, immunomodulatory, and pro-proliferative factors <sup>148,149</sup>. This leads to liver function being restored via the repair of damaged tissue, the suppression of inflammation, and the stimulation of endogenous regeneration through paracrine effects <sup>150</sup>. Finally, isolating hepatic progenitors' cells from liver and their efficient expansion have gained increasingly attention for liver cell-based therapy to regenerate the liver during chronic diseases. Several protocols have been established for isolating HPCs and bipotent stem cells from the human liver or biliary tree <sup>87,151</sup>. Due to the low number of these progenitor cells in the liver, the use of autologous HPCs is probably unfeasible and establishing efficient protocol for their expansion is more likely feasible <sup>76</sup>. Though this approach also raises questions

regarding the engraftment rate of transplanted cells, their proper differentiation in vivo, and the need for immunosuppressant therapy. Despite the promising view of such approaches, acquiring a deep understanding of HPCs nature, their precise role in liver pathophysiology, and how the entire process of regeneration/differentiation is regulated is essential. Given the possible disadvantages of HPC activation, which might exacerbate disease progression or prompt the onset of cancer <sup>152</sup>, addressing all these issues and translating the technology for clinical application need further study and careful examination of cells and their mechanism of action under in vivo condition.

### **Comparing the translational potential of therapeutic components and established platforms for treating liver cirrhosis and their widespread clinical application**

In previous sections currently established technologies with promising potential for treating liver cirrhosis and liver regenerative medicine described. Liver-assistive devices and whole liver bioengineering technologies have witnessed significant progress but still suffering from critical efficacy and technical challenges that hindered their use for widespread clinical application. For instance, liver-assistive devices and external supports are highly complex and costly devices that showed poor efficacy in most trials for patients suffering from acute liver failure to induce their liver inherent regeneration capacity or bridging them to receive a transplant. Donor tissue variability, shortage of cadaveric liver, undefined matrix composition, tricky recellularization process, and low functionality of bioengineered whole-liver organ is also important issue that still need extensive research to offer viable solutions. Liver patches and tissue constructs that fabricated by bioprinting or patterning technology are also demonstrated promising results in animal studies but most of established protocols employed fabrication techniques are not scalable for large scale manufacturing and implantation of constructs need invasive transplantation and open surgery. Therefore, liver cell therapy and liver organoids transplantation can be considered as most promising technology for liver regenerative

medicine. However, currently established protocols for hepatocyte-like cells and expandable hepatocytes mainly resulted in generation of cells with significantly lower functionality and metabolic activity compared to primary hepatocytes and adult liver tissue. On the other hand, liver organoids/buds with complex structure such as vascular network and self-organized structure are gained increasingly attention as therapeutic component since they provide a native liver tissue like structure and recapitulating hepatic functions in tiny scale. Moreover, they are expandable and can be transplanted with non-invasive methods for clinical applications. A comparison of currently available RM technologies base on their translational aspects to meet widespread clinical applications indicating that vascularised liver bud/organoids production from readily available cell source; hPSCs is a highly promising platform for liver regenerative medicine due to fast integration to host for functionalization, significant in vivo maturation, and recapitulating key liver metabolic functions (Table I-1).

However, generation of complex, functional, and vascularized liver organoids/buds has been done under static culture conditions (mainly multi-well and array multi-well plates) that offer poor scalability for mass production or used xenogeneic ECM components for bud formation or organisation, lacking biliary structure/bile metabolism and mainly require using Matrigel as ECM which is not compatible with GMP requirements of therapeutic products manufacturing for human use <sup>20,21</sup>. Thus, developing scalable and robust generation of complex, functional, and vascularized liver organoids for therapeutic applications may provide a valuable platform for liver cirrhosis organoid medicine.

Table I-1. Comparing translational aspects of different regenerative medicine technologies for treating acute liver failure

Platform	Options	Fabrication technique	Cell ingredients	In vitro Functionality / In vivo maturation	Complex/vascularized structure	Cell ingredients production scalability	Defined culture condition	Production process scalability	GMP compatibility of process	Translational potential for allogeneic application
Whole liver bioengineering		Whole organ decellularization/r ecellularization	Hepatic progenitors, endothelial progenitors, parenchymal cells	Poor	+	-	-	-	-	-
Liver tissue constructs: Expandable liver tissue		Bioprinting	Human primary hepatocytes/ Fibroblasts/ Endothelial cells	Good	+	-	-	-	+	-
Liver organoids/buds	Genome-Stable Bipotent Stem Cells derived organoids	Static culture in Matrigel	Liver organoids raised from adult liver tissue biopsy and differentiated to hepatocytes	Good	-	+	-	-	-	-
	hPSCs derived liver organoids	Intergated expansion and differentiation as 3D aggregates	hPSCs	Poor	-	+	+	-	+	+
	liver bud-like tissue generation using GATA6 over expression	Genetic engineering	hiPSCs	Good	+	+	+	-	-	+
	Liver buds generation by mesenchymal stem cells driven self-condensation	Co-culture in Multi-well- Omniwell tech.	hiPSCs/Mesenchymal stem cells/ Endothelial cells	Good	+	+	+	-	+	+
Cell therapy by primary hepatocytes, hepatocyte like cells, hMSCs		Encapsulation in decellularized matrix	hPSCs, liver progenitors, expandable heaptocytes, hMSCs	Good	-	+	+	+	-	+

## **Current challenges in scalable generation and clinical application of vascularized liver buds/organoids**

There are some critical challenges in translating vascularized liver bud's production platform for clinical application that can be generally categorized as technical, functionality, and transplantation challenges highlighted as below:

### **Production scalability issue**

Current platforms for production of vascularized liver buds and organoid depends on co-culture of different cell types such as hepatic progenitors, endothelial cells, and mesenchymal stem cells in 3D culture condition mainly using animal-derived ECM such as Matrigel in a multi-step process. Multi-well plates <sup>20</sup>, micro-well arrays <sup>100</sup>, or (omni)-well-array plates are the most culture systems that were used to generate liver buds/organoids under static culture condition that are offering very good control over the co-culture condition, aggregate size control and self-organization/condensation process but very poor scalability for large scale production of organoids. In addition, using xenogeneic/undefined ECM and culture condition combined with labor-intensive multistep process nature of existing approaches will result in significant variability and low throughput of organoids production.

Other scalability issue is poor scalability of established protocols for required starting cell ingredients production for liver organoid production. In fact, large scale production of organoids would essentially require scalable production of starting cell materials before co-culturing or fabricating organoids. However, most of current protocols for liver organoid generation have employed cell ingredients that generated under static culture condition after extensive optimization of differentiation process in petri dishes or flasks that are not amenable for scalable manufacturing <sup>21</sup>. Moreover, adapting protocols in static culture condition to dynamic culture condition can result in generation of cells exhibiting different fate and functionality and subsequently organoid generation efficacy.

### **Organoids functionality issue**

Although several strategies are available to generate hepatic micro-tissues, buds, and organoids with demonstrated fetal to mature like hepatic functionality, few studies have succeeded in generating a liver organoid with hepatobiliary structure (hepatobiliary organoids) and efficient bile metabolism from hPSCs or liver tissue<sup>153,154</sup>. Bile metabolism and bile ducts structures are essential for normal liver function and preferably should exist in in vitro generated organoids for transplantation. However, these studies have been done in very small scale and static culture conditions which hindered their use for clinical application.

### **Challenges in transplanting liver organoids**

To date, most of the liver organoids transplant in mice for in vivo integration and functionality studies but not to develop an effective transplantation strategy<sup>82</sup>. It was proven that human iPSC-organoids were functional and sustainable relatively long term when implanted into the kidney capsules or the mesentery<sup>20</sup>. Generally, mesentery can be considered as an attractive option for transplanting organoids as “second” liver to support a failing liver. However, direct clinical application of organoid technology faces multiple challenges including potential malignant transformation of the hPSCs derived organoids that is under extensive investigations in animal models are underway to address this concern. Another issue is few hundred to 1 mm scale of organoids diameter size and their size and structure heterogeneity that will make their injection and in vivo integration difficult. Thus, developing a robust process for homogenous organoids generation and an effective transplantation strategy would largely facilitate the future organoid medicine technology.

### **Scalable techniques for generation of liver bud's/organoids**

Nowadays, significant progress in biomaterials development and microfabrication technologies have offered great opportunities and paved the way to recreate 3D tissue/organ models and complex organoids with more physiological relevance in a controllable manner.

Natural <sup>155</sup>, defined <sup>156</sup>, or combinatorial/composite hydrogels <sup>157</sup> as 3D soft scaffolds has been used in several studies to create biomimetic matrices, 3D microenvironments or porous scaffolds, and tissue constructs using different fabrication techniques (e.g. simple substrate coating and advance ones such as micro-molding, 3D bioprinting, photolithography, stereolithography, patterning, and microfluidics) for tissue constructs or organoid formation to reduce their variability. However, most of these technologies are suitable for generation tissue constructs and require extensive lab work that offering poor scalability for large scale production of microscale organoids. Thus, robust scalable production of complex liver buds/organoids remained challenging.

One viable alternative is using core shell hydrogel micro capsules as 3D microenvironment for organoids generation and their scalable and continuous production using electro spray/jetting systems <sup>158</sup> or microfluidic technology <sup>159</sup>. Practically, hydrogel capsules with solid shell and liquid core can be used for loading stem cells or co-culturing different cell types for organoid formation instead of individual wells in micro-wells or array-well plates due to their uniform and tunable morphology, customizable permeability, and the ability in scale-up production <sup>160,161</sup>. Several studies have used core shell hydrogel systems for controlled generation of embryonic bodies <sup>162</sup>, generation of hepatospheres from primary hepatocytes <sup>159</sup> and intestinal or pancreatic organoids <sup>163,164</sup> using elector-spray or microfluidic technology. The microfluidic generation of core shell capsules can be considered as viable choice over electrospray systems because of high reproducibility, consistency, and control over capsules generation and capable of generating wide range of capsules diameter 100-1000  $\mu\text{m}$  which are considered as bottleneck in elector spray systems that are limited to generate capsules with min. 300 $\mu\text{m}$  diameter <sup>165</sup>. However, these studies have been done in small scale for generation of simple organoids or different type spheres using typical microfluidic equipment's but not as platform for scalable and continuous generation of complex and vascularized organoids such as vascularized liver buds or organoids.

## **Aim of Study and Thesis Outline**

In this project, we are going to address two important challenges in translating two most promising liver organoid generation technologies from hPSCs for therapeutic application including scalable generation of functional complex organoids by integrated differentiation process as the first convenient approach, secondly the scalable platform for xeno-free generation of vascularized complex buds/organoids including large scale production of the required starting cell material, and developing an innovative transplantation strategy for delivering organoids will be explored. Accordingly, key bioprocess parameters will be optimized in integrated differentiation of hPSCs toward liver organoids in stirred suspension bioreactor to generate functional liver organoids.

In the next step, we tried to develop a fully scalable and continuous process for generation of functional vascularized liver organoids from hPSCs based on liver bud generation concept by co-culturing and self-organization technique. Two strategies will be explored including co-seeding cells in dynamic suspension culture condition and then co-culturing in core shell capsules by one-step fabrication of dissolvable liquid core and shell capsules using a novel and scalable microfluidic technology that is adaptable for GMP manufacturing. The first phase of co-culture approach study involve developing a robust and fully scalable protocols for large scale production of starting cell ingredients from hPSCs that required for generation of vascularized liver organoids including hepatic progenitors to generate functional hepatocytes, endothelial progenitors for creating vascular structure and improve hepatocytes maturation, and mesenchymal stromal cells for promoting self-condensation and organization under ECM-free dynamic suspension culture . The next phase of the project is developing a scalable and GMP compatible platform for large scale production of vascularized liver organoids and subsequently developing innovative transplantation strategy (Fig 1.13).

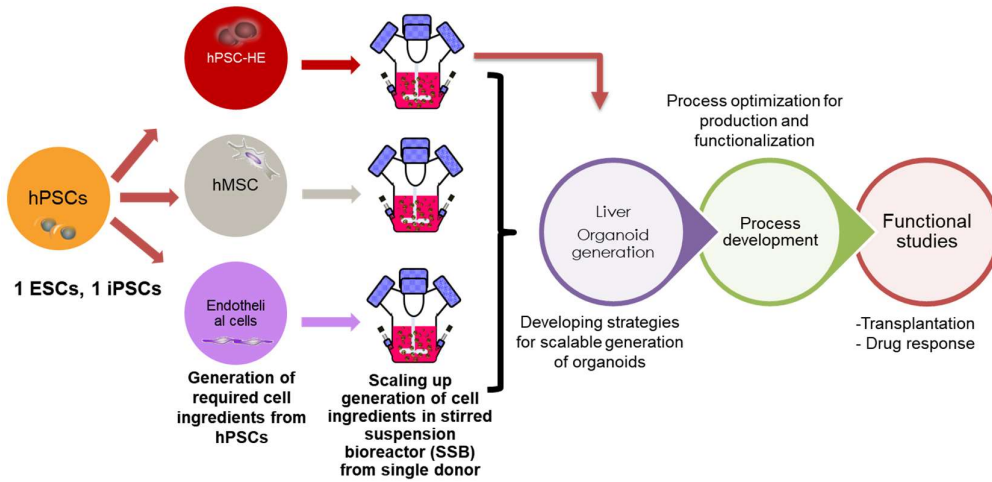


Fig I-13. Thesis project outline for scalable generation of vascularized liver organoids.

## References

- 1 Kuntz, E. Biochemistry and functions of the liver. *Hepatology Principles and Practice: History Morphology Biochemistry Diagnostics Clinic Therapy*, 31-71 (2006).
- 2 Weissman, I. L. Stem cells: units of development, units of regeneration, and units in evolution. *cell* 100, 157-168 (2000).
- 3 Nusrat, S., Khan, M. S., Fazili, J. et al. Cirrhosis and its complications: evidence based treatment. *World Journal of Gastroenterology: WJG* 20, 5442 (2014).
- 4 Shashidhar, K. & Nallagangula, K. S. Pros and Cons of Existing Biomarkers for Cirrhosis of Liver. *Acta Scientific Medical Sciences* 3, 63-72 (2019).
- 5 Hope, A. A. & Morrison, R. S. in *Evidence-Based Practice of Palliative Medicine* 300-307 (Elsevier Inc., 2012).
- 6 Hernaez, R., Solà, E., Moreau, R. et al. Acute-on-chronic liver failure: an update. *Gut* 66, 541-553, doi:10.1136/gutjnl-2016-312670 (2017).
- 7 Nayak, N. C., Jain, D., Vasdev, N. et al. Etiologic types of end-stage chronic liver disease in adults: analysis of prevalence and their temporal changes from a study on native liver explants. *European journal of gastroenterology & hepatology* 24, 1199-1208 (2012).
- 8 Moon, A. M., Singal, A. G. & Tapper, E. B. Contemporary epidemiology of chronic liver disease and cirrhosis. *Clinical Gastroenterology and Hepatology* (2019).
- 9 Tapper, E. B. & Parikh, N. D. Mortality due to cirrhosis and liver cancer in the United States, 1999-2016: observational study. *BMJ* 362, k2817, doi:10.1136/bmj.k2817 (2018).
- 10 Estes, C., Razavi, H., Loomba, R. et al. Modeling the epidemic of nonalcoholic fatty liver disease demonstrates an exponential increase in burden of disease. *Hepatology* 67, 123-133 (2018).
- 11 Marcellin, P. & Kutala, B. K. Liver diseases: A major, neglected global public health problem requiring urgent actions and large-scale screening. *Liver International* 38, 2-6 (2018).
- 12 Jadowiec, C. C. & Taner, T. Liver transplantation: current status and challenges. *World journal of gastroenterology* 22, 4438 (2016).
- 13 Dutkowski, P., Linecker, M., DeOliveira, M. L. et al. Challenges to liver transplantation and strategies to improve outcomes. *Gastroenterology* 148, 307-323, doi:10.1053/j.gastro.2014.08.045 (2015).
- 14 Shukla, A., Vadeyar, H., Rela, M. et al. Liver Transplantation: East versus West. *J Clin Exp Hepatol* 3, 243-253, doi:10.1016/j.jceh.2013.08.004 (2013).
- 15 Tayyeb, A., Azam, F., Nisar, R. et al. Regenerative medicine in liver cirrhosis: promises and pitfalls. *Liver Cirrhosis-Update and Current Challenges*, 236-256 (2017).
- 16 Yamamoto, J., Udono, M., Miura, S. et al. Cell Aggregation Culture Induces Functional Differentiation of Induced Hepatocyte-like Cells through Activation of Hippo Signaling. *Cell Rep* 25, 183-198, doi:10.1016/j.celrep.2018.09.010 (2018).
- 17 Thompson, J., Jones, N., Al-Khafaji, A. et al. Extracorporeal cellular therapy (ELAD) in severe alcoholic hepatitis: a multinational, prospective, controlled, randomized trial. *Liver Transplantation* 24, 380-393 (2018).
- 18 Farzaneh, Z., Najarasl, M., Abbasalizadeh, S. et al. Developing a cost-effective and scalable production of human hepatic competent endoderm from size-controlled pluripotent stem cell aggregates. *Stem cells and development* 27, 262-274 (2018).
- 19 Pla-Palac n, I., Sainz-Arnal, P., Morini, S. et al. Liver Bioengineering Using Decellularized Whole-Liver Scaffolds. (2017).
- 20 Takebe, T., Sekine, K., Enomura, M. et al. Vascularized and functional human liver from an iPSC-derived organ bud transplant. *Nature* 499, 481-484 (2013).
- 21 Takebe, T., Sekine, K., Kimura, M. et al. Massive and Reproducible Production of Liver Buds Entirely from Human Pluripotent Stem Cells. *Cell reports* 21, 2661-2670 (2017).

- 22 Stevens, K. R., Scull, M. A., Ramanan, V. et al. In situ expansion of engineered human liver tissue in a mouse model of chronic liver disease. *Science Translational Medicine* 9, eaah5505 (2017).
- 23 Mardpour, S., Hassani, S. N., Mardpour, S. et al. Extracellular vesicles derived from human embryonic stem cell-MSCs ameliorate cirrhosis in thioacetamide-induced chronic liver injury. *Journal of cellular physiology* 233, 9330-9344 (2018).
- 24 Sussman, N. L. & Kelly, J. H. Extracorporeal liver support: cell-based therapy for the failing liver. *American journal of kidney diseases* 30, S66-S71 (1997).
- 25 Mullon, C. & Pitkin, Z. The HepatAssist® Bioartificial Liver Support System: clinical study and pig hepatocyte process. *Expert opinion on investigational drugs* 8, 229-235 (1999).
- 26 Patzer, J. F., Mazariegos, G. V., Lopez, R. et al. Novel bioartificial liver support system: preclinical evaluation. *Annals of the New York Academy of Sciences* 875, 340-352 (1999).
- 27 Nibourg, G. A., Chamuleau, R. A., Van der Hoeven, T. V. et al. Liver progenitor cell line HepaRG differentiated in a bioartificial liver effectively supplies liver support to rats with acute liver failure. *PloS one* 7 (2012).
- 28 Sauer, I. M. & Gerlach, J. C. Modular extracorporeal liver support. *Artificial organs* 26, 703-706 (2002).
- 29 Patel, P. & Pysopoulos, N. T. in *Liver Diseases* 721-726 (Springer, 2020).
- 30 Fisher, C. & Wendon, J. in *Critical Care Nephrology* 793-799. e792 (Elsevier, 2019).
- 31 Chen, F.-M. & Liu, X. Advancing biomaterials of human origin for tissue engineering. *Progress in polymer science* 53, 86-168 (2016).
- 32 Maghsoudlou, P., Georgiades, F., Smith, H. et al. Optimization of liver decellularization maintains extracellular matrix micro-architecture and composition predisposing to effective cell seeding. *PloS one* 11 (2016).
- 33 Andrews, E. Damage of porcine aortic valve tissue caused by the surfactant sodiumdodecylsulphate. *The Thoracic and cardiovascular surgeon* 34, 340-341 (1986).
- 34 Ott, H. C., Matthiesen, T. S., Goh, S.-K. et al. Perfusion-decellularized matrix: using nature's platform to engineer a bioartificial heart. *Nature medicine* 14, 213-221 (2008).
- 35 Rajabi, S., Pahlavan, S., Ashtiani, M. K. et al. Human embryonic stem cell-derived cardiovascular progenitor cells efficiently colonize in bFGF-tethered natural matrix to construct contracting humanized rat hearts. *Biomaterials* 154, 99-112 (2018).
- 36 He, M. Tissue engineering of the kidney using a whole organ decellularisation approach. (2014).
- 37 Stabler, C. T., Lecht, S., Mondrinos, M. J. et al. Revascularization of decellularized lung scaffolds: principles and progress. *American Journal of Physiology-Lung Cellular and Molecular Physiology* 309, L1273-L1285 (2015).
- 38 Mazza, G., Rombouts, K., Hall, A. R. et al. Decellularized human liver as a natural 3D-scaffold for liver bioengineering and transplantation. *Scientific reports* 5, 13079 (2015).
- 39 Uygun, B. E., Soto-Gutierrez, A., Yagi, H. et al. Organ reengineering through development of a transplantable recellularized liver graft using decellularized liver matrix. *Nature medicine* 16, 814-820 (2010).
- 40 Rossi, E. A., Quintanilha, L. F., Nonaka, C. K. V. et al. Advances in hepatic tissue bioengineering with decellularized liver Bioscaffold. *Stem cells international* 2019 (2019).
- 41 Shaheen, M. F., Joo, D. J., Ross, J. J. et al. Sustained perfusion of revascularized bioengineered livers heterotopically transplanted into immunosuppressed pigs. *Nature biomedical engineering*, 1-9 (2019).
- 42 Barakat, O., Abbasi, S., Rodriguez, G. et al. Use of decellularized porcine liver for engineering humanized liver organ. *Journal of Surgical Research* 173, e11-e25 (2012).
- 43 Verstegen, M. M., Willemse, J., Van Den Hoek, S. et al. Decellularization of whole human liver grafts using controlled perfusion for transplantable organ bioscaffolds. *Stem cells and development* 26, 1304-1315 (2017).

- 44 Mattei, G., Magliaro, C., Pirone, A. et al. Decellularized human liver is too heterogeneous for designing a generic extracellular matrix mimic hepatic scaffold. *Artificial organs* 41, E347-E355 (2017).
- 45 Shafiee, A. & Atala, A. Tissue engineering: Toward a new era of medicine. *Annual review of medicine* 68, 29-40 (2017).
- 46 Gilgenkrantz, H. & de l'Hortet, A. C. Understanding liver regeneration: from mechanisms to regenerative medicine. *The American journal of pathology* 188, 1316-1327 (2018).
- 47 Bizzaro, D., Russo, F. P. & Burra, P. New perspectives in liver transplantation: From regeneration to bioengineering. *Bioengineering* 6, 81 (2019).
- 48 da Silva Morais, A., Vieira, S., Zhao, X. et al. Advanced Biomaterials and Processing Methods for Liver Regeneration: State-of-the-Art and Future Trends. *Advanced Healthcare Materials* 9, 1901435 (2020).
- 49 Jain, E., Damania, A. & Kumar, A. Biomaterials for liver tissue engineering. *Hepatology international* 8, 185-197 (2014).
- 50 Turner, W. S., Schmelzer, E., McClelland, R. et al. Human hepatoblast phenotype maintained by hyaluronan hydrogels. *Journal of Biomedical Materials Research Part B: Applied Biomaterials* 82, 156-168 (2007).
- 51 Burra, P., Arcidiacono, D., Bizzaro, D. et al. Systemic administration of a novel human umbilical cord mesenchymal stem cells population accelerates the resolution of acute liver injury. *BMC gastroenterology* 12, 88 (2012).
- 52 Fu, R.-H., Wang, Y.-C., Liu, S.-P. et al. Differentiation of stem cells: strategies for modifying surface biomaterials. *Cell transplantation* 20, 37-47 (2011).
- 53 Kleinman, H. K. & Martin, G. R. in *Seminars in cancer biology*. 378-386 (Elsevier).
- 54 Wang, H., Shi, Q., Guo, Y. et al. Contact assembly of cell-laden hollow microtubes through automated micromanipulator tip locating. *Journal of Micromechanics and Microengineering* 27, 015013 (2016).
- 55 Hospodiuk, M., Dey, M., Sosnoski, D. et al. The bioink: A comprehensive review on bioprintable materials. *Biotechnology advances* 35, 217-239 (2017).
- 56 Liu, W., Zhang, Y. S., Heinrich, M. A. et al. Rapid continuous multimaterial extrusion bioprinting. *Advanced materials* 29, 1604630 (2017).
- 57 Kang, D., Hong, G., An, S. et al. Bioprinting of Multiscaled Hepatic Lobules within a Highly Vascularized Construct. *Small*, 1905505 (2020).
- 58 Murphy, S. V. & Atala, A. 3D bioprinting of tissues and organs. *Nature biotechnology* 32, 773 (2014).
- 59 Murphy, S. V., Skardal, A. & Atala, A. Evaluation of hydrogels for bio-printing applications. *Journal of Biomedical Materials Research Part A* 101, 272-284 (2013).
- 60 Jammalamadaka, U. & Tappa, K. Recent advances in biomaterials for 3D printing and tissue engineering. *Journal of functional biomaterials* 9, 22 (2018).
- 61 Skardal, A. & Atala, A. Biomaterials for integration with 3-D bioprinting. *Annals of biomedical engineering* 43, 730-746 (2015).
- 62 Kizawa, H., Nagao, E., Shimamura, M. et al. Scaffold-free 3D bio-printed human liver tissue stably maintains metabolic functions useful for drug discovery. *Biochemistry and biophysics reports* 10, 186-191 (2017).
- 63 Yorukoglu, A. C., Kiter, A., Akkaya, S. et al. A concise review on the use of mesenchymal stem cells in cell sheet-based tissue engineering with special emphasis on bone tissue regeneration. *Stem cells international* 2017 (2017).
- 64 Owaki, T., Shimizu, T., Yamato, M. et al. Cell sheet engineering for regenerative medicine: current challenges and strategies. *Biotechnology journal* 9, 904-914 (2014).
- 65 Takagi, S., Ohno, M., Ohashi, K. et al. Cell shape regulation based on hepatocyte sheet engineering technologies. *Cell transplantation* 21, 411-420 (2012).
- 66 Tatsumi, K. & Okano, T. Hepatocyte transplantation: cell sheet technology for liver cell transplantation. *Current transplantation reports* 4, 184-192 (2017).

- 67 Kobayashi, J., Kikuchi, A., Aoyagi, T. et al. Cell sheet tissue engineering: Cell sheet preparation, harvesting/manipulation, and transplantation. *Journal of Biomedical Materials Research Part A* 107, 955-967 (2019).
- 68 Takahashi, H. & Okano, T. Thermally-triggered fabrication of cell sheets for tissue engineering and regenerative medicine. *Advanced drug delivery reviews* 138, 276-292 (2019).
- 69 Nobakht Lahrood, F., Saheli, M., Farzaneh, Z. et al. Generation of Transplantable Three-Dimensional Hepatic-Patch to Improve the Functionality of Hepatic Cells In Vitro and In Vivo. *Stem Cells and Development* 29, 301-313 (2020).
- 70 Kim, K., Ohashi, K., Utoh, R. et al. Preserved liver-specific functions of hepatocytes in 3D co-culture with endothelial cell sheets. *Biomaterials* 33, 1406-1413 (2012).
- 71 Sakai, Y., Koike, M., Hasegawa, H. et al. Rapid fabricating technique for multi-layered human hepatic cell sheets by forceful contraction of the fibroblast monolayer. *PloS one* 8 (2013).
- 72 Sakai, Y., Yamanouchi, K., Ohashi, K. et al. Vascularized subcutaneous human liver tissue from engineered hepatocyte/fibroblast sheets in mice. *Biomaterials* 65, 66-75 (2015).
- 73 Arai, K., Yoshida, T., Okabe, M. et al. Fabrication of 3D-culture platform with sandwich architecture for preserving liver-specific functions of hepatocytes using 3D bioprinter. *Journal of Biomedical Materials Research Part A* 105, 1583-1592 (2017).
- 74 Fujii, M., Yamanouchi, K., Sakai, Y. et al. In vivo construction of liver tissue by implantation of a hepatic non-parenchymal/adipose-derived stem cell sheet. *Journal of tissue engineering and regenerative medicine* 12, e287-e295 (2018).
- 75 Sasaki, K., Akagi, T., Asaoka, T. et al. Construction of three-dimensional vascularized functional human liver tissue using a layer-by-layer cell coating technique. *Biomaterials* 133, 263-274 (2017).
- 76 Schneeberger, K., Sánchez-Romero, N., Ye, S. et al. Large-scale Production of LGR5-positive Bipotential Human Liver Stem Cells. *Hepatology* (2019).
- 77 Nagamoto, Y., Takayama, K., Ohashi, K. et al. Transplantation of a human iPSC-derived hepatocyte sheet increases survival in mice with acute liver failure. *Journal of hepatology* 64, 1068-1075 (2016).
- 78 Wilson, H. A new method by which sponges may be artificially reared. *Science* 25, 912-915 (1907).
- 79 Liu, F., Huang, J., Ning, B. et al. Drug discovery via human-derived stem cell organoids. *Frontiers in pharmacology* 7, 334 (2016).
- 80 Dutta, D., Heo, I. & Clevers, H. Disease modeling in stem cell-derived 3D organoid systems. *Trends in molecular medicine* 23, 393-410 (2017).
- 81 Huch, M., Knoblich, J. A., Lutolf, M. P. et al. The hope and the hype of organoid research. *Development* 144, 938-941 (2017).
- 82 Sakabe, K., Takebe, T. & Asai, A. Organoid Medicine in Hepatology. *Clinical Liver Disease* 15, 3 (2020).
- 83 Lancaster, M. A. & Knoblich, J. A. Organogenesis in a dish: modeling development and disease using organoid technologies. *Science* 345, 1247125 (2014).
- 84 Fatehullah, A., Tan, S. H. & Barker, N. Organoids as an in vitro model of human development and disease. *Nature cell biology* 18, 246-254 (2016).
- 85 Huch, M., Dorrell, C., Boj, S. F. et al. In vitro expansion of single Lgr5+ liver stem cells induced by Wnt-driven regeneration. *Nature* 494, 247-250 (2013).
- 86 Skardal, A., Murphy, S. V., Devarasetty, M. et al. Multi-tissue interactions in an integrated three-tissue organ-on-a-chip platform. *Scientific reports* 7, 1-16 (2017).
- 87 Huch, M., Gehart, H., Van Boxtel, R. et al. Long-term culture of genome-stable bipotent stem cells from adult human liver. *Cell* 160, 299-312 (2015).
- 88 Sgodda, M., Dai, Z., Zweigerdt, R. et al. A scalable approach for the generation of human pluripotent stem cell-derived hepatic organoids with sensitive hepatotoxicity features. *Stem cells and development* 26, 1490-1504 (2017).

- 89 Guye, P., Ebrahimkhani, M. R., Kipniss, N. et al. Genetically engineering self-organization of human pluripotent stem cells into a liver bud-like tissue using Gata6. *Nature communications* 7, 1-12 (2016).
- 90 Ramachandran, S. D., Schirmer, K., Müntz, B. et al. In vitro generation of functional liver organoid-like structures using adult human cells. *PloS one* 10 (2015).
- 91 Ang, C. H., Hsu, S. H., Guo, F. et al. Lgr5+ pericentral hepatocytes are self-maintained in normal liver regeneration and susceptible to hepatocarcinogenesis. *Proceedings of the National Academy of Sciences* 116, 19530-19540 (2019).
- 92 Prior, N., Inacio, P. & Huch, M. Liver organoids: from basic research to therapeutic applications. *Gut* 68, 2228-2237 (2019).
- 93 Hu, H., Gehart, H., Artegiani, B. et al. Long-term expansion of functional mouse and human hepatocytes as 3D organoids. *Cell* 175, 1591-1606. e1519 (2018).
- 94 Yamaguchi, T., Matsuzaki, J., Katsuda, T. et al. Generation of functional human hepatocytes in vitro: current status and future prospects. *Inflammation and regeneration* 39, 13 (2019).
- 95 Sgodda, M., Dai, Z., Zweigerdt, R. et al. A Scalable Approach for the Generation of Human Pluripotent Stem Cell-Derived Hepatic Organoids with Sensitive Hepatotoxicity Features. *Stem Cells and Development* (2017).
- 96 Takebe, T., Enomura, M., Yoshizawa, E. et al. Vascularized and complex organ buds from diverse tissues via mesenchymal cell-driven condensation. *Cell stem cell* 16, 556-565 (2015).
- 97 Zhang, R.-R., Koido, M., Tadokoro, T. et al. Human iPSC-derived posterior gut progenitors are expandable and capable of forming gut and liver organoids. *Stem cell reports* 10, 780-793 (2018).
- 98 Underhill, G. H. & Khetani, S. R. Bioengineered liver models for drug testing and cell differentiation studies. *Cellular and molecular gastroenterology and hepatology* 5, 426-439. e421 (2018).
- 99 Mun, S. J., Ryu, J.-S., Lee, M.-O. et al. Generation of expandable human pluripotent stem cell-derived hepatocyte-like liver organoids. *Journal of hepatology* 71, 970-985 (2019).
- 100 Pettinato, G., Lehoux, S., Ramanathan, R. et al. Generation of fully functional hepatocyte-like organoids from human induced pluripotent stem cells mixed with endothelial cells. *Scientific reports* 9, 1-21 (2019).
- 101 Li, J., Xing, F., Chen, F. et al. Functional 3D human liver bud assembled from MSC-derived multiple liver cell lineages. *Cell transplantation* 28, 510-521 (2019).
- 102 Haideri, S. S., McKinnon, A. C., Taylor, A. H. et al. Injection of embryonic stem cell derived macrophages ameliorates fibrosis in a murine model of liver injury. *NPJ Regenerative medicine* 2, 1-11 (2017).
- 103 Esch, M. B., Prot, J.-M., Wang, Y. I. et al. Multi-cellular 3D human primary liver cell culture elevates metabolic activity under fluidic flow. *Lab on a Chip* 15, 2269-2277 (2015).
- 104 Nejak-Bowen, K. N. & Monga, S. P. S. in *Liver regeneration* 77-101 (Elsevier, 2015).
- 105 Mito, M. & Kusano, M. Hepatocyte transplantation in man. *Cell transplantation* 2, 65-74 (1993).
- 106 Fisher, R. A. & Strom, S. C. Human hepatocyte transplantation: worldwide results. *Transplantation* 82, 441-449 (2006).
- 107 Fox, I. J., Chowdhury, J. R., Kaufman, S. S. et al. Treatment of the Crigler-Najjar syndrome type I with hepatocyte transplantation. *New England Journal of Medicine* 338, 1422-1427 (1998).
- 108 Muraca, M., Gerunda, G., Neri, D. et al. Hepatocyte transplantation as a treatment for glycogen storage disease type 1a. *The Lancet* 359, 317-318 (2002).
- 109 Bilir, B. M., Guinette, D., Karrer, F. et al. Hepatocyte transplantation in acute liver failure. *Liver Transplantation* 6, 32-40 (2000).

- 110 Nicolas, C. T., Hickey, R. D., Chen, H. S. et al. Concise review: liver regenerative medicine: from hepatocyte transplantation to bioartificial livers and bioengineered grafts. *Stem Cells* 35, 42-50 (2017).
- 111 Utoh, R., Tateno, C., Yamasaki, C. et al. Susceptibility of chimeric mice with livers repopulated by serially subcultured human hepatocytes to hepatitis B virus. *Hepatology* 47, 435-446 (2008).
- 112 Kim, Y., Kang, K., Lee, S. B. et al. Small molecule-mediated reprogramming of human hepatocytes into bipotent progenitor cells. *Journal of hepatology* 70, 97-107 (2019).
- 113 Zhang, K., Zhang, L., Liu, W. et al. In vitro expansion of primary human hepatocytes with efficient liver repopulation capacity. *Cell Stem Cell* 23, 806-819. e804 (2018).
- 114 Fu, G.-B., Huang, W.-J., Zeng, M. et al. Expansion and differentiation of human hepatocyte-derived liver progenitor-like cells and their use for the study of hepatotropic pathogens. *Cell research* 29, 8-22 (2019).
- 115 Li, S., Huang, S.-Q., Zhao, Y.-X. et al. Derivation and applications of human hepatocyte-like cells. *World journal of stem cells* 11, 535 (2019).
- 116 Hay, D. C., Fletcher, J., Payne, C. et al. Highly efficient differentiation of hESCs to functional hepatic endoderm requires ActivinA and Wnt3a signaling. *Proceedings of the National Academy of Sciences* 105, 12301-12306 (2008).
- 117 Woo, D. H., Kim, S. K., Lim, H. J. et al. Direct and indirect contribution of human embryonic stem cell-derived hepatocyte-like cells to liver repair in mice. *Gastroenterology* 142, 602-611 (2012).
- 118 Duan, Y., Catana, A., Meng, Y. et al. Differentiation and enrichment of hepatocyte-like cells from human embryonic stem cells in vitro and in vivo. *Stem cells* 25, 3058-3068 (2007).
- 119 Lavon, N., Yanuka, O. & Benvenisty, N. Differentiation and isolation of hepatic-like cells from human embryonic stem cells. *Differentiation* 72, 230-238 (2004).
- 120 Basma, H., Soto-Gutiérrez, A., Yannam, G. R. et al. Differentiation and transplantation of human embryonic stem cell-derived hepatocytes. *Gastroenterology* 136, 990-999. e994 (2009).
- 121 Yamanaka, S. Induced pluripotent stem cells: past, present, and future. *Cell stem cell* 10, 678-684 (2012).
- 122 Kia, R., Sison, R. L., Heslop, J. et al. Stem cell-derived hepatocytes as a predictive model for drug-induced liver injury: are we there yet? *British Journal of Clinical Pharmacology* 75, 885-896 (2013).
- 123 Gómez-Lechón, M. J. & Tolosa, L. Human hepatocytes derived from pluripotent stem cells: a promising cell model for drug hepatotoxicity screening. *Archives of toxicology* 90, 2049-2061 (2016).
- 124 Ang, L. T., Tan, A. K. Y., Autio, M. I. et al. A roadmap for human liver differentiation from pluripotent stem cells. *Cell reports* 22, 2190-2205 (2018).
- 125 Zhao, T., Zhang, Z.-N., Rong, Z. et al. Immunogenicity of induced pluripotent stem cells. *Nature* 474, 212-215 (2011).
- 126 Araki, R., Uda, M., Hoki, Y. et al. Negligible immunogenicity of terminally differentiated cells derived from induced pluripotent or embryonic stem cells. *Nature* 494, 100-104 (2013).
- 127 Zhou, J. & Sun, J. A revolution in reprogramming: small molecules. *Current molecular medicine* 19, 77-90 (2019).
- 128 Si-Tayeb, K., Noto, F. K., Nagaoka, M. et al. Highly efficient generation of human hepatocyte-like cells from induced pluripotent stem cells. *Hepatology* 51, 297-305 (2010).
- 129 Asumda, F. Z., Hatzistergos, K. E., Dykxhoorn, D. M. et al. Differentiation of hepatocyte-like cells from human pluripotent stem cells using small molecules. *Differentiation* 101, 16-24 (2018).
- 130 Roy-Chowdhury, N., Wang, X., Guha, C. et al. Hepatocyte-like cells derived from induced pluripotent stem cells. *Hepatology international* 11, 54-69 (2017).

- 131 Takebe, T., Sekine, K., Enomura, M. et al. Vascularized and functional human liver from an iPSC-derived organ bud transplant. *Nature* 499, 481-484, doi:nature12271 [pii] 10.1038/nature12271 (2013).
- 132 Soltys, K. A., Setoyama, K., Tafaleng, E. N. et al. Host conditioning and rejection monitoring in hepatocyte transplantation in humans. *Journal of hepatology* 66, 987-1000 (2017).
- 133 Vosough, M., Omidinia, E., Kadivar, M. et al. Generation of functional hepatocyte-like cells from human pluripotent stem cells in a scalable suspension culture. *Stem Cells Dev* 22, 2693-2705, doi:10.1089/scd.2013.0088 (2013).
- 134 Wang, Y., Alhaque, S., Cameron, K. et al. Defined and Scalable Generation of Hepatocyte-like Cells from Human Pluripotent Stem Cells. *Journal of visualized experiments: JoVE* (2017).
- 135 Thomas, J. A., Pope, C., Wojtacha, D. et al. Macrophage therapy for murine liver fibrosis recruits host effector cells improving fibrosis, regeneration, and function. *Hepatology* 53, 2003-2015 (2011).
- 136 Forbes, S. J. & Newsome, P. N. New horizons for stem cell therapy in liver disease. *Journal of hepatology* 56, 496-499 (2012).
- 137 Afshari, A., Shamdani, S., Uzan, G. et al. Different approaches for transformation of mesenchymal stem cells into hepatocyte-like cells. *Stem Cell Research & Therapy* 11, 54 (2020).
- 138 Zhan, Y., Wang, Y., Wei, L. et al. in *Transplantation proceedings*. 3082-3085 (Elsevier).
- 139 Terai, S., Takami, T., Yamamoto, N. et al. Status and prospects of liver cirrhosis treatment by using bone marrow-derived cells and mesenchymal cells. *Tissue Engineering Part B: Reviews* 20, 206-210 (2014).
- 140 Rossi, L., Challen, G. A., Sirin, O. et al. in *Stem Cell Migration* 47-59 (Springer, 2011).
- 141 Lagasse, E., Connors, H., Al-Dhalimy, M. et al. Purified hematopoietic stem cells can differentiate into hepatocytes in vivo. *Nature medicine* 6, 1229-1234 (2000).
- 142 Vainshtein, J. M., Kabarriti, R., Mehta, K. J. et al. Bone Marrow-Derived Stromal Cell Therapy in Cirrhosis: Clinical Evidence, Cellular Mechanisms, and Implications for the Treatment of Hepatocellular Carcinoma. *International Journal of Radiation Oncology\* Biology\* Physics* 89, 786-803 (2014).
- 143 Austin, T. W. & Lagasse, E. Hepatic regeneration from hematopoietic stem cells. *Mechanisms of development* 120, 131-135 (2003).
- 144 Thorgeirsson, S. S. & Grisham, J. W. Hematopoietic cells as hepatocyte stem cells: a critical review of the evidence. *Hepatology* 43, 2-8 (2006).
- 145 Nakamura, T., Torimura, T., Sakamoto, M. et al. Significance and therapeutic potential of endothelial progenitor cell transplantation in a cirrhotic liver rat model. *Gastroenterology* 133, 91-107. e101 (2007).
- 146 Lan, L., Liu, R., Qin, L.-Y. et al. Transplantation of bone marrow-derived endothelial progenitor cells and hepatocyte stem cells from liver fibrosis rats ameliorates liver fibrosis. *World journal of gastroenterology* 24, 237 (2018).
- 147 Taniguchi, E., Kin, M., Torimura, T. et al. Endothelial progenitor cell transplantation improves the survival following liver injury in mice. *Gastroenterology* 130, 521-531 (2006).
- 148 Banerjee, A., Bizzaro, D., Burra, P. et al. Umbilical cord mesenchymal stem cells modulate dextran sulfate sodium induced acute colitis in immunodeficient mice. *Stem cell research & therapy* 6, 79 (2015).
- 149 Christ, B., Brückner, S. & Winkler, S. The therapeutic promise of mesenchymal stem cells for liver restoration. *Trends in molecular medicine* 21, 673-686 (2015).
- 150 Andrzejewska, A., Lukomska, B. & Janowski, M. Concise review: Mesenchymal stem cells: From roots to boost. *Stem Cells* 37, 855-864 (2019).

- 151 Lanzoni, G., Cardinale, V. & Carpino, G. The hepatic, biliary, and pancreatic network of stem/progenitor cell niches in humans: A new reference frame for disease and regeneration. *Hepatology* 64, 277-286 (2016).
- 152 Huch, M., Boj, S. F. & Clevers, H. Lgr5+ liver stem cells, hepatic organoids and regenerative medicine. *Regenerative medicine* 8, 385-387 (2013).
- 153 Wu, F., Wu, D., Ren, Y. et al. Generation of hepatobiliary organoids from human induced pluripotent stem cells. *Journal of hepatology* 70, 1145-1158 (2019).
- 154 Vyas, D., Baptista, P. M., Brovold, M. et al. Self-assembled liver organoids recapitulate hepatobiliary organogenesis in vitro. *Hepatology* 67, 750-761 (2018).
- 155 Saheli, M., Sepantafar, M., Pournasr, B. et al. Three-dimensional liver-derived extracellular matrix hydrogel promotes liver organoids function. *Journal of cellular biochemistry* 119, 4320-4333 (2018).
- 156 Broguiere, N., Isenmann, L., Hirt, C. et al. Growth of epithelial organoids in a defined hydrogel. *Advanced Materials* 30, 1801621 (2018).
- 157 Yamada, M., Utoh, R., Ohashi, K. et al. Controlled formation of heterotypic hepatic micro-organoids in anisotropic hydrogel microfibers for long-term preservation of liver-specific functions. *Biomaterials* 33, 8304-8315 (2012).
- 158 Ma, M., Chiu, A., Sahay, G. et al. Core-shell hydrogel microcapsules for improved islets encapsulation. *Advanced healthcare materials* 2, 667-672 (2013).
- 159 Siltanen, C., Diakatou, M., Lowen, J. et al. One step fabrication of hydrogel microcapsules with hollow core for assembly and cultivation of hepatocyte spheroids. *Acta biomaterialia* 50, 428-436 (2017).
- 160 Gonzalez-Pujana, A., Santos, E., Orive, G. et al. Cell microencapsulation technology: current vision of its therapeutic potential through the administration routes. *Journal of Drug Delivery Science and Technology* 42, 49-62 (2017).
- 161 Pajoumshariati, S. R., Azizi, M., Wesner, D. et al. Microfluidic-based cell-embedded microgels using nonfluorinated oil as a model for the gastrointestinal niche. *ACS applied materials & interfaces* 10, 9235-9246 (2018).
- 162 Zhang, W., Zhao, S., Rao, W. et al. A novel core-shell microcapsule for encapsulation and 3D culture of embryonic stem cells. *Journal of materials chemistry B* 1, 1002-1009 (2013).
- 163 Liu, H., Wang, Y., Wang, H. et al. A Droplet Microfluidic System to Fabricate Hybrid Capsules Enabling Stem Cell Organoid Engineering. *Advanced Science* (2020).
- 164 Lu, Y. C., Fu, D. J., An, D. et al. Scalable production and cryostorage of organoids using core-shell decoupled hydrogel capsules. *Advanced biosystems* 1, 1700165 (2017).
- 165 Zhong, Q., Ding, H., Gao, B. et al. Advances of Microfluidics in Biomedical Engineering. *Advanced Materials Technologies* 4, 1800663 (2019).

## **II. Chapter 2. Scalable production of hepatic organoids by integrated differentiation of hPSCs under fully controlled culture condition**

This chapter is based on following paper published Biotechnology and Bioengineering Journal:

**Dissolved oxygen concentration regulates human hepatic organoid formation from pluripotent stem cells in a fully controlled bioreactor published in Biotechnology and bioengineering Journal**

**Dissolved oxygen concentration regulates human hepatic organoid formation from pluripotent stem cells in a fully controlled bioreactor**

Zahra Farzaneh<sup>1</sup>, Saeed Abassalizadeh<sup>1,2</sup>, Mohammad-Hassan Asghari-Vostikolaee<sup>1</sup>, Mehdi Alikhani<sup>1</sup>, Joaquim M.S. Cabral<sup>2</sup>, Hossein Baharvand<sup>1,3\*</sup>

1. Department of Stem Cells and Developmental Biology, Cell Science Research Center, Royan Institute for Stem Cell Biology and Technology, ACECR, Tehran, Iran

2. Department of Bioengineering and iBB - Institute for Bioengineering and Biosciences, Instituto Superior Técnico, Universidade de Lisboa, Lisboa, Portugal

3. Department of Developmental Biology, University of Science and Culture, Tehran, Iran

**Running Title:** Fully controlled production of Hepatic organoids

**Competing financial interests:** The authors declare that they have no competing financial interests.

## Introduction

Liver diseases, including chronic and acute liver failure, are the fifth leading causes of mortality worldwide with over one million deaths annually <sup>1,2</sup>. Although liver transplantation is a highly successful treatment for chronic liver diseases, it is the only available option. Increasing numbers of patients die each day or experience deteriorating health when placed on liver transplantation lists because of the critical local and worldwide shortages of available transplantable livers. There are approximately 25 000 liver transplants available worldwide per year <sup>3,4</sup>. To cope with this unmet medical need, different research groups and companies have focused on developing promising regenerative medicine technologies that use different cell types as starting materials (e.g., human pluripotent stem cells [hPSCs], adult derived progenitors, and induced hepatocyte-like [iHep] cells from somatic cells) to generate functional hepatocyte-like cells, liver organoids, or tissue constructs <sup>5</sup> as therapeutic components for transplantation. These therapeutic components can be used to induce or assist the liver's inherent regeneration capacity and hopefully treat acute or chronic liver failure <sup>6</sup>. Among the different available cell sources, hPSCs are considered one of the most convenient cell types. These cells provide an unlimited source for integrated hepatic differentiation and scalable production of hepatocyte-like cells or liver organoids for translational studies and clinical applications, and are easily amenable for scalable expansion and integrated differentiation <sup>7,8</sup>. However, most studies have used small and/or static (culture dishes and multi-well plates) or dynamic culture (spinner flasks) systems with limited culture working volumes (1.5–50 ml) and uncontrolled culture conditions in an attempt to establish protocols to generate hepatocyte-like cells or hepatic organoids from hPSCs <sup>9-12</sup>. These culture systems are convenient for protocol development and optimization studies; however, they lack adequate scalability to produce clinically relevant cell numbers ( $1-2 \times 10^9$  cells per patient) as essential therapeutic components to treat one or multiple patients with autologous or allogeneic cell therapy strategies <sup>13</sup>. Therefore, this critical technical issue has largely hindered the potential use of

currently established protocols for clinical or commercial applications <sup>12,14</sup>. Other critical issues that should be addressed in established protocols of small scale cultures include issues with quality of the final product such as low differentiation efficacy and functionality of hepatocytes (e.g., poor gene expression profiles and metabolic characteristics) compared to primary hepatocytes; productivity issues such as low cell yields; product homogeneity; and lack of process reproducibility that could be potentially boosted during scale-up trials <sup>14</sup>. Thus, development of robust bioprocess technologies for scalable production of human functional hepatocytes or hepatic organoids is a necessary step prior to the clinical translation of currently developed regenerative medicine technologies.

Previously, we improved the efficacy of our protocol for stepwise and integrated hepatic differentiation of hPSCs as three dimensional (3D) aggregates in a 50 ml dynamic suspension culture by optimizing a hepatic endoderm differentiation strategy (e.g., CHIR and activin A concentration and treatment time) and explored the optimal hPSCs starting aggregate size for beginning the differentiation process <sup>15</sup>. However, we realized that our protocol was not scalable after a 3X volume increase to a 150 ml working volume under the same uncontrolled dynamic culture condition and resulted in the generation of heterogeneous hepatospheres that had limited functionality. Next, we employed fully controlled culture conditions in a bioreactor to scale-up our established integrated hepatic differentiation protocol by regulating pH and optimizing dissolved oxygen (DO) concentrations in the range of liver tissue physiological oxygen concentrations, as a very important cue in hepatic fate determination and liver function <sup>16</sup>. To date, the results of different studies have demonstrated the significant effect of oxygen concentration/gradient on hPSCs hepatic differentiation efficacy, functionality, and maturation. Blood oxygen concentration modulates liver zonation and metabolic activity <sup>17-20</sup> as well as hepatic differentiation from human hPSCs by regulation through intercellular TGF $\beta$  signaling <sup>21</sup>. However, generation of hepatocyte-like cells or liver organoids in fully controlled stirred bioreactors and exploring the effect of DO concentration on integrated hepatic differentiation efficacy of hPSCs as 3D aggregates has not been studied. Therefore, we used a stirred tank

bioreactor to develop a fully controlled integrated hepatic differentiation process and explored the effect of different oxygen concentrations (20%, 30%, and 40% air saturation, which corresponded to 30–60 mmHg pO<sub>2</sub> within liver tissue) on process efficacy and quality attributes of the final product. Stirred suspension/tank bioreactors have been successfully used for scalable production of hPSCs and their potential therapeutic derivatives such as beating cardiomyocytes <sup>22</sup>, neural stem cells <sup>23</sup>, and hepatocytes <sup>14</sup>, and can be considered a superior option for large-scale production of hPSC derivatives, including hepatocyte-like cells and hepatic organoids.

Here, the application of an optimized DO concentration (30% air saturation at 37°C, equal to 40–45 mmHg pO<sub>2</sub> in liver tissue) resulted in the generation of self-organized fetal-like hepatic organoids comprised of functional hepatocytes and red blood cells. We observed that 20% DO and an uncontrolled culture condition generated hepatospheres that had poor functionality. The demonstrated cross-talk between hepatocytes and erythroid cells, which also occurs during human liver bud development, resulted in improved metabolic activity, functionality, and meaningfully higher levels of CYP enzyme activity of the hESC-derived fetal-like hepatic organoids generated in our study <sup>24</sup>. Our data emphasized and highlighted the critical effect of oxygen concentration on integrated differentiation efficacy of hPSCs and its fate determination properties as 3D aggregates, which should be explored and optimized before clinical translation and the commercialization stage of established protocols..

## **Material and Methods**

### ***Expansion and integrated hepatic differentiation of human pluripotent stem cells (hPSCs) under dynamic suspension culture condition***

We selected the human embryonic stem cell line (hESC), RH5 (passages 40–60), <sup>166</sup> as the cell source for this study. We cultured RH5 as 3D aggregates under a dynamic suspension culture as previously described <sup>15</sup>. The hPSCs were passaged in a spinner flask as follows: day 7 hPSpheres were collected in a tube, washed with PBS without Ca<sup>2+</sup>/Mg<sup>2+</sup> and

dissociated by an Accumax™ enzymatic solution treatment. We then transferred  $2 \times 10^5$  cell/ml inoculation density of the hPSCs to a 250 ml glass stirred bioreactor vessel that had a 150 ml working volume of standard hPSC medium, which consisted of DMEM-F12 supplemented with 20% DO (v/v) KOSR, 1% (v/v) MEM-NEAA, 1% (v/v) Glutamax, and 0.1 mM of 2-mercaptoethanol (all from Invitrogen) that had been conditioned with human fetal fibroblasts for 24 h and subsequently supplemented with 100 ng/ml bFGF. The agitation rate was 40 rpm during the hPSCs expansion and integrated differentiation. All dynamic suspension cultures were performed under standard culture conditions of 37 C, 5% CO<sub>2</sub>, and saturated humidity. The integrated hepatic differentiation process for the hPSC aggregates under a dynamic suspension culture was conducted in three developmental steps. Briefly, after 3–4 days of dynamic suspension culture and generation of hPSC aggregates (diameter:  $142 \pm 32$  μm), we harvested all of the aggregates from the spinner flask that had a 150 working volume, and transferred them to a conical tube. The aggregates were allowed to settle down, and extra medium was removed. The aggregates were washed with PBS plus Ca<sup>2+</sup> and Mg<sup>2+</sup> prior to the differentiation process. For endoderm differentiation, we used a basal medium that included RPMI 1640 plus 1X B-27 supplement (without vitamin A) and 0.1% bovine serum albumin (BSA) and 6 μM CHIR99021. After 24 h, the aggregates were washed and treated with basal medium supplemented with activin (10 ng/ml) for 48 h with one medium refreshment after 24 h. For hepatic differentiation, DMEM/F12 plus KOSR (2% v/v) supplemented with hepatocyte growth factor (HGF, 10 ng/ml) and fibroblast growth factor 4 (FGF4, 10 ng/ml) was used for six days. Subsequently, 50% (v/v) of the previous medium was replaced by HCM medium (v/v) that contained Oncostatin M (OSM, 10 ng/ml) and dexamethasone (Dex, 10<sup>-7</sup> M) for 11 days. The medium was refreshed every two days during this period. The diameter of the spheres in each experimental group was determined with ImageJ software (National Institutes of Health) under phase-contrast microscope from three independent images. Approximately 100–500 spheres were counted in each group. Table S1 lists the materials used in this study.

***Integrated hPSpheres to hepatic differentiation organoids under fully controlled culture conditions in a stirred tank bioreactor***

We conducted all of the bioreactor runs in a 250 ml glass stirred bioreactor vessel equipped with a glass bulb impeller that was placed on a magnetic stirred platform (CELLSPIN, Integra Bioscience, Switzerland) in a temperature-controlled chamber at 37 °C. The vessel was equipped with pH and DO probes, and fully monitored and controlled by a PC-based stirred tank bioreactor (New Brunswick™ CelliGen 310, USA) and BioCommand software (Biocommand Bioprocessing Software, New Brunswick, USA). Both the integrated and fully controlled hepatic differentiation processes in the bioreactor and its uncontrolled condition counterpart (control group) had an equal working volume of 150 ml with 40 rpm agitation rate. The pH level in all controlled runs was precisely regulated at  $7.1 \pm 0.1$  by a cascading pH setpoint with a CO<sub>2</sub> gas sparge/flow rate. DO concentrations (20%, 30%, 40% air saturation) were monitored by a polarographic DO probe and automatically regulated by a cascading DO setpoint at three levels with air, N<sub>2</sub>, and O<sub>2</sub> sparge/flow rate, consequently using the bioreactor 4-gas mixing system that included four solenoid valves/TMFCs to control each gas flow rate (0.08–2 VVM) and was controlled by bioreactor controller software. All gases were sparged into the headspace of the bioreactor vessel after passage through a 0.2 μm microfilter membrane (Midistart 2000, Sartorius) and a humidifier to maintain a constant media level during the 20 days of culture. The most important bioprocess parameters of temperature, DO, pH, and gas flow rates were monitored and recorded online at 1 min intervals during the 20-day culture period.

***Gene expression analysis***

Total RNA was extracted using the TRIzol reagent in different stages under different conditions. RNA integrity and purity were verified by 1% agarose gel. cDNA was synthesized with 2 μg total RNA based on the manufacturer's instructions. Real-time PCR reactions were performed as previously reported<sup>15</sup>. The fold change for each gene was normalized against

the *GAPDH* housekeeping gene and calibrated with pluripotent status. Data analysis was performed with StepOne software v2.1 and by the comparative CT method ( $2^{-\Delta\Delta Ct}$ ). Human adult and fetal liver tissues were used as positive controls for gene expression analysis. Table S2 lists the primers used in this experiment.

### ***Immunofluorescence staining***

Spheres were collected from different groups on days 3, 9, and 20 of differentiation as the endoderm, hepatoblast, and hepatocyte steps. Immunofluorescence staining was done as previously described<sup>15</sup>. Briefly, the spheres were fixed overnight with 4% paraformaldehyde and embedded in a 2% agar gel. After processing, the tissues were embedded in paraffin blocks. The paraffin blocks were cut into 6  $\mu$ m sections, which were subsequently deparaffinized and dehydrated before rehydration. Next, the sections were treated by antigen retrieval (Dako and trypsin) and then permeabilized by 0.3% Triton X-100 (except for the membrane protein) before they were blocked. Subsequently, the sections were incubated overnight with diluted primary antibodies at 4 °C followed by incubation with secondary antibodies after a washing step. The nuclei were counterstained with DAPI and the slides were analyzed by a fluorescent microscope (IX71; Olympus).

Immunofluorescent staining in the adherent cells was done according to a previous study<sup>167</sup>. The adherent cells were fixed with 4% paraformaldehyde for 15–20 min. After washing, the cells were blocked and permeabilized with 0.3% Triton X-100 in 1% BSA. Diluted primary antibodies were added to samples and allowed to remain overnight at 4 C, then they were washed and incubated with secondary antibodies. The samples were washed again, DAPI was added, and the samples were analyzed by a fluorescent microscope.

### ***Flow cytometry analysis***

Flow cytometry analysis of the endospheres was done as previously described<sup>167</sup>. Briefly, the dispersed cells were fixed with 4% paraformaldehyde, permeabilized, and blocked. Subsequently, they were incubated overnight with diluted primary antibodies at 4 °C, then

washed and incubated with secondary antibodies for 45 min at room temperature. The expressions of surface red blood cell markers were done in live dispersed hepatic organoids using conjugated primary antibodies, and then incubated for 30 min at room temperature. Flow cytometry analysis was performed with a BD FACSCalibur flow cytometer (Becton-Dickinson, USA).

#### ***DNA and protein extraction***

Briefly, the cells were homogenized with TRIzol reagent and centrifuged at  $12000 \times g$  for 15 min after addition of chloroform. The DNA was precipitated by the addition of 100% ethanol to the lower phases, followed by extraction per the manufacturer's instructions. DNA concentration and quality were evaluated by spectrophotometry.

#### ***Western-blot***

Protein extraction and Western blot analysis were performed as previously described <sup>167</sup>. Briefly, the upper phase of the vial from the previous step was transferred to a new tube, and the proteins were precipitated by centrifugation and washed. Protein pellets were dried at room temperature and dissolved in urea buffer. A Pierce BCA Protein Assay kit was used to determine the protein concentration. For Western blot analysis, 20  $\mu$ g total protein was separated by 10% sodium dodecyl sulfate-polyacrylamide gel electrophoresis (SDS-PAGE), and transferred to a PVDF membrane via a semi-dry blotting system for 2 h at 25 V. The blotted membranes were blocked by 2.5% nonfat milk, then washed with tris-buffered saline that contained 0.1% Tween 20 (TBST) for 5 min. Subsequently, the blots were incubated with primary antibodies against ALB, AFP, and GAPDH for 90 min. After we washed the blots three times for 10 min each, they were incubated for 1 h with secondary antibodies. The blots were washed similar to the previous step, and the protein bands were visualized on X-ray films in a darkroom using an ECL select substrate. The images were scanned using a densitometer (Bio-Rad, USA). Table S3 lists all antibodies used in this experiment.

### ***Functional analysis***

ICG and LDL uptake, and PAS staining were performed to evaluate the maturation extent and metabolic activity of the generated hepatic cells (Table S1).

### ***Albumin (ALB) and fibrinogen secretion and urea production***

To evaluate the albumin (ALB) secretion ability of hepatocytes, the supernatant culture media was collected on day 20 at 48 h after the last media refreshment and stored at 20 °C before the assay. The concentrations of ALB and fibrinogen in the supernatant were assessed by an ELISA kit specific for each protein according to the manufacturer's instructions.

Urea concentration was assayed using a colorimetric assay. Data in these experiments were normalized to the total DNA content in each group.

### ***Cytochrome P450 activity and inducibility***

On day 20, the hepatic organoids generated under fully controlled and uncontrolled culture conditions were divided into two groups. To evaluate the CYP3A4 enzymatic activity of these hepatocytes, we incubated the hepatic organoids for 72 h in basal medium that contained rifampicin (20 µM) as a CYP3A4 inducer or DMSO (0.1%) as the control group. Enzymatic activity was assessed with a P450-Assay Kit (Promega) according to the manufacturer's instructions and a luminometer (Biocompare). Relative activity was measured by taking into consideration the amount of activity in the inducer group relative to DMSO. The data were normalized to the amount of total DNA in each group.

### ***Transplantation***

Acute liver failure was induced in five BALB/C mice (10–12 weeks age) by an intraperitoneal injection of 1 ml/kg of CCL4 diluted 1:10 in corn oil. Under inhaled anesthesia, 10–20 hepatic organoids that were derived under the 30% DO condition were injected into the spleen of each mouse. The animals were monitored daily and received normal food and water. The animals

were sacrificed at 7 and 14 days after the transplantation. The presence of human ALB in the mice sera was evaluated using a human albumin ELISA quantitation kit that did not cross-react with mice ALB (Bethyl Laboratories). Liver and spleen samples were fixed in 10% formalin. After the tissues were processed, they were ready for immunohistochemistry staining for human ALB.

### ***Statistical analysis***

We had a dedicated uncontrolled bioreactor culture for each DO concentration trial with same cell source and differentiation protocol, which included three biological replicates for the different DO concentrations. The samples were derived from 1.5–2 ml suspensions collected from different time points in the bioreactor runs. Data were presented as mean±standard deviation (SD). Comparisons between groups and data were performed with one-way ANOVA and the post-hoc Tukey test.  $P < 0.05$  were considered statistically significant.

## **Results**

### ***Online monitoring of DO concentration and pH during integrated hepatic differentiation of hPSC aggregates in the stirred bioreactor***

The hPSC 3D spheroids (~150  $\mu\text{m}$  mean aggregate diameter; hereafter named hPSpheres, Fig. S1A) were differentiated into a hepatic lineage in three developmental steps that included generation of endodermal cells (endospheres), hepatoblasts (hepatoblastspheres), and hepatocyte-like cells (hepatospheres) over a 20-day culture period as previously described<sup>18</sup> (Fig II.1 A). We used a fully controlled stirred tank bioreactor with a 150 ml working volume to scale-up our established protocol in a 50 ml working volume.

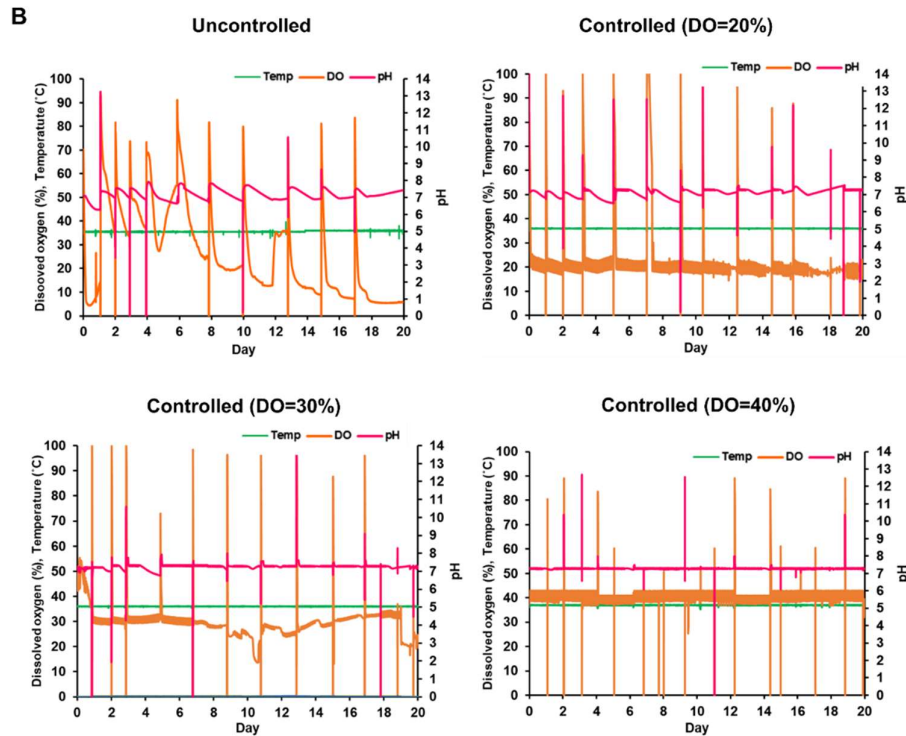
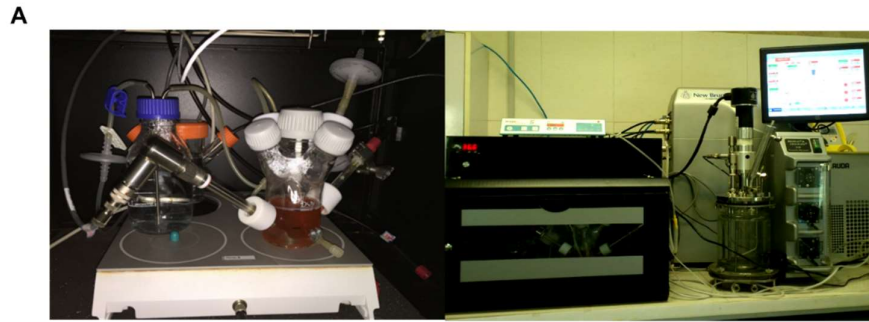


**Figure II-1 Integrated hepatic differentiation of hPSC 3D spheroids (hPSpheres) into hepatic organoids in a stirred tank bioreactor under fully controlled conditions.** (a) Schematic diagram of hepatic organoid generation from hPSpheres. (b, c) A stirred Therefore, we developed a strategy to control the DO concentration (20%, 30%, and 40% air saturation, equal to 30, 45, and 60 mmHg, respectively, at 37 C) in similar range of pO<sub>2</sub> in different regions of the human liver tissue (Brooks, Hammond, Girling, & Beckingham, 2007) and regulated the pH precisely at  $7.2 \pm 0.1$  during different steps of the hepatic differentiation process in an attempt to improve efficacy and productivity of the hepatospheres. The results of all bioreactor runs were compared to their uncontrolled culture condition counterpart, which was conducted under the same time and operation conditions of cell source, working volume, culture vessel, differentiation protocol, and operation time.

Key bioprocesses parameters were monitored during the integrated differentiation to identify potentially important parameters that possibly influenced hepatic differentiation efficacy and might result in the generation of heterogeneous hepatospheres with low functionality and

metabolic activity (Fig II-1 B). Online monitoring of the hepatic differentiation process in the 150 ml working volume under uncontrolled culture conditions revealed unstable and decreasing DO and pH profiles during the different stages of differentiation. The oxygen concentration was not limited during endoderm differentiation (Day 3) and hepatoblast generation (Day 9 of the integrated differentiation process).

However, the oxygen concentration dramatically decreased during the hepatocyte expansion and maturation phase, from approximately 70% after medium refreshment to 5–20% air saturation during 10–20 days of culture. Hence, we considered the oxygen concentration as a variable and a potentially limiting factor during the integrated hepatic differentiation process that should be optimized accordingly (Fig II-1 C). We observed that the pH level was unstable and decreased from 7.8 to 6.2 after medium refreshment, even with continuous introduction of air with 5% CO<sub>2</sub> into the vessel headspace for pH control, which is a standard strategy for maintaining a constant pH during the culture condition.

#### ***The effect of regulating DO concentration on integrated differentiation efficacy into endodermal cells and hepatoblasts***

In the first step, we evaluated the endosphere differentiation efficacy of hPSpheres at different DO concentrations after 3 days of the stepwise and integrated differentiation process. The generated endospheres had a relatively similar morphology under both the controlled and uncontrolled conditions (Fig. II-2 a). We measured the aggregate diameters to estimate cell proliferation kinetics during each point of the stepwise hepatic differentiation. The endospheres had a round and dense morphology with a 220  $\mu\text{m}$  mean diameter size under all culture conditions, except for 40% DO (Fig. II-2 b). The 40% DO resulted in larger endospheres ( $244 \pm 82 \mu\text{m}$ ) with an approximately 33% coefficient of variation (CV), which showed increased heterogeneity of the endosphere sizes (Fig. II-2 b and c). Immunostaining results indicated that the SOX17-positive cells were distributed and well-expressed in each single endosphere under different culture conditions (Fig. II-2 d).

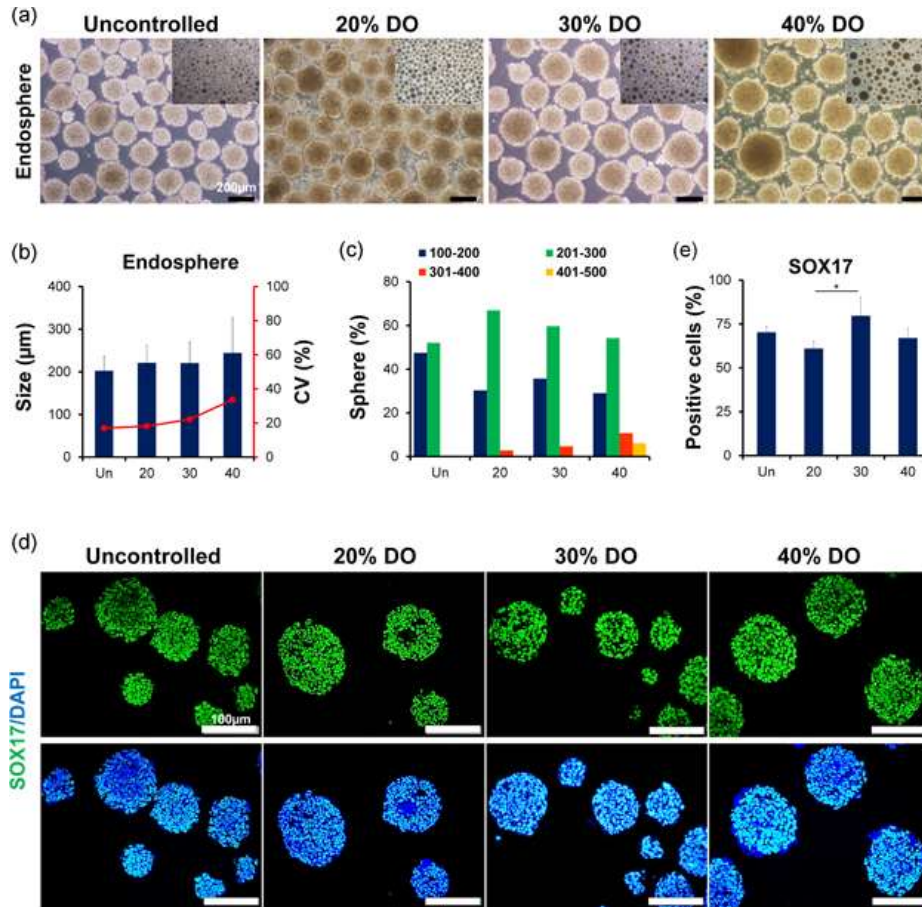


**Figure II-2 The effect of controlled DO on differentiation to endodermal cells.** (a) The morphology of endospheres was relatively similar between groups. Scale bar = 200 µm. Mean size with CV (b) and (c) size distribution of endospheres. Histogram data showed that size heterogeneity increased under 40% DO conditions. About 150–200 spheres were counted in each experimental group. (d) Immunofluorescent images of sectioned endospheres under different culture conditions. (e) Flow cytometry data showed a similar percent of SOX17-positive cells among the groups. The percentage of SOX17 positive cells was higher under 30% DO than 20% DO. Scale bar = 100 µm. Data (mean ± SD) were analyzed with ANOVA and Tukey's post hoc test;  $n = 3$ . 20%, 30% and 40%, differentiation under DO controlled culture conditions in a stirred bioreactor with 20%, 30%, and 40% DO. ANOVA, analysis of variance; CV, coefficient of variation; DAPI, 4',6-diamidino-2-phenylindole; DO, dissolved oxygen; Un, differentiation under uncontrolled culture condition. \* $p < .05$

Flow cytometry analysis also showed that approximately 70% of the cell populations expressed SOX17 under uncontrolled, 20% DO, and 40% DO conditions. The highest SOX17 expression was under 30% DO (about 80%) and was significantly higher than 20% DO ( $p < 0.05$ ; Fig. II-2 e and II-S2). Thus, controlling the DO concentration during endoderm differentiation resulted in higher expressions of endoderm markers at 30% DO and lower expressions at 20% DO. In the next step, the endospheres were treated for an additional 6 days in HGF and FGF4 supplemented medium for integrated differentiation to hepatoblasts as 3D aggregates (hepatoblastspheres).

The hepatoblastspheres generated in all of the trials had a round and mostly dense morphology (Fig. II-3 a,f, 4',6-diamidino-2-phenylindole staining).

The aggregate mean diameter size increased in the higher DO concentrations until it reached a maximum diameter of 260  $\mu\text{m}$  at 40% DO with higher CV compared with the other groups (Fig. II-3 b). The hepatoblastspheres size distribution was more homogenous at 20% and 30% DO, and increased heterogeneity was observed under the uncontrolled and 40% DO conditions (Fig. II-3 b,c).

Gene expression analysis showed that the hepatoblasts generated in all groups well-expressed *-fetoprotein (AFP)*, *albumin (ALB)*, *HNF4A*, and *TTR* in a similar manner (Figure II-3 d). AFP expression, as a key marker of hepatic progenitors, was also validated by western blot analysis.

The results showed no significant differences in AFP expression levels among the different trials (Fig. II-3 e and II-S3A). Immunostaining analysis also showed that AFP was well-expressed in the cytoplasm of cells distributed through all hepatoblastspheres generated under the different trials, except for those generated under 20% DO where AFP expression was not detected in some spheres.

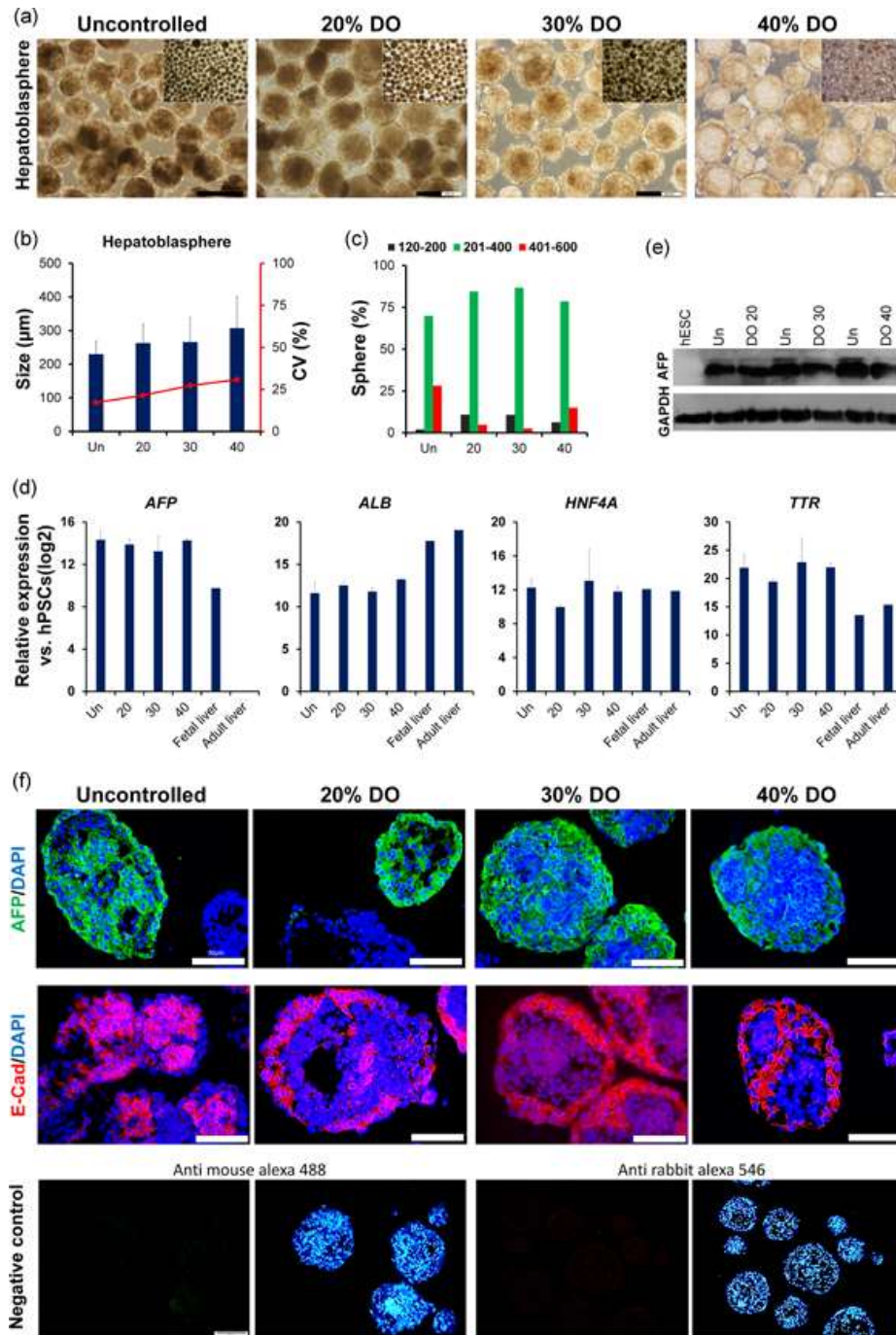


**Figure II-3 The effect of controlled DO on hepatoblast differentiation.** (a) Hepatoblastspheres in different groups had a similar morphology. Scale bar = 200 µm. (b) and (c) Mean size, CV, and size distribution of hepatoblastspheres. The mean size of the hepatoblastspheres was 260 µm; 70% of the hepatoblastspheres were 200–400 µm. About 100–150 spheres were counted in each experimental group. (d) Gene expression analysis of hepatoblastspheres showed high expression levels of *TTR*, *AFP*, *HNF4A*, and *ALB* in the groups. (e) Western blot for AFP expression in hepatoblastspheres. (f) Representative immunofluorescent images of sectioned hepatoblastspheres in different conditions showed expressions of AFP and E-cad. Scale bar = 50 µm. Data (mean ± SD) were analyzed with ANOVA and Tukey's post hoc test;  $n = 3$ . 20%, 30%, and 40%, differentiation under DO

controlled culture conditions in the stirred bioreactor; AFP,  $\alpha$ -fetoprotein; ALB, albumin; CV, coefficient of variation; DAPI, 4',6-diamidino-2-phenylindole; DO, dissolved oxygen; E-cad, E-cadherin; Un, differentiation under uncontrolled culture condition

E-cadherin (E-cad), an early surface hepatic marker, expressed in cells that were mainly located around the hepatoblastospheres under fully controlled DO conditions, which was similar to liver organoids derived from the human liver (Fig. II-3 f). Thus, the results of gene and protein expression analyses indicated that the integrated differentiation efficacy to hepatoblasts was similar under the controlled DO conditions and the uncontrolled condition.

### **Generation of human fetal-like hepatic organoids during integrated hepatoblast expansion and maturation**

There was a significant change in hepatosphere morphology after Day 11 in both the fully controlled and uncontrolled conditions (Fig. II-4a). The average diameter sizes of Day 20 hepatospheres in all groups were approximately 370  $\mu\text{m}$ , except for the 30% DO group that had a smaller diameter size compared to the other conditions (mean diameter: approximately 300  $\mu\text{m}$ ) with more uniform morphology and lower CV (Fig. II-4b,c). More important, the fully controlled conditions significantly decreased the generation of hepatospheres that had cystic morphologies. The majority of hepatospheres generated under the uncontrolled culture condition had a cystic/transparent ( $59 \pm 9\%$ ) structure and morphology (Fig. II-4d) compared to  $4 \pm 0.1\%$  at 20% DO ( $p < .001$ ),  $16 \pm 10\%$  at 30% DO ( $p < .01$ ), and  $30 \pm 12\%$  at 40% DO. These results indicated that the fully controlled culture condition could reduce final product morphology heterogeneity in favor of dense hepatosphere production (Fig. II-4 a,d). Third, measurement of total DNA content in the final products, as an indirect method for estimation of cell numbers, showed that the total cell production yield after the 20-day culture increased by 1.4–1.6-fold under the fully controlled conditions compared to the uncontrolled culture conditions ( $p < .01$ ; Fig. II-4 e).

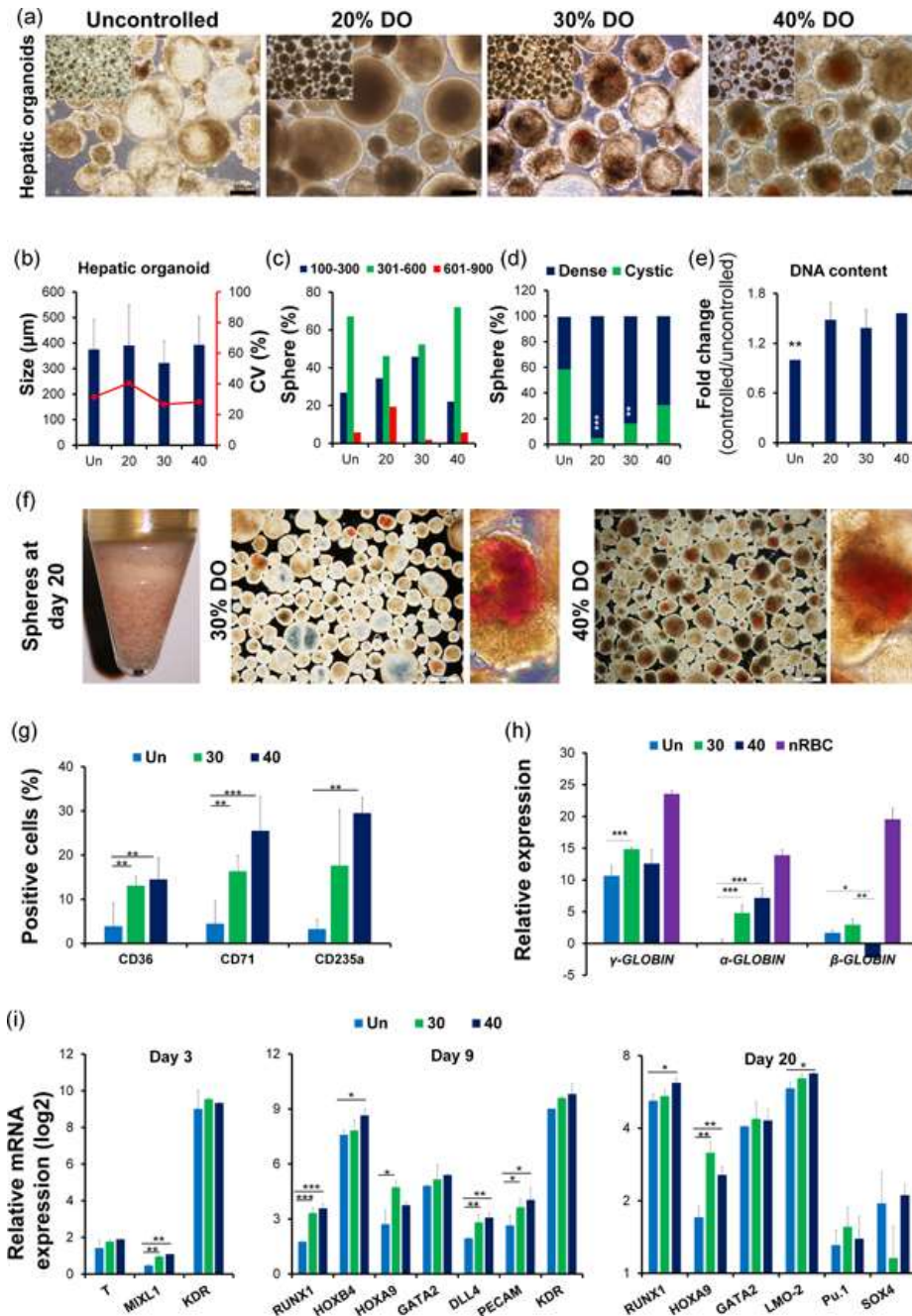


**Figure II-4 The effect of controlled DO on differentiation to hepatocyte-like cells.** (a) Morphology of hepatic organoids differed among the groups. Scale bar = 200 µm. (b, c) Mean size, CV, and size distribution of hepatic organoids. The mean size of the hepatic organoids was approximately 370 µm. The size distribution of the hepatic organoids showed a vastly distributed heterogeneous population, except under the 30% DO condition. About 70–150 spheres were counted in each experimental group. (d) Different appearance of hepatic organoids, dense or cystic. Hepatic organoids under the uncontrolled culture condition had a significantly more cystic population than the controlled condition. (e) Fold change of cells by total DNA concentration of hepatocytospheres. DNA concentration showed an increase in the total yield of cells produced under the controlled conditions. (f) Controlled bioreactor produced red clusters in hepatic organoids under 30% and 40% DO conditions. Morphology of red clusters inside the hepatic organoids. During differentiation of hepatoblasts to hepatocytes, we observed the appearance of several red clusters in spheres in the 30% or 40% DO conditions harvested after 20 days of culture. (g) Flow cytometry data for erythroid markers. Flow data revealed that a small

fraction of the dispersed hepatic organoids expressed erythroid precursor markers CD36, CD71, and CD235a. (h) qRT-PCR data for  $\alpha$ -,  $\gamma$ - and  $\beta$ -*globin* expressions showed that samples derived under 30% and 40% DO controlled conditions significantly expressed  $\alpha$ -*globin* and  $\gamma$ -*globin*, but not  $\beta$ -*globin*, compared to the uncontrolled condition. Nucleated RBCs derived from cord blood were used as the positive control that highly expressed all *globin* genes. (i) qRT-PCR data for expression of HSC markers during three differentiation steps. Data (mean  $\pm$  *SD*) were analyzed with ANOVA and Tukey's post hoc test. 20%, 30%, and 40%, differentiation under DO controlled culture conditions in stirred bioreactor; CV, coefficient of variation; DO, dissolved oxygen; nRBC, nucleated red blood cell; qRT-PCR, quantitative reverse-transcription polymerase chain reaction; Un, differentiation under uncontrolled culture condition. ( $n = 3$ . \* $p < .05$ ; \*\* $p < .01$ ; \*\*\* $p < .001$ )

Fourth, we observed the appearance of red cell clusters inside the hepatic endoderm aggregates under 30% DO and 40% DO controlled conditions, which was an interesting morphological change.

The red spots in the aggregates were visible from 11 to 13 days of the integrated hepatic differentiation and these areas were increasing onward until Day 20. We counted the hepatospheres with red spots at Day 20 and found that  $27.8 \pm 6.3\%$  and  $31.7 \pm 6.0\%$  of the total hepatospheres (small or large, cystic or dense) contained red blood cells under 30% and 40% DO, respectively (Fig. II-4 f). The red cells generated within the hepatospheres were characterized after harvesting all aggregates at the end of the differentiation process (Fig. II-4 g,h).

Flow cytometry analysis of these red cell populations revealed a relatively small population of cells that expressed early erythroblast markers CD36 and CD71. Approximately  $13 \pm 2\%$  of this population expressed CD36 in 30% DO and  $14.5 \pm 5\%$  in 40% DO, whereas  $16 \pm 4\%$  of cells expressed CD71 in 30% DO and  $25.5 \pm 7\%$  in 40% DO (Fig. II-4 g). CD235a, an erythroid precursor surface marker, was expressed in  $18 \pm 12\%$  of the hepatosphere cell population under 30% DO and in  $29.5 \pm 3.5\%$  of these cells under 40% DO. A significant difference existed in expressions of these markers under 30% DO and 40% DO compared to the uncontrolled culture condition, where approximately  $4 \pm 5\%$  of the erythroid markers were expressed with the same differentiation culture media and strategy. This data showed a direct effect of increased DO concentration on regulation of the hPSC fate inside the hepatic endoderm aggregates, which resulted in co-generation of hepatocytes and red blood cells.

We evaluated relative RNA expression of  $\alpha$ -,  $\gamma$ -, and  $\beta$ -*globin*, an erythroid specific marker, in hepatospheres generated under controlled and uncontrolled conditions, and compared the results to nucleated red blood cells (nRBC) derived from cord blood (positive control; Fig. II-4 h). Cell populations derived from 30% DO ( $p < .001$ ) and 40% DO ( $p < .05$ ) expressed fetal erythroid markers such as  $\alpha$ - and  $\gamma$ -*globin* at significantly higher levels than the uncontrolled condition.  $\beta$ -*globin*, an adult *HB*, was expressed at low levels in these cell populations. *HB* expression in the hepatic organoids was lower than in nRBC, which demonstrated the fetal nature of these generated erythroid cells within the hepatospheres. Quantitative reverse-transcription polymerase chain reaction (qRT-PCR) analysis was performed on Days 3, 9, and 20 to assess the temporal expressions of the mesoderm and hematopoietic markers at 30% and 40% DO.

*MIXL1*, a hematopoiesis promoter and mesoendodermal marker <sup>26</sup>, upregulated significantly at Day 3 of differentiation under the fully controlled culture condition (Fig. II-4 i). However, the expressions of the mesodermal and hematopoiesis markers, *T* or *Brachyury* and *KDR* <sup>27-29</sup> did not change significantly at Day 3. Day 9 gene expression results showed that *RUNX1*, *HOXA9*, *HOXB4*, *DLL4*, and *PECAM* were significantly upregulated under controlled conditions compared to the uncontrolled condition. *RUNX1* is a master regulator of hematopoiesis, which is essential in the initial and final stages of hematopoiesis <sup>30</sup>. *HOXA9* <sup>31</sup> and *HOXB4* are important for hematopoietic stem cell (HSC) fate determination <sup>32</sup>. *DLL4* and *PECAM* are important for both HSC maintenance and erythroid lineage commitment <sup>32</sup>.

Expression analysis of the cells at Day 20 showed a significant increase in *LMQ-2* expression (HSC and erythropoiesis marker <sup>34</sup>) under controlled conditions compared to the uncontrolled culture condition (Fig. II-4 i).

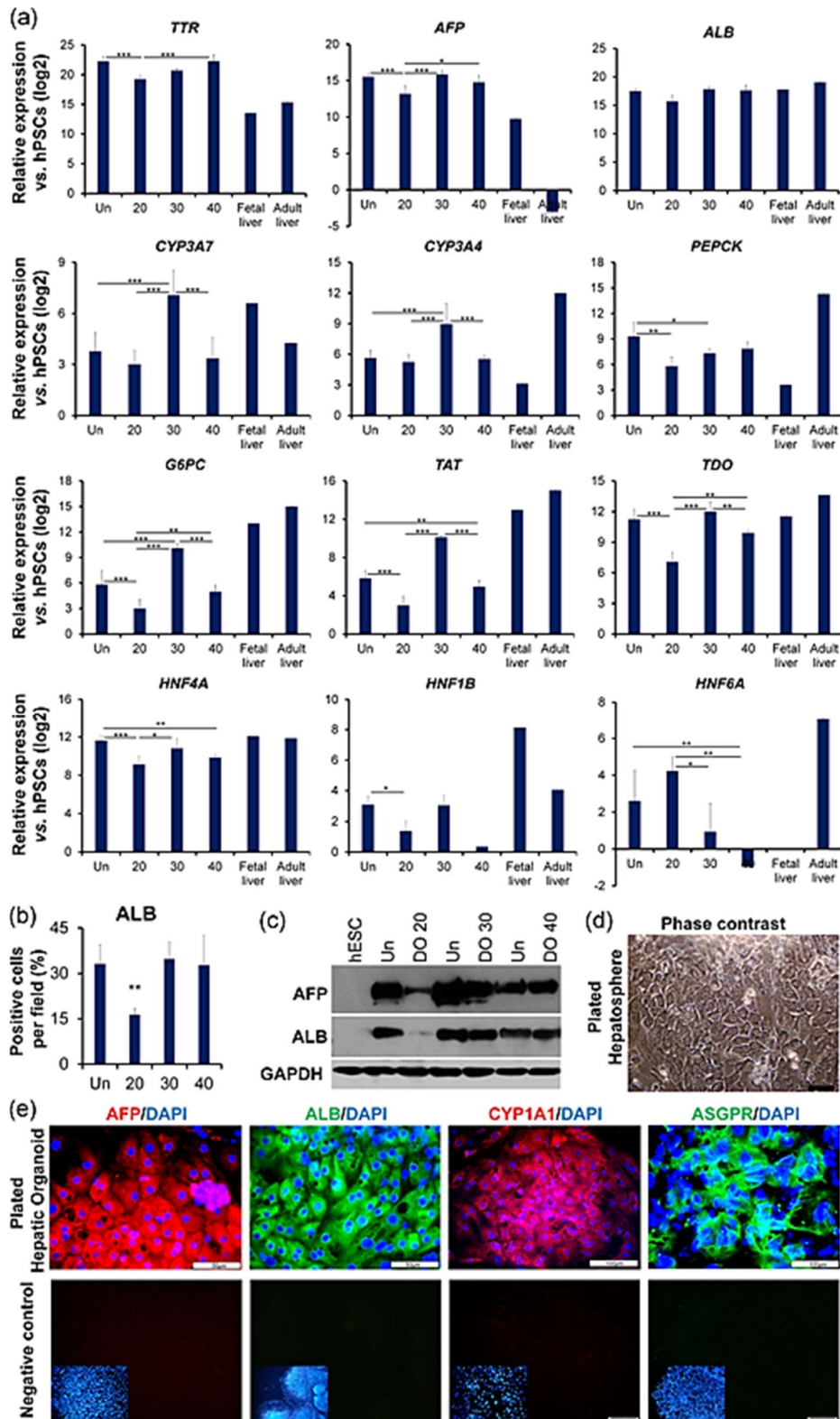


**Figure II-5 The gene and protein expression of the hepatic organoids.** (a) Gene expression analysis of hepatic organoids showed that hepatic gene expression in 20% DO was significantly lower than the uncontrolled condition. Expression of some mature genes in the 30% DO condition was significantly higher than under the uncontrolled condition. (b) The percentage of ALB-positive cells in the hepatic organoid cell population was calculated by counting positive cells from different immunofluorescent

images of sectioned hepatospheres generated in 30% DO. (c) Western blot for AFP and ALB expression in hepatic organoids. (d) Representative phase contrast images of plated hepatic organoid. (e) Immunofluorescent staining of plated hepatic organoids AFP, ALB, CYP1A1, and ASGPR as mature hepatic markers in the 30% DO condition. Scale bar = 50  $\mu$ m. Data (mean  $\pm$  *SD*) were analyzed with ANOVA and Tukey's post hoc test; *n* = 3. 20%, 30%, and 40%, differentiation under DO controlled culture conditions; AFP, -fetoprotein; ALB, albumin. ANOVA, analysis of variance; DAPI, 4',6-diamidino-2-phenylindole; DO, dissolved oxygen; GAPDH, glyceraldehyde 3-phosphate dehydrogenase; Un, differentiation under uncontrolled culture condition. \**p* < .05; \*\**p* < .01; \*\*\**p* < .001 In contrast to 30% DO, expressions of other hepatic markers (CYP3A7, CYP3A4, PEPCK, G6PC, TAT, and TDO) significantly downregulated in 20% DO and TAT significantly downregulated in 40% DO compared to the uncontrolled culture condition (Fig. II.5a). We also evaluated hepatic nuclear factor expressions in the differentiated cells. HNF4A and HNF1B had significantly lower expressions in the 20% and 40% DO conditions compared to the uncontrolled condition, as well as HNF6A expression at 30% and 40% DO compared to the uncontrolled and 20% DO conditions (Fig. II-5 a).

There were no significant changes in expressions of *PU.1* (marker for myeloid or lymphoid precursors cells) <sup>35</sup>, *SOX4* <sup>36</sup>, *GATA2* (HSC and erythroid lineage) <sup>37</sup>, and hepatoblast markers (Fig. II-4 i) <sup>27</sup>. These results indicated that the DO concentration regulated the fate of the hPSC aggregates through endoderm as well as mesoderm induction. This regulation was concentration dependent. Regulation of DO at higher (30%) air saturation resulted in partial generation of mesoderm cells, an erythroid lineage, and subsequently red blood cells in addition to endodermal, hepatic endoderm, and hepatic cells.

We quantified the hepato-specific gene expressions of the differentiated cells after 20 days of integrated differentiation and found that hepatocyte cells were generated under all the tested conditions and they expressed the basic hepatic markers *TTR*, *AFP* and *ALB*. The expression levels of these basic hepatic markers were comparable to fetal liver expression levels; however, they were not similar to the adult liver expression pattern because *AFP* is not normally expressed in the adult liver (Fig. II-5 a). Gene expression analysis results showed that fully controlled integrated differentiation at 30% DO resulted in the highest expression of important mature hepatic markers (*CYP3A*, *G6PC*) compared to the other DO concentrations and the uncontrolled culture condition, which provided evidence for the enhanced maturation and functionality of these generated cells (*p* < .001).

We attempted to conduct a cell population study of the generated hepatospheres with different treatments. However, we were unable to dissociate the hepatospheres into viable single cell populations for flow cytometry analysis when we used different enzymatic or mechanical

treatments or their combinations because of the highly intact structure of these hepatospheres. We hypothesized that the hepatospheres became intact in response to dynamic shear stress in the stirred bioreactor by the secretion of the ECM around the spheres. To obtain a rough estimate of the number of ALB-positive cells in the hepatic organoids, we counted the ALB-positive cells in different immunofluorescent images of the cross-sectioned hepatospheres. The results showed that about 35% of the population per microscopic field were ALB-positive under the 30% DO condition (Fig. II-5b and S1B) and were dispersed in all hepatosphere sizes and morphologies (Fig. II-S1B). The ALB-positive cells were significantly less under the 20% DO condition compared with the other groups ( $p < .05$ ; Fig. II-5b and S1B).

Data from western blot analysis also confirmed the expressions of AFP and ALB in all the trials (Fig. II-5 c). Quantitative analysis showed significantly lower expressions of AFP ( $p < 0.05$ ) and ALB ( $p < .01$ ) in the 20% DO group compared to the uncontrolled, 30% DO, and 40% DO groups. These markers had similar expression patterns in the 30% DO and 40% DO groups (Fig. II-S3 B). To assess the morphology of hepatocytes generated within hepatospheres under the two-dimensional (2D) culture condition, we plated hepatospheres that had been generated under the 30% DO condition on Matrigel-coated plates. After 3 days of plating, polygonal cells with large nuclei had migrated from each hepatosphere (Fig. II-5 d). We observed that they expressed AFP, ALB, CYP1A1, and ASGPR as demonstrated by immunostaining (Fig. II-5e).

These results demonstrated the co-generation of functional fetal hepatocyte-like cells and red blood cell populations within hepatospheres after 20 days of integrated differentiation under the 30% and 40% DO concentrations. Thus, we called these hepatospheres fetal-like hepatic organoids because of their similar cell population and functionality to the human fetal liver, which is mainly populated by these two cell types.

To further evaluate the functionality of the generated hepatocyte-like cells within these organoids, we analyzed the metabolic activity of these cells by exploring the secretion profiles

of hepatic specific metabolites in samples collected from hepatic organoid conditioned medium after Day 20 of differentiation (Fig. II-6 a–d).

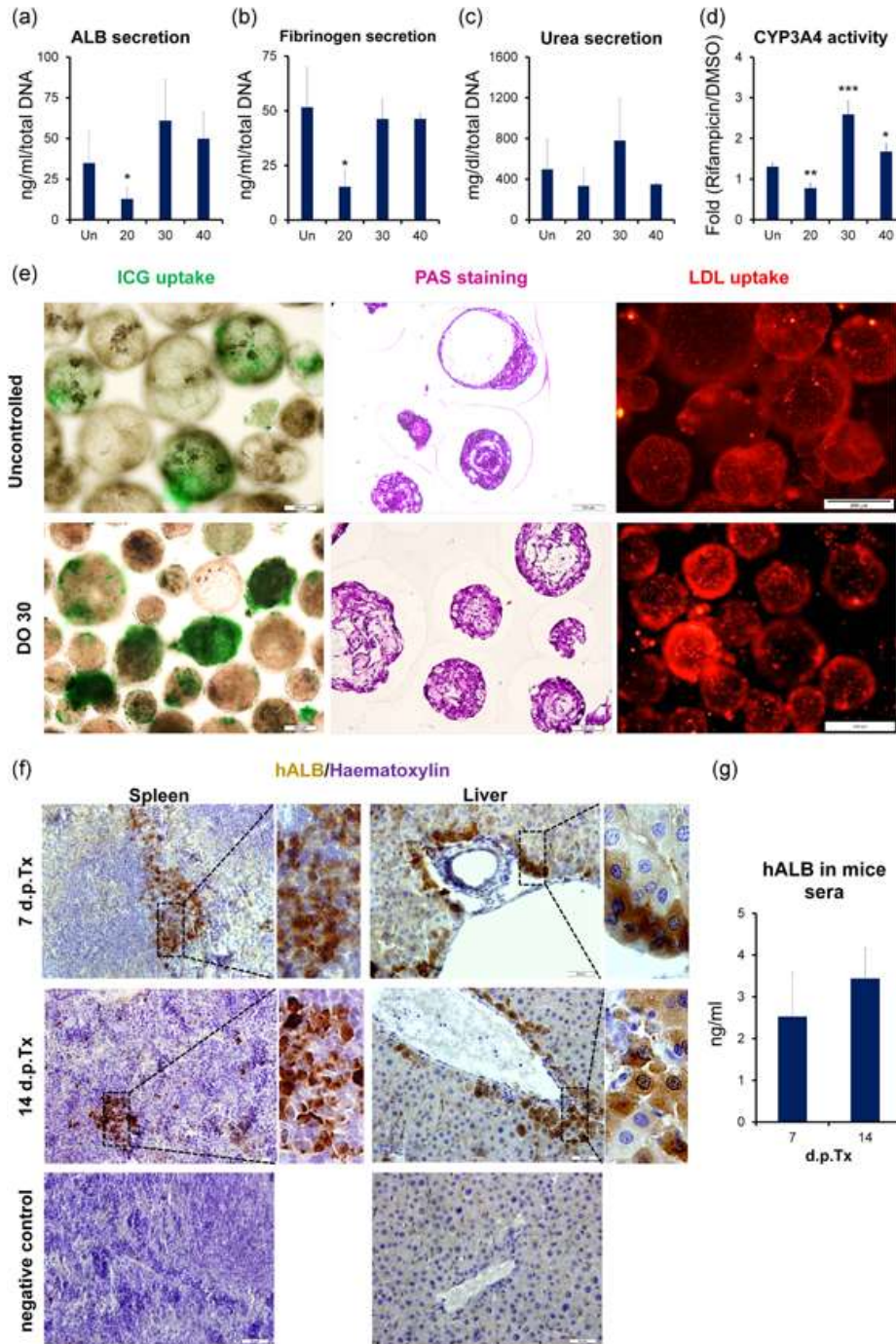


**Figure II-6 The functional activity of hepatic organoids.** The hepatic organoids performed major hepatic functions. (a) ALB and (b) fibrinogen secretion. ALB and fibrinogen secretions decreased significantly in the 20% DO. (c) Urea secretion. (d) Evaluation of the detoxification activity. Data showed that CYP3A4 enzyme activity increased significantly in response to rifampicin compared to DMSO as the control group under 30% DO and it reduced under 20% DO. (e) Representative images for uptake of LDL, stored glycogen in their cytoplasm, and ICG under the uncontrolled culture condition and 30% DO. Scale bar = 100  $\mu$ m. (f) Engraftment of hepatic organoids cells derived under 30% DO in mice

spleen. Representative immunohistochemistry images showed the transplanted hepatic organoid cells distributed as clusters or single human ALB-positive cells in the spleen and liver of mice at days 7 and 14 post-transplantation. (g) Engrafted cells secreted human ALB into mice sera at Days 7 and 14. Data are mean  $\pm$  *SD* and analyzed with ANOVA and Tukey's post hoc test;  $n = 3$ ; 20%, 30% and 40%, differentiation under DO controlled culture conditions; AFP, alpha-fetoprotein; ALB, albumin. ANOVA, analysis of variance; DO, dissolved oxygen; Un, differentiation under uncontrolled culture condition. \*\* $p < .01$ ; \*\*\* $p < .001$

The hepatic organoids generated under 30% and 40% DO had relatively higher secretion levels of ALB (Fig. II-6 a) and fibrinogen (Fig. II-6 b) compared to the 20% and uncontrolled conditions. In addition, hepatospheres and hepatic organoids derived under all tested conditions had the ability to produce urea as a key and essential metabolic activity of hepatocytes (Fig. II-6 c).

The drug detoxification ability of hepatic organoids was also tested by analysis of CYP3A4 activity, as an important enzyme of xenobiotic metabolism. We treated the hepatic organoids with rifampicin, a CYP3A4 inducer, for 3 days and compared the results to the DMSO control group, which represented basal CYP3A4 enzyme activity in the hepatocytes.

The results showed a significant fold increase in CYP3A4 enzyme activity compared to DMSO in the 30% DO condition and a decrease in the 20% DO (Fig. II-6 d). Further evaluation of these cells in the 30% DO condition showed that they had additional hepatic specific functions of indocyanine green (ICG) and low-density lipoprotein (LDL) uptake, as well as glycogen storage in their cytoplasm in the uncontrolled culture condition (Fig. II-6 e).

Uptake results showed that about  $59.0 \pm 9.9\%$  and  $71.1 \pm 13.5\%$  of the hepatospheres could uptake ICG and became partially or entirely green under the uncontrolled and 30% DO conditions, respectively. Additionally,  $76.5 \pm 5.6\%$  of the hepatospheres could uptake LDL under the uncontrolled culture condition and  $78.4 \pm 7.6\%$  could uptake LDL under the 30% DO condition.

Altogether, differentiation under the 30% DO controlled bioreactor condition resulted in the generation of fetal-like hepatic aggregates that had a more homogenous morphology and diameter size distribution, higher cell yield, hepatic metabolic activity

(particularly *CYP* activity), hepatic functions, and gene expression compared with the other DO concentrations and the uncontrolled culture condition.

Finally, to demonstrate the in vivo functionality of hepatic organoids generated under the fully controlled condition, we transplanted the whole organoids derived under the 30% DO condition into the spleen of an acute liver mouse model. We observed a human ALB-positive cell population that was distributed as clusters or single cells within the mice spleens at 7- and 14-day post-transplantation (Fig. II-6 f). Most human ALB-positive cells were positioned around the large capillaries in the liver on days 7 and 14 post-transplantation (Fig. II-6 f).

These cells secreted  $2.5 \pm 1$  ng/ml human ALB into the mice sera 7 days post-transplantation and  $3.4 \pm 0.7$  ng/ml human ALB into the mice sera 14 days post-transplantation (Fig. II-6g). The results indicated that the human fetal-like hepatic organoids had successfully engrafted into the spleen and liver of the mouse model and had a demonstrated ability to secrete human ALB into the mice sera.

***Reproducibility of the developed integrated hepatic differentiation process at the 30% DO concentration***

Finally, we validated the reproducibility of the developed integrated differentiation process by conducting three independent bioreactor runs under the 30% DO concentration. Similar gene expression profiles and culture outcomes confirmed the reproducibility of this established protocol (Fig. II-7 a). We showed that increasing the integrated hepatic differentiation working volume from 50 to 150 ml without key bioprocess parameter controls (DO and pH) caused a significant decrease in mature hepatic differentiation, which could be overcome by conducting the process at 30% DO under fully controlled culture conditions in the stirred bioreactor (Fig. II-7 b,c).

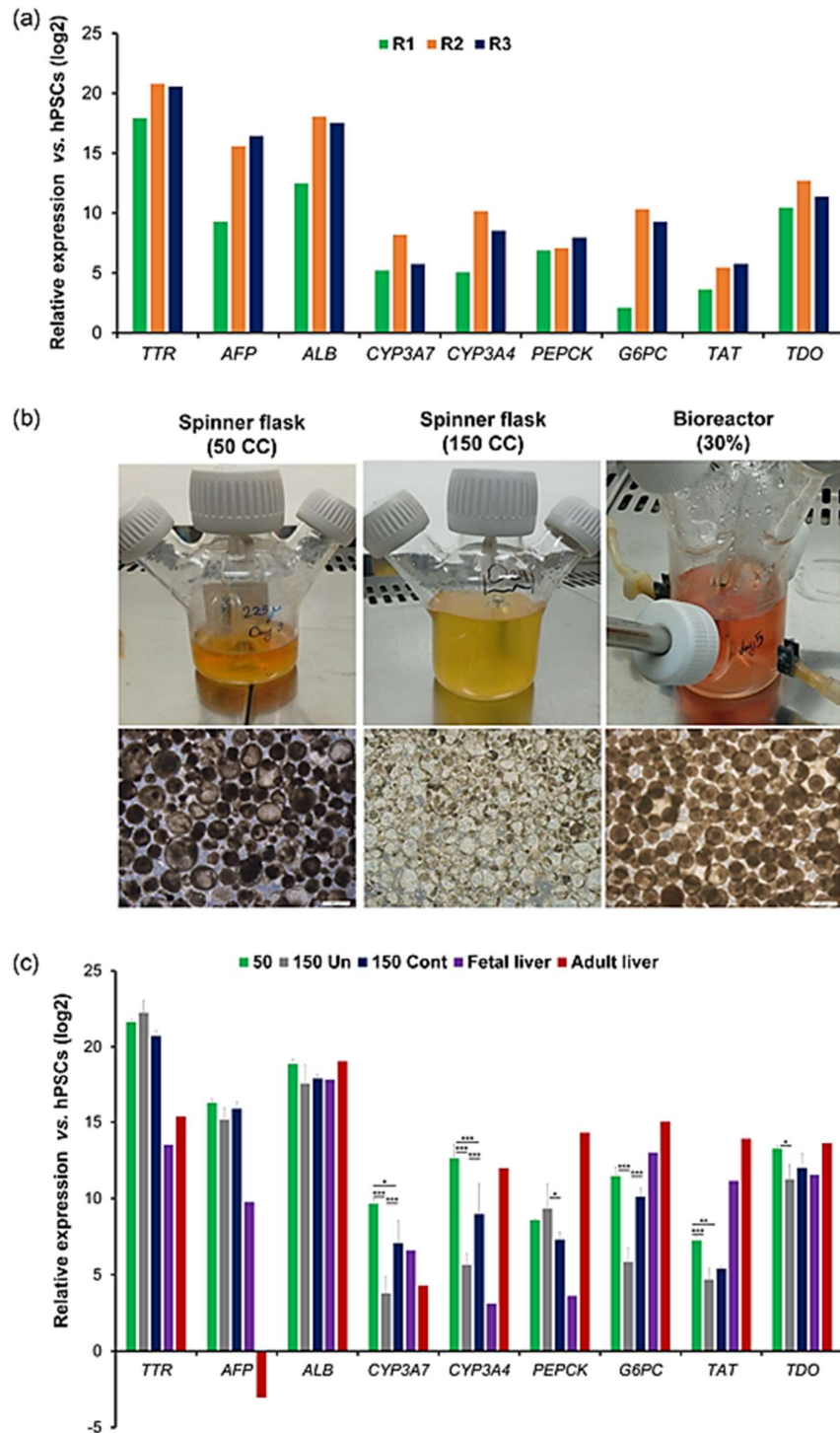


**Figure II-7 Validation of the developed integrated hepatic differentiation protocol at 30% DO concentration.** (a) Important hepatic marker gene expressions in fetal-like hepatic organoids generated with three different bioreactor runs at 30% DO concentration. (b) Production of hepatic organoids under uncontrolled (50 and 150 ml) and fully controlled conditions (30% DO, 150 ml). (c) Their important hepatic marker gene expression compared to the fetal and adult livers. Data (mean  $\pm$  SD) were analyzed with ANOVA and Tukey's post hoc test;  $n = 3$ . ANOVA, analysis of variance; DO, dissolved oxygen. \* $p < .01$ ; \*\* $p < .01$ ; \*\*\* $p < .001$

## Discussion

Previously, we developed a scalable culture system for large-scale production of hepatocytes from hPSC aggregates under a dynamic suspension culture. However, that protocol suffered from low differentiation efficacy, decreased hepatosphere size, lack of a homogeneous morphology (approximately 50% cystic and 50% dense spheres, and poor productivity<sup>14</sup>. It has been reported that cystic or dense hepatospheres generated under uncontrolled culture conditions exhibited differences in marker expression levels and distribution of expressed spatial markers within the hepatospheres. For instance, dense hepatospheres contained higher percentages of hepatocytes that expressed mature specific markers, whereas the same markers were downregulated in hepatocytes populated in cystic hepatospheres. Subsequently, we attempted to improve the efficacy of this protocol by establishing a cost-effective, efficient differentiation process to optimize the size of the initial hPSC aggregates before starting integrated hepatic differentiation under a dynamic suspension culture in a 50 ml working volume. Optimization trials resulted in improved efficacy of the differentiation protocol with decreased cystic hepatospheres formation with poor functionality and improved hepatocyte function inside the cystic hepatospheres<sup>15</sup>. We attempted to scale up this protocol for large scale production of functional hepatocyte-like cells from hPSCs. However, scale-up trials with only three-fold (150 ml) working volume with the same improved and optimized differentiation protocol were not successful because of a significant increase in cystic hepatosphere generation and decreased expressions of some important mature hepatic markers along with their significant downregulation during the integrated differentiation process. Therefore, we determined that the poor scalability of the uncontrolled culture condition was a critical issue that should be addressed before translating established protocols to clinical or commercial applications. Here, we monitored the key bioprocess parameters during integrated and stepwise hepatic differentiation in the bioreactor with 150 ml working volume under an uncontrolled culture condition. It was our intent to explore possible limiting parameters that resulted in the generation of hepatospheres with low functionality. We

observed that pH values and DO concentration were largely unstable and had a decreasing trend during integrated hepatic differentiation. Practically, the DO concentration profile suddenly decreased during the hepatoblast phase (day 9 of culture) as determined by online monitoring of these parameters during 20 days of culture. We hypothesized that the DO concentration was a limiting and important factor during the hepatocyte expansion/maturation phase, which possibly affected the efficacy and productivity of the hepatic differentiation process. Theoretically, the amount of oxygen available for cells can become limited when expansion and integrated differentiation is conducted with large culture working volumes (i.e., more than 1 L) under dynamic suspension without DO and pH control because of a lower cell culture surface to volume ratio (e.g., spinner flask culture). Under uncontrolled cultures, the amount of DO largely depends on culture vessel geometry, agitation speed, liquid/air interface area to depth of the medium ratio, cell density, cellular respiration, and oxygen level in the incubator 38,39.

Several studies have demonstrated the critical effects of the oxygen concentration/gradient as a developmental morphogen and cell fate modulator (e.g., stem cell maintenance or cellular differentiation) in a concentration-dependent manner for neural, cardiomyocyte, endoderm, and mesodermal lineages, which were mainly under static culture conditions with limited working volumes 40-42.

Regarding hepatic differentiation of hPSCs, it has been shown that a hypoxic or normoxic culture condition can regulate the differentiation process efficacy and outcome. Hypoxic culture conditions can promote mesoderm, endoderm, and hepatoblast differentiation; however, it has an adverse effect on hepatic endoderm cell proliferation and maturation, which will lead to inhibition of mature hepatocyte induction in a 2D adherent culture 43. The hypoxic culture condition activates hypoxia-inducible factors (HIF-1 $\alpha$  molecules that control and regulate stem cell behavior and regulate the Wnt, Notch, and TGF $\beta$  signaling pathways) 44 that promote differentiation of hepatoblasts to a cholangiocyte fate 21. However, it has been shown to decrease the metabolism, functional polarization, gene expression, and drug

clearance of hepatocytes 45. CYP3A4, a hepatic maturation marker, has been shown to downregulate under hypoxic conditions and recover under normoxic culture conditions 43. Thus, a hypoxic culture condition (2%–5% O<sub>2</sub>) is not efficient for the entire hepatic differentiation process. Proliferation of hepatic progenitors and their further maturation would require a normoxic culture condition (20% O<sub>2</sub>).

The significant effect of DO concentration on the integrated differentiation process was reported for different cell types, including neural cells 46, red blood cells 47, and skin-derived precursor cells 48 that were produced in fully controlled bioreactors. However, for liver and integrated hepatic differentiation of hPSCs, most studies were conducted in small scale culture systems under uncontrolled culture conditions in an attempt to explore the role of the oxygen concentration/gradient in hepatic differentiation and functionality, liver development, and primary hepatocyte maintenance and function.

In terms of the effect of oxygen concentration on hepatocyte structure and metabolic activity in human liver tissue, an oxygen concentration gradient exists in the adult liver lobule that induces the formation of three different zones in the liver for over 500 metabolic activities. Around the portal vein, the oxygen concentration is approximately 60–65 mmHg, whereas it decreases to 30–35 mmHg in regions closer to the central vein <sup>16</sup>. Gluconeogenesis and ureagenesis occur in the majority of periportal hepatocytes, whereas the pericentral zone is the site of glycolysis and detoxification activities <sup>16</sup>.

However, there is no report about the effect of physiological levels of DO concentrations during the integrated hepatic differentiation process and large-scale production of hPSC derived hepatocytes in fully controlled bioreactors. Therefore, we evaluated three DO concentration levels (20%, 30%, and 40% equal to 30, 45, and 60 mmHg at 37°C, respectively) in the range of human liver tissue oxygen concentration levels (30–60 mmHg pO<sub>2</sub> at different regions) combined with an automatic pH control of 7.1±0.1 to explore the effect of these DO concentrations on hepatic organoid formation.

Our data showed that high oxygen concentrations (30% and 40% DO) had no significant effects on endoderm and hepatic endoderm differentiation efficacy compared to the uncontrolled culture condition. The 20% DO concentration generated hepatic endoderm that had poor functionality. The uncontrolled culture condition with 150 ml working volume had a DO concentration above 50%–70% after media refreshment during endoderm and hepatic endoderm generation; therefore, it could not be considered a limiting factor. Thus, the lower DO concentration (20%) compared to other trials generated hepatic endoderm with lower specific marker expressions and a DO concentration of approximately 30% employed during the integrated hepatic endoderm generation phase.

During the hepatic endoderm proliferation and maturation phase, the 30% DO concentration generated functional fetal-like liver organoids that had a uniform size and better homogeneity. Interestingly, different DO concentrations also resulted in hepatocytes that were generated with different metabolic activities and functionalities or mixed cell populations. For instance, there were significantly greater G6PC gene expression, which functions in the gluconeogenesis and glycogenolysis processes, and CYP3A7 and CYP3A4 activities (as xenobiotic factors responsible for the detoxification process) in the 30% DO, which resembled the oxygen concentration in the pericentral liver zone. It was reported that rat hepatocytes cultured in a 30% DO controlled bioreactor resulted in long-term maintenance of metabolic activity compared to the uncontrolled culture condition <sup>49</sup>.

At 40% DO, there was no difference in the expression levels of the related genes compared to the uncontrolled condition, whereas more erythrocyte cells were produced compared to 30% DO due to induction of erythroid cell generation by the higher DO concentration. Thus, hepatocytes with special zone characteristics might be produced if we extended the differentiation process for a longer period and regulated the oxygen concentration at different levels.

Another important outcome of this study is the regulation effect of the oxygen concentration (30% and 40% DO) on hPSCs fate and generation of hepatic organoids that consisted of red

blood cells and functional hepatocyte-like cells with similar characteristics to the human fetal liver cell population <sup>24</sup>. During embryogenesis, primary erythropoiesis transfers from the yolk sac to the fetal liver and definitive erythropoiesis occurs <sup>50</sup>. The resident hepatoblasts secrete erythropoietic cytokines such as stem cell factor (SCF) and erythropoietin to promote differentiation of hematopoietic stem cells to erythroid cells and produce red blood cells <sup>51</sup>. Although the production of red blood cells in conjunction with hepatocytes can result in decreased hepatocyte production, it resulted in improved functionality of the hepatocytes generated under 30% DO with higher CYP activities, which was possibly due to cell-cell interaction and cross-talk between these two cell populations. HSC secrete OSM, which promotes hepatocyte maturation <sup>52</sup>. We demonstrated that erythroblasts produced within our hepatic organoids under 30% and 40% DO conditions have a fetal identity similar to cells generated during fetal liver development.

Therefore, we hypothesized that this was a direct result of regulating oxygen concentrations over 30% DO and inducing co-generation of mesoderm and endoderm cells within the hPSCs aggregates from day 3 of the integrated differentiation process. This was confirmed by qRT-PCR analysis of mesoderm related genes, which showed significant upregulation of *MIXL1* under 30% and 40% DO compared to the uncontrolled culture condition, as well as T to a lesser extent on day 3 of differentiation. Previous studies showed that a hypoxic culture condition <sup>53</sup> and treatment with CHIR99021 <sup>54</sup> could promote mesoderm and hemangioblast differentiation of hPSCs. We had one day of CHIR treatment in our protocol that mainly induced mesoendoderm generation and activin treatment that mainly promoted endoderm differentiation <sup>15</sup>. We believe that the higher DO concentration regulated the CHIR treated/mesoendoderm induced hPSC aggregate fate and induced mesoderm differentiation in parallel with endoderm differentiation. Jin et al. reported similar results and concluded that reactive oxygen species enhanced differentiation of human embryonic stem cells into a mesendodermal lineage under a static culture condition <sup>55</sup>.

The fully controlled culture at 30% and 40% DO resulted in enhanced expressions of some hematopoietic progenitor cell related genes (*RUNX1*, *HOXA9*, *HOXB4*, *DLL4*, and *PECAM*) compared to the uncontrolled culture condition on day 9 of culture. However, most of these hematopoietic specific markers and receptors are commonplace with hepatic progenitor cells and could not be solely related to erythropoietic differentiation. This similarity made it difficult to characterize HSC generation during integrated hepatic differentiation. It has been reported that hepatic progenitor cells derived from hPSCs also expressed CD31, CD133, and GATA2 markers that are also related to hematopoietic cell markers <sup>29</sup>. Nevertheless, the expression of erythroid related genes was higher under controlled conditions from the hepatic endoderm generation step to further maturation and generation of functional hepatic organoids.

Finally, we injected whole organoids into the spleens of mice that had induced acute liver injuries to assess the transplantability of these fetal liver organoids that were generated under the fully controlled 30% DO condition. The results showed the existence of viable and metabolically active human ALB-positive cells and clusters in the spleens of this animal model 7- and 14-days post-transplantation, along with their increased metabolic activity as demonstrated by increased levels of human ALB in mice sera two weeks after the transplantation.

## **Conclusions**

We have developed a scalable platform for fully controlled large-scale production of hepatic organoids by optimizing DO concentration during the integrated differentiation process (Fig. II-8). Our data emphasize that oxygen concentration is a very important bioprocess parameter that regulates proliferation, differentiation efficacy, and generated hepatocyte metabolic activity. Thus, this parameter should be carefully optimized during the integrated hepatic differentiation process for a scalable production of hepatic cells. The results show that the oxygen concentration regulates the fate of these hPSC aggregates by inducing simultaneous endoderm and mesoderm in a concentration-dependent manner, which results

in the generation of fetal-like hepatic organoids and red blood cells. The functionality and metabolic activities of hepatocytes were improved at 30% DO. The oxygen switching during differentiation could be used to generate hepatocytes with different metabolic activity profiles that mimic those different zones of liver tissue. This integrated hepatic differentiation strategy might facilitate large-scale production of organoids for potential medical applications, fabrication of liver tissues/organs in the laboratory, and drug discovery applications.

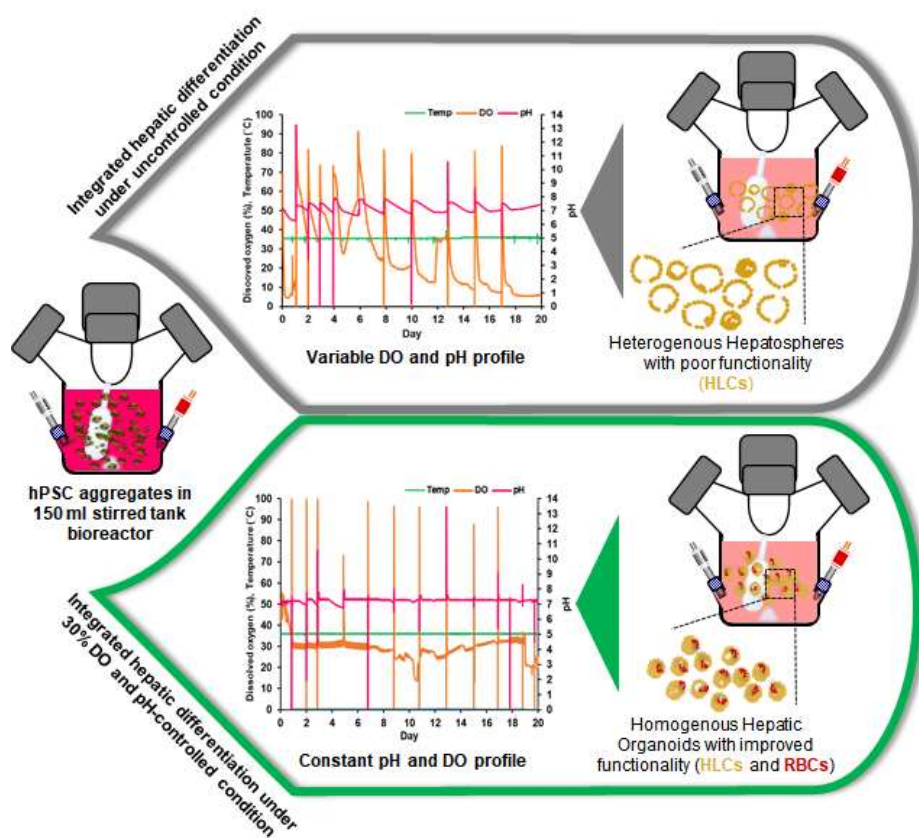


**Figure II-8** Employing fully controlled dissolved oxygen (DO) at physiologically relevant concentration level similar to liver tissue and pH during integrated differentiation process led to regulating the fate of human pluripotent stem cell (hPSC) aggregates and generation of fetal-like hepatic organoids including red blood cells (RBCs). The homogeneity, functionality, and metabolic activities of hepatocyte-like cells (HLCs) were improved at 30% DO including improved CYP activity within organoids.

## Acknowledgments

We express our appreciation to Hassan Ansari at Royan Institute for his technical assistance. This study was funded by Royan Institute, the Iranian Council of Stem Cell Research and Technology, the Iran National Science Foundation (INSF), and the Ministry of Health and Medical Education (no. 56700/147) to H.B.

## References

- 1 Olson, J. C. Acute-on-chronic and Decompensated Chronic Liver Failure: Definitions, Epidemiology, and Prognostication. *Crit Care Clin* 32, 301-309, doi:10.1016/j.ccc.2016.02.001 (2016).
- 2 Alwahsh, S. M., Rashidi, H. & Hay, D. C. Liver cell therapy: is this the end of the beginning? *Cell Mol Life Sci* 75, 1307-1324, doi:10.1007/s00018-017-2713-8 (2018).
- 3 Dutkowski, P., Linecker, M., DeOliveira, M. L., Mullhaupt, B. & Clavien, P. A. Challenges to liver transplantation and strategies to improve outcomes. *Gastroenterology* 148, 307-323, doi:10.1053/j.gastro.2014.08.045 (2015).
- 4 Shukla, A., Vadeyar, H., Rela, M. & Shah, S. Liver Transplantation: East versus West. *J Clin Exp Hepatol* 3, 243-253, doi:10.1016/j.jceh.2013.08.004 (2013).
- 5 Yamamoto, J., Udono, M., Miura, S., Sekiya, S. & Suzuki, A. Cell Aggregation Culture Induces Functional Differentiation of Induced Hepatocyte-like Cells through Activation of Hippo Signaling. *Cell Rep* 25, 183-198, doi:10.1016/j.celrep.2018.09.010 (2018).
- 6 Zhang, J. et al. A decade of progress in liver regenerative medicine. *Biomaterials* 157, 161-176, doi:10.1016/j.biomaterials.2017.11.027 (2018).
- 7 Kwok, C. K. et al. Scalable stirred suspension culture for the generation of billions of human induced pluripotent stem cells using single-use bioreactors. *J Tissue Eng Regen Med* 12, e1076-e1087, doi:10.1002/term.2435 (2018).
- 8 Abbasalizadeh, S., Larijani, M. R., Samadian, A. & Baharvand, H. Bioprocess development for mass production of size-controlled human pluripotent stem cell aggregates in stirred suspension bioreactor. *Tissue Eng Part C Methods* 18, 831-851, doi:10.1089/ten.TEC.2012.0161 (2012).
- 9 Takebe, T. et al. Vascularized and functional human liver from an iPSC-derived organ bud transplant. *Nature* 499, 481-484, doi:nature12271 [pii] 10.1038/nature12271 (2013).
- 10 Takebe, T. et al. Massive and Reproducible Production of Liver Buds Entirely from Human Pluripotent Stem Cells. *Cell Rep* 21, 2661-2670, doi:10.1016/j.celrep.2017.11.005 (2017).
- 11 Pettinato, G. et al. Generation of fully functional hepatocyte-like organoids from human induced pluripotent stem cells mixed with Endothelial Cells. *Sci Rep* 9, 8920, doi:10.1038/s41598-019-45514-3 (2019).
- 12 Sgodda, M. et al. A Scalable Approach for the Generation of Human Pluripotent Stem Cell-Derived Hepatic Organoids with Sensitive Hepatotoxicity Features. *Stem cells and development* 26, 1490-1504, doi:10.1089/scd.2017.0023 (2017).
- 13 Tzanakakis, E. S., Hess, D. J., Sielaff, T. D. & Hu, W. S. Extracorporeal tissue engineered liver-assist devices. *Annu Rev Biomed Eng* 2, 607-632, doi:10.1146/annurev.bioeng.2.1.607 (2000).

- 14 Vosough, M. et al. Generation of functional hepatocyte-like cells from human pluripotent stem cells in a scalable suspension culture. *Stem Cells Dev* 22, 2693-2705, doi:10.1089/scd.2013.0088 (2013).
- 15 Farzaneh, Z., Najarasl, M., Abbasalizadeh, S., Vosough, M. & Baharvand, H. Developing a Cost-Effective and Scalable Production of Human Hepatic Competent Endoderm from Size-Controlled Pluripotent Stem Cell Aggregates. *Stem cells and development* 27, 262-274, doi:10.1089/scd.2017.0074 (2018).
- 16 Kietzmann, T. Metabolic zonation of the liver: The oxygen gradient revisited. *Redox Biol* 11, 622-630, doi:S2213-2317(16)30449-9 [pii] 10.1016/j.redox.2017.01.012 (2017).
- 17 Jungermann, K. & Kietzmann, T. Oxygen: modulator of metabolic zonation and disease of the liver. *Hepatology* 31, 255-260, doi:10.1002/hep.510310201 (2000).
- 18 Nishikawa, M. et al. Optimal oxygen tension conditions for functioning cultured hepatocytes in vitro. *Artif Organs* 20, 169-177, doi:10.1111/j.1525-1594.1996.tb00723.x (1996).
- 19 Khakpour, S. et al. Oxygen transport in hollow fibre membrane bioreactors for hepatic 3D cell culture: A parametric study. *Journal of Membrane Science* 544, 312-322 (2017).
- 20 Pimton, P. et al. Hypoxia enhances differentiation of mouse embryonic stem cells into definitive endoderm and distal lung cells. *Stem Cells Dev* 24, 663-676, doi:10.1089/scd.2014.0343 (2015).
- 21 Ayabe, H. et al. Optimal Hypoxia Regulates Human iPSC-Derived Liver Bud Differentiation through Intercellular TGFB Signaling. *Stem Cell Reports* 11, 306-316, doi:10.1016/j.stemcr.2018.06.015 (2018).
- 22 Fonoudi, H. et al. A Universal and Robust Integrated Platform for the Scalable Production of Human Cardiomyocytes From Pluripotent Stem Cells. *Stem Cells Transl Med* 4, 1482-1494, doi:sctm.2014-0275 [pii] 10.5966/sctm.2014-0275 (2015).
- 23 Nemati, S., Abbasalizadeh, S. & Baharvand, H. Scalable Expansion of Human Pluripotent Stem Cell-Derived Neural Progenitors in Stirred Suspension Bioreactor Under Xeno-free Condition. *Methods in molecular biology* 1502, 143-158, doi:10.1007/7651\_2015\_318 (2016).
- 24 Dzierzak, E. & Speck, N. A. Of lineage and legacy: the development of mammalian hematopoietic stem cells. *Nat Immunol* 9, 129-136, doi:10.1038/ni1560 (2008).
- 25 Brooks, A. J., Hammond, J. S., Girling, K. & Beckingham, I. J. The effect of hepatic vascular inflow occlusion on liver tissue pH, carbon dioxide, and oxygen partial pressures: defining the optimal clamp/release regime for intermittent portal clamping. *The Journal of surgical research* 141, 247-251, doi:10.1016/j.jss.2006.10.054 (2007).
- 26 Ng, E. S. et al. The primitive streak gene *Mixl1* is required for efficient haematopoiesis and BMP4-induced ventral mesoderm patterning in differentiating ES cells. *Development* 132, 873-884, doi:10.1242/dev.01657 (2005).
- 27 Ziegler, B. L. et al. KDR receptor: a key marker defining hematopoietic stem cells. *Science* 285, 1553-1558, doi:10.1126/science.285.5433.1553 (1999).
- 28 Han, S., Goldman, O. & Gouon-Evans, V. Liver progenitor cell and KDR. *Cell Cycle* 13, 1051-1052, doi:10.4161/cc.28213 (2014).
- 29 Goldman, O., Cohen, I. & Gouon-Evans, V. Functional Blood Progenitor Markers in Developing Human Liver Progenitors. *Stem Cell Reports* 7, 158-166, doi:10.1016/j.stemcr.2016.07.008 (2016).
- 30 Yzaguirre, A. D., de Bruijn, M. F. & Speck, N. A. The Role of *Runx1* in Embryonic Blood Cell Formation. *Advances in experimental medicine and biology* 962, 47-64, doi:10.1007/978-981-10-3233-2\_4 (2017).
- 31 Ramos-Mejia, V. et al. *HOXA9* promotes hematopoietic commitment of human embryonic stem cells. *Blood* 124, 3065-3075, doi:10.1182/blood-2014-03-558825 (2014).

- 32 Forrester, L. M. & Jackson, M. Mechanism of action of HOXB4 on the hematopoietic differentiation of embryonic stem cells. *Stem Cells* 30, 379-385, doi:10.1002/stem.1036 (2012).
- 33 Ayllon, V. et al. The Notch ligand DLL4 specifically marks human hematoendothelial progenitors and regulates their hematopoietic fate. *Leukemia* 29, 1741-1753, doi:10.1038/leu.2015.74 (2015).
- 34 Baumann, C. I. et al. PECAM-1 is expressed on hematopoietic stem cells throughout ontogeny and identifies a population of erythroid progenitors. *Blood* 104, 1010-1016, doi:10.1182/blood-2004-03-0989 (2004).
- 35 Burda, P., Laslo, P. & Stopka, T. The role of PU.1 and GATA-1 transcription factors during normal and leukemogenic hematopoiesis. *Leukemia* 24, 1249-1257, doi:10.1038/leu.2010.104 (2010).
- 36 Laurenti, E. et al. The transcriptional architecture of early human hematopoiesis identifies multilevel control of lymphoid commitment. *Nat Immunol* 14, 756-763, doi:10.1038/ni.2615 (2013).
- 37 Vicente, C., Conchillo, A., Garcia-Sanchez, M. A. & Odero, M. D. The role of the GATA2 transcription factor in normal and malignant hematopoiesis. *Critical reviews in oncology/hematology* 82, 1-17, doi: 10.1016/j.critrevonc.2011.04.007 (2012).
- 38 Csete, M. Oxygen in the cultivation of stem cells. *Ann N Y Acad Sci* 1049, 1-8, doi:1049/1/1, 10.1196/annals.1334.001 (2005).
- 39 Wion, D., Christen, T., Barbier, E. L. & Coles, J. A. PO(2) matters in stem cell culture. *Cell Stem Cell* 5, 242-243, doi:S1934-5909(09)00394-4 [pii] 10.1016/j.stem.2009.08.009 (2009).
- 40 Niebruegge, S. et al. Generation of human embryonic stem cell-derived mesoderm and cardiac cells using size-specified aggregates in an oxygen-controlled bioreactor. *Biotechnol Bioeng* 102, 493-507, doi:10.1002/bit.22065 (2009).
- 41 Medley, T. L. et al. Effect of oxygen on cardiac differentiation in mouse iPS cells: role of hypoxia inducible factor-1 and Wnt/beta-catenin signaling. *PLoS One* 8, e80280, doi:10.1371/journal.pone.0080280 PONE-D-13-13205 [pii] (2013).
- 42 Horton, R. E. & Auguste, D. T. Synergistic effects of hypoxia and extracellular matrix cues in cardiomyogenesis. *Biomaterials* 33, 6313-6319, doi:S0142-9612(12)00617-5 [pii] 10.1016/j.biomaterials.2012.05.063 (2012).
- 43 van Wenum, M. et al. Oxygen drives hepatocyte differentiation and phenotype stability in liver cell lines. *J Cell Commun Signal* 12, 575-588, doi:10.1007/s12079-018-0456-4 (2018).
- 44 Bogaerts, E., Heindryckx, F., Vandewynckel, Y. P., Van Grunsven, L. A. & Van Vlierberghe, H. The roles of transforming growth factor-beta, Wnt, Notch and hypoxia on liver progenitor cells in primary liver tumours (Review). *Int J Oncol* 44, 1015-1022, doi:10.3892/ijo.2014.2286 (2014).
- 45 Kidambi, S. et al. Oxygen-mediated enhancement of primary hepatocyte metabolism, functional polarization, gene expression, and drug clearance. *Proc Natl Acad Sci U S A* 106, 15714-15719, doi:10.1073/pnas.0906820106 (2009).
- 46 Serra, M., Brito, C., Costa, E. M., Sousa, M. F. & Alves, P. M. Integrating human stem cell expansion and neuronal differentiation in bioreactors. *BMC Biotechnol* 9, 82, doi:1472-6750-9-82 10.1186/1472-6750-9-82 (2009).
- 47 Bayley, R. et al. The productivity limit of manufacturing blood cell therapy in scalable stirred bioreactors. *J Tissue Eng Regen Med* 12, e368-e378, doi:10.1002/term.2337 (2018).
- 48 Agabalyan, N. A. et al. Enhanced Expansion and Sustained Inductive Function of Skin-Derived Precursor Cells in Computer-Controlled Stirred Suspension Bioreactors. *Stem Cells Transl Med* 6, 434-443, doi:10.5966/sctm.2016-0133 (2017).
- 49 Miranda, J. P. et al. Towards an extended functional hepatocyte in vitro culture. *Tissue Eng Part C Methods* 15, 157-167, doi:10.1089/ten.tec.2008.0352 (2009).

- 50 Palis, J. Primitive and definitive erythropoiesis in mammals. *Front Physiol* 5, 3, doi:10.3389/fphys.2014.00003 (2014).
- 51 Sugiyama, D., Kulkeaw, K., Mizuochi, C., Horio, Y. & Okayama, S. Hepatoblasts comprise a niche for fetal liver erythropoiesis through cytokine production. *Biochem Biophys Res Commun* 410, 301-306, doi:10.1016/j.bbrc.2011.05.137 (2011).
- 52 Kinoshita, T. & Miyajima, A. Cytokine regulation of liver development. *Biochim Biophys Acta* 1592, 303-312, doi:S0167488902003233 [pii] (2002).
- 53 Ramírez-Bergeron, D. L. et al. Hypoxia affects mesoderm and enhances hemangioblast specification during early development. *Development* 131, 4623-4634 (2004).
- 54 Galat, Y. et al. Application of small molecule CHIR99021 leads to the loss of hemangioblast progenitor and increased hematopoiesis of human pluripotent stem cells. *Exp Hematol* 65, 38-48 e31, doi:10.1016/j.exphem.2018.05.007 (2018).
- 55 Ji, A.-R. et al. Reactive oxygen species enhance differentiation of human embryonic stem cells into mesendodermal lineage. *Experimental & molecular medicine* 42, 175-186 (2010).

## Supplementary Material

### Supplementary Tables and Figures

#### Supplementary Table II-1 List of materials used in this study.

Material	Company	Cat. no.
DMEM/F12	Life Technologies	21331021
MEM Non-essential Amino Acids	Life Technologies	11140035
Glutamax	Life Technologies	35050-038
Serum Replacement	Life Technologies	10828028
bFGF	Royan Biotech	-
DPBS	Life Technologies	14040117
PBS without Ca <sup>2+</sup> and Mg <sup>2+</sup>	Life Technologies	21600-010
Insulin-transferrin-selenium	Life Technologies	41400-045
Mitomycin C	Sigma Aldrich	M4287
Y-27632	Sigma Aldrich	Y0503
Trypsin-EDTA 0.5%	Life Technologies	25300054
FBS	Life Technologies	10437
RPMI 1640	Life Technologies	52400041
B-27 Supplement without vitamin A	Life Technologies	12587-010
Bovine serum albumin (BSA)	Sigma Aldrich	A3311-100G
CHIR99021	Stemgent	04-0004
Activin A	R&D Systems	338-AC
Fibroblast growth factor (FGF4)	Royan Biotech	-
Hepatocyte growth factor (HGF)	R&D Systems	294-HG
Oncostatin M (OSM)	R&D Systems	295-OM
Dexamethasone (Dex)	Sigma Aldrich	D2915
HCM Bullet Kit	Lonza	CC-3189
TRizol	Sigma Aldrich	T9424
cDNA Synthesis Kit	Takara	RR037A
Real Time PCR Kit	Takara	RR820L
Cardiogreen	Sigma Aldrich	I2633
Dil-Ac-LDL	BTI (Biomedical Technology)	BT-902
Human Albumin ELISA Quantitation Set	Bethyl Laboratories	E80-129
P450-Glo™ CYP3A4 Assay Kit	Promega	V9002
Fibrinogen ELISA Quantitation Set	Genway	10-288-22856
BCA	Thermo Fisher Scientific	23225
Sigma coat	Sigma	FI2-100 ml

**Supplementary Table II-2** The list of primer sequences.

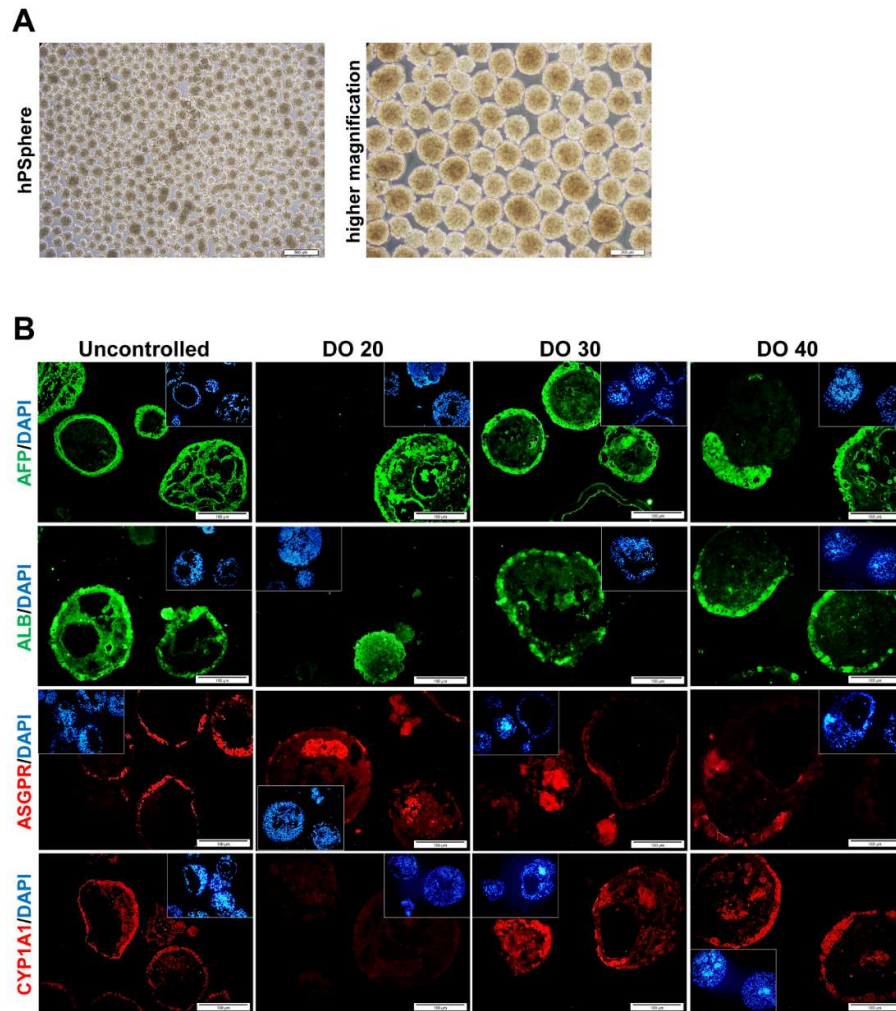
<b>Gene Name</b>	<b>Forward primer sequence</b>	<b>Reverse primer sequence</b>
<i>AFP</i>	AAA TGC GTT TCT CGT TGC TT	GCC ACA GGC CAA TAG TTT GT
<i>ALB</i>	CTT CCT GGG CAT GTT TTT GT	TGG CAT AGC ATT CAT GAG GA
<i>TTR</i>	GAGGAGGAATTTGTAGAAGGGA	CGTGGTGGAAATAGGAGTAGG
<i>HNF4A</i>	CGATGACAATGAGTATGCCT	GTCGTTGATGTAGTCCTCCA
<i>TAT</i>	ATG CTG ATC TCT GTT ATG GG	CAC ATC GTT CTC AAA TTC TGG
<i>CYP3A4</i>	TTTTTGGATCCATTCTTTCTCTCAA	ATCCACTCGGTGCTTTTGTG
<i>CYP3A7</i>	GACCGTAAGTGGAGCCTGATTC	ACAGACCATGAGAGAGCACAA
<i>TDO</i>	GGT TTA GAG CCA CAT GGA TT	ACA GTT GAT CGC AGG TAG TG
<i>G6PC</i>	GTG GAT TCT CTT TGG ACA GC	AGC AAG GTA GAT TCG TG
<i>HNF1B</i>	TCACAGATACCAGCAGCATCAGT	GGGCATCACCAGGCTTGTA
<i>HNF6A</i>	GCTTAGCAGCATGCAAAAGGA	CTGACAGTGCTCAGCTCCAA
<i>PEPCK</i>	GGCTGAAGAAGTATGACAACTG	AAATCCTCCTCTGACATCCA
<i>HBA</i>	AAGGTCGGCGCGCACGCT	CTCAGGTCGAACTGCGGG
<i>HBB</i>	GGCACCTTTGCCCACTG	CACTGGTGGGGTGAATTCTT
<i>HBG</i>	GGACAAGGCTACTATCACAAGC	GGAAGTCAGCACCTTCTTGC
<i>GAPDH</i>	CTC ATT TCC TGG TAT GAC AAC GA	CTT CCT CTT GTG CTC TTG CT

**Supplementary Table II-3** The list of antibodies.

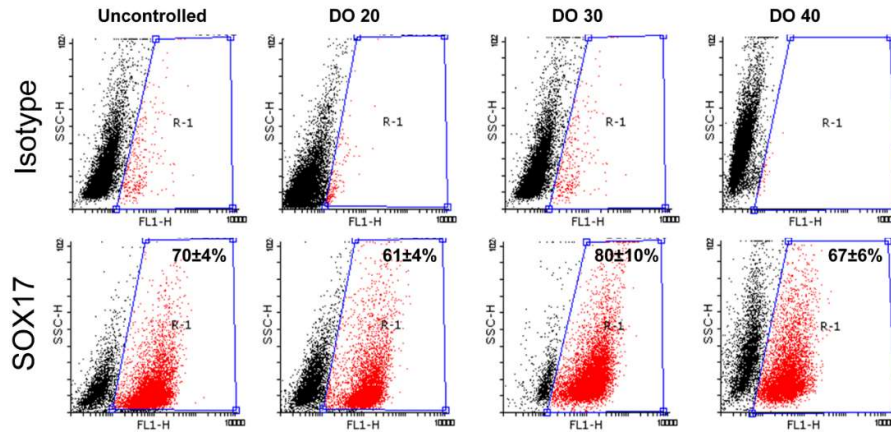
<b>Primary antibody</b>	<b>Type</b>	<b>Company</b>	<b>Cat. no.</b>	<b>Dilution</b>	<b>Dilution (Western)</b>
<b>SOX17</b>	Goat	R&D	AF1924	1:300	-
<b>ALB</b>	Goat	Bethyl Lab	A80-229A	1:100	1:5000
<b>AFP</b>	Mouse	R&D	Mab1368	1:200	1:5000
<b>E-cad</b>	Rabbit	Santa Cruz	SC7870	1:100	-
<b>CYP1A1</b>	Mouse	Santa Cruz	SC-48432	1:100	-
<b>ASGPR</b>	Goat	Santa Cruz	SC-13467	1:100	-
<b>CD36</b>	Mouse	BD	561820	1:100	-
<b>CD71</b>	Mouse	BD	555536	1:100	-
<b>CD235a</b>	Mouse	BD	561051	1:100	-
<b>GAPDH</b>	Mouse	Cell Signaling	97166	-	1:10 000
<b>Secondary antibody</b>	<b>Type</b>	<b>Company</b>	<b>Cat. no.</b>	<b>Dilution</b>	<b>Dilution (Western)</b>
<b>Anti-goat IgG Alexa Fluor®488</b>	Donkey	Invitrogen	A11055	1:500	-
<b>Anti-rabbit IgG Alexa Fluor®546</b>	Donkey	Invitrogen	A10040	1:500	-
<b>Anti-mouse IgG Alexa Fluor®546</b>	Donkey	Invitrogen	A10036	1:300	-
<b>Anti-mouse IgG Alexa Fluor®488</b>	Donkey	Invitrogen	A21202	1:500	-
<b>FITC Mouse IgG2a, κ Isotype Control</b>	Mouse	BD	553456	1:100	-
<b>PE Mouse IgG2b κ Isotype Control</b>	Mouse	BD	555743	1:100	-
<b>Anti-mouse IgG HRP</b>	Goat	Sigma-Aldrich	A4416	-	1:50 000

## Figure legends

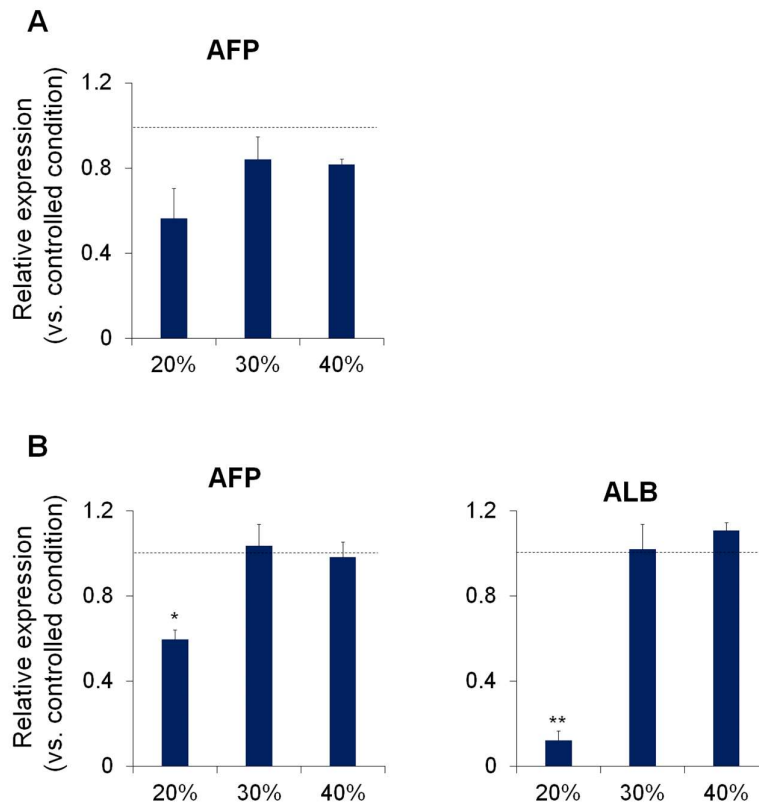
**Supplementary Figure II-1** (A) The morphology of human pluripotent stem cell (hPSC) spheres under dynamic culture conditions. (B) Immunofluorescent staining for hepatic markers in hepatic organoids under the uncontrolled and all the controlled dissolved oxygen (DO) conditions.



**Supplementary Figure II-2.** Flow cytometry analysis. Upper panel shows the isotype control population. Lower panel shows the representative dot plots and percent of SOX17-positive cells in endspheres derived under different dissolved oxygen (DO) conditions.



**Supplementary Figure II-3. The quantification of western blot data.** The expression of hepatospecific markers at day 9 (A) and day 20 (B) of differentiation procedure under different DO conditions in compared to uncontrolled condition (as dotted line). Data (mean±SD) were analyzed with ANOVA and Tukey's post hoc test. n=3. \*:  $p < 0.05$ ; \*\*:  $p < 0.01$



This chapter will be as supplementary section of next chapter related manuscript which is under review of project supervisors and US patent pending for submission through MIT TLO office:

**III. Chapter 3. Scalable production of hepatic endoderm, endothelial progenitors, and mesenchymal stromal cell derived from hPSCs for scalable vascularized liver bud/organoid generation.**

## Chapter Introduction

As mentioned in aims and project scope section, the vascularized liver bud generation technology that recapitulated the developmental stages of hepatogenesis is one the most promising RM platforms for treating acute liver failure as unmet medical need. However, the technology is mainly facing protocol and production scalability issue for widespread clinical application since currently established protocol that claimed as mass production platform capable of producing about 100 million cells for treating one pediatric patient.

In this platform that established by Takebe group, three progenitor populations identified and generated that could effectively generate liver buds in a highly reproducible manner: hepatic endoderm, endothelium, and septum mesenchyme. However, these 3 populations were generated under static culture condition that is not amenable for large scale manufacturing and can be considered as critical bottleneck issue in large scale production of vascularized liver buds <sup>21</sup>. Here, we established protocols for scalable production of these progenitor's population under dynamic suspension culture.

## Scalable production of definitive and hepatic endoderm cells as 3d aggregates

### Introduction

Takebe group have performed massive “reverse” screen experiments by comparing the multiple endoderm stages based on the resultant organoid quality as well as employing most reproducible published mature hepatocyte differentiation protocols. This has been done to precisely determine the best endoderm stages for iPSC-LB functionality by starting LB culture from day 0 to day 20 cells. They realized that only the day 6 and day 10 endodermal cells exhibited the highest hepatic functions after extended culture using 3 days treatment of hiPSCs with Activin A (100ng/ml), Wnt3a (50ng/ml), and sodium butyrate (0.5 mM) followed by another 3 days treatment with Activin A (100 ng/ml), Wnt3a (50 ng/ml) as optimized protocol for endoderm differentiation under static culture condition. Subsequently, human iPSC-derived endodermal cells were treated further with RPMI-1640 with 1% B27, 10 ng/ml human basic FGF, and 20 ng/ml human BMP4 for 2 days to derive a TBX3- and ADRA1B-positive transitional hepatic endoderm population (tHE). These day 8 cells were the only population capable of maintaining highly homogeneous LBs within 100–200  $\mu\text{m}$  in size after co-culture<sup>21</sup>. However, this protocol has been done under static adherent culture condition using iMatrix-511-coated dishes that is not fully defined and not amenable for large scalable production of tHE cells for scalable liver bud generation. Other groups also published protocols for efficient generation of liver progenitors from hPSCs but used same small scale and static culture system for establishing the protocol<sup>124</sup>. Our previous experiences showed that protocols established under static culture condition using monolayer culture system cannot be easily adopted for differentiation of hPSCs as 3D aggregates under dynamic suspension culture conditions and re-optimization of differentiation protocols maybe required<sup>168</sup>.

Previously, it has been shown that definitive endoderm (DE) differentiation in suspension is feasible<sup>169</sup> that facilitating the culture scale-up in stirred suspension bioreactors for integrated differentiation to hepatic endoderm and subsequently hepatocytes<sup>18,170</sup>. It has been also

reported that integrated differentiation at suspension may be superior to adherent culture differentiation since DE markers appear faster with more strongly expression. Despite promising prospects to use suspension cultures for DE and hepatic differentiation, most of these protocols have done in small scale under undefined culture condition without optimizing the differentiation protocol under dynamic suspension culture that is crucial for generating a large population of liver progenitors within 3D aggregates. Practically, massive numbers of liver progenitors (even in billions scale) are essentially required as starting material for scalable vascularized liver buds/organoids generation for potential clinical application. Here, we optimized the DE and hepatic progenitors generation from hPSC aggregates under dynamic suspension culture condition by optimizing definitive endoderm differentiation protocol and then optimizing HGF concentration and hepatic differentiation day by tracing key liver progenitors' markers that introduced in other studies (e.g. TBX3, ADRA1B (alpha-1b Adrenergic Receptor), EPCAM, CD90, and Hnf4 $\alpha$ <sup>21,124</sup>). This has been done to achieve 3D aggregated populated and enriched by liver progenitors for subsequent dissociation and incorporation in vascularized liver bud's/organoids generation process under scalable and reproducible manner (Fig. III-1).

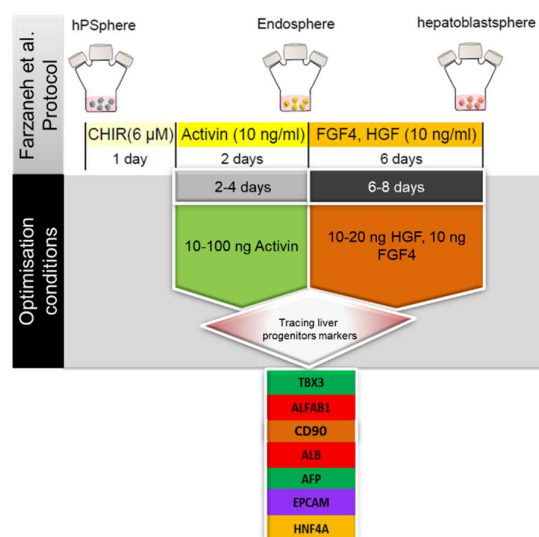


**Figure III-1. Integrated differentiation protocol for scalable generation of liver progenitors from hPSCs as 3D aggregates under dynamic suspension culture condition.**

## **Material and Methods**

### ***hPSC aggregate culture***

Here, we used hESC line (H9, passages: 25-50, WiCell Research Institute, Inc., Madison, WI, <http://www.wicell.org>)<sup>166</sup> and the hiPSC line (Gibco™ Episomal hiPSC, passages: 25-45) for definitive endoderm and hepatic defined differentiation protocol development under fully defined culture condition. Both cells lines were maintained on Vitronectin XF™ coated plates in mTeSR™ Plus medium before transferring to static suspension culture. We developed a suspension culture of 3D hPSC aggregates in spinner flasks as previously described with some modification<sup>171</sup>. After 2 or 3 passages in a static suspension culture (low attachment culture dish),  $1.5 \times 10^7$  dispersed cells were transferred to 50 ml of mTeSR™ Plus medium (STEMCELL Technologies) in 100ml spinner flask with a 40 rpm agitation rate<sup>172</sup>. All hPSCs culture procedures were performed under standard cell culture conditions of 37 °C and 5% CO<sub>2</sub> with approximately 95% relative humidity.

### ***Integrated differentiation of hPSpheres***

3 to 4 days hPSCs aggregates (after reaching to mean 150µm aggregate diameter size) were washed in phosphate-buffered saline plus Ca<sup>2+</sup> and Mg<sup>2+</sup>, and then cultured in basal medium for differentiation to endodermal cells (endospheres). The basal medium consisted of RPMI 1640 (Life Technologies), 1X B-27 without vitamin A (-vit A) or insulin (-Ins; Life Technologies), and 0.1% human serum albumin (HSA; Sigma Aldrich). On the first day, 6 µM CHIR99021 (CHIR; Stemgent) was added to the basal medium. After 24 h, the cells were washed before refreshing the medium. Then, Activin A with 10 to 100 ng/ml concentration (R&D Systems, hereafter Activin) or plus Wnt3a (50 ng/ml) was added during day 2 to 5 to induce the hPSCs into a definitive endoderm. Generated endodermal aggregates were called endospheres.

The efficacy of this protocol has also compared with Takebe group protocol for endoderm generation from hiPSC but using hPSCs aggregated with same diameter size under dynamic

suspension culture (i.e. 3 days treatment of hPSCs aggregates with Activin A (100 ng/ml), Wnt3a (50 ng/ml), and sodium butyrate (0.5 mM) <sup>21</sup>.

Then, the endospheres that were generated by optimized definitive endoderm differentiation protocol, induced for hepatic differentiation as previously described with some modifications <sup>173</sup>. Integrated hepatic differentiation of endospheres were conducted in DMEM/F12 supplemented with 2% knockout serum replacement (KOSR; Life Technologies), fibroblast growth factor 4 (FGF4, 10 ng/ml; Invitrogen) and hepatocyte growth factor (HGF, 10-20 ng/ml; R&D Systems) for 6-12 days to trace liver progenitor markers by gene expression and immunostaining.

#### ***Aggregates size and morphology evaluation***

The morphology and the size distribution of spheres in each step were assessed by a phase-contrast microscope (EVOS XL; Thermofisher Scientific). The diameter size of aggregates (approximately 100 aggregates per sample) was measured by the microscope software.

#### ***Gene expression profiling by RT-qPCR***

RNA was extracted using Qiagen mini-RNA extraction kit. Reverse transcription was performed with random primers (Applied Biosystems RT kit) to generate cDNA. Gene expression was quantified using gene-specific primers and KAPA SYBR® Fast qPCR kit (KAPA Biosystems, KK4602). NCBI primer designing tool was used to design gene-specific primer sequences. The primers used were validated for their specificity and those with efficiency between 90-110% were used (Table III.S4). Gene expression profile was analyzed using Microsoft excel and heatmaps were generated using GenePattern version 2.0 <sup>174</sup>.

#### ***Immunofluorescence staining and flow cytometry***

Differentiated aggregates collected, washed, and fixed overnight in 4% paraformaldehyde at 4 °C for immunofluorescence staining or confocal microscopy. The fixed spheres were incorporated in an Histogel (2%). After processing, they were embedded in paraffin blocks

and sectioned into 6  $\mu\text{m}$  sections with a microtome (Microm™, HM325). We followed the standard protocol for immunofluorescence staining. Fixed aggregates were also stained with direct antibody staining protocol and suspended in glycerol/fructose solution in glass bottom 24-well plates (Cellvis) for imaging the confocal microscopy (Olympus FV1200 Laser Scanning Confocal Microscope).

For flow cytometry analysis, we dissociated the differentiated spheres into single cells using Accutase® cell detachment solution or 20 mg/mL collagenase type I (Sigma-Aldrich). Dispersed cells were fixed in 4% paraformaldehyde at 4 °C for 20 min, permeabilized, blocked in bovine serum, and allowed to incubate overnight with diluted dye conjugated antibodies for direct staining method or diluted primary antibodies at 4 °C and then washed and incubated with secondary antibodies for 45 min at room temperature. Flow cytometry analysis was performed with a BD LSRFortessa™ flow cytometer (Becton Dickinson).

### ***Statistical analysis***

Data were presented as mean  $\pm$  standard deviation (SD). T-squared test was used to compare two independent groups. Comparisons between groups and data were performed with one-way ANOVA and the post-hoc Tukey test and  $p \leq 0.05$  were considered statistically significant. The analyzes were performed using SPSS 16 software.

## Results

First, we employed Takebe group static monolayer protocols for generation of DE and tHE cells<sup>21</sup> and adapted it for integrated differentiation of hPSCs aggregates for production definitive endoderm cells as 3D aggregates and compared its efficacy to our group protocol which was optimized for hepatic endoderm's production in our previous reports under suspension culture condition<sup>18</sup>. Results showed that Takebe group endoderm differentiation protocol was not efficient for endoderm differentiation of hPSCs aggregates since significant cell death and aggregates dissociation observed within aggregates after starting the differentiation process and then a heterogeneous population of small or large number of aggregates were generated after 5 days of differentiation process under dynamic suspension culture for both of H9 and Episomal iPSCs lines (Fig. III-2). On the other side, Farzaneh protocols that was optimized for endospheres production from hPSCs aggregates using RH5 and RH6, (hESCs, passages no: 25-50) and the hiPSC4 lines (passages no: 40-45) resulted in homogenous generation of endospheres from H9 and Episomal hiPSC lines<sup>18</sup>.

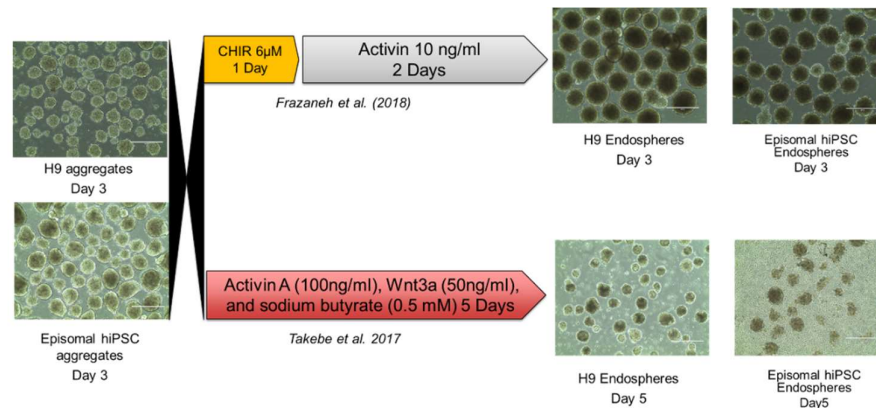


**Figure III-2. Integrated differentiation of hPSCs (H9, and Episomal hiPSC) using two different protocols for scalable generation of DE endospheres<sup>21,168</sup>.** H9 and Episomal hiPSC cells were expanded as 3D aggregated and differentiated when aggregates size reached to about 150-170 µm diameter size by either Farzaneh et al.<sup>18</sup> or Takebe group<sup>21</sup> protocols for generation of transitional hepatic endoderm's..

However, optimizing integrated differentiation protocol for maximizing the generation of liver progenitors was not conducted in Farzaneh protocol and not published yet so far.

Here, we sought to determine the optimal differentiation strategy for generating liver progenitors as 3D aggregates by optimizing the endoderm differentiation steps through exploring optimum Activin A treatment period (2 to 4 days) from day 2 to 5 of the differentiation process and its concentration (10, 25, 50, 75, 100 ng/ml) (Fig. III-3 A) after one day of priming with 6 $\mu$ M CHIR. Then, we explored the effect Wnt3a (50ng/ml) addition to optimized Activin A treatment strategy from day 2 to 5 of differentiation process because of the critical role of Wnt signaling pathway in hepatic endoderm generation from hPSCs and hepatogenesis<sup>168,175</sup>.

Results showed that one day treatment with 6  $\mu$ M CHIR followed by 3 to 4 days treatment with 50 ng/ml Activin A can result in more efficient generation of DE cells as endospheres from H9 cell line since about 82% of the total endospheres cell population double expressed SOX17 and FOXA2 as key DE markers after 3 days treatment, respectively ( $p < 0.05$ , Fig. III-3 B). Increasing Activin A concentration to 75 and 100 ng/ml and continuing treatment for 4 days was not resulted in significant increase in DE markers expression compared to 3 days treatment with 50 ng/ml Activin A.

Integrated differentiation trials with 50 ng/ml Activin A treatment with addition of 50 ng/ml Wnt3A supplementation at different days revealed that Wnt3A supplementation for 3 days (Day 4 of the differentiation process) can improve DE differentiation efficacy since 85-90% of the total endospheres cell population double expressed SOX17 and FOXA2 as key DE markers for H9 and hiPSC cell lines ( $p < 0.05$ , Fig. 3.2.3 C). Extended supplementation of Wnt3a for 4 days was not resulted in significant increase in DE markers expression for both of tested the cell lines. Thus, 6  $\mu$ M CHIR treatment followed by 3 days treatment with 50 ng/ml Activin A plus 50 ng/ml Wnt3a selected as optimal differentiation strategy for endospheres generation from hPSCs for liver progenitor's generation trials.

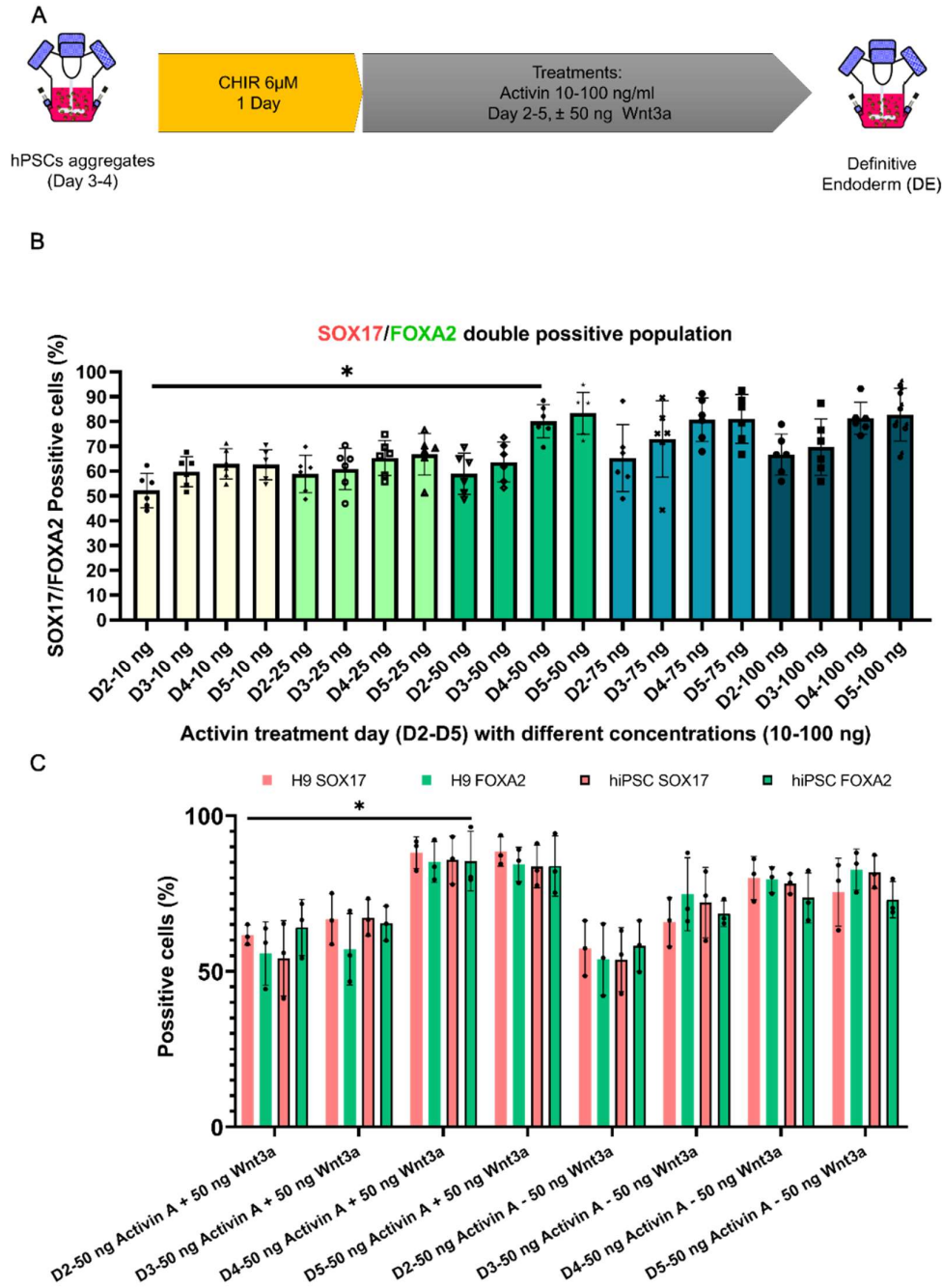


**Figure III.3 Schematic design of the protocol optimization for generation of endospheres from hPSCs under dynamic suspension culture condition (A).** Flowcytometry data of SOX17 and FOXA2 expression of cell population within endospheres generated from H9 cell line after Activin A treatment with different period (2 to 4 days) from day 2 to 5 of the differentiation process and different concentrations (10, 25, 50, 75, 100 ng/ml) (B). Flowcytometry data of SOX17 and FOXA2 expression of cell population within endospheres generated from H9 and Episomal hiPSC cell lines after 1-4 days 50 ng/ml Activin A treatment plus 50 ng/ml Wnt3a or without Wnt3a (C). Data are presented as mean  $\pm$  SD (n=3-6). Data were analyzed using ANOVA followed by the post hoc Tukey's tests, \*:  $p < 0.05$ .

To generate hepatic endoderm aggregates populated by liver progenitors expressing key liver progenitors' markers (e.g. *TBX3*, *ADRA1B*, *EPCAM*, *CD90*, and *Hnf4a*), H9 and Episomal hiPSC derived endospheres were further treated with 10 or 20 ng HGF and 10 ng FGF4 for 5 days and generated hepatic endoderm aggregates were analyzed by quantitative gene expression for *Hnf4a* and *TTR* genes as important markers of hepatic progenitors. Results showed that supplementation with 20 ng HGF (as a key growth factor for hepatic differentiation) will results in higher expression of *Hnf4a* and *TTR* genes compared to 10 ng/ml HGF for both cell lines ( $P < 0.05$ , Fig. III-4 B). Therefore, endospheres were treated with 20 ng/ml HGF and 10 ng/ml FGF4 for 7days from day 5 to day 13 of the differentiation process and aggregate samples were taken from each day of hepatic differentiation process for tracing liver progenitors related markers expression (Fig III-4 C). Quantitate gene expression analysis of aggregate samples revealed that most the hepatic progenitors marker genes were started to express from day 8 of the differentiation process and all progenitors marker genes reached to their maximum expression levels during day 10 and 11 of the integrated differentiation process (i.e. *TBX3*, *ADRA1B*, *EPCAM*, *CD90*, *AFP*, and *Hnf4a*). AFP and Albumin markers expressions has also increased after Day 9 of differentiated process indicating the undergoing hepatic maturation process from liver progenitors to hepatocyte like cells (Fig. III-4 C). Thus, the established protocol repeated using H9 cell line to monitor the proliferation and key markers/genes expression differentiation process (Fig. III-4 D).

Microscopic observation of aggregates revealed that hPSCs aggregates size increased during endoderm differentiation from  $150 \pm 25 \mu\text{m}$  to  $178 \pm 32 \mu\text{m}$  diameter size for endospheres and then increased to about  $210 \pm 34 \mu\text{m}$  after 11 days of differentiation for hepatic endoderm aggregates (Fig. III-4 E, F, G). Immunostaining of Day 4 endospheres showed that cells are double positive for SOX17/FOXA2 indicating efficient DE differentiation (Fig III-4 H). They also started to express *TBX3* and *alfab1* as key THE markers as well as E-cadherin from day 8 of the differentiation process which were previously introduced as a reliable cell surface marker for liver specific stem cells <sup>176</sup>.

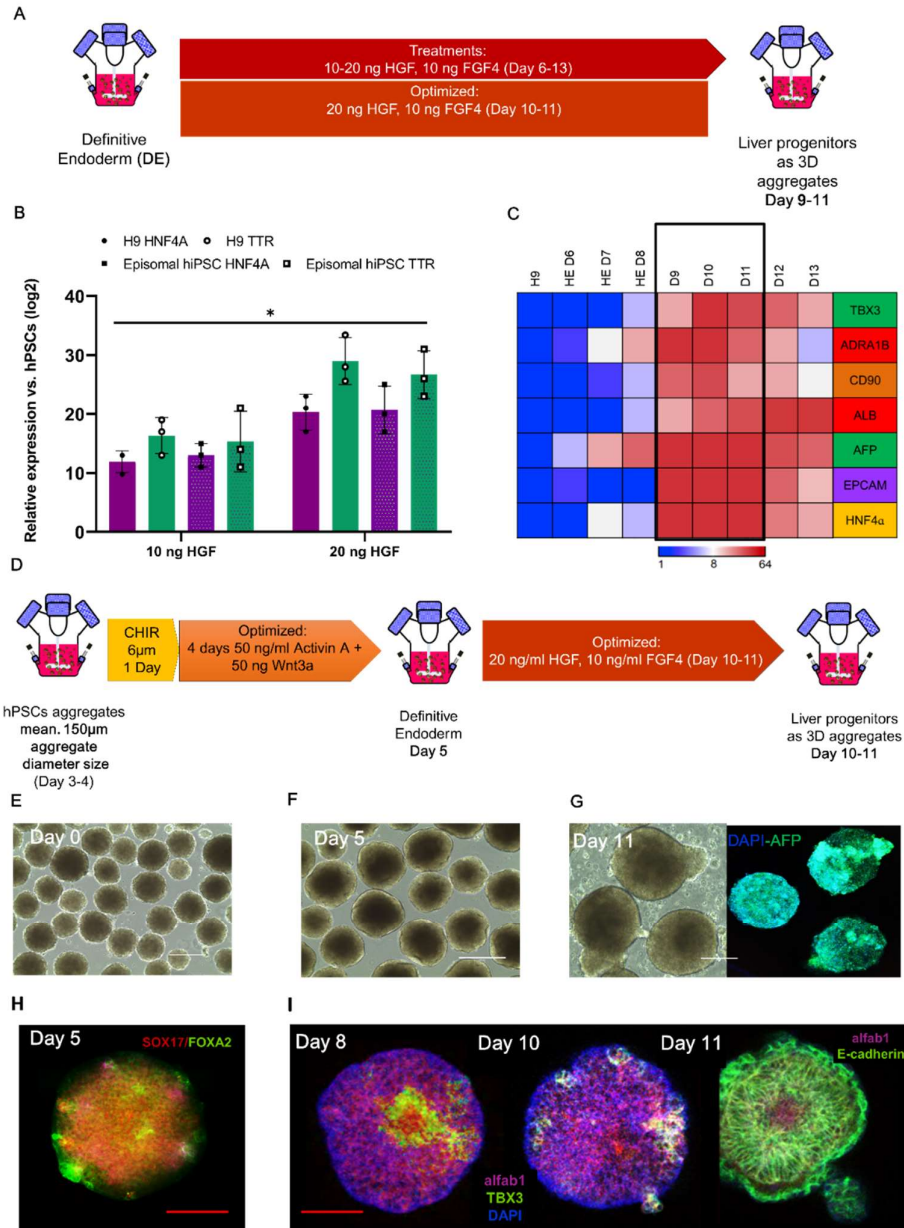


**Figure III-4 Schematic design of the protocol optimization for generation of hepatic endoderm aggregates form endospheres under dynamic suspension culture condition (A), Comparing two concentration of HGF including 10 ng/ml and 20 ng/ml for hepatic differentiation of H9 and Episomal hiPSC cell as 3D aggregates (B)..RT-qPCR analysis for key liver progenitors' markers expression (e.g. TBX3, ADRA1B, EPCAM, CD90, and Hnf4a as well as AFP and Albumin as markers for hepatic endoderm) from day 6 to day 13 of integrated hepatic differentiation of H9 (C). Schematic design of optimized differentiation strategy to generate 3D hepatic endoderm aggregates populated by liver progenitors (D). Morphology of endospheres (E) and hepatic endoderm aggregates at day 4 (F) and day 11 (G). SOX17 and FOXA2 expression in H9 endospheres detected by immunostaining and confocal imaging (H), tracing liver progenitors' markers by immunostaining of hepatic endoderm cells at day 8, 10, and 11 of the differentiation processes for TBX3, alfab1, and E-cadherin markers (I). (White scalebars: 200µm, Red scalebars: 100µm)**

Interestingly, hepatic endoderm aggregates were also started to budding and generating small aggregates from Day 9 of the differentiation process may be due to high proliferation capacity of hepatic progenitors (Fig III-4 I).

Expression of liver progenitors' and hepatic endoderm markers were decreased from Day 12 of integrated hepatic differentiation process while albumin expression increased in parallel as an indication for starting hepatic maturation process towards hepatocytes.

Similar results obtained by Takebe group using different protocol done under static culture condition that introduced day 8 of the differentiation process as the starting day for expression of the related markers <sup>21</sup>. Farzaneh et al. have also introduced Day 9 of the differentiation process for generating hepatoblasts as 3D aggregates under dynamic suspension culture <sup>18</sup>.

Thus, hepatic endoderm aggregates generated from Day 8 to 11 were selected for conducting co-culture studies with endothelial cells and hPSCs derived hMSCs and exploring optimal conditions of cell ratio and culture conditions to achieve vascularized liver buds/organoids through self-organization/self-condensation. The established platform can be also used for scalable production of hepatic progenitors as 3D aggregates in stirred bioreactors for other applications such as tissue constructs fabrication and recellularization of whole liver decellularized scaffold.

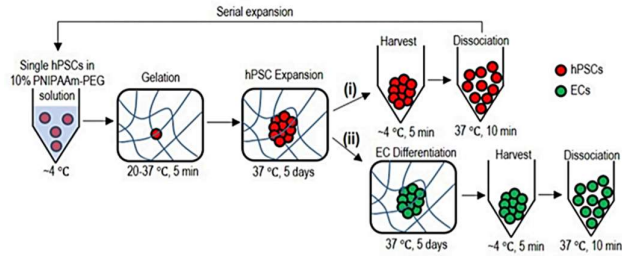
## Scalable production of progenitors and mature endothelial cells from hPSCs

### Introduction

During last 5 years, scalable manufacturing of endothelial cells (ECs) and endothelial colony forming cells (ECFCs) capable of differentiating to regenerate endothelial cell populations has gained increasingly attention due to significant progress in vascularized organs, tissues, or organoids/bud's fabrication using these unique cells for in vitro vascularization as well as their support for proliferation and maturation of liver or pancreatic progenitors<sup>21,177,178</sup>. Recently, "endothelial cell therapy" has also gained increasingly attention for therapeutic angiogenesis as a new and exciting approach to the treatment of cardiovascular diseases<sup>179-181</sup>.

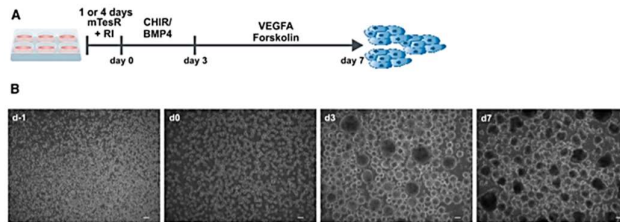
To date, few reports available that established protocols for scalable production of endothelial cells from hPSCs using different approaches including expansion and differentiation in thermo-responsive gel-based platform<sup>182</sup>, integrated differentiation of hPSCs aggregates followed by MACS separation of CD31 positive cells<sup>183</sup>, and using an alginate hydrogel column based approach for hPSCs seeding and integrated differentiation to endothelial cells (Fig. III-5)<sup>184</sup>. Lin *et al.* expanded and differentiated hPSCs into ECs in a 3D thermoreversible PNIPAAm-PEG hydrogel that resulted in high-culture efficiency of expansion/differentiation culture system including high-viability (>90%), high-purity (>80%), and high-volumetric productivity yield ( $2.0 \times 10^7$  cells/ml). Moreover, genome-wide gene expression analysis revealed that ECs generated in scalable culture system had higher expression of genes related to vasculature development, extracellular matrix, and glycolysis, while 2D-ECs had higher expression of genes related to cell proliferation<sup>182</sup>. This platform introduced an innovative strategy for production of endothelial cells but purity of CD31<sup>+</sup> cells was reported about 80% that should be improved to min 90% for potential applications. Moreover, scalability of hydrogel based hPSCs expansion and differentiation should be demonstrated at larger scales. Olmer *et al.* have also established a scalable strategy for production of functional endothelial cells from hPSCs as 3D aggregates in dynamic suspension culture system from

static suspension culture to agitated Erlenmeyer flasks, and finally transfer to a 120ml bioreactor. They reported production of up to 76.8% CD31<sup>+</sup> cells in dynamic suspension culture using CHIR and BMP4 for KDR positive cells generation and VEGFA plus forskolin for generation of mature endothelial cells 185.



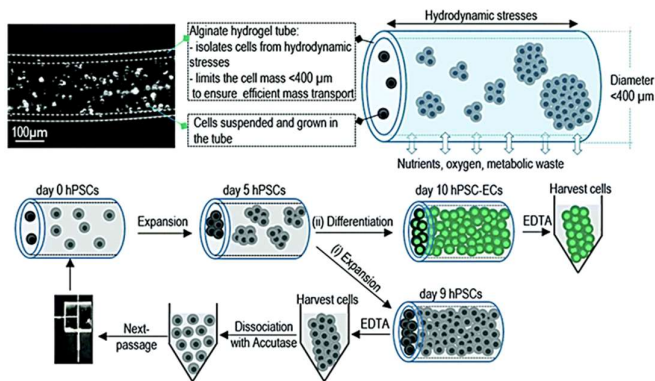
**Thermoresponsive gel-based platform**  
*Lin et. Al. Stem Cell Reports. (2018)*

**Scalability Issue due to hydrogel based culture/Cost**



**hPSC 3D aggregate differentiation and MACS SEPARATION**  
*Olmer et. Al. Stem Cell Reports. (2018)*

**Necessity of MACS purification that can result in significant cell loss!**



**Alginate based column production**  
*Lin et. Al. Biomaterial Science. (2019)*

**Scalability Issue due to hydrogel-based culture/Cost**

**Figure III-5. Comparing currently established protocols for scalable production of functional endothelial cells from hPSCs 182,184,185.**

By applying CD31-based magnetic-activated cell sorting (MACS) separation on day 7 of differentiation, the proportion of CD31 positive cells could be increased from 74.7% ± 8.6% to 98.3% CD31<sup>+</sup> cells that could be further expanded on fibronectin coated plates. This platform is high promising for scalable production of endothelial cells since adapted for 3D suspension culture of hPSCs and their integrated differentiation <sup>185</sup>. However, the necessity of using MACS purification system for generating mature endothelial cells can be considered as drawback of the protocol since it can result is significant cell loss during purification process. The alginate hydrogel-based protocol that developed by Lin *et al.* is also suffering from scalability issue due to hydrogel column fabrication steps for scalable production and harvesting that should be also adapted for GMP manufacturing <sup>184</sup>.

Thus, developing a scalable approach for production of pure population of endothelial progenitors, endothelial colony forming cells, and functional CD31<sup>+</sup> cells can facilitate the large-scale production of this unique cells for potential clinical and organoids/tissue fabrications applications. Here, we tried to establish a scalable approach for production of ECFCs, EPCs, and the further maturation to ECs from hPSCs using 3D aggregate culture as well as microcarrier culture under defined culture conditions (Fig. III-6).

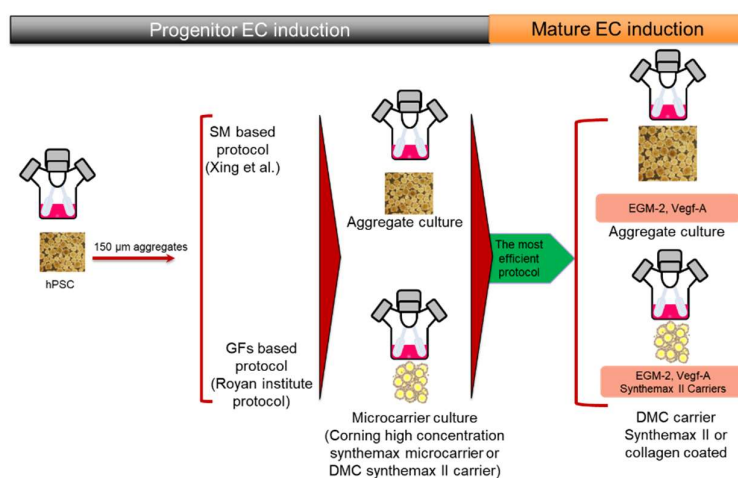


**Figure III-6 Scalable endothelial differentiation strategy under dynamic culture using small molecule or growth factor-based differentiation strategy as well as culture mode (3D aggregate vs. micro-carrier culture approach).**

## **Materials and Methods**

### ***Integrated differentiation of hPSCs to endothelial cells***

We used hESC lines RH5 (passages: 22-41, Royan institute, Iran), H9 (passages: 25-50, WiCell Research Institute, Inc., Madison, WI, <http://www.wicell.org>) and the hiPSC line (Gibco™ Episomal hiPSC, passages: 25-45) for definitive endoderm and hepatic differentiation protocol development. All cell lines were maintained on Vitronectin XF™ coated plates in mTeSR™ Plus medium before transforming to static suspension and then dynamic suspension culture. We employed a protocol for suspension culture of 3D hPSC aggregates in spinner flasks as previously described with some modification <sup>171</sup>. After 2 or 3 passages in a static suspension culture (low attachment surface culture dish, Corning),  $1.5 \times 10^7$  dispersed cells were transferred to 50 ml of mTeSR™ Plus medium (STEMCELL Technologies, Canada) in 100ml spinner flask with a 40 rpm agitation rate to generate hPSCs as 3D aggregates <sup>172</sup>. All hPSCs culture procedures were performed under standard cell culture conditions of 37 °C and 5% CO<sub>2</sub> with approximately 95% relative humidity.

### **Integrated differentiation of hPSCs to endothelial cells as 3D aggregates**

#### ***Integrated differentiation of hPSCs to endothelial progenitor cells as 3D aggregates using growth factors***

To start differentiation cultures as 3D aggregates with growth factors, 3 to 4 days hPSCs aggregates produced in dynamic suspension culture (after reaching to mean 150 μm aggregate diameter size) were washed in phosphate-buffered saline plus Ca<sup>2+</sup> and Mg<sup>2+</sup>, and then treated by 12μm CHIR99021 for one day in RPMI 1640 medium (11875093, Gibco) medium supplemented with B27 (A3582801, Gibco). After 24 hours, medium refreshed with RPMI/B27 without CHIR99021 for another 24 hours. Then, 25 ng/ml BMP4 (R&D systems, 314-BP-010), 50 ng/ml VEGF-A (aa 207-318, R&D biosystems.), 10 μm purmorphamine (SML0868-5MG, Sigma) and 10μm SB431542 (S4317, Sigma) were added to the cell medium and kept for 48 hours. All cultures have conducted in CELLSPIN spinner flask system using

50 ml medium in 125 ml spinner flask with 40 rpm agitation rate under standard cell culture condition.

#### ***Integrated differentiation of hPSCs to endothelial progenitor cells as 3D aggregates using SMs***

To start differentiation cultures as 3D aggregates, 3 to 4 days hPSCs aggregates (after reaching to mean 150  $\mu\text{m}$  aggregate diameter size) were washed in phosphate-buffered saline plus  $\text{Ca}^{2+}$  and  $\text{Mg}^{2+}$ , and then treated by 6  $\mu\text{M}$  CHIR9901 (4423, Tocris Bioscience) and 100  $\mu\text{g}/\text{ml}$  ascorbic acid (A8960, Sigma Aldrich) for 2 days in defined media containing DMEM High Glucose (11965, Life Technologies,) according to Xiaoping *et al.* report that established a monolayer differentiation culture for generation of endothelial cells from hPSCs under chemically defined culture conditions<sup>186</sup>. Then, CHIR9901 was removed by refreshing media with DMEM High Glucose supplemented with ascorbic acid at a concentration of 100  $\mu\text{g}/\text{ml}$  for another 4 days. All differentiation cultures conducted in CELLSPIN spinner flask system using 50 ml medium in 125 ml spinner flask under standard cell culture condition.

#### ***Integrated differentiation of hPSCs to endothelial progenitor cells on microcarriers***

In this approach, hPSCs expanded as aggregates and then dissociated after 5 days of culture with Accumax cell dissociation solution and single cells seeded cell corning synthamax II high concentration microcarriers with 25000 cells/ $\text{cm}^2$  cell density in mTeSR™ Plus media. About 3 - 4 days after seeding and reaching to 60-70% confluency on microcarriers surface, the hPSC expansion media was refreshed with DMEM high glucose medium supplemented with 6 $\mu\text{M}$  CHIR9901 and 100  $\mu\text{g}/\text{ml}$  ascorbic acid in for 2 days. CHIR9901 was removed after two days and the cells were cultured for extra 4 days in media supplemented with 100  $\mu\text{g}/\text{ml}$  ascorbic acid. All cultures have conducted in CELLSPIN spinner flask system using 50 ml medium in 125 ml spinner flask with 40 rpm agitation rate under standard cell culture condition.

***Integrated differentiation of endothelial progenitors to mature endothelial cells under 3D dynamic culture condition***

At the day 6 of differentiation process when reaching to maximum endothelial progenitor cells population, endothelial colony forming cells/progenitors sorted based on KDR expression with BD FACSAria III Cell Sorter and isolated KDR+ cells were cultured on cell culture plates coated with collagen type 1 (Sigma Aldrich C3867) in EGM-2 (Lonza CC-3162) supplemented with 50 ng/ml VEGF-A (R&D biosystems) for two more days to generate mature CD31 positive endothelial cells.

As an alternative scalable strategy, endothelial progenitors were harvested from DMC carrier and seeded on denaturated collagen coated dissolvable microcarriers (denaturated collagen DMC) or collagen coated microcarriers with 20,000-50,000 cell/cm<sup>2</sup> seeding density without a sorting step in same medium to generate mature CD31<sup>+</sup> endothelial cells on microcarriers under dynamic suspension culture.

***Monitoring endothelial differentiation process***

Expressions of Brachyury (Mesodermal and also endodermal differentiation marker), CD34 (Colony forming endothelial progenitor marker), KDR (Endothelial progenitor marker) and CD31 (Mature endothelial marker) were measured during the differentiation process of all trials by RT-qPCR and flowcytometry to monitor the integrated differentiation process for generation of endothelial progenitors.

Endothelial maturation markers such as CD31, VE-cadherin, VWF, and LDL uptake were also examined after 8 days of culture in integrated differentiation of endothelial progenitors by immunocytochemistry and flow cytometry techniques to validate the functionality of cells and efficacy of the differentiation process.

### ***Flow cytometry and cell sorting***

During the differentiation, at day 2,4,6 and 8, cells were dissociated with trypsin/EDTA (15400-054, Gibco-Invitrogen) or Accumax cell dissociation solution. For dissolvable microcarrier cultures, cells were harvested by with a solution of EDTA and pectinase for dissolving carriers and releasing cells. Following neutralization with DMEM supplemented with 10% FBS, cells were washed in PBS that contained 2% FBS (FACS buffer). Subsequently, cells were incubated for 1 h at 4 °C with mouse IgG1 monoclonal anti-human KDR, and then washed with FACS buffer. Secondary polyclonal rat anti-mouse IgG1-PE or FITC was added and cells incubated for 1 h at 4 C. After washing with FACS buffer, KDR positive cells were sorted by BD FACSAria III Cell Sorter (USA). This method was also used for sorting CD31-positive cells in EGM-2 medium. After differentiation of KDR positive cells into ECs in EGM-2 medium, the cells were dissociated using trypsin/EDTA after reaching confluency. Afterwards, cells were fixed with 4% paraformaldehyde (Sigma-Aldrich, P6148) and stained with monoclonal antibodies for CD31, CD144, CD146, FLK1, and CD45. Cells were washed twice with PBS before being analyzing by flow cytometer (FACS Aria, BD).

### ***Quantitative PCR and RT-PCR***

Reverse transcription reactions were performed using SuperScript III reverse transcription (Invitrogen). The resulting cDNA was used for quantitative PCR (qPCR) and RTPCR. qPCR was performed with Power SYBR Green PCRMasterMix (Applied Biosystems) according to the manufacturer's instructions. The signals were detected with a 7900HT Fast Real-Time PCR system (Applied Biosystems).

### ***Immunostaining and confocal imaging***

For 2D immunostaining, cells were harvested form aggregates of microcarriers and fixed with 4% paraformaldehyde (PFA) overnight at 4 °C, permeabilized with 0.25% Triton X-100 for 30 min and blocked with 5% donkey serum for 1 h before incubating with primary antibodies or

Alexa Fluor® conjugated primary antibodies at 4°C overnight. After extensive washing, secondary antibodies, and 10 mM, DAPI in 2% BSA was added and incubated at room temperature for 4 hr. Cells were washed with PBS three times before imaging. For 3D immunostaining of cells on microcarriers, hPSCs were fixed with 4% PFA at 4°C overnight, and then incubated with PBS± 0.25% Triton X-100+ 5% (vol/vol) goat serum+ Alexa Fluor® conjugated primary antibodies at 4°C for 48 hr. After washing with PBS three times, microcarriers suspended in glycerol/fructose solution in glass bottom 24-well plates (Cellvis) for imaging the confocal microscopy (Olympus FV1200 Laser Scanning Confocal Microscope).

#### ***Tube formation assay***

Tube formation assay conducted for endothelial cells generated from optimal culture condition using Angiogenesis Assay Kit (Abcam, ab204726). Briefly, extracellular matrix solution added to empty culture plate and incubated for 1 hr at 37°C to allow the solution to form a gel. Then, endothelial cells as single cells were added to plates at 50,000 cells/well for 3-4 hours and then examined in EVOS XL light microscope. Tubes were quantified with Image J software.

#### ***Statistical analysis***

Data were presented as mean ± standard deviation (SD). T-squared test was used to compare two independent groups. Comparisons between groups and data were performed with one-way ANOVA and the post-hoc Tukey test.  $p \leq 0.05$  were considered statistically significant. The analyzes were performed using SPSS 16 software.

## Results

### Integrated endothelial differentiation of hPSCs as 3D aggregates

As mentioned in experimental procedure section, two strategies were employed for scalable generation endothelial cells including 3D aggregate culture and microcarrier culture using two different differentiation protocols including growth factor and small molecule-based differentiation (Fig. III-7A).

After employing the integrated differentiation strategy with RH5 3D aggregates using growth factor-based protocol, Flowcytometry analysis of Brachyury expression- as a mesoderm marker- in cells treated with CHIR99021 showed that 85% of cells were Brachyury positive. After further treatment of aggregates with BMP4, Purmorphamine, SB431542 and VEGF for 4 days, heterogeneous population of aggregates were generated and flowcytometry analysis showed that only 30% of the cell's population are KDR positive (VEGFR2 positive) (Fig 3.7 B). Thus, this strategy resulted in poor efficacy for generation of endothelial progenitor cells that will require a sorting step for isolation of progenitors for further differentiation and maturation to CD31 positive endothelial cells which is not amenable for scalable manufacturing.

In integrated differentiation of RH5 aggregates with chemically defined protocol, aggregates with mean 150  $\mu\text{m}$  aggregate diameter were exposed to CHIR99021 small molecule with concentration of 6  $\mu\text{M}$  and 100  $\mu\text{g} / \text{ml}$  ascorbic acid for 2 days in DMEM high glucose. Then, CHIR was removed from the cell environment by media refreshing with DMEM High Glucose and 100  $\mu\text{g} / \text{ml}$  ascorbic acid for more 4 days to generate endothelial progenitors and colony forming cells. Flowcytometry analysis on day 6 differentiated cells indicated 6.25% for CD34 marker (primary precursor cell) and 11.64% of the cells were positive for KDR marker (Fig III-7C). This result indicating that Xiaoping et al. protocol that has been established for endodermal differentiation of hPSCs ad monolayer culture cannot be adopted for integrated differentiation of hPSCs as 3D aggregates <sup>186</sup>.

### **Integrated endothelial differentiation of hPSCs on microcarriers**

Here, RH5 and H9 human embryonic stem cells were expanded as aggregates and then coated on Corning microcarriers with Synthemax surface (Corning high concentration synthemax II microcarriers) at optimal density of 25000 cells/cm<sup>2</sup> (5000-75000 cells/cm<sup>2</sup> range) in 100 ml spinner flasks with 50 ml working volume and 14 gr/L microcarrier concentration (about 500 cm<sup>2</sup> surface per 100 ml culture medium).

After 3-4 days and reaching to about 60-70% confluency, expansion medium was removed, and cells exposed to 6 µm CHIR99021 and 100 µg/ml ascorbic acid for 2 days in DMEM high glucose medium. After 48 hours, CHIR99021 was removed and cells were cultured in DMEM High glucose + 100 µg / ml Ascorbic acid for 4 days (Fig. III-7 D). Samples were taken at days 2,4,6 and 8 of differentiation process and analyzed with different techniques to monitor the differentiation process.

Flow-cytometry analyzes revealed the highest expression of Brachyury at the protein level on day 2 at about 80%, and 70% of cells differentiated on microcarriers were KDR<sup>+</sup> at day 6 of the differentiation process which was highest expression obtained among different tested trials. The maximum CD31 expression was also at day 6 reached to about 13% expression (Fig. III-7 C). Real-Time PCR analysis also confirmed the results and showed the highest expression of Brachyury marker at day 2 with about 1,000 times increase compared to hPSCs expression level, the highest expression of KDR was on day 6 and about 150 times, and the highest expression of CD31 was about 17.5 times higher at day 6 (Fig. III-7 D). Thus, days 6 selected as optimal day for generating endothelial progenitors' cells for further maturation to CD31 mature endothelial cells.

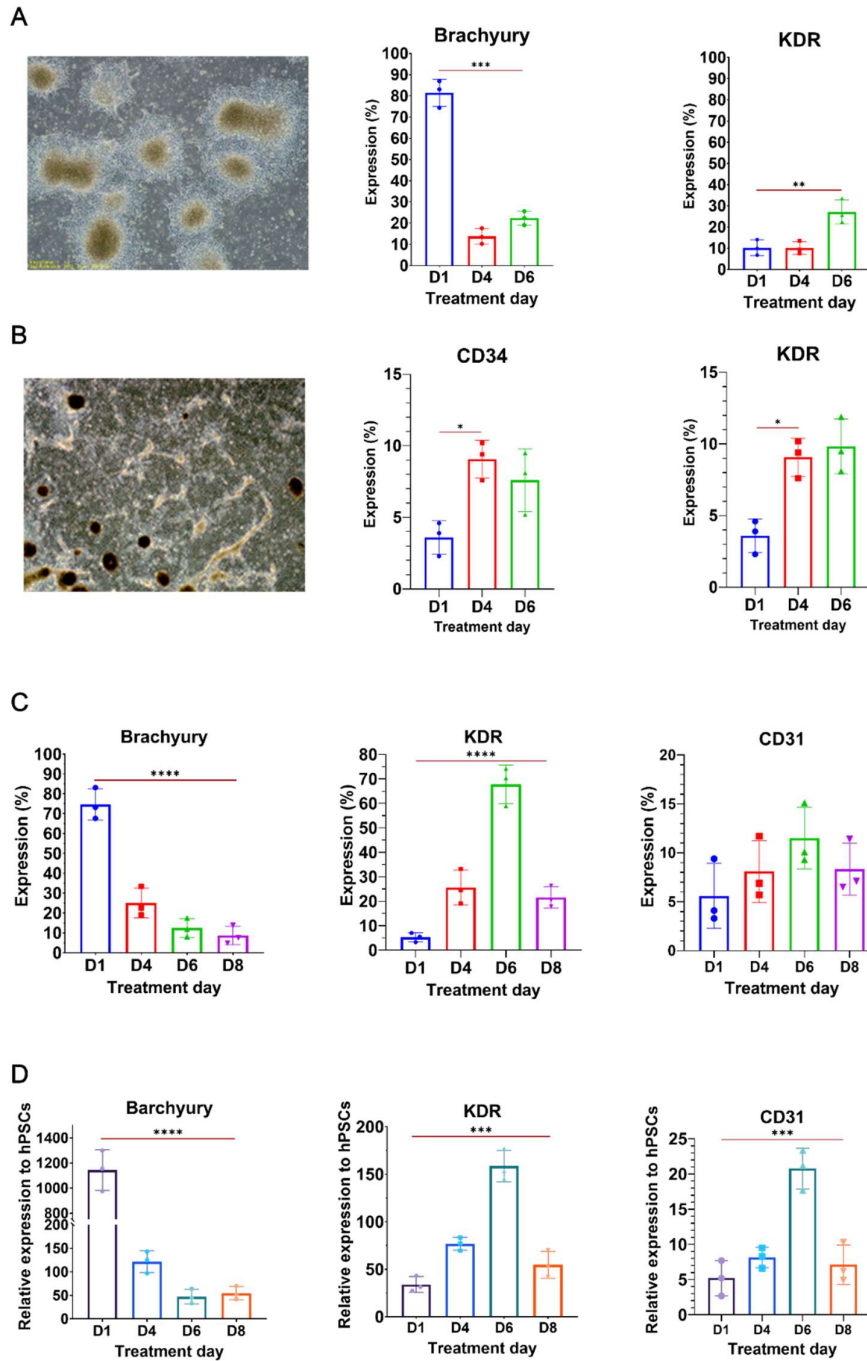


**Figure III-7 Integrated differentiation of hPSCs to endothelial progenitors**, Integrated differentiation of RH5 cells as 3D aggregates using two different approaches including growth factor or small molecule based approach, Morphology of aggregates generated after 6 days treatment with growth factor based approach as well their Brachyury and KDR expression analyzed by flowcytometry (A). Morphology of aggregates generated after 6 days treatment with small molecule-based approach as well their CD34 and KDR expression analyzed by flowcytometry (B). Integrated differentiation of hPSCs to endothelial progenitor's cell on microcarriers using two small molecule-based approach (C), Expression levels of Brachyury, KDR, and CD31 quantified by Flowcytometry (E) and RT-qPCR (D). (n=3; \* $p < 0.05$ , \*\* $p < 0.01$ , \*\*\* $p < 0.001$ )

### **Integrated maturation of endothelial progenitor cells towards mature endothelial cells on collagen coated microcarriers**

In this experiment, H9 cells seeded and grown on Corning® High Concentration Synthemax™ II Microcarriers treated with chemically defined approach for generation of KDR<sup>+</sup> cells. Afterwards, KDR<sup>+</sup> cells generated on surface of microcarriers were harvested from at day 6 of the differentiation process and then seeded on Corning® denatured collagen dissolvable microcarriers or collagen coated microcarriers with 40,000 cells/cm<sup>2</sup> density (500 cm<sup>2</sup>/100 ml surface) in EGM-2 medium (Lonza) supplemented 50 ng / ml VEGF-A Growth Factor (Fig. III-8 A, B, C, D).

Results showed that hPSCs and KDR<sup>+</sup> cells successfully attached to selected microcarriers and expanded on the carrier surface (Fig. III-8 B, C, D). Moreover, endothelial progenitor cells that grown and expanded on microcarriers were highly proliferative and started to form tubular-like structures out of carrier surface at day 6 of differentiation process. They also efficiently differentiated to CD31<sup>+</sup> cells on collagen coated microcarriers that imaged by confocal microscopy through direct staining with dye conjugated antibody (Fig. III-8 E). Flowcytometry analysis revealed that about 70% of cells were KDR<sup>+</sup> at Day 6 of integrated differentiation process (Fig. III-8 F). After harvesting generated KDR<sup>+</sup> endothelial progenitor cells and seeding on collagen coated microcarriers without sorting step, 93.7% of cell population expressed CD31 and mature endothelial cell markers as well as 94.1% expressed vascular endothelial (VE)-cadherin (CD144) as adhesion molecule that mediates cell-cell contact between endothelial cells. However, denatured collagen dissolvable microcarriers were not supported endothelial progenitors' cells efficient attachment and differentiation to CD31<sup>+</sup> mature endothelial cells since only 12 % and 14.9 % of cell population expressed CD31 and CD144, respectively (Fig. III-8 G). H9 and Episomal hiPSCs derived endothelial cells on collagen microcarriers also showed typical morphology of endothelial cells after plating as monolayers culture (Fig. III-8 H&I).

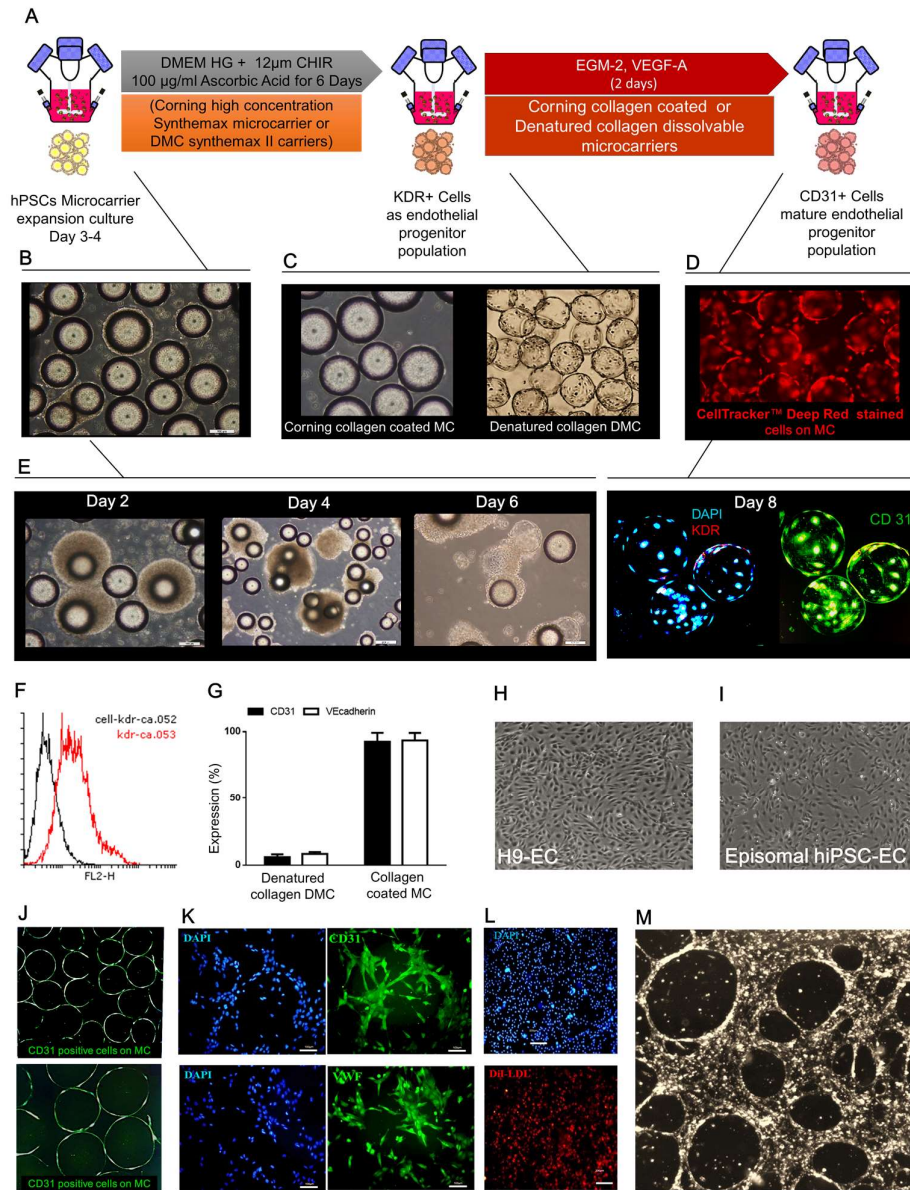


**Fig III-8 Schematic design of integrated endothelial differentiation of hPSCs under 3D dynamic suspension culture.** Attachment and growth of hPSCs, endothelial progenitors, and endothelial cells on microcarriers (B, C, and D). Proliferation of endothelial progenitor cells and tubular-like structures on microcarriers during 6 days of differentiation process and CD31 expression after day 8 of culture (E). Flowcytometry analysis of KDR+ at Day 6 of integrated differentiation process (F). CD31 vascular endothelial (VE)–cadherin expression at day 8 by Flowcytometry (CD144) (G). Morphology of H9 and Episomal hiPSCs derived endothelial cells after plating as monolayers culture (H&I). Immunostaining of generated cells for CD31 (on collagen coated microcarriers) (J) and CD31 and vWF expression under static suspension culture (K). LDL uptake (L) and generation of tube-like structure after seeding generated cells on collagen type I 3D scaffold (M). (Scale bars= 100 µm).

Immunostaining of generated cells on collagen microcarriers (Imaged by confocal microscopy) and plated cells also confirmed CD31 expression as well as of vWF expression under static suspension culture (Fig. III-8 J&K). They also could uptake LDL and generated tube-like structure after seeding on collagen type I 3D scaffold (Fig. III-8 L&M). Tube formation assay also showed that H9 derived endothelial cells generated larger tubes, higher number of branch points, and larger tube area compared to HUVEC cells and endothelial cells generated on denaturated collagen microcarriers

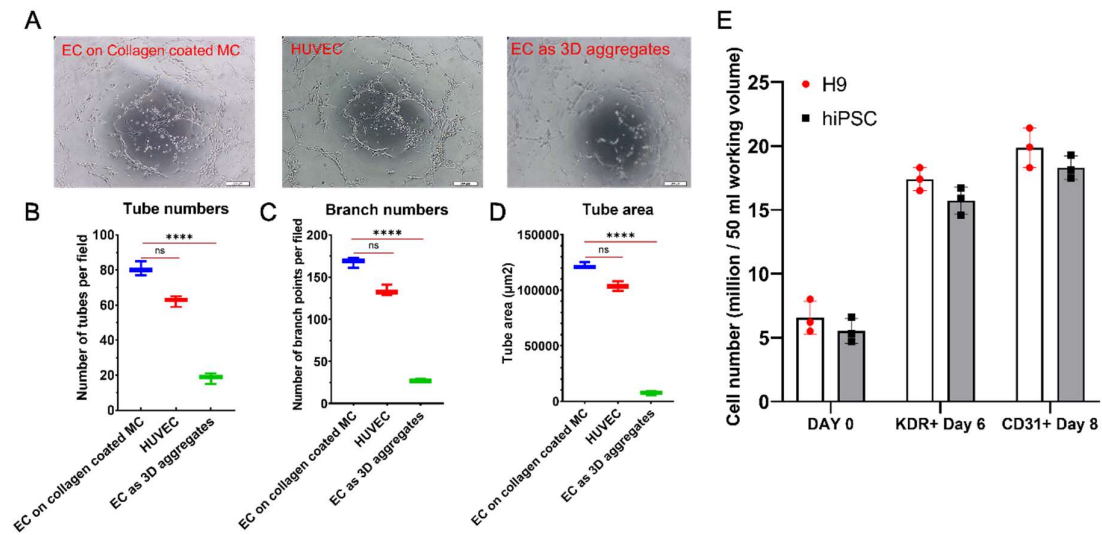


**Figure III-9 Tube formation assay of H9 derived endothelial cells.** (A) including number of tubes (B), number of branch points (C), tube area (D) compared to HUVEC cells and endothelial cells generated on denaturated collagen microcarriers. Cell density during endothelial differentiation of hPSCs (H9 and Episomal hiPSC) after 6 days of culture and generation 70% KDR+ cells and 2 days after harvesting reseeding KDR+ cells on collagen coated carriers and generation of mature CD31+ endothelial cells. (Fig. III-9 A, B, C, and D). (n=3; \* $p < 0.05$ , \*\* $p < 0.01$ , \*\*\* $p < 0.001$ )

Finally, the productivity of integrated differentiation of hPSCs on microcarrier culture for generation of mature CD31+ endothelial cells was about 4.3- and 4-fold increase for H9 and Episomal hiPSC cell lines, respectively (Fig. III-9 E). These results indicating that the established microcarrier platform can be employed for scalable production endothelial progenitors and mature cells for scalable generation of vascularized liver buds/organoids

under defined culture condition without using hydrogels as matrix <sup>184</sup> or cell sorting step (MACS separation) <sup>185</sup> as the main bottlenecks of previously established protocols.

## Scalable and GMP-compatible production of hMSCs derived from human pluripotent stem cells

### Introduction

Developing efficient protocols for generation of human pluripotent stem cell derived mesenchymal stem cells has gained increasingly attention during last 5 years for providing a readily available cell source for potential clinical applications including treatment of a series of autoimmune, inflammatory, and degenerative diseases where promising results observed in animal studies <sup>187-189</sup>. However, most of the established hPSC-MSCs derivation and expansion protocols rely on two-dimensional (2D) static culture systems, which are inefficient and offering poor scalability for large-scale production as prerequisite for most the intended therapeutic applications. Meanwhile, recent findings about critical role of mesenchymal stem cells in self-organization and condensation of organoids and tissues called as “mesenchymal cell-driven condensation” has boosted this need for scale up culture as essential cell ingredient for scalable liver bud formation <sup>96</sup>. Although numerous studies have published aiming scalable manufacturing of hMSCs isolated from various tissue sources for allogeneic cell therapy application <sup>190,191</sup>, only one study reported a scalable approach to generate hESC-derived MSCs using 3D aggregate culture of hESCs <sup>192</sup>. Yan et. al. demonstrated that hESC spheroids can directly differentiate into MSC spheroids (EMSC<sub>Sp</sub>) within 20 days in one vessel without passaging and the system is scalable to any desired size of vessel. EMSC<sub>Sp</sub> successfully differentiated into osteocytes and chondrocytes in spheres or demineralized bone matrix while also retains immune-modulatory effects *in vitro* and therapeutic effects on two mouse models of colitis after dissociation. Interestingly, suspension derived EMSC cells had faster proliferation and higher yield and develop less apoptosis and slower senescence compared to monolayered derived cells. However, for each batch of production, hPSCs should be expanded in large scale followed by integrated differentiation to hMSCs that could increase the cost of the process due to high cost of hPSCs media and differentiation reagents. In this

project, we tried to establish a more cost-effective approach by generation of expandable MSCs from hPSCs under static culture condition following banking homogenous population of isolated hMSCs and then their scalable expansion on dissolvable microcarriers for facilitated scale up and harvesting.

## **Materials and Methods**

### ***Generation and characterization of ES-MSCs***

Human embryonic stem cell line H9 (WiCell Research Institute, Inc., Madison, WI, <http://www.wicell.org>),) was cultured on Vitronectin XF™ coated plates in mTeSR™ Plus medium. Every other day, the medium was changed and every four days the colonies were passaged using Gentle Cell Dissociation Reagent (STEMCELL Technologies, Canada). To induce hPSCs differentiation into hMSCs, spontaneous differentiation was performed. Briefly, hPSC colonies were dissociated using Gentle Cell Dissociation Reagent (STEMCELL Technologies, Canada) and plated on 6 cm<sup>2</sup> non-adherent culture petri dish at 2 X 10<sup>5</sup> cells/cm<sup>2</sup> in ESC medium supplemented with RevitaCell Supplement (1X) (Thermofisher, USA) in the absence of bFGF. The medium was refreshed every other day to generate embryoid bodies (EBs) after 7 days. Then, generated EBs were plated on gelatin-coated plates in Alpha Modified Eagle's Medium (α-MEM, Life technologies) supplemented with 5% GMP-grade Human platelet lysate (PLTGold, Merck Millipore, USA) and 2 mM L-glutamine for 7-10 days. The outgrowing differentiated cells were collected and subsequently re-plated and cultured for additional days. Then, resulted ES-MSCs of passage 0 were passaged at 80% confluency until 4 passages and then banked as 5 × 10<sup>6</sup> cells/ml in 5 ml cryovials for microcarrier expansion trails.

### ***Microcarrier suspension culture***

Dissolvable microcarriers (Synthemax II-coated dissolvable microcarriers, surface area of 5000 cm<sup>2</sup>/g, Corning Life Sciences) were used for dynamic suspension culture of hPSCs derived MSCs. To hydrate dry powder of dried microcarriers, 5,000 cm<sup>2</sup> (1 g) dissolvable microcarriers were aseptically transferred to a 500 ml sterile bottle. Next, 150 mL sterile water (Gibco, USA) was added to the bottle (150 mL water per gram microcarriers), and the mixture was gently swirled in order to resuspend the microcarriers and incubated for 10 minutes at RT to allow complete hydration. Then, water was removed from the settled microcarrier bed and washed with 100 ml StemPro® MSC SFM medium to minimize dilution of the culture medium due to residual water from the hydration step. Next, the microcarriers were resuspended in StemPro MSC SFM medium to a final volume of 50 mL (500 cm<sup>2</sup>/ml microcarrier concentration) in 100 ml corning disposable spinner flask and then incubated in a cell culture incubator for ~30 minutes to allow the media to equilibrate.

To prepare cells for microcarrier cultures, LN2 cryopreserved hMSCs were thawed and seeded directly into gelatin coated T75 flasks at 5,000 cells/cm<sup>2</sup> in StemPro® MSC SFM CTS™ serum-free medium (SFM) medium (Thermofisher), incubated for 5-6 days in a cell culture incubator (at 37 °C, 5% CO<sub>2</sub> and saturated humidity) and refreshed by same media at day 3. To harvest, cells were twice with 15 ml DPBS (Thermofisher) and then incubated with 4-5 mL TrypLE™ Select Enzyme (1X) (Thermo Fisher) for 6-8 minutes. Following cell dissociation, cells were centrifuged at 200 *xg* for 3-4 minutes and then resuspended in 25 ml of same medium for inoculating to microcarrier culture.

### ***Dynamic suspension culture in spinner flask***

Harvested cells were seeded at a density of 6,000 cells/cm<sup>2</sup> in spinner flask and cultures was mixed for 18-24h at 25 rpm using CELLSPIN SYSTEM (Pfeiffer, Germany) inside a CO<sub>2</sub> Incubator. Cell attachment was monitored by taking a 1 mL sample of the microcarrier culture and visual observation by EVOS XL microscope. After 24h, agitation rate was increased to 40

rpm till day 3 and 50 rpm by day 7. Half-volume media exchanges were performed on days 3 and 5.

#### ***Cells harvesting from microcarriers***

Cells were harvested from the dissolvable microcarriers after 5 to 7 days of expansion when reaching to confluency on microcarrier surface. First, spinner flasks transferred to biosafety cabinet for microcarriers settle down and spent media removed by aspiration then. Next, the microcarriers were washed with 50 mL DPBS and allowed to settle again after the addition of DPBS and the supernatant was then removed. 50 ml of pre-warmed dissociation solution including 100 U/mL pectinase (P2611, MilliporeSigma), 10 mM EDTA (46-034-CI, Corning), 5X TryPLE™ Select (A12177-01, Thermo Fisher) diluted in DPBS (21-031-CM, Corning) added to microcarriers and spinner flasks was incubated on a stir platform for 10-15 minutes at 35 rpm. Once a single-cell suspension was observed, the cells were centrifuged at 200 xg for 5 minutes in a two 25 mL centrifuge tubes and then resuspended in media for characterization studies.

#### ***Monitoring microcarriers culture and determining cell yield***

Microscopic inspection was performed daily to monitor the morphology of cells by taking 0.5 ml sample and observing by EVOS XL camera microscope. In addition, cell counts, and viability measurement were performed at least on day 5,6, and 7 for spinner cultures using Countess™ II Automated Cell Counter (Thermo Fisher Scientific) by Trypan blue method.

#### ***Surface marker expression***

Expression of surface markers was determined on cell samples that were cryopreserved on day 7. Cells were thawed and evaluated for H-CAM, STRO-1, THY-1, CD45 and CD-146 markers expression by immunostaining and flowcytometry. Data acquisition was performed

on a FACSCanto using Diva-software (BD LSRFortessa™, USA). The data was analyzed using Flow-jo software.

### ***Multipotency determination***

Expanded hMSCs were differentiated into adipocytes and osteocytes to demonstrate their multipotency potential. The cryopreserved cells were thawed and washed in culture medium to remove the freezing medium. For adipocyte and osteocyte differentiation, the cells were re-seeded in Corning CellBIND surface 6-well plates and differentiated according to manufacturer's recommendations (SCR020 and SCR028, EMD Millipore). After 2-3 weeks of differentiation process, cells were fixed in 2% paraformaldehyde and stained for characteristic markers of differentiation: adipocytes (O1516-250ML, Oil Red O; MilliporeSigma), osteocytes (TMS-008-C, Alizarin Red; MilliporeSigma).

### ***Karyotyping***

The cells were seeded in culture flasks to stimulate proliferation, treated with colcemid (4-6 h at 0.15 µg/mL), and detached using trypsin and concentrated by centrifugation. The pelleted cells were treated with hypotonic solution (75 mM KCl, 3 min), centrifuged again, and fixed with 10 volumes fixative 1 [methanol-acetic acid 9:1 (v/v)]. The cells were concentrated and subsequently fixed with 10 volumes fixative 2 [methanol-acetic acid 3:1 (v/v)]. The fixed cell dropped onto microscope slides after another concentration step and allowed to dry and aged overnight at 60 °C. The slides were re-hydrated in 2 SSC and subsequently in PBS, treated with trypsin (0.07%, 3 min) and finally stained at room temperature for 3–4 min using 1 ml Giemsa (Merck) and 3 mL Leishman stain (Merck) in 60 ml Gibco® Gurr Buffer. The slides were dried and mounted in Eukitt® before observation.

### ***Statistical analysis***

Data were presented as mean ± standard deviation (SD). T-squared test was used to compare two independent groups. Comparisons between groups and data were performed with one-

way ANOVA and the post-hoc Tukey test.  $p \leq 0.05$  were considered statistically significant. The analyzes were performed using SPSS 16 software.

## Results

### *Generation and characterization of ES-MSCs*

To produce hPSCs-MSCs, hPSCs were cultured in hPSC medium in the absence of bFGF to form EBs. Then, EBs were plated in gelatin-coated plates and cultured in StemPro™ MSC SFM CTS™ as cell therapy grade xeno and serum-free media as reported previously with some modification<sup>23</sup>. Spontaneous differentiating of EBs resulted in outgrowth of ES-MSCs around the colonies. Generated MSC-like cells were further passaged four times to acquire a homogenous population with spindle-shaped morphology (Fig III-10 A). The resulting cells were cryopreserved after 4 passages under static culture condition and used for scaling up trials using corning Synthemax II dissolvable microcarriers (Fig III-10 A). Cryopreserved hPSC-MSCs were transferred to two T-flasks to prepare seed culture for microcarriers culture after thawing and inoculated to spinner flask culture systems for 3D dynamic suspension culture at 6000 cells/cm<sup>2</sup> seeding density in 75ml working volume and 500 cm<sup>2</sup> surface area per 100ml culture medium. Generated cells were characterized after 5-6 passages in microcarrier culture for MSC markers expression by immunostaining and flowcytometry (Fig. III-10 B, C). Results showed that MSC expanded on microcarriers in multiple passages no longer expressing OCT4 as pluripotency marker and expressed H-CAM, STRO-1, THY-1 and CD146 MSC markers (Fig III-10 B). These results were confirmed by flowcytometry and 72.1 %, 66.3%, 99.7%, and 81,3% of cells well expressed H-CAM, STRO-1, THY-1 and CD146 markers, respectively (Fig III-10 B). Moreover, differentiation studies demonstrated that generated MSCs are multipotent since successfully differentiated after 21 days culture in adipogenic differentiation medium to mature adipocytes as indicated by the accumulation of lipid vacuoles stained with Oil Red O compared to control sample (Fig. III-10 D (A, B, C)).

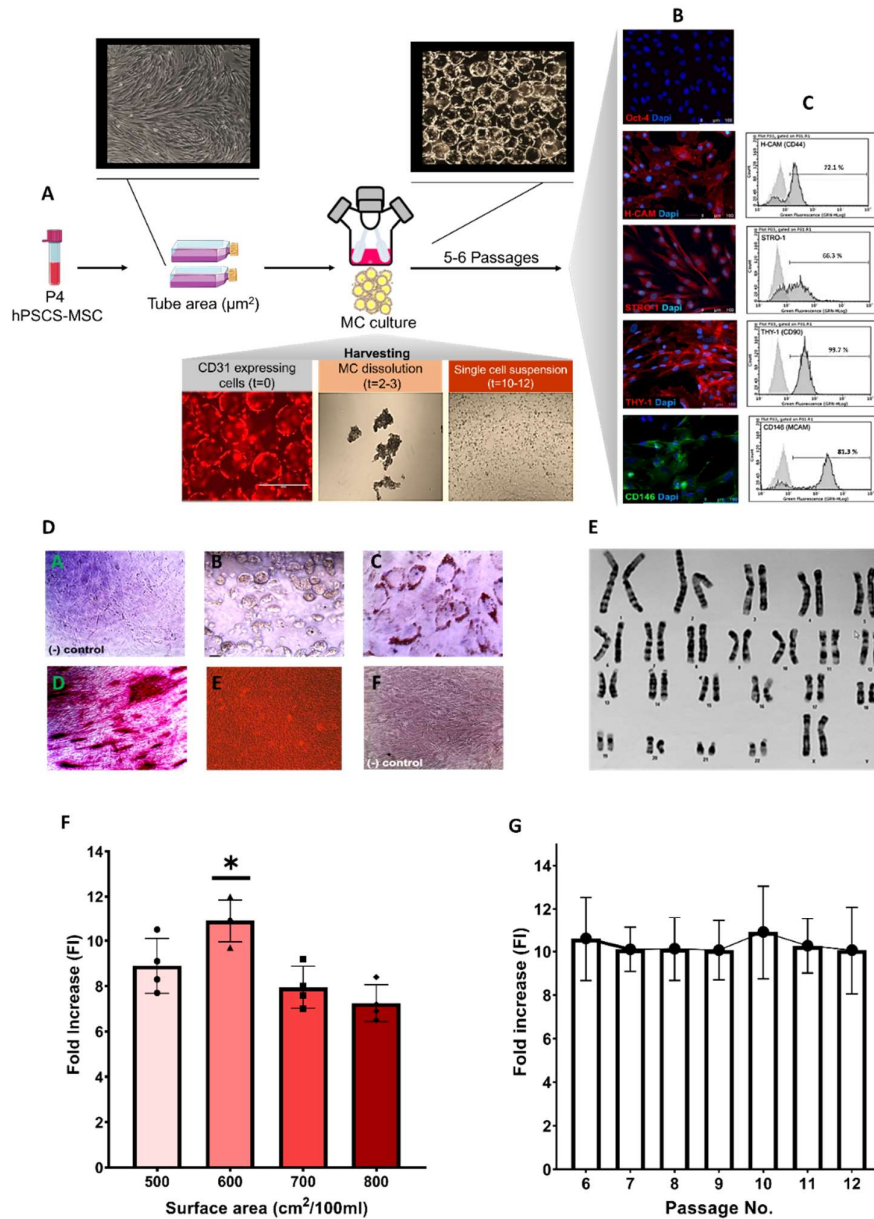


**Figure III-10. Scalable expansion of hPSC-MSC using Synthmex II dissolvable microcarriers from P4 cryopreserves cells including their harvest procedure after each passage.** Immunostaining of MSC markers STRO-1, THY-1 (CD90), CD146 as well as OCT4 as hPSCs pluripotency marker (B). Flowcytometry analysis of MSC markers STRO-1, THY-1 (CD90), CD146 (C). H9 derived MSCs differentiated in adipogenic (D(B), D(C)) and osteogenic (D(D), D(E)) differentiation medium. Generated cells differentiated after 21 days to mature adipocytes as indicated by the accumulation of lipid vacuoles that stain with Oil Red O (D(B), unstained; D(C), 40X magnification). Control untreated human mesenchymal stem cells did not contain any lipid droplets D(A). H9 derived MSCs also differentiated to an osteocyte lineage as demonstrated by alkaline phosphatase (D(D), 10X magnification) and Alizarin Red S (ARS) D(E) staining. Alizarin Red S staining demonstrates mineral deposition throughout the culture that was not observed in control untreated cells D(F). Karyotyping of H9 derived MSC after 10 passages under dynamic suspension culture (E). Optimizing the microcarriers surface area in 100 ml culture medium for increasing the FI (F), Exploring the proliferation capacity of H9 generated MSCs during six passage after thawing conducted in spinner flask with 50 ml defined StemPro® MSC SFM medium (G). (n=3-4 ; \* $p < 0.05$ )

They also differentiated to osteocyte lineage as indicated by alkaline phosphatase with demonstrates mineral deposition through staining with Alizarin Red S (ARS) (Fig. III-10 D (D, E, F)) Karyotyping also demonstrated preserved genetic stability of MSCs during derivation, banking, and 5-6 passages on microcarriers (Fig III-10 E).

To optimize the MSC cells yield in microcarrier culture, different microcarriers area surface was used in similar working volume. Results showed that maximum cell yield can be achieved by 600 cm<sup>2</sup> microcarrier surface area that lead to about 11-fold increase in single cell inoculation density (Figure III-10 F). To demonstrate the robustness of the protocol, cells cultured on microcarriers until passage 12 that demonstrated their preserved proliferation capacity after multiple passages which is essentially required for scalable manufacturing of cells for commercial application (Figure III-10 G). Thus, the established differentiation strategy and microcarrier based expansion platform can be considered as viable strategy for creating a universal bank of MSCs from different hPSCs lines and their robust expansion under defined and serum-free culture condition for production of clinical grade cells required for scalable of liver/organoids buds through MSC driven self-condensation under clinical grade settings.

**References of this chapter are merged with the next chapter.**

#### **IV. Chapter 4. Large scale and continuous production of vascularized liver organoids using scalable microfluidic technology**

This chapter is based on following paper prepared under review of project supervisors and US patent pending for submission through MIT TLO office:

**Continuous Production of Vascularized Hepatobiliary Organoids from Human Pluripotent Stem Cells Using a Scalable Microfluidic Platform**

**Introduction**

Generating complex and vascularized organoids derived from self-organizing stem cells-derived progenitors or somatic cells is considered as a major technological breakthrough in regenerative medicine field. These organoids have potential to revolutionize the current standard care and treatment protocols and raising hope for developing efficient treatment for unmet patients' needs through "Organoids medicine"<sup>82</sup> as well as discovery of more safe and effective drugs for personalized medicine using organoids as models system<sup>193</sup>. Current protocols for generating vascularized and highly functional liver organoids mainly depends on co-culture of different cells type with precise cell ratio in animal derived matrixes (e.g. Matrigel) or coated microwell plates using static culture system (e.g. multi-well and array-well plates) through a labor-intensive multi-step process that are not amenable for scalable manufacturing of organoids in clinically relevant cell numbers for clinical application<sup>21,100</sup>. Moreover generated liver buds/organoids lacking vascular<sup>153</sup> of biliary structure/bile metabolism<sup>21,194</sup> that are essential for proper liver function and preferably should be present in generated complex organoids as therapeutic component.

Therefore, generating complex, functional, and multicellular organoids such as liver organoids in a reproducible and high-throughput manner remained challenging and hindered their therapeutic and commercial application. To date, significant advances and progress in hydrogel science and microfabrication technologies have opened new doors and offered great opportunities to recreate 3D tissue/organ models with more physiological relevance in a controllable manner<sup>195,196</sup>. Several groups have attempted to create bioinspired hydrogels as soft and biomimetic matrices or 3D scaffolds for liver organoid/tissue formation to increase

their functionality and reduce variability in the generation process <sup>197-199</sup>. These hydrogels have been created using different fabrication techniques (e.g. Bioprinting) and formats such as inverted colloidal crystal poly (ethylene glycol) scaffold for liver organoids generation <sup>200</sup>, patterned substrates for expandable liver tissue generation <sup>22</sup>, and microfibers for generation of hepatic micro-organoids <sup>157</sup>. Despite the progress, most of these technologies are offering poor scalability for production of required cell ingredients or their process for generating organoids in reproducible manner and large-scale production of complex organoids under defined culture conditions remained challenging. Microfluidic or electrospray generation of liquid core and hydrogel-shell made microcapsules using natural biopolymers such as biodegradable alginate or alginate-chitosan based shell material or non-degradable PEG based microcapsules have been suggested as proper 3D culture environment for different applications including human organoids generation <sup>195</sup>. For example, uniform aggregate formation of hPSCs <sup>201</sup>, primary hepatocytes encapsulation and co-culture with fibroblast <sup>159</sup> or HepG2 cells with HUVEC cells <sup>202</sup>, and encapsulation/transplanting of human islets or stem cells derived islets for clinical application <sup>158,163</sup> has been successfully done owing to hydrogel microcapsules tunable permeability, and adaptability for scale-up production. Among different microcapsules generation technologies, the microfluidic technology for generating core and shell microcapsules can be considered as proper choice for continuous production of organoids due its capability to achieve uniform morphology and size-controlled capsules with tunable mechanical properties and permeability in a fully controlled manner. However, currently established droplet microfluidic platforms mainly used natural biopolymers such as alginate/chitosan-based materials for microcapsules production that can result in batch to batch variation in microcapsules production process and their size homogeneity due to the natural source of shell material and its inherent composition variability <sup>195</sup>. GelMa and 4-arm PEG network hydrogels providing more defined materials with tunable diffusion properties but not offering degradability for organoids release after generation which is essential for scalable

culture for further maturation, integrating to host tissue, or fabricating a tissue in lab settings for either autologous or allogeneic organoid based therapy <sup>159,202</sup>.

Moreover, almost all studies that using microcapsules for cell encapsulation/culture/co-culture used PDMS material for fabrication of the 3D flow-focusing chip which require intensive work for fabrication and prone to change its hydrophobicity/surface properties during the microcapsule's generation process that can result in capsules adhesion to microfluidic chip wall and stopping the process. Accordingly, PDMS chips have not translated well to a commercial scale and mass-production manufacturing due to their multi-step and labor-intensive fabrication processes such as etching (glass and silicon) or embossing and injection molding (thermoplastics) <sup>163,203</sup>. Moreover, most of the microfluidic platforms used typical syringe pump systems that working with limited working volume (e.g. 50 ml for each stream), with no option for efficient mixing of cells suspension in core solution to avoid cells settling down and aggregation that make them unsuitable for continues and scalable generation of droplets and organoids. In fact, it seems that almost all related studies have done in small scale as proof-of concept studies rather that process development for scalable manufacturing of microcapsules and large-scale organoid production.

Here, we first established a scalable platform for large scale production of hepatic progenitors as 3D aggregates, progenitor and mature endothelial cells, and mesenchymal stem cells from individual hPSC lines as required cell ingredients for scalable generation of functional vascularized liver buds through co-culture and self-organization. Then, we established a fully scalable and continuous biodegradable microcapsules production process using pressure driven microfluidic pumps / remote pressurized vessels under control of an automated microfluidic system to address scalability issue of previous established protocols for liver organoid production through co-culturing technique. The microfluidic platform combined with medical grade polycarbonate (PC) made chip or ready-to-use polyester made 3D-printed-3D-flow focusing chip for one-step fabrication and continuous production of biodegradable microcapsules under aseptic culture condition. Fully degradable hydrogel materials including

synthesized 4arm-PEG-MMP-sensitive peptide or PGA hydrogel microcapsules were also used for continuous generation of vascularized hepatobiliary organoids through self-organization/ condensation mechanism. We demonstrated that liquid core microcapsules with proper size, permeability, mechanical properties, and degradability allowed co-culture of liver progenitors, endothelial cells and mesenchymal stromal cells derived from hPSCs under defined and animal-free culture condition in single step to generate mono-dispersed vascularized hepatobiliary liver organoids and their subsequent release to the dynamic suspension culture for further maturation. We showed that 3D dynamic suspension culture of organoid resulted in generation of highly functional and self-organized hepatobiliary organoids that showed future maturation and formation of *in vivo* liver tissue like biliary and vascular structures after 7 days of culture. The cell ingredients scalable production process combined with the established microfluidic platform offering a promising approach for large production of highly functional hPSC derived vascularized hepatobiliary organoids under defined culture conditions that can be employed as manufacturing platform to commercialize “Organoid medicine” as allogeneic organoids therapy platform.

## **Materials and Methods**

### ***Optimizing co-culturing conditions and density optimisation for liver bud/organoid generation***

To explore the optimum cell density and ratio for generating human liver organoids 9-12 days hepatic endoderm cells, KDR+/CD31+ endothelial cells and hPSCs-derived mesenchymal stromal cells were resuspended at different cell densities ( $1-60 \times 10^6$  cells/ml) and ratio 10:8:5, 10:8:2, 10:5:5, 10:5:2, 10:2:2 were resuspended in a mixture of endothelial cell growth medium (EGM, Lonza) and hepatocyte culture medium (HCM, Lonza containing 0.1 mM dexamethasone ; Sigma-Aldrich, St. Louis, MO) without using FBS, Oncostatin M (10 ng/mL; R&D biosystem), hepatocyte growth factor (HGF) (20 ng/mL, R&D biosystem), and 2% PLTGold® Human Platelet Lysate in 40  $\mu$ l volume for each well and transferred to Corning® 384-well Round Bottom Ultra-Low Attachment Spheroid Microplate after passing through a

reversible strainer (37  $\mu$ m, STEMCELL technologies). The bud/organoid formation Kinetic was monitored by phase-contrast imaging plus time-laps video capture using IncuCyte® S3 Live-Cell Analysis System (Essen bioscience).

#### ***Delaying cell aggregation after co-culture in spinner flask***

Here, we used 1-5% Mebiol® Gel PNIPAAm-PEG 3D (Cosmo bio, US) as and 1 g/L dextran sulfate (40 kDa, Sigma Aldrich) as culture medium densifiers for delaying cell clumps during co-culture under 3D dynamic suspension culture and avoiding cell clumps transfer to the microfluidic chip <sup>204</sup>. Aggregation kinetics were monitored by co-culturing cells in 125 ml spinner flask with 50 ml working volume and taking 2 ml samples each 2 h for observing under inverted light microscope (Evos XL, Life technologies).

#### ***Synthesis of biodegradable 4arm-PEG-MMP sensitive peptide as shell material***

4-arm-PEG-4-Maleimide (10 and 40 kDa, >95% end-group substitution) was purchased from the Jenkem Technology Co., Ltd. (USA). Fast MMP1 degradable peptide with one thiol group (NH<sub>2</sub>-CGPQGIWGQGRK-CONH<sub>2</sub>) was synthesized proteomics core facility of Koch institute for integrative cancer research. Sulfo-MBS purchased from Click chemistry (US) and triethanolamine (TEA), KRB buffer, mineral oil, human recombinant MMP1, and Dithiothreitol (DTT) purchased from Sigma Aldrich.

A schematic of the hydrogel formation and degradation concept is presented in (Fig. IV-1). 4-arm-PEG-MAL-MMP were prepared by Michael-type addition of fast MPP1 sensitive peptide (NH<sub>2</sub>-CGPQGIWGQGRK-CONH<sub>2</sub>) to 4-arm-10K PEG-MAL or 4-arm-40K PEG-MAL. Practically, 4-arm-PEG maleimide was dissolved in phosphate buffered saline to prepare a stock solution (25 mM). In parallel, peptide solution ( 101 mM in 1X PBS , 0.05 mmol, 5 equiv, 1.25 equiv. per maleimide, concentration checked by UV) was prepared in tri(2-carboxyethyl) phosphine hydrochloride (TCEP) (36 mg, 0.025 mmol, 2.5 equiv.) and stirred at RT for 30 min. Next, 4-arm-PEG maleimide (25 mM, 0.01 mmol, 1 equiv.) solution was added

to the peptide solution to make a final reaction solution (10 mM). After 3 h of continuous vigorous shaking, the reaction mixture was passed through an Amicon® filter (MWCO 50K) and washed with PBS 1 X (3 times), concentrated, and characterised by microflex™ LT/SH MALDI-TOF mass spectrometer. Then, the modified PEG with MMP sensitive peptide has been used directly for the next step after coupling confirmation.

In the next step Maleimide group was added to synthesized 4arm-PEG-MAL-MMP to create 4arm-PEG-MAL-MMP-MAL that can be crosslinked by thiol groups to create a hydrogel network. Briefly, Sulfo-MBS (42 mg, 0.1 mmol, 10 equiv.) was added to the reaction mixture and vortexed to make the solution homogenous. The mixture was vigorously shaken till the solution turned clear. It was then again passed through an Amicon® filter (MWCO 50K) and washed with PBS 1X and characterised by NMR and MALDI-TOF mass spectrometer.

***Scalable microfluidic platform for continuous production of liquid core and shell microcapsules***

We used 3D flow-focusing microfluidic polycarbonate or polyester made chip with hydrophobic surface combined with a fully scalable and continuous microfluidic platform for generation of liquid core and biodegradable microcapsules. The Microfluidic platform consisted of four pressure pumps (Mitos P-Pump, Dolomite Microfluidics, UK) equipped with in-line Mitos Flow Rate Sensors to monitor and control the streams flow rates by integrated pressure and flow sensor (Figure IV-1).

Four flow rate sensors, two 30 - 1000 µl/min and two 1 - 50 µl/min were employed in the organic lines and aqueous lines to pulse-free delivery of stream to the chip, respectively.

An air compressor (California AirTools) equipped with 0.2 microfilter for air inlet and outlet provided the supply pressure for the remote P-Pumps to control different streams flow rates by regulation pressure.

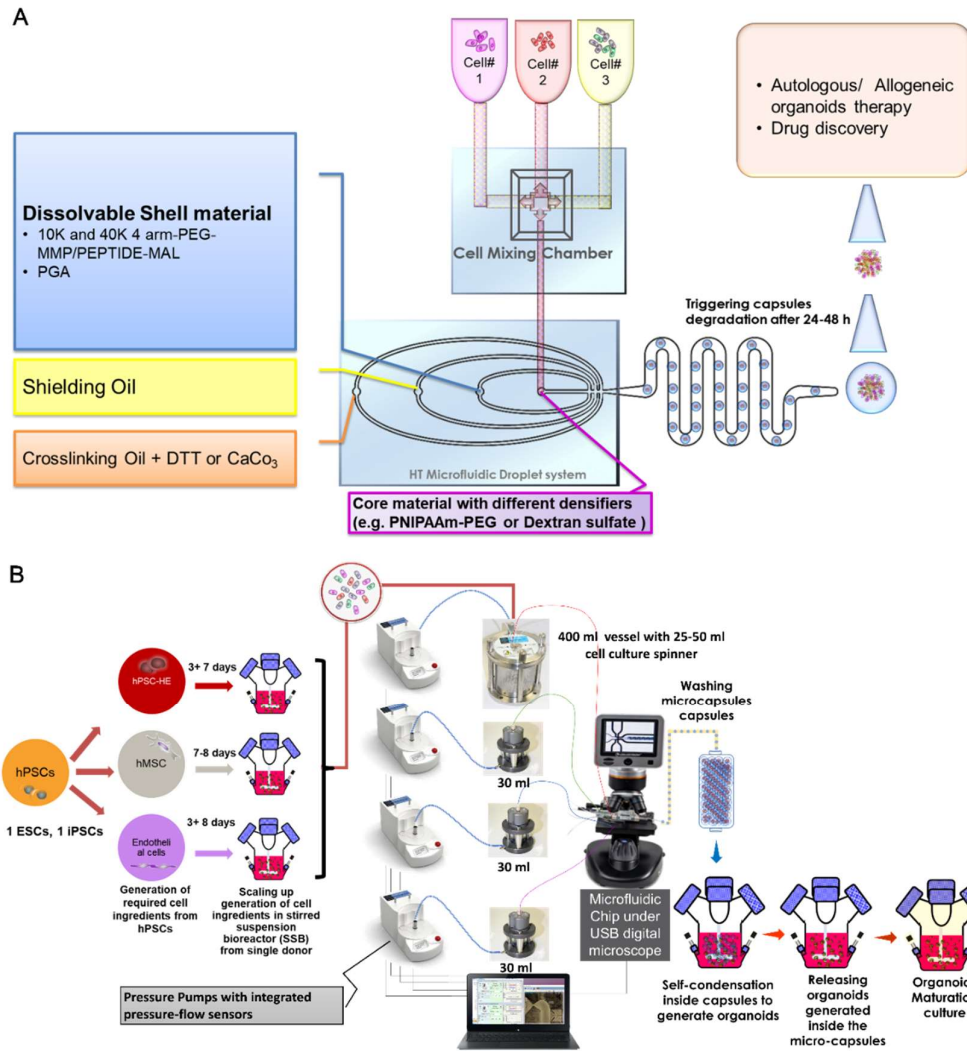


**Figure IV-1. Schematic design of 3D flow focusing chip and scalable microfluidic platform for generation of liver organoids.** Concept of droplet microfluidic chip including information about different streams including core, shell, shielding oil or crosslinking oil compositions (A). PC-controlled scalable microfluidic droplet generation platform using pressure-based remote pumps and vessels for aseptic production of microcapsules and vascularized liver organoids, and their further maturation under dynamic suspension culture condition (B).

The pumps were connected to three 30ml remote pressure vessels for shell, shielding oil and crosslinking oil streams and one 400 ml remote pressure vessel with a two arm 50 ml cell culture spinner flask (Wheaton scientific) inside placed on magnetic stirrer for continuous stirring of cells suspension delivering them as single cells to the chip during microcapsules production process.

A USB camera microscope (AM4113T, Dino-lite, US) was also used for continuous monitoring of capsules generation process in PC. The whole set-up was controlled by Flow Control Centre

software through a PC and all components except Pumps and air compressor placed inside A2 Biosafety cabinet for aseptic production of microcapsules for optimisation trials and the shell solution also microfiltered before use and sterile mineral oil and reagents were used for shielding oil and crosslinking oil preparation (Fig. IV-1).

#### ***Fabrication of polycarbonate 3D flow focusing chip***

Polycarbonate chips were from TUFFAK® Polycarbonate Sheet (thicknesses of 2 and 3 mm; Bayer, Germany) and were processed with laser cutter before making channels. Top and Bottom masters were prepared by Othermill Pro mini CNC machine. We designed the channels with AutoCad 2019 software and generated the CNC code, and created toolpaths with Bantam Tools software (BANTOM TOOLS, USA). Prior to bonding all master and bottom pieces were cleaned from debris with pressurized water and then with detergent and several rinsing steps with distilled water. Then both PC pieces were transferred to a 2L vacuum chamber with 5 ml dichloromethane in a glass vial (DCM, Sigma) with 10 mbar vacuum pressure to create a swelled surface layer on PC parts after exposing to DCM solvent vapor for 30 min. Then, slabs with swelled surface were immediately transferred between a silicon rubber sheets to a preheated thermal press (Carver, US) at 135 °C for 40 min at 0.4 MPa for bonding two parts together. After bonding and cooling, required ports were created by drilling and stainless-steel needles were used to create ports for 4 different streams.

#### ***Fabrication of 3D printed 3D flow focusing chip***

3D printed microfluidic chips including ports (i.e. Top and Bottom slabs) were designed in AutoCad 2019 software and 3D printed from VeroClear material which is a transparent polyester based material that simulates PMMA (polymethyl methacrylate) using Stratasys Objet30 Pro (Stratasys, USA). Support material were removed from printed parts and cleaned parts were soaked in 2 M NaOH for 2 h for support materials residues cleaning and rinsed

multiple times with distilled water. Then, slabs were bonded using medium viscosity medical instant glue (Loctite 403, Japan) by embedding paraffin in channels and removing after bonding by heating at 50° for 30 min in laboratory oven.

### ***Microfluidic device operation, microcapsule fabrication, and separation***

Microfluidic 3D flow-focusing devices for both chip types were infused with 4 different solutions to generate capsules: 1) a core solution composed of different densifiers 2 % w/v Mebiol® Gel PNIPAAm-PEG thermo responsive gel, 1 g/L 40 kDa Dextran sulfate in EGM2- HGM 50:50 culture medium including hepatic endoderm, endothelial progenitors, and mesenchymal stem cells with different cell densities from 1-40 x 10<sup>6</sup> cells/ml at 1: 0.8 :0.2 ratio, respectively. The cell suspension mix filled in autoclaved 50 ml spinner flask and transferred to 400 ml pressure chamber under aseptic condition and the chamber were purged with humidified sterile air with 5% CO<sub>2</sub> and transferred to incubator to keep the chamber at 37 °C, 2) a shell solution containing 8% w/v 4-arm MAL-MMP sensitive peptide-Mal and 10 mM triethanolamine (TEA) dissolved in KRB buffer or 2% w/v polygalacturonic acid (PGA) in KRB buffer ( adjusted at pH=7 by Sodium bicarbonate, 3) shielding organic phase of mineral oil with 1% v/v Span-80 surfactant, and 4) crosslinking organic phase of mineral oil with 3% Span-80 and a 1:15 emulsion of 35 mg/mL dithiothreitol (DTT) dissolved in DI water (emulsion was generated by sonicating oil/water mixture for 30 min in an ultrasonic bath) for PEG based capsule and 10% acetic acid in oil and 2% calcium carbonate (w/w in proportion to oil, emulsion was generated by sonicating oil/water mixture for 30 min in an ultrasonic bath). Shell, shielding, and crosslinking solutions were sterilized with 0.2 µm centrifuge filters, and injected into respective microfluidic inlets with Mitos remote pressure pumps at flow rates of 3-8 µL/min for core, 3-8 µL/min for shell, 30-50 µl/min for shielding oil, and 40-60 µl/min for cross linking oil. Generated microcapsules were collected in another spinner flask after passing through an in-line mesh filter and washed min 3 times with PBS and resuspended in co-culture media for 2-3 days for further maturation. After 3-4 days and generation self organised organoids, Microcapsules

were digested enzymatically (recombinant MMP1, collagenase or pectinase), and organoids were kept in refreshed culture medium for another 4 days for further maturation.

#### ***Microcapsule characterization***

The size of the microcapsules with different shell material, shell flow rates were captured using an inverted light microscope (EVOS XL, Life technologies) and measured using imageJ as well as microscope built-in software.

#### ***Permeability studies using labelled dextran***

Diffusive properties of PGA and 4armPEG-MAL-MMP-MAL derived capsules were visualized by imaging transport of fluorescent dextran polymers across capsule shell barriers. Briefly, microcapsules were incubated in a solution of 800 µg/mL TRITC-labeled dextran (65-85 kDa, Sigma Aldrich) in PBS until saturated, then washed with fresh PBS in a microfluidic flow chamber and monitored over time with a fluorescence microscope. Average pixel intensities inside capsules (n=10) were quantified in ImageJ.

#### ***Characterization of Hepatobiliary organoids***

##### ***Immunostaining, fluorescent, and confocal imaging***

Generated hepatobiliary organoids collected, washed, and fixed overnight in 4% paraformaldehyde at 4 °C for immunofluorescence staining or confocal microscopy. The fixed spheres were incorporated in an Histogel (2%). After processing, they were embedded in paraffin blocks and sectioned into 6 µm sections with a microtome (Microm™, HM325). We followed the standard protocol for immunofluorescence staining. Fixed aggregates were also stained with direct antibody staining protocol and suspended in glycerol/fructose solution in glass bottom 24-well plates (Cellvis, US) for imaging the confocal microscopy (Olympus FV1200 Laser Scanning Confocal Microscope).

Cell viability was evaluated at the end of the differentiation process by LIVE/DEAD staining (Catalog # L-7013, Molecular Probes) to determine the presence of any core necrosis in generated organoids according to the manufacturer's instruction. Fluorescent images were acquired by confocal microscopy using Olympus FV1200 laser scanning confocal microscope.

### ***Flowcytometry***

For flow cytometry analysis, we dissociated the organoids into single cells using Accutase® cell detachment solution with 20 mg/mL collagenase type I (Sigma-Aldrich). Dispersed cells were fixed in 4% paraformaldehyde at 4 °C for 20 min, permeabilized, blocked in serum, and allowed to incubate overnight with diluted dye conjugated antibodies for direct staining method or diluted primary antibodies at 4 °C and then washed and incubated with secondary antibodies for 45 min at room temperature. Flow cytometry analysis was performed with a BD LSRFortessa™ Flow cytometer (Becton Dickinson, US).

### ***Metabolic activity determination***

ICG and LDL uptake were performed to evaluate the maturation extent and metabolic activity of the generated hepatic cells (Vosough et al., 2013). PAS staining was performed with Periodic Acid-Schiff (PAS) Kit (395B, Sigma Aldrich) according to manufacturer instruction.

### ***Albumin (ALB) and fibrinogen secretion and intracellular urea assay***

To evaluate the albumin (ALB) secretion ability of hepatobiliary organoids, the supernatant culture media was collected 48 h after the last media refreshment and stored at -80 °C before the assay. The concentrations of ALB and fibrinogen in the supernatant were assessed by an ELISA kit specific for each protein or metabolite according to the manufacturer's instructions including Human Albumin ELISA kit (ab108788, Abcam), Alpha Fetoprotein Human SimpleStep ELISA kit (ab193765, Abcam), and Fibrinogen Human SimpleStep ELISA Kit (ab171578, Abcam). Hepatobiliary organoids were digested with a specific buffer of a

commercial Urea Assay Kit (ab83362, Abcam), total Urea content within the generated hepatobiliary organoids during maturation process was measured, according to the manufacturer's instructions. All the samples were carried out in triplicate.

### ***CYP activity assays***

CYP activity of organoids were conducted according to the manufacturer's instructions. Different P450 enzymes activity were tested including CYP3A4 (P450-Glo CYP3A4 (Luciferin-IPA) – V9002 – Promega), CYP2B6 (P450-Glo CYP2B6 – V8322 – Promega), CYP1A1 (P450-Glo CYP1A1 – V8752 – Promega) by incubating them with different inducers.

Undifferentiated hPSC, primary hepatocytes and differentiated HLCs were incubated with basal medium containing 20  $\mu$ M Rifampicin solution (Sigma Aldrich), or DMSO (0.1%) for 72 hours for the CYP3A4 activity assay. For the CYP2B6 activity assay, undifferentiated hPSC, primary hepatocytes and differentiated HLCs were incubated with basal medium containing 1000  $\mu$ M Phenobarbital solution (Sigma), or DMSO (0.1%) for 72 hours. For the CYP1A1 activity assay, undifferentiated hPSC, primary hepatocytes and differentiated HLCs were incubated with basal medium containing 50  $\mu$ M Omeprazole solution (Sigma), or DMSO (0.1%) for 72 hours. The activity of each enzyme was measured by reading the luminescence using luminometer instrument (Luminoskan™ Microplate Luminometer – Thermo Scientific) according to the manufacturer's instructions. All the experiments were performed in triplicate.

### ***Gene expression analysis***

RNA was extracted using Qiagen mini-RNA extraction kit. Reverse transcription was performed with random primers (Applied Biosystems RT kit) to generate cDNA. Gene expression was quantified using gene-specific primers and KAPA SYBR® Fast qPCR kit (KAPA Biosystems, KK4602). NCBI primer designing tool was used to design gene-specific primer sequences. The primers used were validated for their specificity and those with efficiency between 90-110% were used (Table S IV-3). Gene expression profile was analyzed

using Microsoft excel and heatmaps were generated using Prism Graph Pad Ver. 8 or GenePattern version 2.0 <sup>174</sup>.

For control samples, Total RNA, Fetal Liver, Human purchased from Agilent Technologies (19-37gwk pool Fetal Liver Tissue) and Adult human liver Total RNA also obtained (7yrs, 25 yrs., 42 yrs. old Adult Liver Tissues) from Ambion®.

### ***Western Blot analysis and total DNA content measurement***

Protein extraction and western blot analysis of VHOs was done using a method as previously described <sup>18</sup>. Briefly, the upper phase of vial in previous step, was transferred to a new tube and the proteins were precipitated by centrifugation and washed. Protein pellets were dried in RT and dissolved in urea buffer. Pierce BCA protein assay Kit was used for determining the protein concentration. For western blot analysis, 20 µg total protein was separated by 10% sodium dodecyl sulfate-polyacrylamide gel electrophoresis (SDS-PAGE), and transferred to PVDF membrane via a semi-dry blotting system for two hours at 25 V. Blotted membranes were blocked by 2.5% nonfat milk, and then washed by tris-buffered saline, containing 0.1% Tween 20 (TBST) for 5 min. Subsequently, blots were incubated with primary antibodies against ALB, AFP, CK19, and GAPDH for 90 min. After three times washing (10 min each), blots were incubated for one hour with secondary antibodies. Blots were washed like previous step, and the protein bands were visualized on x-ray films in a darkroom using ECL select substrate. Images were scanned using a densitometer (Bio-Rad, USA).

For DNA content measurement, organoids were homogenized in Trizol reagent and centrifuged at 12000 × *g* for 15 min after addition of chloroform. The DNA was precipitated by adding 100% ethanol to the lower phases and extracted as manufacture instruction. DNA concentration/quality was evaluated by spectrophotometry.

### ***Statistical analysis***

Data were presented as mean  $\pm$  standard deviation (SD). T-squared test was used to compare two independent groups. Comparisons between groups and data were performed with one-way ANOVA and the post-hoc Tukey test. P 0.05 were considered statistically significant. The analyzes were performed using SPSS 16 or Prism 8 software's.

## Results

### *Optimum cell density and ratio for self-condensation of hepatic endoderm, endothelial cells, and mesenchymal stem cells co-culture and liver bud/ organoid formation*

Hepatic endoderm cells at different transitional hepatic differentiation day, endothelial cells (EC), and hPSC derived mesenchymal stem cells (MSC) generated under dynamic suspension culture in scalable manner were used to optimize cell ratio and cell density for generation of vascularized liver bud/organoids through co-culture technique and MSC-driven self-condensation<sup>96</sup>. Results showed that mixing Day 10-11 HE (TBX3<sup>+</sup> /ADRA1B<sup>+</sup>), CD31<sup>+</sup> EC, and MSC in 10:8:5 and 10:8:2 ratio at  $40 \times 10^6$  cells/ml density in low attachment spheroid wells resulted in efficient condensation of these cell types to a dense 3D bud/ organoid like structure after 18-24 h with  $110 \pm 22 \mu\text{m}$  diameter size. Decreasing endothelial cells ratio for 80% to 50% of total hepatic endoderm cells numbers resulted in less self-condensation and a loose 3D structure formation ( $140\text{--}160 \mu\text{m}$  diameter size). Similar outcome observed for decreasing mesenchymal stromal cells ratio from 50% to 20% that resulted in lower self-condensation and creating pf clump like structure ( $150\text{--}190 \mu\text{m}$  diameter size). Decreasing endothelial cells and mesenchymal stem cells to 25% and 10 % total hepatic endoderm cells numbers resulted no self-conception and single cells created small clumps after 24 h. Thus, these results demonstrating that both endothelial and mesenchymal stromal cells ratio is highly important parameters for regulating cell-condensation and creating a 3D liver bud/organoid structure (Fig. IV-2 A). The 10:8:2 ratio has been selected for other optimisation trials because of efficient cell condensation with lower MSC ratio as starting cell ingredient. In the next step, we explored again the optimal day of transitional hepatic endoderm cells (Day 9-12 of differentiation) and total cell mix density (20, 40, and 60 million cells/ml) that can result in more efficient and reproducible self-condensation and liver organoid generation. Results showed that using Day11 hepatic endoderm cells that well-expressed liver progenitors' markers (e.g. TBX3, ADRA1B (alpha-1b Adrenergic Receptor), EPCAM, CD90, and Hnf4 $\alpha$ ) resulted in robust generation of liver organoids as 3D structures. Moreover, cells self-

condensation was happened using different cell densities from 20 to 40 million cells/ml while liver organoids structure generated with 20 and 40 million cells/ml resulted in generation of more homogenous 3D structure compared to 60 million cell/ml cell density that resulted in generation of heterogenous 3D structures (Fig. IV-2 B). The outcome of these trials and findings were used to establish the co-culturing conditions of cells in core solution of microfluidic system for continuous microcapsules production as well as co-culture trials under dynamic suspension culture in spinner flask.

***Delaying cell aggregation after co-culture in spinner flask and co-culture trial under dynamic suspension culture***

We identified that cells aggregation is an important technical issue in continuous microfluidic generation of complex liver organoids using co-culture technique. Practically, hepatic endoderm cells showed high tendency to form aggregates during dynamic suspension culture after 4-6h of inoculation as single cells that got boosted by co-culturing with endothelial and mesenchymal stromal cells at high cell densities. This aggregation will result in creating cell clumps in spinner flask before delivering them to the chip and blocking microfluidic tubing's/channels, or heterogenous encapsulation of cells in microcapsules and subsequently heterogenous organoids formation.

To overcome the problem, we used 1-5% Mebiol® Gel PNIPAAm-PEG 3D (Cosmo bio, US) thermo-responsive polymer because of its high biocompatibility and 3D hydrogel formation properties and/or 2% dextran sulfate (40 kDa, Sigma Aldrich) as culture medium densifiers to minimize risk of aggregation<sup>182,204</sup>. We evaluated aggregation kinetics for delaying cell aggregation during continuous production of cells loaded microcapsules using microfluidic system. Results showed that 6-10% w/v Mebiol® Gel PNIPAAm-PEG 3D thermo-responsive polymer in culture media is in liquid form at 4 °C and forming a stable hydrogel at 37 °C that fully compatible with different cells types and can be used for generation of cell aggregates, differentiation under 3D culture condition, and creating 3D tissue constructs<sup>205-207</sup>. Its has

been also reported that dextran sulfate offering high biocompatibility with mammalian cells and can reduce cell clumping and aggregation and clumping during CHO culture for monoclonal antibody production.

Accordingly, used lower concentrations of Mebiol® Gel PNIPAAm-PEG 3D (1-4% w/v) as liquid densifier were used to increase the density of culture media combined with 1% 40kDa dextran sulfate to delay aggregation and enabling continuous production of cells loaded microcapsules.

Dynamic suspension co-culture of cells at optimized cells ratio and seeding density conditions in 50 ml spinner flask showed that small cell clumps appeared after 4h in co-culture media without any densifier. The size of small clumps was increased after 8-12 h of culture and condensed clumps in form of heterogenous aggregates were generated after 24h culture. On the other hand, different concentrations of Mebiol® Gel PNIPAAm-PEG 3D were tested with and without dextran sulfate addition to minimize clump formation. Results showed that combination of 2% Mebiol® Gel PNIPAAm-PEG 3D and 1 g/L dextran sulfate addition could delay aggregate formation for up to 10 h and relatively homogeneous aggregate formation observed after 24h (Fig. IV-2 C).

After obtaining satisfactory results in generating homogenous aggregates using culture medium densifies, we hypothesized that this protocol may be also useful for scalable production of vascularized liver organoids by co-culturing tHE/EC/MSC cells at optimized cell density and ratio under dynamic suspension culture in spinner flask at 50 ml working volume. Results showed that heterogeneous aggregates (100-700  $\mu\text{m}$  diameter) were generated by co-culturing H9-derived HE, EC, and MSC cells and integrated differentiation/maturation after 3, 5, and 7 days that indicated inefficient generation of liver organoids in reproducible manner (Fig. IV-2 D).

Therefore, the established combination/ratio has been used in preparation of core solution for all microcapsules production trials using the microfluidic platform for subsequent production of homogenous liver organoids.

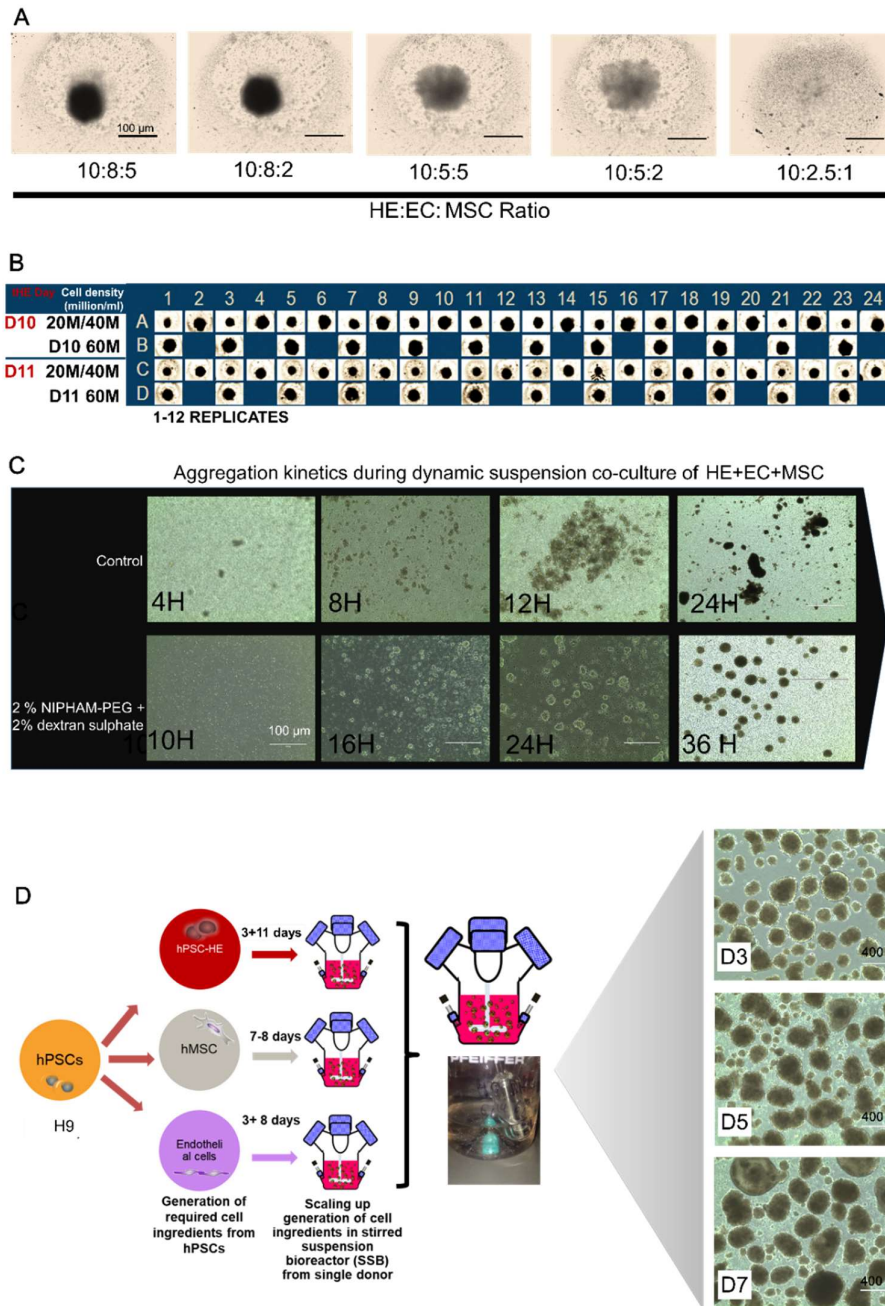


**Figure IV-2. Optimizing cell ratio and cell density co-culture condition for efficient self-condensation of hPSCs derived tHE, EC, and MSC for generation of liver bud like structure.** Hepatic endoderm cells, KDR+/CD31+ endothelial cells and hPSCs-derived mesenchymal stromal cells were resuspended at different ratio 10:8:5, 10:8:2, 10:5:5, 10:5:2, 10:2:2 in co-culture medium transferred to Corning® 384-well Round Bottom Ultra-Low Attachment Spheroid Microplate and monitored by light microscopy after 24h (A). Explored the transitional hepatic endoderm cells differentiation day (Day 9-12) and total cell mix density (20,40, and 60 million cells/ml) on self-condensation efficacy and liver organoid generation (B). Delayed aggregate formation after using combination of 2% Mebiol® Gel PNIPAAm-PEG 3D and 1g/L dextran sulfate addition to co-culture media compared to control group (C). Dynamic suspension co-culture of tHE, EC, and MSC for generation of liver bud like structure (D).

### ***Synthesis of biodegradable 4arm-PEG-MMP sensitive peptide as shell material***

To date, most of the degradable hydrogel microcapsules for cells encapsulation or organoid formation made from natural sources biomaterials such as alginate<sup>158</sup>, alginate-chitosan<sup>195</sup> or gelatin-based materials<sup>202</sup> that suffer from lot-to-lot variation and variability in microcapsules generation process. Degrading alginate-based capsules require addition of chelating agents for divalent cations such as citrate and ethylenediaminetetraacetic acid (EDTA) or hexametaphosphate that can also have adverse effect on cells/organoids viability<sup>208</sup>. Non-degradable PEG derived hydrogels have been also used for microfluidic generation of liquid core and shell droplets for human hepatocytes encapsulation that offering more reproducibility and defined condition for robust generation of microcapsules<sup>159</sup>. However, these microcapsules are non-degradable and only suitable for applications that require a shell as immune barrier layer between therapeutic cells and host immune system such as encapsulated human islet transplantation. Here, we synthesized a 4arm-PEG-MMP1-sensitive peptide (Fast degradable MMP1- CGPQGIWGQGRK) material that can be degraded by either MMP1 secreted by endothelial cells or mesenchymal stromal cells<sup>209,210</sup>, or low concentrations of collagenase for releasing organoids from microcapsules for further maturation under dynamic suspension culture and potential allogeneic cell therapy applications.

4-arm-PEG-MAL with 10 kDa and 40 kDa PEG molecular weight were used as starting material and the fast degradable MMP1 sensitive peptide with one cysteine (thiol group) were conjugated to 4 maleimide groups (Fig IV-3 A) of 4-arm PEG. In the next step, another maleimide group was added to MPP-peptide end using Sulfo-MBS reagent containing maleimide group because of its fast cross-linking kinetics with DTT (Fig IV-3 B). Interestingly, only 4-arm-10 K PEG-MAL- PEPTIDE -MAL was soluble in water (8% w/v) and synthesized 4-arm-10 K PEG-MAL-MMP-MAL formed a stiff hydrogel after desalting and concentration without adding a crosslinking agent (Fig IV-3 C).

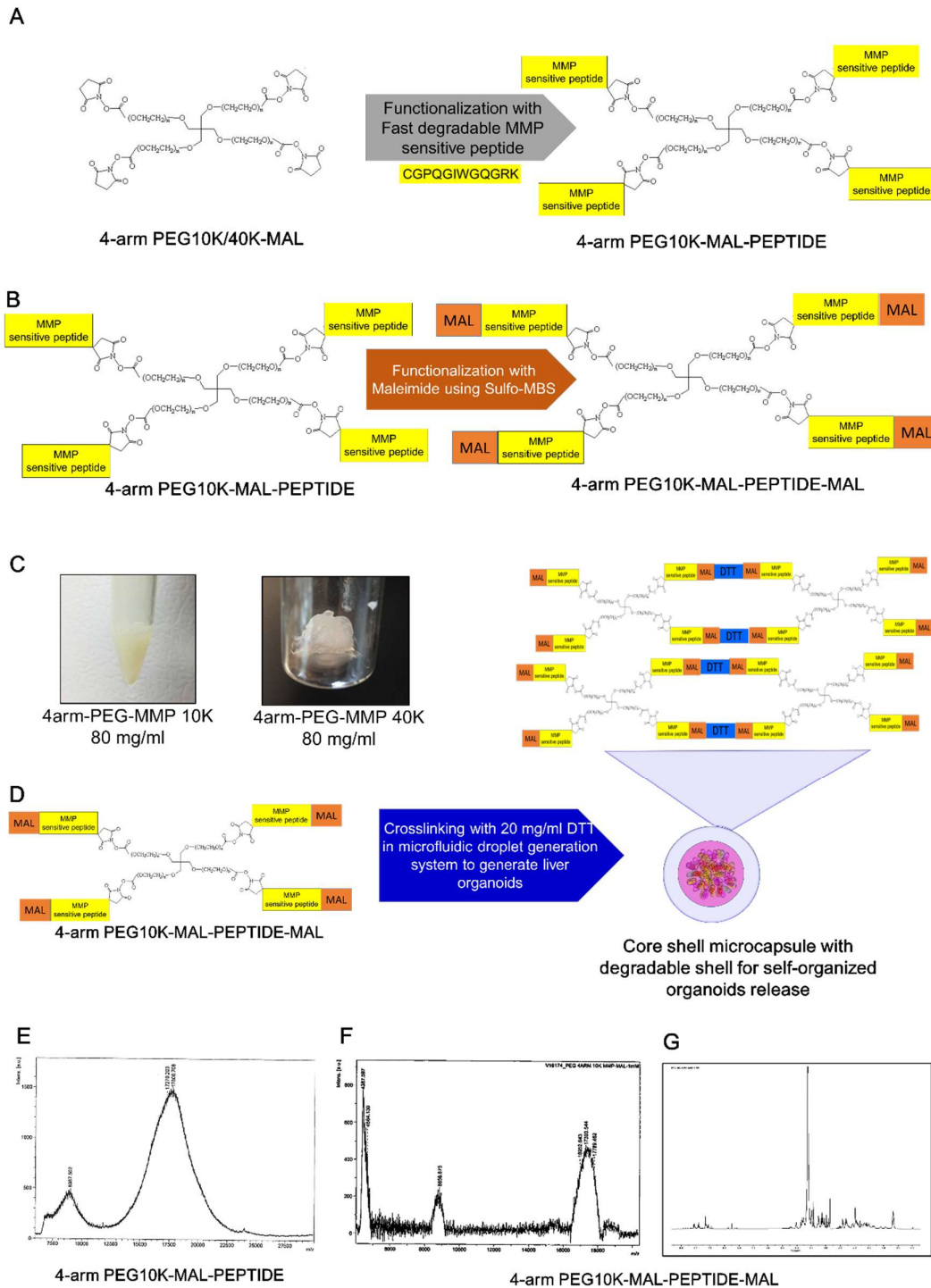


**Figure IV-3. Synthesis of biodegradable 4arm-PEG-MMP sensitive peptide as shell material.** Conjugation of fast degradable MMP1 sensitive peptide to 4-arm-10/40 PEG-MAL for generation of biodegradable hydrogel (A), Adding maleimide group to 4-arm-10/40 PEG-PEPTIDE using Sulfo-MBS (B). Synthesized 4-arm-10K PEG-PEPTIDE and 4-arm-40K PEG-PEPTIDE (C) Crosslinking concept of 4-arm-10/40 PEG-PEPTIDE for generation of biodegradable shell microcapsule (D). Mass-spectrometry characterization of 4-arm-10K PEG-PEPTIDE (E), Mass-spectrometry characterization of 4-arm-10K PEG-PEPTIDE-MAL (F) and its NMR (G).

Thus, the synthesized 4-arm-10K PEG-MAL-MMP-MAL prepared at 8% concentration as shell solution and tested for creating hydrogel with DTT cross-linker.

Results showed that dissolved 4-arm-10K PEG-MAL-PEPTIDE-MAL rapidly formed a stiff gel by adding crosslinking solution with minimum 20 mg/ml DTT concentration. Moreover, synthesized 4-arm-10K PEG-MAL- PEPTIDE and 4-arm-10K PEG-MAL-PEPTIDE-MAL were characterized by MALDI-TOF mass spectrometry and NMR that confirmed conjugations completion for MMP1 degradable peptide (Fig IV-3 E) as well as secondary MAL group (Fig IV-3 E). Thus, 4-arm-10K PEG-MAL- MMP sensitive PEPTIDE-MAL selected as shell material for fabrication of microcapsules that can be crosslinked with crosslinkers with thiol groups such as DDT to form a mechanically stable hydrogel shell in microfluidic system. The main advantage of the PEG-PEPTIDE hydrogel is its easily degradability by peptidase enzymes or MMP1 secreted by cells after self-condensation inside microcapsules to harvest organoids and subsequent integrated maturation under dynamic suspension culture in scalable manner (Fig IV-3 F&G).

#### ***Fabrication of polycarbonate and 3D printed 3D flow focusing chips***

Polycarbonate chip was fabricated in different channel configuration designs including round or U bottom shapes channels, 45° or 90° channel designs (Fig. IV-4 A) , and channels depth configuration to achieve homogeneous droplet production, minimize channels blocking, achieve uniform flow for all streams, and maximize productively with smaller microcapsules size (150-200 µm diameter). Small microcapsules are preferable since capable generating liver organoids with smaller size for facilitated transplantation and minimizing creation necrotic cores during growing in hepatic maturation phase (Fig. IV-4 A). After testing different designs and evaluating generated microcapsules size and size distribution profile (data not shown), U-bottom type channels with 90° channel junctions and 200 µm depth for core, 250 µm for shell channels and 400 µm depth for shielding and crosslinking oil channels was selected as optimal design for homogenous streams flow and generation of microcapsules from 4-arm-PEG-

Peptide (Fig IV-4 B&C). 3D printed microfluidic chip has also made by same design and both the microfluidic chips (Fig. IV-4 D&E) were capable for generation of uniform PGA (Fig. IV-4 F) and 4-arm-PEG-Peptide (Fig. IV-4 G) microcapsules with about 150  $\mu\text{m}$  diameter.

***Optimising cell loaded microcapsules production process for generation of organoids through self-organisation***

As mentioned before, the optimal microcapsules size for liver organoids generation can be considered around 100-150  $\mu\text{m}$  to generated organoids with about 100  $\mu\text{m}$  diameter size that will minimize formation of necrotic cores in the organoids during further expansion and maturation under in vitro culture condition and facilitate their handling and transplantation. It has been demonstrated that dense cell aggregates/organoids with diameter size larger than 300-400  $\mu\text{m}$  diameter are prone to reducing viability and creation of necrotic core because of potential limited diffusion of metabolites or morphogens<sup>211,212</sup>. On the other hand, maximizing microcapsules production speed will facilitate the continuous and high throughput production of organoids and minimizing risk of aggregation or cells clumps formation during co-culture mixing. Other key important parameter of microcapsules as 3D culture environment is their mechanical stability allowing them to be stable under dynamic cell culture and respective shear stress during mixing. Diffusive properties of microcapsules are also high important for providing efficient metabolites, morphogens, and by-products exchange through the shell to support cells viability, proliferation, and function. In fact, a balanced mechanical stability and diffusive properties should be established for successful cells encapsulation and organoids formation. Among different variables in droplet generation process, core and shell flow rate and their respective composition are the most important parameters that can be modified to tune these properties. Here, we first tried to maximize core solution flowrate to increase the productivity of cells encapsulation and organoid generation. To optimize the flow rates and the concentration of the 4-arm-10k PEG-Peptide-MAL and PGA, we measured the core diameter (CD), the shell thickness (ST), and the overall diameter (OD) under different conditions by light microscopy.

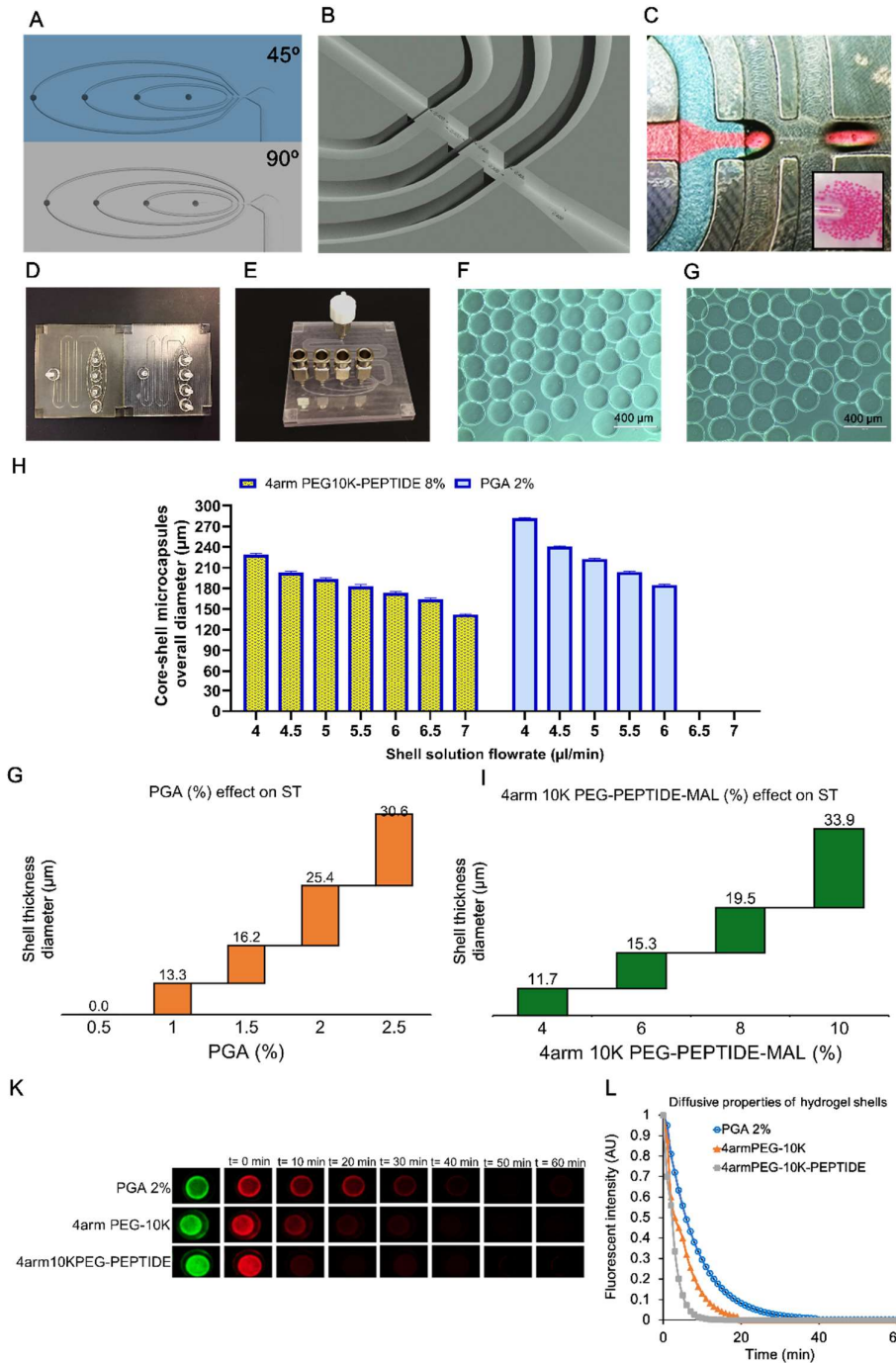


**Figure IV-4. 3D flow focusing chip design and fabrication.** Different channel junction configuration 45° and 90° junction design (A). Channels depth configuration at 90° (B). Core and shell flow and droplet formation (C). 3D printed 3D flow focusing chip using VeroClear material (D) Polycarbonate based 3d flow focusing chip (E). PGA based microcapsules (F) 4-arm 10k PEG-PEPTIDE based microcapsules (G). Effect of shell flow rate on overall dimension (OD) of PGA and 4-arm 10K PEG-PEPTIDE microcapsules diameter (OD) (H), Effect of PGA concentration on shell thickness of microcapsules (I) Release of 75kDa rhodamine-dextran (red) from capsules of 2% PGA, 8% 4-arm 10K PEG, and 8% 4-arm 10K PEG-PEPTIDE. Fluorescein-labeled PEG (green) is used to visualize shell (J) Fluorescence intensity of capsules over time. Dotted lines represent  $\pm$  SD from measured numbers of capsules (n=10).

After applying different core and shell flow rates from 4 to 10  $\mu\text{l}/\text{min}$  with 20  $\mu\text{l}/\text{min}$  flow rate for shielding and crosslinking oil, we identified that 8  $\mu\text{l}/\text{min}$  core flow rate is the maximum flowrate that can be applied for the continuous microcapsule generation. In the next step, we explored effect of the shell flow rate and composition to achieve a mechanically stable microcapsule with proper diffusive properties.

Trials with fixed core flow rate (8  $\mu\text{l}/\text{min}$ , 160 mbar pressure) and different shell flow rates showed that the outer diameter (OD) of generated microcapsules decreased from  $231.3 \pm 8.4$   $\mu\text{m}$  diameter to  $153.4 \pm 3.3$   $\mu\text{m}$  diameter by increasing shell flow rate from 4  $\mu\text{l}/\text{min}$  to 6  $\mu\text{l}/\text{min}$  for 1.5% PGA based microcapsules, respectively. There was no PGA microcapsules formation at 6.5  $\mu\text{l}/\text{min}$  and 7  $\mu\text{l}/\text{min}$  flow rates due to no droplet formation in the chip. Similar microcapsules size profile obtained with 8% 4-arm-10k PEG-Peptide-MAL and increasing shell flow rate from 4 to 7  $\mu\text{l}/\text{min}$  resulted in microcapsules size decrease from  $282.2 \pm 9.1$   $\mu\text{m}$  diameter to  $135.3 \pm 2.2$   $\mu\text{m}$  diameter (Figure IV-4 H). Thus, 7  $\mu\text{l}/\text{min}$  and 8  $\mu\text{l}/\text{min}$  shell flow rates were selected to explore the effect of PGA (0.5 % to 2 % w/v) and 4-arm-10k PEG-Peptide-MAL (4 % to 10 % w/v) different concentrations on shell thickness (ST) and its diffusive properties, respectively.

Results showed that the ST were increased from 13.3  $\mu\text{m}$  to 30.6  $\mu\text{m}$  by increasing concentration of PGA from 1% to 2.5% while no stable microcapsule generated at 0.5% PGA. 4-arm-10k PEG-Peptide-MAL made microcapsules ST were also decreased by increasing the polymer concentration from 4 to 10 % from 11.7  $\mu\text{m}$  to 33.9  $\mu\text{m}$  (Figure IV-4 G&I). It has been reported that microcapsules with low ST ( $\sim 10\text{-}15$   $\mu\text{m}$ ) are mechanically unstable capsules<sup>159</sup>. We have seen same instability and shrinkage in capsules after transferring to spinner flask under dynamic suspension culture and identified that capsules with about 20  $\mu\text{m}$  ST correspond to 2% PGA and 8% 4-arm-10k PEG-Peptide-MAL are mechanically stable after 3 days mixing in spinner flask and selected for studying diffusive properties.

Release profiles of 75 kDa rhodamine-dextran from capsules of 2% PGA, 8% 4-arm-10k PEG, and 8% 4-arm-10k PEG-Peptide hydrogel compositions are shown in Fig. IV-4 K&L. Results

showed that the 'half life' ( $t_{1/2}$ ) of encapsulated dextran increased ~3.5-fold for 4% w/v PGA capsules compared to 8% 4-arm-10K PEG-PEPTIDE. It also demonstrated that 8% 4-arm-10K PEG-PEPTIDE is more diffusive compared to 8% 4-arm-10K PEG of peptide conjugation (Fig. IV-4 K&L). Thus, the 4-arm-10K PEG-PEPTIDE hydrogel as shell provided more diffusive properties compared to other hydrogels while maintaining mechanical stability properties. These properties can facilitate metabolites and maturation induction growth factors/small molecules exchange through the shell and support cells self-condensation and liver buds/organoids generation.

***Scalable and continuous production of liquid core and shell microcapsules using microfluidic platform***

Cells loaded microcapsules production trials were conducted under aseptic culture condition using optimized protocols for cell ingredients production in scalable manner, preparation of core solution including tHE/EC/MSC cells mixing ratio, and shell material preparation composition that resulted in generation of microcapsules with proper size and diffusive properties (i.e. 7  $\mu\text{l}/\text{min}$  core flow, 8  $\mu\text{l}/\text{min}$  shell flow containing 8% 4-arm 10K PEG-PEPTIDE) (Fig. IV-5 A, B,C, and D). The minimum achievable biodegradable PGA microcapsules size was about mean 153.4  $\mu\text{m}$  OD that was bigger than 4-arm-10K PEG-PEPTIDE microcapsules with  $135.2 \pm 2.2 \mu\text{m}$ . Thus, the 4-arm-10K PEG-PEPTIDE based microcapsules were selected for vascularized organoids production trials because of their smaller size, good diffusive properties, and defined chemical composition that offer more reproducibility to minimize variability between different batches of production.

To start cells loaded microcapsules production using scalable microfluidic platform, we first tested again different cells inoculation densities in core solution from  $1 \times 10^6$  to  $40 \times 10^6$  cells/ml with 1:0.8:0.2 ratio comprising hepatic endoderm, endothelial cells, and mesenchymal stem cells during microcapsules generation process. Results showed that cells successfully loaded in microcapsules as single cells with no clump or aggregate formation during dynamic

suspension mixing in spinner flask, transferring to the chip, and microcapsule generation (Fig. IV-5 E). Confocal imaging of microcapsules with  $40 \times 10^6$  cells/ml cells inoculation density “as preferred density” also demonstrated that different cell types were efficiently mixed, and ALB<sup>+</sup> cells and CD31<sup>+</sup> as major parts of cell population of the mixture were present in the mixture and homogeneously distributed (Fig. IV-5 F). The generated microcapsules were collected in 50ml jacketed temperature-controlled spinner flask and transferred to another 100ml spinner flask or PBS-MINI Air-Wheel bioreactor (Air-Wheel Bioreactor, PBS Biotech, Inc, US) with 50 ml working volume of co-culture media after separation/washing from core solution and mineral oil to proceed with hepatic differentiation maturation (Fig. IV-5 G, H, I).

Monitoring microcapsules by light microscopy revealed that cells formed a liver bud like structure with 80-90  $\mu\text{m}$  diameter size through self-condensation after 24-48 h of microcapsules generation. The generated buds/organoids were grown slightly inside the microcapsule and reached to 110-120  $\mu\text{m}$  diameter size. After 3 days of co-culture, microcapsules shell started degradation because of potential MMP1 secretion by hepatic endoderm cells <sup>213</sup>, endothelial cells <sup>214</sup> and mesenchymal stromal cells that degraded the fast degradable MMP-1 peptide linker in hydrogel structure. The shell hydrogel was largely degraded at Day 3-4 of co-culture (Fig. IV-5 J), but the generated organoids could not be easily separated from partially degraded hydrogel. Human recombinant MMP1 (MMP-1 human, SRP6269, Sigma-Aldrich) was added to culture media at optimized 20 nM concentration for complete solubilization of the shell hydrogel that allowed simple harvesting of generated organoids by 70  $\mu\text{m}$  reversible strainer mesh (27260, STEMCELL technologies).

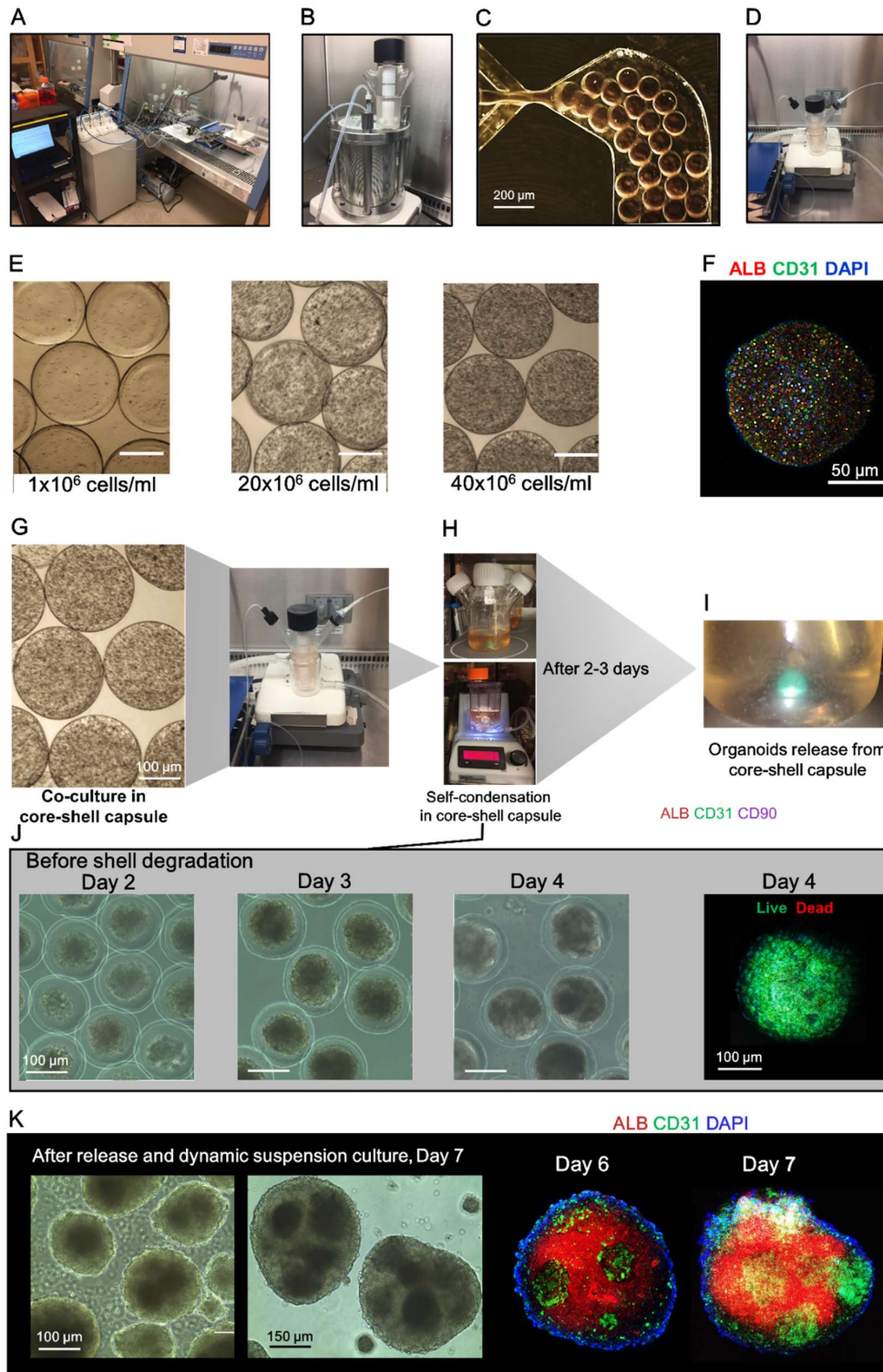


**Figure IV-5 Scalable and continuous production of liquid core and shell microcapsules using microfluidic platform.** Microfluidic set-up for continuous production of microcapsules including liver organoids under aseptic culture condition (A). 50 ml cell mixing spinner in 400ml pressure chamber for introducing core solution to the droplet generation chip (B). Droplet generation chip generating 4-arm 10K PEG-PEPTIDE microcapsule with uniform size at optimal flow rates (C). Jacketed/temperature-controlled spinner flask for collecting generated microcapsules (D). Microcapsules generated with different co-

culture densities in core solution including  $1 \times 10^6$  cells/ml,  $20 \times 10^6$  cells/ml, and  $40 \times 10^6$  cells/ml. Immunostaining of albumin (tHE) and CD31<sup>+</sup> (Endothelial cells) inside microcapsules (F). Microcapsules generation process comprising generated microcapsules at  $40 \times 10^6$  cells/ml density (G), dynamic suspension culture of microcapsules in spinner flask and AirWheel bioreactors for self-condensation of 3 cell types tHE, EC, MSC (H), Dynamic suspension culture of vascularized liver buds/organoids released from microcapsules for further integrated differentiation/maturation (I). Self-condensation of 3 cell types tHE, EC, MSC in microcapsules after 48h and release after 4 days including viability of cells in generated vascularized organoid (J). Phase-contrast images of self-organized organoids after 7 days culture under dynamic suspension condition including immunostaining of organoids after 6- and 7-days culture for ALB<sup>+</sup> and CD31<sup>+</sup> cells (K).

Harvested organoids were then cultured again in FBS-free co-culture media supplemented with 2% PL and growth factors under dynamic suspension culture for another 3 days and characterized for structure and hepatic functionality from days 1 to 7 after co-culture. Confocal imaging of day 2 and day 3 generated buds revealed that albumin positive cells population surrounded by endothelial cells.

Live/Dead imaging of day 3 buds also showed that microcapsules supported high viability of liver buds cell population and further hepatic maturation since the albumin positive cell population area were increase from day 2 to day3 of co-culture (Fig. IV-5 J). Continuing liver buds/organoids culture for 7 days under dynamic suspension culture resulted in generation of self-organized structure inside the buds comprising 3D dense structures inside aggregates with  $250 \pm 40 \mu\text{m}$  diameter (Fig. IV-5 K).

Confocal imaging of Day 6 and Day 7 liver organoids using direct Alexa-flour conjugated antibodies staining protocol showed that hepatocyte cells populated in dark areas of generated organoids and surrounded by CD31<sup>+</sup> endothelial cells. Interestingly, dark areas were interconnected and formed a 3D like structure during maturation under 3D dynamic suspension culture (Fig. IV-5 K).

***Generation of highly functional and vascularized hepatobiliary organoids after 7 days culture under dynamic suspension culture***

To further characterize the generated 3D structure in generated organoids, a non-linear pulsed laser scanning of whole organoid was conducted in  $4 \mu\text{m}$  steps by multiphoton microscopy

(Fig. IV-6 A). Results showed that the self-organised 3D structure created in red color (Fig. IV-5 K) include ALB<sup>+</sup> transitional hepatic endoderm's or hepatocytes (Dark red, APC) in surrounding of CK19<sup>+</sup> cells (light Red, Alexa flour 594) that formed small interconnected tubular duct-like structures (Fig. IV-6 A).

Moreover, analyzing different layers at different organoid diameter levels (88  $\mu$ m, 112  $\mu$ m, and 65  $\mu$ m depth) revealed that all formed tubular structures are interconnected and created a 3D structure ALB<sup>+</sup> and CK19<sup>+</sup> cells. Endothelial cells (Green CD31<sup>+</sup>, Alexa flour 488) were also dispersed through the organoids and created vascular structures visible as green dots and spots (Fig. IV-6 A). From localization point of view, CK19<sup>+</sup> cholangiocytes cells were formed small ducts-like structures as well as a population around the ducts with a ring/tube like structure with lower cell numbers out of biliary duct.

Hepatic endoderm cells (ALB<sup>+</sup>) were also localized around and in between of ducts while endothelial cells dispersed all over the organoid and formed small vascular-like structure (Fig. IV-6 B). Characterization of biliary ducts with higher magnification (30X magnification) clearly showed the localization of CK-7<sup>+</sup> cholangiocytes around the ducts as well the ring like structure (Fig. IV-6 C). Moreover, cells inside the bile ducts well-expressed E-cadherin as well as cytokeratin-19 (CK-19) and albumin around the ducts that are reliable markers for cholangiocytes and hepatocytes (Fig. IV-6 D) <sup>215,216</sup>.

To track self-condensation/organisation events/progress after co-culturing under during dynamic suspension culture, samples were taken every 24h after co-culturing in microcapsules as well as subsequent release and analyzed by multi-photon microscopy at the same day. Captured images showed increasingly hepatocytes like cells population expansion, growing of created 3D structure, and self-organisation as interconnected 3D structure during this period.

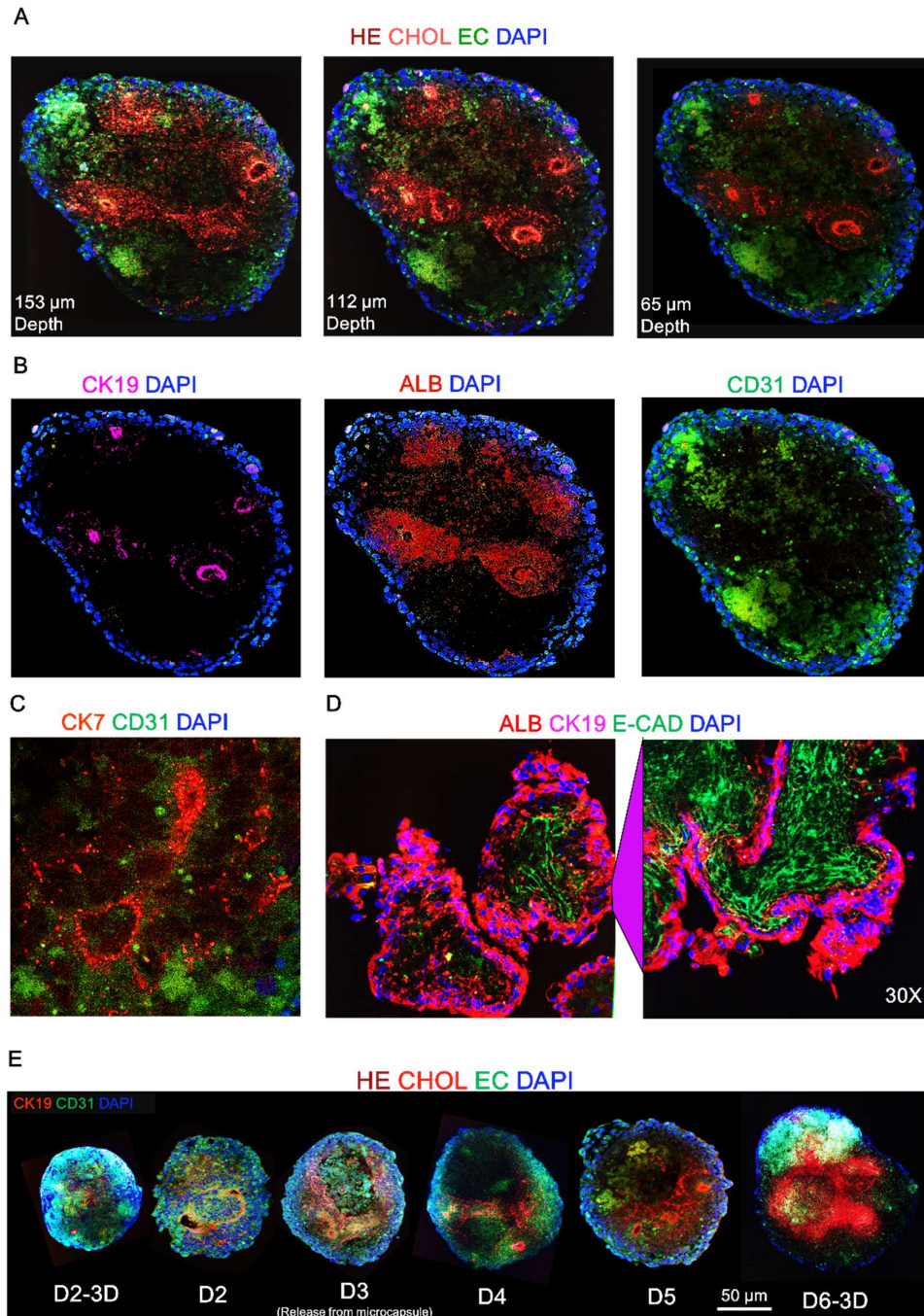


**Figure IV-6 Generation of highly functional and vascularized hepatobiliary organoids.** (A) Multiphoton microscopy of a 7-day hepatobiliary organoid at different depth (55-153  $\mu\text{m}$ ) to show the self-organized structure, (B) Generated biliary structures (CK19-pink) that surrounded by hepatocyte like cells expressing albumin (ALB-red) and endothelial cells (CD31-green). (C) Magnified view of biliary tubes stained with direct CK-7 antibody (Red, 30X magnification). (D) Multiphoton images of biliary tubes with 30X magnification showing co-existence of hepatocyte like cells, cholangiocytes, and endothelial cells as well expression of e-cadherin in biliary structures (30X magnification). (E) monitoring hepatobiliary organoid growth and self-organization during day 2 to 6 culture under dynamic suspension culture after co-culturing in microcapsules.

Creation of biliary ducts started from Day 2 and emerged to form a completely self-organized ducts during 5 days under dynamic suspension culture. A fully self-organized and vascularized liver organoid generated after 6-7 days of dynamic suspension culture with similar structure of fetal liver tissue (Fig. IV-6 E).

***Fully vascularized structure of generated hepatobiliary organoids and their CYP expression***

A critical feature and functional property of a complex functional liver organoid is their vascularization that will improve the maturation of hepatocytes and their fast integration with host vascular network for further proliferation and maturation.

To better illustrate vascularized nature of the generated organoids and angiogenesis progress after co-culturing cells. Vascular networks were directly stained by CD31 conjugated antibody and the whole organoid scanned by multiphoton and confocal microscopy. Results revealed the creation of self-organized endothelial cells populations that were well-dispersed all-over the organoids in between of hepatocyte/cholangiocyte like cells 3D structure (Fig. IV-7 A&B). The created network were also visible as small holes in 6  $\mu\text{m}$  cross section of organoid as characterized By IHC (Fig. IV-7 C).

Moreover, the 3D image of 5 days organoid showed the interconnected nature of created vascular networks that extended from inside to surface of organoids (Fig. IV-7 D and E). Same structure observed for 7 days organoid where the hepatobiliary organoids diameter size increased while preserving the self-organized structure. To verify the localisation of endothelial cells in created vascular structure, an image captured from cross section of a vascular tube using 60X objective where showing CD31<sup>+</sup> endothelial cells formed a vascular tube and surrounded by ALB<sup>+</sup> hepatocytes likes cells (Fig. IV-7 F).

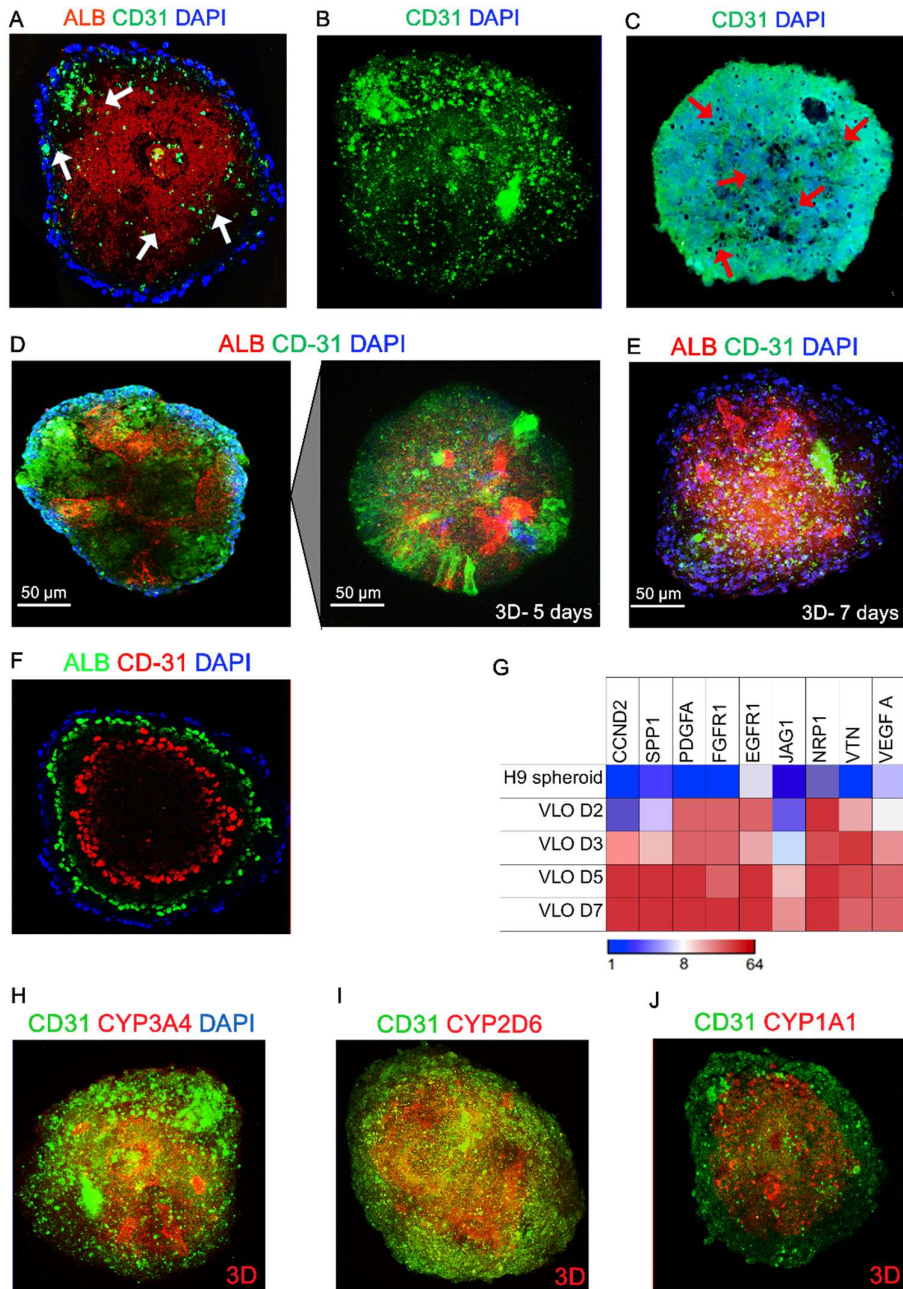


**Figure IV-7 Vascularized structure of generated hepatobiliary organoids and their CYP expression.**

(A) Vascularized hepatobiliary organoids including CD31+ cells stained by direct antibody that dispersed in whole organoid and created vascular structure, (B) CD31+ cells network in hepatobiliary organoid, (C) Immunohistochemistry of hepatobiliary organoid cross section including CD31+ cells and small holes related to generated vasculature, (D) 3D image of 5 days and (E) 7 days hepatobiliary organoid including CD31+ cells that created 3D vascular structure through angiogenesis. (F) Cross section of single vasculature including CD31+ cells surrounded by ALB+ cells captured by multiphoton microscopy with 60 X magnification. (G) qRT-PCR analysis of angiogenesis related genes in 3, 5, and 7 days hepatobiliary organoids. (H, I, and J) expression of CYP enzymes markers including CYP3A4, CYP2D6, and CYP1A1 in multiphoton microscopy images of 7 days multiphoton microscopy.

Gene expression analysis also confirmed the expression of key angiogenesis related genes (e.g. *SPP1*, *PDGFA*, *FGFR1*, and *VEGFA*) in generated organoids and their increasing expression during 7 days of maturation after co-culturing in microcapsules as an indication for InProgress angiogenesis (Fig. IV-6 G). Thus, we named these organoids as vascularized hepatobiliary organoids (VHO) that showed high similarity with the liver structure.

Finally, to demonstrate the functionality of hepatocyte like cells generated in vascularized hepatobiliary organoids, direct staining with CYP enzymes antibodies (CYP3A4, CYP2D6, and CYP1A1) were conducted for 7 days vascularized hepatobiliary organoids that showed their well expression as 3D structure same to albumin positive expressing cells structure. To further characterize the hepatobiliary organoids metabolite activity and liver proteins secretion profile were evaluated.

#### ***Metabolic activity of vascularized hepatobiliary organoids***

To explore metabolic activity of generated vascularized hepatobiliary organoids, absorption, and release of ICG, glycogen storage, and lipid processing was evaluated. As shown in Fig. IV-8, the ability of 7 days VHO under dynamic suspension culture was assessed for different metabolites storage. Results showed that 7 days VHOs are presenting high functionality with respect to indocyanine green (ICG - Cardiogreen) absorption and release after 6-8 hours (Fig. IV-8 A), glycogen storage determined by PAS staining (Fig. IV-8 B), and acetylated low-density lipoprotein (Dil-ac-LDL) uptake (Fig. IV-8 C). Interestingly, the fully vascularized and interconnected tubular biliary structure of organoids were also clearly visible in LDL uptake images. H9 cell line was used as negative control and did not show any of the functions studied.

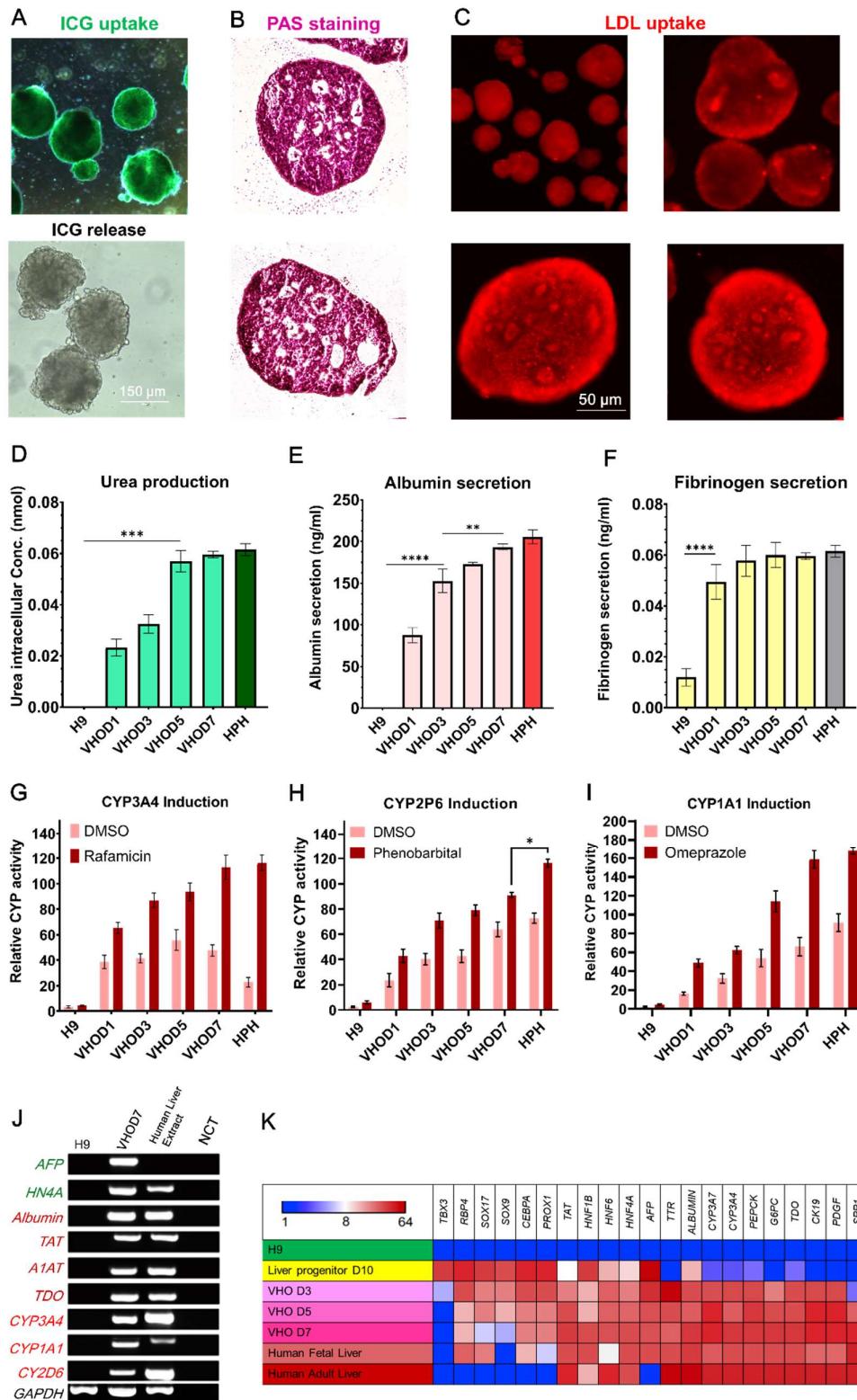


**Figure IV-8 Metabolic activity properties of VHOs and their key genes and protein expression**

The VHOs showed key hepatocyte functional activities, such as (A) Indocyanine green (ICG - Cardiogreen) uptake and release after 6-8 hours; (B) glycogen storage indicated by PAS staining; and

(C) Acetylated low density lipoprotein (Dil-ac-LDL) uptake in red. Secretion pattern of three hepatic proteins by VHOs. Conditioned media from organoids culture were collected after 48 hours from the completion of the differentiation protocol for different groups with and without cells. (D) Inter-cellular Urea, (E) Albumin and (F) Fibrinogen were detected. The results are representative of at least three independent experiments. Data presented as mean  $\pm$  SD (n = 3). \* $p < 0.05$ ; \*\* $p < 0.01$ ; \*\*\* $p < 0.001$ ; Detoxification property analysis of VHOs. Cytochrome P450 (CYP450) induction analysis, three important CYP enzymes were assessed through incubation of the differentiated VHOs with specific inducers: Rifampicin for the CYP3A4 (G), Phenobarbital for the CYP2B6 (H), Omeprazole for the CYP1A1(I) in a period of 72 hours. DMSO was used as control to test the basal activity of the different CYP450. Data presented as mean  $\pm$  SD (n = 3). \* $p < 0.05$ ; \*\* $p < 0.01$ ; \*\*\* $p < 0.001$ . (J) Representative gel electrophoresis of RT-PCR products from VHOD7 and HPH for mRNAs associated with the *AFP* and *HNF4A* as hepatic endoderm genes, hepatocyte-maturation markers (*TAT*, *A1AT*, and *TDO*), cytochrome P450 family (e.g., *CYP3A4*, *CYP2D6*, and *CYP1A1*), obtained from independently triplicated experiments. H9 cells were used as a control, and a liver extract from a healthy donor was used as a positive control. (K)

### ***Urea metabolism and proteins secretion***

The intracellular urea concentration in VHOD1 and VHOD3 was significantly lower than HPH while VHOD5 and VHOD7 had comparable urea concentration (about 95% of HPH, 0.057 and 0.059 nmol for VHOD5 and VHOD7 vs. 0.061 nmol for HPH, respectively) that indicating their higher maturation (Fig IV-8 D).

Relatively similar secretion profile was observed for albumin secretion but only VHOD7 had comparable secretion with HPH (about 95% of HPH, 194 ng/ml vs. 205 ng/ml for  $5 \times 10^5$  cells, respectively) (Fig IV-8 E). Fibrinogen secretion had different trend where VHOD1 to VHOD7 had comparable secretion with HPH (from 0.049 to 0.059 vs. 0.61 for HPH) and only H9 secretion was significantly lower than other groups ( $p = 0.001$ ).

### ***CYP enzymes activity***

The *in vitro* detoxification capacity of 1, 3, 5, and 7 days VHO was measured by characterizing the activities of three important Cytochrome P450 (CYP450) family enzymes (CYP3A4, CYP2B6, and CYP1A1) and DMSO was used as a control/basal activity in cell culture. Results indicated the increasing trend of activities after co-culturing/during maturation of organoids as well as significant increases in the activities of all the tested isoforms of CYP450 relative to the DMSO control during organoid maturation process (Fig. IV-8 G, H, and I). VHO's displayed

increased CYP450 activity when compared to DMSO group in response to induction with Rifampicin (CYP3A4: from 65.36% to 112.9% for VHOD1 and VHOD7 vs. 38.73% to 47.77% for DMSO, respectively), Phenobarbital (CYP2B6: from 42.86 to 91.03 for VHOD1 and VHOD7 vs. 23.63 to 63.76 for DMSO, respectively), and Omeprazole (CYP1A1: from 48.66 to 158.53 for VHOD1 and VHOD7 vs. 16.23 to 91.4 for DMSO, respectively). Moreover, the VHOD7 displayed comparable CYP450 activity relative to HPH for CYP3A4 and CYP1A1 isoforms (CYP3A4: 112.9 vs. 116.33,  $p < 0.01$ ; CYP1A1: 158.53 vs. 167.63,  $p < 0.01$ ) while the activity for CYP2B6 of were significantly lower than HPH ( $p < 0.05$ ).

We believe that CYP activities could be improved with further maturation under dynamic suspension culture since activities for all isoforms were improved after co-culturing and during dynamic suspension culture.

#### ***Gene expression analysis of hepatobiliary organoids***

To confirm the gene expression associated with hepatic differentiation, we conducted quantitative RT-PCR (Fig IV-8 J) for VHOD7 and HPH to evaluate the maturation extent of generated VHO. Results showed that VHOD7 still expressing hepatic endoderm related genes (*AFP* and *HNF4A*) while also expressing mature hepatocyte markers including *TAT*, *A1AT*, and *TDO* as well as CYP enzymes related genes will less extent.

A gene expression profile study by q-PCR was also conducted for liver progenitor's population at day 10 before starting the co-culturing process with endothelial progenitor cells and mesenchymal stem cells as starting material as well as VHO's generated at days 3 to 7 of hepatic differentiation/maturation process to realize if the correct developmental path followed during entire differentiation process ((Fig IV-8 K). H9 cells also used as control for the q-PCR study.

Results showed that day 10 liver progenitors expressing key endoderm, early hepatic, and transitional hepatic endoderm markers related genes including *TBX3*, *RBP4*, *SOX17*, *SOX9*,

*CEBPA, PROX1, TAT, HNF1B, HNF6, HNF4A, AFP* that indicating their suitability to be used as starting cell ingredient for vascularized liver organoids production. The expression of these genes was decreased after co-culturing and the initiation of hepatic differentiation process under dynamic suspension culture.

After 3 days of co-culturing and during hepatic differentiation process, expression of mature hepatocyte genes (e.g. *TTR, ALBUMIN, CYP3A7, CYP3A4, PEPCK, G6PC, TDO, PDGF*, and *SPP1*) was increased and this trend continued until day 7 of the maturation process when the gene expression profile of VHOD7 become similar to fetal liver gene expression profile. High expression of mature hepatic genes such as CYP enzymes and cholangiocytes related gene (i.e. *CK19*) was also detected after 5 days of hepatic differentiation process.

The VHOD7 gene expression profile was more similar to human fetal liver gene expression profile but with higher expression for some key hepatic maturation genes including *CYP3A7, CYP3A4, PEPCK, G6PC, TDO, and PDGF* as well as *CK19* gene as a marker of cholangiocyte that can be related to generation of hepatobiliary structures inside the vascularized hepatobiliary organoids. The CK19 expression was largely increased after 5 days of co-culture during the hepatic differentiation process.

#### ***Western blot analysis of hepatobiliary organoids***

The gene expression pattern of VHOs was further analyzed by Western blot. The results of Western blotting (Fig. IV-9 A) confirmed the progression of gene expression detected by reverse transcription-PCR (RT-PCR) and q-PCR gene expression profiling. The VHDO3, VHDO5, and VHDO7 well expressed proteins related hepatic endoderm, hepatocytes and cholangiocytes. Moreover, the expression of hepatic endoderm protein (AFP) decreased during the maturation process and was comparable to human fetal liver expression for VHDO7 rather than HPH. On the other hand, expression of hepatocyte (ALB) and cholangiocyte related protein (CK19) increased during the maturation process after co-culturing in microcapsules.

These results indicating that the generated organoid still has fetal level maturity and may undergo more maturation after extended culture under dynamic suspension culture.

Finally, measurement of total DNA content of VHOs as an indirect method for estimation of cell numbers showed the proliferation of VHO after coculturing and during the maturation process and total DNA content of VHOD7 increased by 2.4 fold compared to the self-condensed organoid after co-culturing (Fig. IV-9 B).

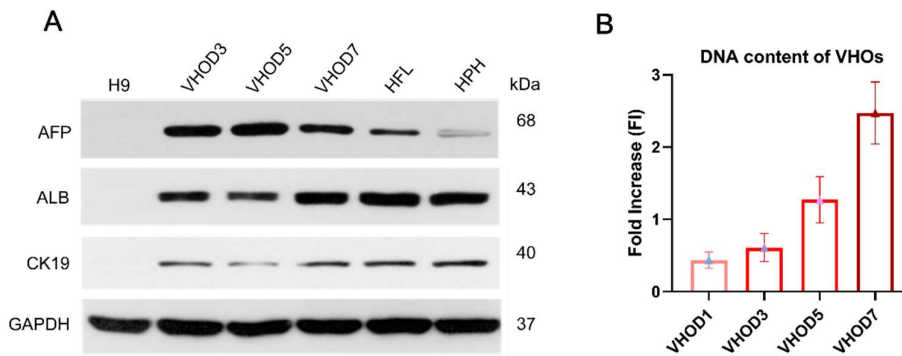


**Figure IV-9 Western blot analysis and VHOs total DNA content.** (A) Western blotting of AFP, albumin, and CK19 proteins showing upregulation of hepatic endoderm, hepatocyte, and cholangiocyte genes expression during the differentiation process under dynamic suspension culture. (B) Total DNA concentration of VHOs at different culturing days after co-culture in microcapsules showed that the total yield of cells increased during maturation process for about 2.4 FI by day 7 of culture.

## Discussion

Organoid technology has showed enormous potential to bridges the gap between conventional cell therapy using individual tissue specific cells (such as hepatocyte like cells that mainly demonstrated poor clinical efficacy in previous studies) and large tissue constructs/grafts or whole organ bioengineering transplantation (such as bioengineered livers<sup>217</sup>) that are showed promising results but currently suffering from significant fabrication and/or fabrication process scalability issues for large scale production and subsequently widespread clinical application. Thus, complex organoids can be considered as a new class of cell-based therapeutic products since they can offer significant higher functionality compared to individual cells, more facilitated scalable production due to their smaller scale compared to tissue constructs or whole organ, and capability for generation from expandable hPSCs or adult derived liver progenitors for potential clinical application<sup>82,218</sup>. In this study, we developed a continuous process for fully scalable and xeno-free generation of complex and highly functional vascularized hepatobiliary organoids from hPSCs with similar structure to native tissue. This has been achieved by optimizing and scaling up the production of all required cell ingredients for vascularized liver organoids generation including transitional hepatic endoderm cells, endothelial progenitor cells, and mesenchymal stromal cells from individual hPSC lines and then developing a continuous process for 3D co-culturing of these cells in uniform size biodegradable hydrogel microcapsules using microfluidic technology. Novel 4-arm-PEG-fast degradable MPP sensitive peptide made microcapsules containing required cells ingredients with optimized mixing ratio and total cells density were generated in fully scalable droplet microfluidic platform for self-condensation/self-organisation of cells under 3D and xeno-free culture condition and their subsequent release to mimic *In Vivo* liver bud development process to generate vascularized liver organoids generation. The dynamic and integrated 3D culture of generated organoids after co-culturing (Maximum 7 days) resulted in generation of self-organized vascularised hepatobiliary organoids that contained large population of ALB+ hepatocyte like cells pollution in surrounding of interconnected vascular structures created by

endothelial cells angiogenesis as well as biliary duct structure that created by cholangiocyte cells. Monitoring the organoids self-organization events with confocal microscopy together with gene expression and metabolic activity profiles revealed a very interesting combined maturation and self-organisation process that resulted in generation of highly functional hepatobiliary organoids. The established platform has addressed four important key challenges of previous protocols for generation of complex, vascularized, and functional liver buds/organoids from hPSCs <sup>21,100</sup> including poor scalability of starting cell ingredients production, poor scalability of co-culturing technique and vascularized liver bud/organoids generation (Up to  $10^8$  cells per batch of production which is enough for one pediatric patient), necessity of using xeno-derived ECM for self-organisation of organoids (e.g. Matrigel) or coating of micro-well surfaces, and lacking biliary duct structure and self-organized cholangiocyte cells in generated organoids which is essential for normal liver function, metabolism, and organoids proper structure and functionality. To date, few studies established protocols for generating functional liver organoids with hepatobiliary structure from hPSCs called "Hepatobiliary organoids" but all of them were able to only generate few organoids in culture dish under 2D static culture condition that could no be adopted for scalable production to meet requirement for future clinical application <sup>153,154</sup>. Moreover, there is no report published for generation of liver organoids with both vascularized and biliary structure from hPSCs or adult derived progenitor cells as cell source that indicating the importance of obtained results.

Therefore, a critical current bottleneck and technical issue in translating the established organoids generation technologies for clinical application and "organoid medicine" is limited scalability of protocols for production of sufficient therapeutic doses of liver cells as complex and functional hepatic organoids for effective therapy. Practically, treating one adult patient with acute liver failure require more than  $2 \times 10^9$  functional hepatocytes cells or as organoids/microtissues while few hundred billion of cells as organoids are required as off-the-shelf therapeutic product for allogeneic liver cell therapy enabling their widespread clinical

application <sup>132</sup>. To generate this massive numbers of cells/organoids, billion numbers of transitional human hepatic endoderm/functional hepatocytes are also essentially required as starting cell material for scalable production of liver organoids since the human liver contains more than 100 billion hepatocytes <sup>177</sup> comprising 70-80% of total cell population and clinical reports indicating that at least 10-20 % of liver cell population is required for an effective liver regenerative therapy <sup>219</sup>. To overcome this issue, developing scalable technologies for large scale production of clinical grade liver progenitors/hepatic endoderm's and more importantly high quality/functional human hepatocyte cells/hepatic organoids from a proper and readily available cell source (hPSCs) or adult derived progenitors (LGR5-positive bipotential human liver stem cell) has been explored by different research groups using different platforms such as microwell array plates <sup>21</sup> and stirred suspension bioreactors <sup>18,76,220</sup>.

Among different potential cell sources, hPSCs are considered one of the most convenient stem cell types for hepatocyte or liver organoid generation and production for potential personalized and allogeneic cell therapy application. They provide a readily available and unlimited cell source that easily adaptable for expansion and integrated differentiation in scalable suspension culture systems for production of stem cells progenitors (e.g. endothelial progenitors and mesenchymal progenitors required for vascularized liver bud formation) and their therapeutic derivatives with potential autologous and allogeneic cell therapy applications <sup>96,172,221</sup>. There are different reports that succeeded in generation of liver progenitors expressing key liver progenitors markers and resulted in generation of functional hepatocyte like cells or liver buds <sup>21,124,200,222</sup> but few reports generated these cells in scalable manner as prerequisite for large scale production of liver organoids/buds, bioengineered liver constructs, and whole liver bioengineering <sup>18</sup>.

In this study, we first optimized our previously established integrated dynamic and scalable suspension protocol for generation hepatic endoderm cells to achieve a liver progenitor population expressing key markers reported by other studies for liver bud generation (e.g. TBX3, ADRA1B (alpha-1b Adrenergic Receptor), EPCAM, CD90, and Hnf4α) from hPSCs as

3D aggregates<sup>21,124</sup>). Optimizing Activin and Wnt3A concentration and treatment strategy for endoderm differentiation and then HGF concentration at 20 ng/ml for hepatic differentiation resulted in generation of a cell population in aggregates with 88% SOX17/FOXA2 double positive cells and then rich population of liver progenitor's as 3D aggregates that well expressed key liver progenitors markers during day 9-11 of the integrated hepatic differentiation process and cells derived from all days was suitable for self-condensation and liver organoid generation in multi-well plates and microcapsules format. Tan *et al.* reported the maximum liver progenitors population (94.1%  $\pm$  7.35% TBX3<sup>+</sup>HNF4A<sup>+</sup> human liver bud progenitors) at Day 6 of hPSCs differentiation process by temporally dynamic manipulation of extracellular signals<sup>124</sup> and Takebe group reported that Day 8 of hiPSC-derived transitional hepatic endoderm cells as the only progenitor population suitable for liver bud generation, both done under static adherent culture condition. We evaluated the Takebe group protocol for integrated hepatic differentiation of hPSCs as 3D aggregates that was not successful and resulted in dissociation of aggregates and significant cell death and after 2-3 days of induction. The result indicating that the culture mode (2D vs. 3D) and differentiation protocol largely affect the differentiation process outcome and should be optimized for each intended application and we used the optimized hepatic progenitors production protocol as 3D aggregates for all co-culture optimization trials .

In parallel, we established robust protocols for scalable production of mesenchymal stem cells (a promoter of self-condensation mechanism and improving hepatic differentiation) and endothelial progenitor cells (as promoter of angiogenesis and improving hepatic differentiation) from individual hPSC lines under dynamic suspension culture condition as prerequisite for large scale co-culturing and generation of vascularized liver organoids in scalable manner. Stable generation and scalable production of ES-derived mesenchymal stem cells and their EVs has gained increasingly attention during recent years for cell therapy applications of a variety of diseases, including degenerative and chronic ones such as allogenic skin grafts, cartilage repair and cerebral ischemia. These cells can offer same

advantage of tissue derived MSCs but with lower immunological issues and limitations <sup>223,224</sup>. To date, several protocols and reports published that aimed to develop scalable expansion of hMSCs from different sources <sup>225</sup> but there is no report for expansion of hPSC-derived MSCs in scalable manner. The established protocol in this study can be used for massive production of functional hPSC-derived hMSCs using microcarrier technology with very good fold increase in multiple passages (about 11 FI for 12 passages) for scalable complex organ buds/organoids production by mesenchymal stem cells driven self-condensation mechanism <sup>96</sup> and other potential applications.

Scalable production of endothelial cells is another essential prerequisite of large-scale vascularized liver organoid production as cell ingredient responsible for creating vascular structure within organoids or microtissues through angiogenesis. The created vascular structure can facilitate nutrient delivery and metabolite removal within organoids and their fast integration to the host vascular structure to support proliferation, further maturation, and function <sup>226,227</sup>. It has been also demonstrated that endothelial cells improved maturation of hepatocyte like cells after co-culture with hepatic endoderm cells and resulted in generation of highly functional liver organoids <sup>100</sup>. Few reports established protocols for scalable production of endothelial cells for potential tissue fabrication and clinical application as 3D aggregate under dynamic suspension culture <sup>185</sup> or hydrogel based 3D culture system <sup>184</sup>. However, these protocols require purification step for isolation of CD31<sup>+</sup> cells <sup>185</sup> or depends on using thermoresponsive gels <sup>184</sup> for endothelial cells generation that will largely increase the complexity of process and its costs. In this study, we established a robust and fully scalable integrated differentiation protocol for production of endothelial KDR<sup>+</sup> progenitors (about 75% at day 6 ) and mature CD31<sup>+</sup> cells (about 95% at day 8) from hESC and hPSC lines using microcarrier technology without need a purification step or hydrogels based culture system to generated CD31<sup>+</sup> positive cells with more than 90% purity. Thus, the established platform can be used for large scale production of endothelial cells for scalable liver organoids generation

and or other potential applications aimed to create vascular microtissue or tissue constructs or direct transplantation.

After successful development of robust and scalable protocols for production of required cell ingredients for liver organoids generation including tHE, hMSC, and ECs from hPSCs under defined and xeno-free culture condition. We explored different platforms for fully controlled co-culture of these cells in scalable and customizable manner under 3D environment for subsequent self-condensation and creating vascularized liver organoids. To date, different platforms have been employed for co-culturing different cell types under 3D culture conditions including multi-well plates with one drop of soft ECM gel such as Matrigel™ for facilitating cells self- condensation to organoids <sup>131</sup>, micro-well arrays <sup>100</sup>, omni-well plates as high-throughput version of multi-well plates coated with biopolymers (e.g. HEMA) <sup>21</sup>, liquid core and solid shell hydrogel microcapsules generated by either elector-spraying encapsulator <sup>164</sup>, air-driven droplet generator <sup>228</sup>, microfluidic flow-focusing droplet generation systems <sup>159</sup>, and a very simple strategy including dynamic co-culture in spinner flask which offering superior scalability but poor control for mixing cells with defined ratio <sup>229</sup>.

Therefore, we first tried the simplest and scalable strategy by co-culturing tHE, hEC, and hMSCs, and EC cells in glass spinner system or AirWheel bioreactor (PBS biotech, US) with 50 working volume under dynamic suspension culture condition to generate homogenous vascularized organoids in scalable manner. However, results showed that heterogeneous spheroids formed with diverse morphology that indicating the poor mixing efficacy of cells with defined ratio (10:8:2, respectively) in this culture system. Practically, inoculated cells were formed spheroid after 4h of inoculation mainly consisting hepatic progenitors' population due to high tendency of tHE for re-aggregation while EC and MSCs has showed low tendency for aggregation under dynamic suspension culture.

Among other platform technologies, the micro-well plates can offer very good reproducibility for providing a completely uniform 3D environment for co-culturing of required cell components for self-condensation and vascularized liver organoid formation under static culture condition.

However, generating massive numbers of organoids using this platform would be a labor-intensive and multi-step process that is not amenable for scalable manufacturing of organoids with clinically relevant cell numbers for clinical application. For instance, a multi-well-array plate consist of over 20,000 micro spots per well were capable of producing liver buds with  $10^8$  cells which is only enough for treating one pediatric patient with acute liver failure while treating an adult patient would require to use at least 10 plates in parallel for producing  $10^9$  cells <sup>21,230</sup>.

As an alternative 3D microenvironment platform, biodegradable hydrogel microcapsules generated by flow-focusing/droplet microfluidic chips can be used as 3D environment for co-culturing different cell types, generation of organoids/micro-tissues, and their subsequent release from capsules instead of using micro-wells in array plates <sup>231</sup>. The hydrogel microcapsules technology has gained increasingly attention during last ten years as fully controllable 3D environment for spheroids formation <sup>159</sup>, cells/islet encapsulation <sup>232</sup>, co-culturing different cells for microtissues formation <sup>233</sup>, organoid generation (e.g. intestinal organoids), and cryopreservation for direct injection to body after thawing <sup>164</sup>. The completely tunable properties of hydrogel micro-capsules using different combinations of biomaterials and fabrication technologies, continuous production capability, and more importantly enabling dynamic suspension culture of generated micro-tissues/organoids culture inside of microcapsules has largely boosted their potential applications as preferable 3D microenvironment <sup>162,231</sup>.

The conventional microfluidic technology mainly consists of syringe pumps (Max. 50 ml volume for each stream) for delivering different streams to individual microfluidic chip for droplet generation which is not scalable for mass production of microcapsules in continuous manner <sup>159</sup>. The electrospray generation of liquid core and shell microcapsules can offer superior scalability for high throughput generation of cells loaded microcapsules but suffering from important technical issues such as batch to batch variation of microcapsules size and their physical and mechanical properties (e.g. shell thickness and shape) due to air flow and

voltage based driven mechanism of microcapsules generation that will result in heterogenous microtissue/organoid formation as well as routine spray nozzle clogging by hydrogel solidification that require multiple pauses during the production process for nozzle cleaning <sup>234,235</sup>.

Therefore, a scalable microfluidic technology for generating core and shell microcapsules (e.g. using flow-focusing microfluidic chips) can be considered as proper choice for continuous production of organoids through self-condensation mechanism due its capability to achieve highly uniform morphology and size-controlled microcapsules with tunable mechanical properties and permeability in a fully controlled manner. However, most of the established droplet microfluidic platforms mainly used natural biopolymers as shell material (e.g. alginate/chitosan-based materials) for microcapsules production that are offering tunable barrier/immune-barrier properties and biodegradability but also suffer from batch to batch variation in composition that subsequently results in low reproducibility of capsules production process and poor size distribution homogeneity due to the natural source of these materials <sup>236</sup>. As more defined alternatives, GelMa and 4-arm PEG network hydrogels or their combination have been used a shell material that providing chemically defined materials with completely tunable diffusion and mechanical properties for cells encapsulation <sup>159,202,237,238</sup>. Although these biomaterials presenting defined and good immune-barrier, and metabolites permeability properties, but they are not degradable to release generate organoid/buds after self-condensation and formation. A fully degradable shell material using will allow the organoids release after self-condensation for further maturation under dynamic suspension culture as essential perquisite for autologous or allogeneic cell/organoid therapy application (Siltanen, Diakatou et al. 2017, Wang, Liu et al. 2019). The degradation method/strategy should be effective enough to completely dissolve the material, while at the same time, without any detrimental effect on cells/organoids viability. For instance, the alginate made microcapsules can be degraded/removed by ethylenediaminetetraacetic acid (EDTA) that also can dissociate cell spheroids/aggregated and decrease the cells viability <sup>159,164</sup>.

In this study and to meet the cell-friendly degradation process criteria, we designed a fully biodegradable 4-arm PEG-MAL based hydrogel to be used as shell material by conjugating a fast degradable-MMP sensitive peptide to each arm of 4-arm-PEG-MAL and then added another maleimide group to the MMP sensitive peptide chain that enabled its crosslinking with sulfide groups (e.g. DTT). We also used polygalacturonic acid (PGA) as shell material for fabrication of microcapsules that can be crosslinked by calcium Ion and degraded by adding pectinase enzyme after organoids self-condensation as cheaper alternative and mild degradation potential with pectinase enzyme since pectinase doesn't have any effect of cells. Results showed that both uniform size microcapsules can be generated by flow focusing droplet microfluidic chip to offer a good 3D environment for co-culturing cell ingredients and subsequent organoid release by degradation. However, the PEG-Peptide based microcapsules were preferred for other trials because of its defined properties that resulted in more uniform and smaller microcapsules minimum size (i.e.  $135.3 \pm 2.2 \mu\text{m}$  diameter) and higher permeability for metabolites exchange. They can be also used as smart microcapsules that could be automatically degraded after organoid formation by secreted MMP enzymes by mainly endothelial cells <sup>239,240</sup>.

Another issue with conventional droplet microfluidic technology for microcapsules generation is that most of the currently established protocols for generation of core and shell microcapsules and encapsulating cells employed PDMS, glass, or their combination made flow-focusing chip that are suffering from important technical issues for continuous droplet generation <sup>159,241,242</sup>. Preparing these 3D flow-focusing chips require intensive work for fabrication and their contact parts with streams/cells suspension that are prone to change their hydrophobicity/surface properties during the microcapsule's generation process. Modification of channels surface properties and gradually removal of coating can result in capsules/cells adhesion to microfluidic chip channels wall that will result is microcapsules generation process instability or stop. Accordingly, PDMS and glass based microfluidic chips have not translated well to a commercial scale and mass-production manufacturing due to their multi-step and

labor-intensive fabrication processes such as etching (glass and silicon) or embossing and injection molding (thermoplastics). Furthermore, all of these fabrication approaches are limited by the range of features that can be created, with a move from 2.5D (structures with varying width but identical depth) to 3D structures significantly increasing processing cost and reducing success rates (Chen, Mehl et al. 2016, Liu, Wang et al. 2020).

In this study, we fabricated microfluidic chips using either 3D printing technology by polyester material (VeroClear®) or polycarbonate-based chip material (Medical grade polycarbonate sheet) that offering significant advantage for continuous generation of microcapsules. Both materials are inert and do not need channels surface treatment during fabrication for microcapsules generation process. In addition they can be fabricated in one or few simple steps and could be used for aseptic microcapsules generation by sterilizing the fabricated chips by either gamma irradiation (polyester based chip) or steam sterilization (polycarbonate made chip). Employing these materials and 3D printed chips for microfluidic application has gained increasing during last 5 years <sup>243-246</sup>. After fabrication trials and testing chips performance during continuous microcapsules generation, we preferred to use polycarbonate based chips with stainless steel inlets because of its thermal and chemical stability, very low cell attachment properties, clear transparency for better monitoring the generation process, and availability of medical grade sheets for fabrication and use under GMP environment.

In order to establish a fully scalable microfluidic platform for microcapsules generation, we employed pressure-driven microfluidic pumps and fully scalable remote pressure chambers commercially available from 30 ml to 400 ml (Mitos P-Pump Remote Chamber, Dolomite Microfluidic, UK) and even few liters scale volume for delivering streams to the microfluidic chip or multiple microfluidic chips in parallel that offering superior scalability, precision, and flow stability for delivering pulse-free flow for the microcapsules production process by integrating the pressure and flowrate sensors of each stream. This platform can be also easily adapted for GMP manufacturing of microcapsules under aseptic condition for clinical grade organoids production as well as drug loaded hydrogel microcapsules <sup>247</sup>.

In the next step and to generate cells loaded microcapsules in continuous manner, we first optimized the cells ratio densities, total cell density, and optimum hepatic progenitors day (10 or 11 day hepatic progenitor cells that well expressed hepatic progenitors markers) in 384-well spheroid plates with low-attachment surface and employed the optimal mixing conditions (1:0.8:0.2 for tHE, EC, and MSCs, Day 11 hepatic progenitors, 20 million cells per ml) for microfluidic microcapsules generation trials. Then, tried to prepare homogeneous mixture of cells in 50 ml spinner flask with 25 ml working volume for delivering cells suspension to the chip as core solution with defined ratio that optimized for self-condensation and vascularized liver organoid formation. However, we realized an important bottleneck here after single cell inoculation of the three cell ingredients in spinner flask since heterogeneous small aggregates and clumps formed in core solution in few hours (3-4 h) that resulted in microfluidic channels clogging. The problem was resolved by supplementing core solution with combination of 2% W/V Mebiol® Gel PNIPAAm-PEG 3D and 1g/L dextran sulfate addition resulted in delayed aggregate formation for up to 10 h and relatively homogeneous aggregate formation after 24h. Using polymeric densifiers have been suggested by many publications for reducing the risk of cell clumps or aggregates formation in mammalian cells and human pluripotent stem cells <sup>172</sup> under dynamic suspension culture with proved efficacy and minimal cytotoxicity. Here, we used an optimized concentration of dextran sulphate and Mebiol® Gel PNIPAAm-PEG combination that were individually reported before for safe use in suspension and 3D cell culture without cytotoxicity <sup>182,204</sup>.

Therefore, the microfluidic process can be continuously run for up to 8-10 h for generation of microcapsules after each single cell inoculation to 50 spinner flask located inside remote pressurized vessel and multiple chips can be run in parallel to maximize the cells loaded microcapsules productivity (Fig S-IV.1). Moreover, maximum three co-culturing trials can be done at day 11 of hepatic progenitors' differentiation to increase the productivity and continue the process for 24 h. Parallel and high-throughput droplet microfluidic production of hydrogel in one chip have been done previously that can be also used to increase the productivity of

cells loaded microcapsules production process that can result in production about 2.5 billion cells as vascularized organoid using 25 ml medium for co-culturing in the 50 ml spinner flask<sup>242</sup>. This cell yield could be hopefully used for an adult patient for bridging to transplantation or even treatment because of VHO high proliferation capacity.

Another novelty of this project is integrated dynamic suspension culture of cells entrapped in microcapsules for self-condensation of cells to form vascularized liver organoid, release of organoids from microcapsules after 3 days by degrading the PEG-MMP sensitive hydrogel as shell, and then continuing of the hepatic maturation process under dynamic suspension culture. Dynamic suspension culture of microcapsules can increase the nutrients and metabolite exchange through the shell for supporting self-condensation/ organization of vascularized organoid during first days after co culture. Interestingly, the microcapsules shell started to become lose after 2 days of culture and partially degraded after 3-4 culture because of secreted MMP effect on MMP sensitive peptide sequence in 4-arm-PEG-peptide hydrogel by cells proliferation inside the capsule. However, the degradation was not complete and media was supplemented with recombinant MMP to completely dissolve the microcapsule and releasing organoids. Previous studies demonstrated that endothelial/endothelial progenitor's cells and mesenchymal stem cells incorporating in MMP-mediated soft matrix degrading for promoting cells migration, angiogenesis, and tissue formation<sup>248-250</sup>. They also showed the capability and high activity for degrading synthetic MMP-sensitive PEG hydrogels during migration and angiogenesis<sup>250-254</sup>. Some reports also detected MMP produced by liver cells including hepatic stellate cells and hepatocytes<sup>255</sup>. So, we believe MMPs produced by these cell<sup>239,256</sup> mainly incorporated in partially degradation of microcapsule hydrogel that facilitated the organoid release from microcapsules.

Continuing the dynamic suspension culture of generated organoids after release from microcapsules resulted in generation of fully self-organized and vascularized hepatobiliary organoids including interconnected bile ducts with gene expression, metabolic activity, CYP activity profiles, key proteins expression for both hepatocytes and cholangiocytes similar to

fetal liver and very close to mature hepatocytes. Moreover, the structure of generated organoids employing fully scalable microfluidic platform was very similar to native tissue because of creating of interconnected vascular and biliary ducts structure within organoids during 3D dynamic suspension culture. The generated structure completely shows the extent of self-organization, complexity, and similarity of the vascularized hepatobiliary organoids (VHO) produced in this study to liver tissue in comparison to other studied used same co-culture strategy to generated vascularized liver buds/organoids but under static culture conditions<sup>21,100</sup>. Moreover, the similar studies have not detected any bile duct formation using the co-culture technique (Fig IV. 10).

The significant effect of 3D and dynamic suspension culture on haptic cell lines<sup>257</sup> or primary hepatocytes<sup>258</sup> maintenance, metabolite activity and function improvement has been reported in different studies that cultured cells as spheroids or in 3D matrix using perfusion bioreactors<sup>259-261</sup>.

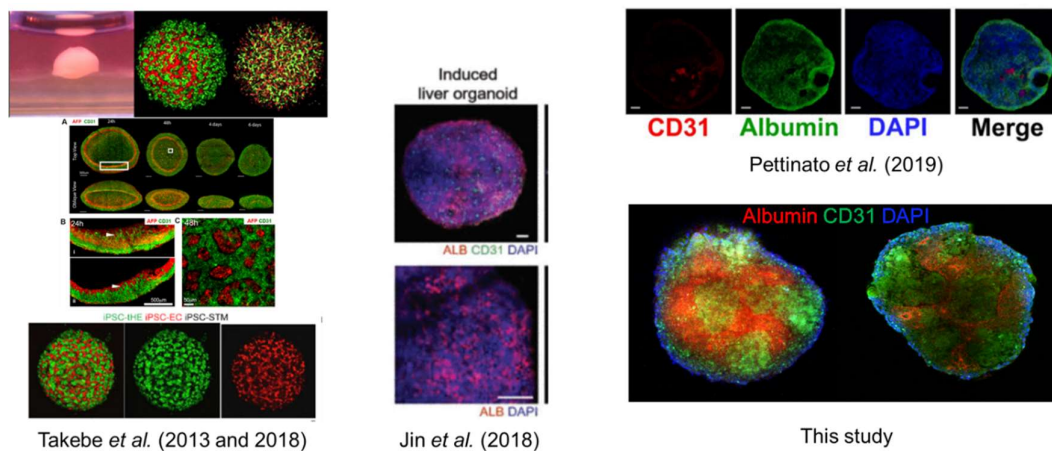


**Fig IV. 10. Comparing the structure on vascularized hepatobiliary organoid generated in this study to other similar studies.**

These 3D culture systems are designed in a way that could provide more *in vivo* like environment to improve functionality and provide *in vivo* like gradients of morphogens such as Wnt, hedgehog, hormones or growth factors as well as oxygen for creating zonation and distinct metabolic activities for providing a better model for drug testing from primary

hepatocytes or hepatic cell lines <sup>261</sup>. It has been also reported that co-culturing of primary hepatocytes or stem cells derived hepatic progenitors with fibroblast, mesenchymal stem cells, and endothelial cells for better maintenance of primary hepatocytes <sup>262,263</sup> and improved differentiation of hepatic progenitors for generation of functional vascularized liver buds <sup>21</sup>, liver organoids or liver microtissues <sup>100,264</sup>.

MSCs and ECs are two main cell types that play an essential role in organogenesis, through mainly cell-cell signaling and secreting organ-specific growth factors, ECMs, and MMPs for tissue morphogenesis and angiogenesis during organ development and repair <sup>265</sup>. The secreted factors are key elements that promote orchestrate induction, specification, and guidance of organ generation processes included liver development as well as maintenance of homeostasis and metabolism. ECs playing pivotal role in liver bud generation prior to the circulation of body fluids within the developing <sup>266</sup>.

In this study, we employed the combination of 3D culture under dynamic suspension culture condition and co-culturing with MSCs and ECs derived from individual hPSC lines in microcapsules under 3D and natural ECM-free culture condition using fully scalable microfluidic platform to generate highly functional organoids in scalable manner. The established platform resulted in generation of functional vascularized hepatobiliary organoids through self-organisation with similar structure to liver tissue and addressed two main drawback of previously established protocols for vascularized liver bud/organoids formation including poor scalability and lack of bile duct formation <sup>21 95,133,134</sup>. The generated VHO can offer great potential for both autologous and allogenic organoid therapy as well drug discovery for personalized medicine using different hiPSC cell lines due to their very good drug response and CYP450 activity.

However, development of a robust, GMP (good manufacturing practice) compatible culture system and fully controlled bioprocess for large scale production of vascularized hepatobiliary organoids and establishing an efficient organoids transplantation strategy are also necessary step that should be taken before the clinical translation of established protocol. We showed in

our previous study that dissolved oxygen can regulated hPSCs fate and adopting the established protocol to a fully controlled bioprocess may change the process outcome including organoids metabolic activity and functionality <sup>220</sup>.

## Acknowledgements

This research was supported by the Royan institute grant, Iranian stem cell council grant, ACECR grant, and Langer lab NIH grant at Koch institute-MIT. We highly appreciate Dr. Giovanni Traverso for mentorship of project part done at MIT as well as financially support of the project. We also highly appreciate Prof. Langer for his support for accommodations during stay in Boston and S.A appointment at MIT.

## References

- 1 Kuntz, E. Biochemistry and functions of the liver. *Hepatology Principles and Practice: History Morphology Biochemistry Diagnostics Clinic Therapy*, 31-71 (2006).
- 2 Weissman, I. L. Stem cells: units of development, units of regeneration, and units in evolution. *cell* **100**, 157-168 (2000).
- 3 Nusrat, S., Khan, M. S., Fazili, J. *et al.* Cirrhosis and its complications: evidence based treatment. *World Journal of Gastroenterology: WJG* **20**, 5442 (2014).
- 4 Shashidhar, K. & Nallagangula, K. S. Pros and Cons of Existing Biomarkers for Cirrhosis of Liver. *Acta Scientific Medical Sciences* **3**, 63-72 (2019).
- 5 Hope, A. A. & Morrison, R. S. in *Evidence-Based Practice of Palliative Medicine* 300-307 (Elsevier Inc., 2012).
- 6 Hernaez, R., Solà, E., Moreau, R. *et al.* Acute-on-chronic liver failure: an update. *Gut* **66**, 541-553, doi:10.1136/gutjnl-2016-312670 (2017).
- 7 Nayak, N. C., Jain, D., Vasdev, N. *et al.* Etiologic types of end-stage chronic liver disease in adults: analysis of prevalence and their temporal changes from a study on native liver explants. *European journal of gastroenterology & hepatology* **24**, 1199-1208 (2012).
- 8 Moon, A. M., Singal, A. G. & Tapper, E. B. Contemporary epidemiology of chronic liver disease and cirrhosis. *Clinical Gastroenterology and Hepatology* (2019).
- 9 Tapper, E. B. & Parikh, N. D. Mortality due to cirrhosis and liver cancer in the United States, 1999-2016: observational study. *BMJ* **362**, k2817, doi:10.1136/bmj.k2817 (2018).
- 10 Estes, C., Razavi, H., Loomba, R. *et al.* Modeling the epidemic of nonalcoholic fatty liver disease demonstrates an exponential increase in burden of disease. *Hepatology* **67**, 123-133 (2018).
- 11 Marcellin, P. & Kutala, B. K. Liver diseases: A major, neglected global public health problem requiring urgent actions and large-scale screening. *Liver International* **38**, 2-6 (2018).

- 12 Jadowiec, C. C. & Taner, T. Liver transplantation: current status and challenges. *World journal of gastroenterology* **22**, 4438 (2016).
- 13 Dutkowski, P., Linecker, M., DeOliveira, M. L. *et al.* Challenges to liver transplantation and strategies to improve outcomes. *Gastroenterology* **148**, 307-323, doi:10.1053/j.gastro.2014.08.045 (2015).
- 14 Shukla, A., Vadeyar, H., Rela, M. *et al.* Liver Transplantation: East versus West. *J Clin Exp Hepatol* **3**, 243-253, doi:10.1016/j.jceh.2013.08.004 (2013).
- 15 Tayyeb, A., Azam, F., Nisar, R. *et al.* Regenerative medicine in liver cirrhosis: promises and pitfalls. *Liver Cirrhosis-Update and Current Challenges*, 236-256 (2017).
- 16 Yamamoto, J., Udono, M., Miura, S. *et al.* Cell Aggregation Culture Induces Functional Differentiation of Induced Hepatocyte-like Cells through Activation of Hippo Signaling. *Cell Rep* **25**, 183-198, doi:10.1016/j.celrep.2018.09.010 (2018).
- 17 Thompson, J., Jones, N., Al-Khafaji, A. *et al.* Extracorporeal cellular therapy (ELAD) in severe alcoholic hepatitis: a multinational, prospective, controlled, randomized trial. *Liver Transplantation* **24**, 380-393 (2018).
- 18 Farzaneh, Z., Najarasl, M., Abbasalizadeh, S. *et al.* Developing a cost-effective and scalable production of human hepatic competent endoderm from size-controlled pluripotent stem cell aggregates. *Stem cells and development* **27**, 262-274 (2018).
- 19 Pla-Palac n, I., Sainz-Arnal, P., Morini, S. *et al.* Liver Bioengineering Using Decellularized Whole-Liver Scaffolds. (2017).
- 20 Takebe, T., Sekine, K., Enomura, M. *et al.* Vascularized and functional human liver from an iPSC-derived organ bud transplant. *Nature* **499**, 481-484 (2013).
- 21 Takebe, T., Sekine, K., Kimura, M. *et al.* Massive and Reproducible Production of Liver Buds Entirely from Human Pluripotent Stem Cells. *Cell reports* **21**, 2661-2670 (2017).
- 22 Stevens, K. R., Scull, M. A., Ramanan, V. *et al.* In situ expansion of engineered human liver tissue in a mouse model of chronic liver disease. *Science translational medicine* **9**, eaah5505 (2017).
- 23 Mardpour, S., Hassani, S. N., Mardpour, S. *et al.* Extracellular vesicles derived from human embryonic stem cell-MSCs ameliorate cirrhosis in thioacetamide-induced chronic liver injury. *Journal of cellular physiology* **233**, 9330-9344 (2018).
- 24 Sussman, N. L. & Kelly, J. H. Extracorporeal liver support: cell-based therapy for the failing liver. *American journal of kidney diseases* **30**, S66-S71 (1997).
- 25 Mullon, C. & Pitkin, Z. The HepatAssist® Bioartificial Liver Support System: clinical study and pig hepatocyte process. *Expert opinion on investigational drugs* **8**, 229-235 (1999).
- 26 Patzer, J. F., Mazariegos, G. V., Lopez, R. *et al.* Novel bioartificial liver support system: preclinical evaluation. *Annals of the New York Academy of Sciences* **875**, 340-352 (1999).
- 27 Nibourg, G. A., Chamuleau, R. A., Van der Hoeven, T. V. *et al.* Liver progenitor cell line HepaRG differentiated in a bioartificial liver effectively supplies liver support to rats with acute liver failure. *PloS one* **7** (2012).
- 28 Sauer, I. M. & Gerlach, J. C. Modular extracorporeal liver support. *Artificial organs* **26**, 703-706 (2002).
- 29 Patel, P. & Pyrsopoulos, N. T. in *Liver Diseases* 721-726 (Springer, 2020).
- 30 Fisher, C. & Wendon, J. in *Critical Care Nephrology* 793-799. e792 (Elsevier, 2019).
- 31 Chen, F.-M. & Liu, X. Advancing biomaterials of human origin for tissue engineering. *Progress in polymer science* **53**, 86-168 (2016).
- 32 Maghsoudlou, P., Georgiades, F., Smith, H. *et al.* Optimization of liver decellularization maintains extracellular matrix micro-architecture and composition predisposing to effective cell seeding. *PloS one* **11** (2016).
- 33 Andrews, E. Damage of porcine aortic valve tissue caused by the surfactant sodiumdodecylsulphate. *The Thoracic and cardiovascular surgeon* **34**, 340-341 (1986).

- 34 Ott, H. C., Matthiesen, T. S., Goh, S.-K. *et al.* Perfusion-decellularized matrix: using  
nature's platform to engineer a bioartificial heart. *Nature medicine* **14**, 213-221 (2008).
- 35 Rajabi, S., Pahlavan, S., Ashtiani, M. K. *et al.* Human embryonic stem cell-derived  
cardiovascular progenitor cells efficiently colonize in bFGF-tethered natural matrix to  
construct contracting humanized rat hearts. *Biomaterials* **154**, 99-112 (2018).
- 36 He, M. Tissue engineering of the kidney using a whole organ decellularisation  
approach. (2014).
- 37 Stabler, C. T., Lecht, S., Mondrinos, M. J. *et al.* Revascularization of decellularized  
lung scaffolds: principles and progress. *American Journal of Physiology-Lung Cellular  
and Molecular Physiology* **309**, L1273-L1285 (2015).
- 38 Mazza, G., Rombouts, K., Hall, A. R. *et al.* Decellularized human liver as a natural 3D-  
scaffold for liver bioengineering and transplantation. *Scientific reports* **5**, 13079 (2015).
- 39 Uygun, B. E., Soto-Gutierrez, A., Yagi, H. *et al.* Organ reengineering through  
development of a transplantable recellularized liver graft using decellularized liver  
matrix. *Nature medicine* **16**, 814-820 (2010).
- 40 Rossi, E. A., Quintanilha, L. F., Nonaka, C. K. V. *et al.* Advances in hepatic tissue  
bioengineering with decellularized liver Bioscaffold. *Stem cells international* **2019**  
(2019).
- 41 Shaheen, M. F., Joo, D. J., Ross, J. J. *et al.* Sustained perfusion of revascularized  
bioengineered livers heterotopically transplanted into immunosuppressed pigs. *Nature  
biomedical engineering*, 1-9 (2019).
- 42 Barakat, O., Abbasi, S., Rodriguez, G. *et al.* Use of decellularized porcine liver for  
engineering humanized liver organ. *Journal of Surgical Research* **173**, e11-e25 (2012).
- 43 Versteegen, M. M., Willemse, J., Van Den Hoek, S. *et al.* Decellularization of whole  
human liver grafts using controlled perfusion for transplantable organ bioscaffolds.  
*Stem cells and development* **26**, 1304-1315 (2017).
- 44 Mattei, G., Magliaro, C., Pirone, A. *et al.* Decellularized human liver is too  
heterogeneous for designing a generic extracellular matrix mimic hepatic scaffold.  
*Artificial organs* **41**, E347-E355 (2017).
- 45 Shafiee, A. & Atala, A. Tissue engineering: Toward a new era of medicine. *Annual  
review of medicine* **68**, 29-40 (2017).
- 46 Gilgenkrantz, H. & de l'Hortet, A. C. Understanding liver regeneration: from  
mechanisms to regenerative medicine. *The American journal of pathology* **188**, 1316-  
1327 (2018).
- 47 Bizzaro, D., Russo, F. P. & Burra, P. New perspectives in liver transplantation: From  
regeneration to bioengineering. *Bioengineering* **6**, 81 (2019).
- 48 da Silva Morais, A., Vieira, S., Zhao, X. *et al.* Advanced Biomaterials and Processing  
Methods for Liver Regeneration: State-of-the-Art and Future Trends. *Advanced  
Healthcare Materials* **9**, 1901435 (2020).
- 49 Jain, E., Damania, A. & Kumar, A. Biomaterials for liver tissue engineering. *Hepatology  
international* **8**, 185-197 (2014).
- 50 Turner, W. S., Schmelzer, E., McClelland, R. *et al.* Human hepatoblast phenotype  
maintained by hyaluronan hydrogels. *Journal of Biomedical Materials Research Part  
B: Applied Biomaterials* **82**, 156-168 (2007).
- 51 Burra, P., Arcidiacono, D., Bizzaro, D. *et al.* Systemic administration of a novel human  
umbilical cord mesenchymal stem cells population accelerates the resolution of acute  
liver injury. *BMC gastroenterology* **12**, 88 (2012).
- 52 Fu, R.-H., Wang, Y.-C., Liu, S.-P. *et al.* Differentiation of stem cells: strategies for  
modifying surface biomaterials. *Cell transplantation* **20**, 37-47 (2011).
- 53 Kleinman, H. K. & Martin, G. R. in *Seminars in cancer biology*. 378-386 (Elsevier).
- 54 Wang, H., Shi, Q., Guo, Y. *et al.* Contact assembly of cell-laden hollow microtubes  
through automated micromanipulator tip locating. *Journal of Micromechanics and  
Microengineering* **27**, 015013 (2016).

- 55 Hospodiuk, M., Dey, M., Sosnoski, D. *et al.* The bioink: A comprehensive review on bioprintable materials. *Biotechnology advances* **35**, 217-239 (2017).
- 56 Liu, W., Zhang, Y. S., Heinrich, M. A. *et al.* Rapid continuous multimaterial extrusion bioprinting. *Advanced materials* **29**, 1604630 (2017).
- 57 Kang, D., Hong, G., An, S. *et al.* Bioprinting of Multiscaled Hepatic Lobules within a Highly Vascularized Construct. *Small*, 1905505 (2020).
- 58 Murphy, S. V. & Atala, A. 3D bioprinting of tissues and organs. *Nature biotechnology* **32**, 773 (2014).
- 59 Murphy, S. V., Skardal, A. & Atala, A. Evaluation of hydrogels for bio-printing applications. *Journal of Biomedical Materials Research Part A* **101**, 272-284 (2013).
- 60 Jammalamadaka, U. & Tappa, K. Recent advances in biomaterials for 3D printing and tissue engineering. *Journal of functional biomaterials* **9**, 22 (2018).
- 61 Skardal, A. & Atala, A. Biomaterials for integration with 3-D bioprinting. *Annals of biomedical engineering* **43**, 730-746 (2015).
- 62 Kizawa, H., Nagao, E., Shimamura, M. *et al.* Scaffold-free 3D bio-printed human liver tissue stably maintains metabolic functions useful for drug discovery. *Biochemistry and biophysics reports* **10**, 186-191 (2017).
- 63 Yorukoglu, A. C., Kiter, A., Akkaya, S. *et al.* A concise review on the use of mesenchymal stem cells in cell sheet-based tissue engineering with special emphasis on bone tissue regeneration. *Stem cells international* **2017** (2017).
- 64 Owaki, T., Shimizu, T., Yamato, M. *et al.* Cell sheet engineering for regenerative medicine: current challenges and strategies. *Biotechnology journal* **9**, 904-914 (2014).
- 65 Takagi, S., Ohno, M., Ohashi, K. *et al.* Cell shape regulation based on hepatocyte sheet engineering technologies. *Cell transplantation* **21**, 411-420 (2012).
- 66 Tatsumi, K. & Okano, T. Hepatocyte transplantation: cell sheet technology for liver cell transplantation. *Current transplantation reports* **4**, 184-192 (2017).
- 67 Kobayashi, J., Kikuchi, A., Aoyagi, T. *et al.* Cell sheet tissue engineering: Cell sheet preparation, harvesting/manipulation, and transplantation. *Journal of Biomedical Materials Research Part A* **107**, 955-967 (2019).
- 68 Takahashi, H. & Okano, T. Thermally-triggered fabrication of cell sheets for tissue engineering and regenerative medicine. *Advanced drug delivery reviews* **138**, 276-292 (2019).
- 69 Nobakht Lahrood, F., Saheli, M., Farzaneh, Z. *et al.* Generation of Transplantable Three-Dimensional Hepatic-Patch to Improve the Functionality of Hepatic Cells In Vitro and In Vivo. *Stem Cells and Development* **29**, 301-313 (2020).
- 70 Kim, K., Ohashi, K., Utoh, R. *et al.* Preserved liver-specific functions of hepatocytes in 3D co-culture with endothelial cell sheets. *Biomaterials* **33**, 1406-1413 (2012).
- 71 Sakai, Y., Koike, M., Hasegawa, H. *et al.* Rapid fabricating technique for multi-layered human hepatic cell sheets by forceful contraction of the fibroblast monolayer. *PloS one* **8** (2013).
- 72 Sakai, Y., Yamanouchi, K., Ohashi, K. *et al.* Vascularized subcutaneous human liver tissue from engineered hepatocyte/fibroblast sheets in mice. *Biomaterials* **65**, 66-75 (2015).
- 73 Arai, K., Yoshida, T., Okabe, M. *et al.* Fabrication of 3D-culture platform with sandwich architecture for preserving liver-specific functions of hepatocytes using 3D bioprinter. *Journal of Biomedical Materials Research Part A* **105**, 1583-1592 (2017).
- 74 Fujii, M., Yamanouchi, K., Sakai, Y. *et al.* In vivo construction of liver tissue by implantation of a hepatic non-parenchymal/adipose-derived stem cell sheet. *Journal of tissue engineering and regenerative medicine* **12**, e287-e295 (2018).
- 75 Sasaki, K., Akagi, T., Asaoka, T. *et al.* Construction of three-dimensional vascularized functional human liver tissue using a layer-by-layer cell coating technique. *Biomaterials* **133**, 263-274 (2017).
- 76 Schneeberger, K., Sánchez-Romero, N., Ye, S. *et al.* Large-scale Production of LGR5-positive Bipotential Human Liver Stem Cells. *Hepatology* (2019).

- 77 Nagamoto, Y., Takayama, K., Ohashi, K. *et al.* Transplantation of a human iPSC-derived hepatocyte sheet increases survival in mice with acute liver failure. *Journal of hepatology* **64**, 1068-1075 (2016).
- 78 Wilson, H. A new method by which sponges may be artificially reared. *Science* **25**, 912-915 (1907).
- 79 Liu, F., Huang, J., Ning, B. *et al.* Drug discovery via human-derived stem cell organoids. *Frontiers in pharmacology* **7**, 334 (2016).
- 80 Dutta, D., Heo, I. & Clevers, H. Disease modeling in stem cell-derived 3D organoid systems. *Trends in molecular medicine* **23**, 393-410 (2017).
- 81 Huch, M., Knoblich, J. A., Lutolf, M. P. *et al.* The hope and the hype of organoid research. *Development* **144**, 938-941 (2017).
- 82 Sakabe, K., Takebe, T. & Asai, A. Organoid Medicine in Hepatology. *Clinical Liver Disease* **15**, 3 (2020).
- 83 Lancaster, M. A. & Knoblich, J. A. Organogenesis in a dish: modeling development and disease using organoid technologies. *Science* **345**, 1247125 (2014).
- 84 Fatehullah, A., Tan, S. H. & Barker, N. Organoids as an in vitro model of human development and disease. *Nature cell biology* **18**, 246-254 (2016).
- 85 Huch, M., Dorrell, C., Boj, S. F. *et al.* In vitro expansion of single Lgr5+ liver stem cells induced by Wnt-driven regeneration. *Nature* **494**, 247-250 (2013).
- 86 Skardal, A., Murphy, S. V., Devarasetty, M. *et al.* Multi-tissue interactions in an integrated three-tissue organ-on-a-chip platform. *Scientific reports* **7**, 1-16 (2017).
- 87 Huch, M., Gehart, H., Van Boxtel, R. *et al.* Long-term culture of genome-stable bipotent stem cells from adult human liver. *Cell* **160**, 299-312 (2015).
- 88 Sgodda, M., Dai, Z., Zweigerdt, R. *et al.* A scalable approach for the generation of human pluripotent stem cell-derived hepatic organoids with sensitive hepatotoxicity features. *Stem cells and development* **26**, 1490-1504 (2017).
- 89 Guye, P., Ebrahimkhani, M. R., Kipniss, N. *et al.* Genetically engineering self-organization of human pluripotent stem cells into a liver bud-like tissue using Gata6. *Nature communications* **7**, 1-12 (2016).
- 90 Ramachandran, S. D., Schirmer, K., Münst, B. *et al.* In vitro generation of functional liver organoid-like structures using adult human cells. *PloS one* **10** (2015).
- 91 Ang, C. H., Hsu, S. H., Guo, F. *et al.* Lgr5+ pericentral hepatocytes are self-maintained in normal liver regeneration and susceptible to hepatocarcinogenesis. *Proceedings of the National Academy of Sciences* **116**, 19530-19540 (2019).
- 92 Prior, N., Inacio, P. & Huch, M. Liver organoids: from basic research to therapeutic applications. *Gut* **68**, 2228-2237 (2019).
- 93 Hu, H., Gehart, H., Artegiani, B. *et al.* Long-term expansion of functional mouse and human hepatocytes as 3D organoids. *Cell* **175**, 1591-1606. e1519 (2018).
- 94 Yamaguchi, T., Matsuzaki, J., Katsuda, T. *et al.* Generation of functional human hepatocytes in vitro: current status and future prospects. *Inflammation and regeneration* **39**, 13 (2019).
- 95 Sgodda, M., Dai, Z., Zweigerdt, R. *et al.* A Scalable Approach for the Generation of Human Pluripotent Stem Cell-Derived Hepatic Organoids with Sensitive Hepatotoxicity Features. *Stem Cells and Development* (2017).
- 96 Takebe, T., Enomura, M., Yoshizawa, E. *et al.* Vascularized and complex organ buds from diverse tissues via mesenchymal cell-driven condensation. *Cell stem cell* **16**, 556-565 (2015).
- 97 Zhang, R.-R., Koido, M., Tadokoro, T. *et al.* Human iPSC-derived posterior gut progenitors are expandable and capable of forming gut and liver organoids. *Stem cell reports* **10**, 780-793 (2018).
- 98 Underhill, G. H. & Khetani, S. R. Bioengineered liver models for drug testing and cell differentiation studies. *Cellular and molecular gastroenterology and hepatology* **5**, 426-439. e421 (2018).

- 99 Mun, S. J., Ryu, J.-S., Lee, M.-O. *et al.* Generation of expandable human pluripotent stem cell-derived hepatocyte-like liver organoids. *Journal of hepatology* **71**, 970-985 (2019).
- 100 Pettinato, G., Lehoux, S., Ramanathan, R. *et al.* Generation of fully functional hepatocyte-like organoids from human induced pluripotent stem cells mixed with endothelial cells. *Scientific reports* **9**, 1-21 (2019).
- 101 Li, J., Xing, F., Chen, F. *et al.* Functional 3D human liver bud assembled from MSC-derived multiple liver cell lineages. *Cell transplantation* **28**, 510-521 (2019).
- 102 Haideri, S. S., McKinnon, A. C., Taylor, A. H. *et al.* Injection of embryonic stem cell derived macrophages ameliorates fibrosis in a murine model of liver injury. *NPJ Regenerative medicine* **2**, 1-11 (2017).
- 103 Esch, M. B., Prot, J.-M., Wang, Y. I. *et al.* Multi-cellular 3D human primary liver cell culture elevates metabolic activity under fluidic flow. *Lab on a Chip* **15**, 2269-2277 (2015).
- 104 Nejak-Bowen, K. N. & Monga, S. P. S. in *Liver regeneration* 77-101 (Elsevier, 2015).
- 105 Mito, M. & Kusano, M. Hepatocyte transplantation in man. *Cell transplantation* **2**, 65-74 (1993).
- 106 Fisher, R. A. & Strom, S. C. Human hepatocyte transplantation: worldwide results. *Transplantation* **82**, 441-449 (2006).
- 107 Fox, I. J., Chowdhury, J. R., Kaufman, S. S. *et al.* Treatment of the Crigler–Najjar syndrome type I with hepatocyte transplantation. *New England Journal of Medicine* **338**, 1422-1427 (1998).
- 108 Muraca, M., Gerunda, G., Neri, D. *et al.* Hepatocyte transplantation as a treatment for glycogen storage disease type 1a. *The Lancet* **359**, 317-318 (2002).
- 109 Bilir, B. M., Guinette, D., Karrer, F. *et al.* Hepatocyte transplantation in acute liver failure. *Liver Transplantation* **6**, 32-40 (2000).
- 110 Nicolas, C. T., Hickey, R. D., Chen, H. S. *et al.* Concise review: liver regenerative medicine: from hepatocyte transplantation to bioartificial livers and bioengineered grafts. *Stem Cells* **35**, 42-50 (2017).
- 111 Utoh, R., Tateno, C., Yamasaki, C. *et al.* Susceptibility of chimeric mice with livers repopulated by serially subcultured human hepatocytes to hepatitis B virus. *Hepatology* **47**, 435-446 (2008).
- 112 Kim, Y., Kang, K., Lee, S. B. *et al.* Small molecule-mediated reprogramming of human hepatocytes into bipotent progenitor cells. *Journal of hepatology* **70**, 97-107 (2019).
- 113 Zhang, K., Zhang, L., Liu, W. *et al.* In vitro expansion of primary human hepatocytes with efficient liver repopulation capacity. *Cell Stem Cell* **23**, 806-819. e804 (2018).
- 114 Fu, G.-B., Huang, W.-J., Zeng, M. *et al.* Expansion and differentiation of human hepatocyte-derived liver progenitor-like cells and their use for the study of hepatotropic pathogens. *Cell research* **29**, 8-22 (2019).
- 115 Li, S., Huang, S.-Q., Zhao, Y.-X. *et al.* Derivation and applications of human hepatocyte-like cells. *World journal of stem cells* **11**, 535 (2019).
- 116 Hay, D. C., Fletcher, J., Payne, C. *et al.* Highly efficient differentiation of hESCs to functional hepatic endoderm requires ActivinA and Wnt3a signaling. *Proceedings of the National Academy of Sciences* **105**, 12301-12306 (2008).
- 117 Woo, D. H., Kim, S. K., Lim, H. J. *et al.* Direct and indirect contribution of human embryonic stem cell-derived hepatocyte-like cells to liver repair in mice. *Gastroenterology* **142**, 602-611 (2012).
- 118 Duan, Y., Catana, A., Meng, Y. *et al.* Differentiation and enrichment of hepatocyte-like cells from human embryonic stem cells in vitro and in vivo. *Stem cells* **25**, 3058-3068 (2007).
- 119 Lavon, N., Yanuka, O. & Benvenisty, N. Differentiation and isolation of hepatic-like cells from human embryonic stem cells. *Differentiation* **72**, 230-238 (2004).

- 120 Basma, H., Soto–Gutiérrez, A., Yannam, G. R. *et al.* Differentiation and transplantation of human embryonic stem cell–derived hepatocytes. *Gastroenterology* **136**, 990-999. e994 (2009).
- 121 Yamanaka, S. Induced pluripotent stem cells: past, present, and future. *Cell stem cell* **10**, 678-684 (2012).
- 122 Kia, R., Sison, R. L., Heslop, J. *et al.* Stem cell-derived hepatocytes as a predictive model for drug-induced liver injury: are we there yet? *British Journal of Clinical Pharmacology* **75**, 885-896 (2013).
- 123 Gómez-Lechón, M. J. & Tolosa, L. Human hepatocytes derived from pluripotent stem cells: a promising cell model for drug hepatotoxicity screening. *Archives of toxicology* **90**, 2049-2061 (2016).
- 124 Ang, L. T., Tan, A. K. Y., Autio, M. I. *et al.* A roadmap for human liver differentiation from pluripotent stem cells. *Cell reports* **22**, 2190-2205 (2018).
- 125 Zhao, T., Zhang, Z.-N., Rong, Z. *et al.* Immunogenicity of induced pluripotent stem cells. *Nature* **474**, 212-215 (2011).
- 126 Araki, R., Uda, M., Hoki, Y. *et al.* Negligible immunogenicity of terminally differentiated cells derived from induced pluripotent or embryonic stem cells. *Nature* **494**, 100-104 (2013).
- 127 Zhou, J. & Sun, J. A revolution in reprogramming: small molecules. *Current molecular medicine* **19**, 77-90 (2019).
- 128 Si-Tayeb, K., Noto, F. K., Nagaoka, M. *et al.* Highly efficient generation of human hepatocyte–like cells from induced pluripotent stem cells. *Hepatology* **51**, 297-305 (2010).
- 129 Asumda, F. Z., Hatzistergos, K. E., Dykxhoorn, D. M. *et al.* Differentiation of hepatocyte-like cells from human pluripotent stem cells using small molecules. *Differentiation* **101**, 16-24 (2018).
- 130 Roy-Chowdhury, N., Wang, X., Guha, C. *et al.* Hepatocyte-like cells derived from induced pluripotent stem cells. *Hepatology international* **11**, 54-69 (2017).
- 131 Takebe, T., Sekine, K., Enomura, M. *et al.* Vascularized and functional human liver from an iPSC-derived organ bud transplant. *Nature* **499**, 481-484, doi:nature12271 [pii] 10.1038/nature12271 (2013).
- 132 Soltys, K. A., Setoyama, K., Tafaleng, E. N. *et al.* Host conditioning and rejection monitoring in hepatocyte transplantation in humans. *Journal of hepatology* **66**, 987-1000 (2017).
- 133 Vosough, M., Omidinia, E., Kadivar, M. *et al.* Generation of functional hepatocyte-like cells from human pluripotent stem cells in a scalable suspension culture. *Stem Cells Dev* **22**, 2693-2705, doi:10.1089/scd.2013.0088 (2013).
- 134 Wang, Y., Alhaque, S., Cameron, K. *et al.* Defined and Scalable Generation of Hepatocyte-like Cells from Human Pluripotent Stem Cells. *Journal of visualized experiments: JoVE* (2017).
- 135 Thomas, J. A., Pope, C., Wojtacha, D. *et al.* Macrophage therapy for murine liver fibrosis recruits host effector cells improving fibrosis, regeneration, and function. *Hepatology* **53**, 2003-2015 (2011).
- 136 Forbes, S. J. & Newsome, P. N. New horizons for stem cell therapy in liver disease. *Journal of hepatology* **56**, 496-499 (2012).
- 137 Afshari, A., Shamdani, S., Uzan, G. *et al.* Different approaches for transformation of mesenchymal stem cells into hepatocyte-like cells. *Stem Cell Research & Therapy* **11**, 54 (2020).
- 138 Zhan, Y., Wang, Y., Wei, L. *et al.* in *Transplantation proceedings*. 3082-3085 (Elsevier).
- 139 Terai, S., Takami, T., Yamamoto, N. *et al.* Status and prospects of liver cirrhosis treatment by using bone marrow-derived cells and mesenchymal cells. *Tissue Engineering Part B: Reviews* **20**, 206-210 (2014).

- 140 Rossi, L., Challen, G. A., Sirin, O. *et al.* in *Stem Cell Migration* 47-59 (Springer, 2011).
- 141 Lagasse, E., Connors, H., Al-Dhalimy, M. *et al.* Purified hematopoietic stem cells can differentiate into hepatocytes in vivo. *Nature medicine* **6**, 1229-1234 (2000).
- 142 Vainshtein, J. M., Kabarriti, R., Mehta, K. J. *et al.* Bone Marrow–Derived Stromal Cell Therapy in Cirrhosis: Clinical Evidence, Cellular Mechanisms, and Implications for the Treatment of Hepatocellular Carcinoma. *International Journal of Radiation Oncology\* Biology\* Physics* **89**, 786-803 (2014).
- 143 Austin, T. W. & Lagasse, E. Hepatic regeneration from hematopoietic stem cells. *Mechanisms of development* **120**, 131-135 (2003).
- 144 Thorgeirsson, S. S. & Grisham, J. W. Hematopoietic cells as hepatocyte stem cells: a critical review of the evidence. *Hepatology* **43**, 2-8 (2006).
- 145 Nakamura, T., Torimura, T., Sakamoto, M. *et al.* Significance and therapeutic potential of endothelial progenitor cell transplantation in a cirrhotic liver rat model. *Gastroenterology* **133**, 91-107. e101 (2007).
- 146 Lan, L., Liu, R., Qin, L.-Y. *et al.* Transplantation of bone marrow-derived endothelial progenitor cells and hepatocyte stem cells from liver fibrosis rats ameliorates liver fibrosis. *World journal of gastroenterology* **24**, 237 (2018).
- 147 Taniguchi, E., Kin, M., Torimura, T. *et al.* Endothelial progenitor cell transplantation improves the survival following liver injury in mice. *Gastroenterology* **130**, 521-531 (2006).
- 148 Banerjee, A., Bizzaro, D., Burra, P. *et al.* Umbilical cord mesenchymal stem cells modulate dextran sulfate sodium induced acute colitis in immunodeficient mice. *Stem cell research & therapy* **6**, 79 (2015).
- 149 Christ, B., Brückner, S. & Winkler, S. The therapeutic promise of mesenchymal stem cells for liver restoration. *Trends in molecular medicine* **21**, 673-686 (2015).
- 150 Andrzejewska, A., Lukomska, B. & Janowski, M. Concise review: Mesenchymal stem cells: From roots to boost. *Stem Cells* **37**, 855-864 (2019).
- 151 Lanzoni, G., Cardinale, V. & Carpino, G. The hepatic, biliary, and pancreatic network of stem/progenitor cell niches in humans: A new reference frame for disease and regeneration. *Hepatology* **64**, 277-286 (2016).
- 152 Huch, M., Boj, S. F. & Clevers, H. Lgr5+ liver stem cells, hepatic organoids and regenerative medicine. *Regenerative medicine* **8**, 385-387 (2013).
- 153 Wu, F., Wu, D., Ren, Y. *et al.* Generation of hepatobiliary organoids from human induced pluripotent stem cells. *Journal of hepatology* **70**, 1145-1158 (2019).
- 154 Vyas, D., Baptista, P. M., Brovold, M. *et al.* Self-assembled liver organoids recapitulate hepatobiliary organogenesis in vitro. *Hepatology* **67**, 750-761 (2018).
- 155 Saheli, M., Sepantafar, M., Pournasr, B. *et al.* Three-dimensional liver-derived extracellular matrix hydrogel promotes liver organoids function. *Journal of cellular biochemistry* **119**, 4320-4333 (2018).
- 156 Broguiere, N., Isenmann, L., Hirt, C. *et al.* Growth of epithelial organoids in a defined hydrogel. *Advanced Materials* **30**, 1801621 (2018).
- 157 Yamada, M., Utoh, R., Ohashi, K. *et al.* Controlled formation of heterotypic hepatic micro-organoids in anisotropic hydrogel microfibers for long-term preservation of liver-specific functions. *Biomaterials* **33**, 8304-8315 (2012).
- 158 Ma, M., Chiu, A., Sahay, G. *et al.* Core–shell hydrogel microcapsules for improved islets encapsulation. *Advanced healthcare materials* **2**, 667-672 (2013).
- 159 Siltanen, C., Diakatou, M., Lowen, J. *et al.* One step fabrication of hydrogel microcapsules with hollow core for assembly and cultivation of hepatocyte spheroids. *Acta biomaterialia* **50**, 428-436 (2017).
- 160 Gonzalez-Pujana, A., Santos, E., Orive, G. *et al.* Cell microencapsulation technology: current vision of its therapeutic potential through the administration routes. *Journal of Drug Delivery Science and Technology* **42**, 49-62 (2017).

- 161 Pajoumshariati, S. R., Azizi, M., Wesner, D. *et al.* Microfluidic-based cell-embedded  
microgels using nonfluorinated oil as a model for the gastrointestinal niche. *ACS*  
*applied materials & interfaces* **10**, 9235-9246 (2018).
- 162 Zhang, W., Zhao, S., Rao, W. *et al.* A novel core-shell microcapsule for encapsulation  
and 3D culture of embryonic stem cells. *Journal of materials chemistry B* **1**, 1002-1009  
(2013).
- 163 Liu, H., Wang, Y., Wang, H. *et al.* A Droplet Microfluidic System to Fabricate Hybrid  
Capsules Enabling Stem Cell Organoid Engineering. *Advanced Science* (2020).
- 164 Lu, Y. C., Fu, D. J., An, D. *et al.* Scalable production and cryostorage of organoids  
using core-shell decoupled hydrogel capsules. *Advanced biosystems* **1**, 1700165  
(2017).
- 165 Zhong, Q., Ding, H., Gao, B. *et al.* Advances of Microfluidics in Biomedical  
Engineering. *Advanced Materials Technologies* **4**, 1800663 (2019).
- 166 Baharvand, H., Ashtiani, S. K., Taei, A. *et al.* Generation of new human embryonic  
stem cell lines with diploid and triploid karyotypes. *Development, growth &*  
*differentiation* **48**, 117-128, doi:10.1111/j.1440-169X.2006.00851.x (2006).
- 167 Farzaneh, Z., Najarasl, M., Abbasalizadeh, S. *et al.* Developing a Cost-Effective and  
Scalable Production of Human Hepatic Competent Endoderm from Size-Controlled  
Pluripotent Stem Cell Aggregates. *Stem cells and development* **27**, 262-274,  
doi:10.1089/scd.2017.0074 (2018).
- 168 Farzaneh, Z., Najarasl, M., Abbasalizadeh, S. *et al.* Developing a Cost-Effective and  
Scalable Production of Human Hepatic Competent Endoderm from Size-Controlled  
Pluripotent Stem Cell Aggregates. *Stem cells and development* (2018).
- 169 Yabe, S. G., Nishida, J., Fukuda, S. *et al.* Definitive endoderm differentiation is  
promoted in suspension cultured human iPS-derived spheroids more than in adherent  
cells. *Int. J. Dev. Biol* **63**, 271-280 (2019).
- 170 Rashidi, H., Luu, N.-T., Alwahsh, S. M. *et al.* 3D human liver tissue from pluripotent  
stem cells displays stable phenotype in vitro and supports compromised liver function  
in vivo. *Archives of toxicology* **92**, 3117-3129 (2018).
- 171 Baharvand, H., Larijani, M. R. & Yousefi, M. Protocol for expansion of undifferentiated  
human embryonic and pluripotent stem cells in suspension. *Methods in molecular*  
*biology* **873**, 217-226, doi:10.1007/978-1-61779-794-1\_13 (2012).
- 172 Abbasalizadeh, S., Larijani, M. R., Samadian, A. *et al.* Bioprocess development for  
mass production of size-controlled human pluripotent stem cell aggregates in stirred  
suspension bioreactor. *Tissue Eng Part C Methods* **18**, 831-851,  
doi:10.1089/ten.TEC.2012.0161 (2012).
- 173 Farzaneh, Z., Pakzad, M., Vosough, M. *et al.* Differentiation of human embryonic stem  
cells to hepatocyte-like cells on a new developed xeno-free extracellular matrix.  
*Histochem Cell Biol* **142**, 217-226, doi:10.1007/s00418-014-1183-4 (2014).
- 174 Reich, M., Liefeld, T., Gould, J. *et al.* GenePattern 2.0. *Nature genetics* **38**, 500-501  
(2006).
- 175 Nejak-Bowen, K. & Monga, S. P. Wnt/ $\beta$ -catenin signaling in hepatic organogenesis.  
*Organogenesis* **4**, 92-99 (2008).
- 176 Ueberham, E., Aigner, T., Ueberham, U. *et al.* E-cadherin as a reliable cell surface  
marker for the identification of liver specific stem cells. *Journal of molecular histology*  
**38**, 359-368 (2007).
- 177 Visconti, R. P., Kasyanov, V., Gentile, C. *et al.* Towards organ printing: engineering an  
intra-organ branched vascular tree. *Expert opinion on biological therapy* **10**, 409-420  
(2010).
- 178 Citro, A., Moser, P. T., Dugnani, E. *et al.* Biofabrication of a vascularized islet organ  
for type 1 diabetes. *Biomaterials* **199**, 40-51 (2019).
- 179 Battig, M. R., Fishbein, I., Levy, R. J. *et al.* Optimizing endothelial cell functionalization  
for cell therapy of vascular proliferative disease using a direct contact co-culture  
system. *Drug delivery and translational research* **8**, 954-963 (2018).

- 180 Reed, D. M., Foldes, G., Harding, S. E. *et al.* Stem cell-derived endothelial cells for cardiovascular disease: a therapeutic perspective. *British journal of clinical pharmacology* **75**, 897-906 (2013).
- 181 Qiu, J. & Hirschi, K. K. Endothelial Cell Development and Its Application to Regenerative Medicine. *Circulation research* **125**, 489-501 (2019).
- 182 Lin, H., Du, Q., Li, Q. *et al.* A scalable and efficient bioprocess for manufacturing human pluripotent stem cell-derived endothelial cells. *Stem cell reports* **11**, 454-469 (2018).
- 183 Olmer, R., Engels, L., Usman, A. *et al.* Differentiation of Human Pluripotent Stem Cells into Functional Endothelial Cells in Scalable Suspension Culture. *Stem Cell Reports* **10**, 1657-1672, doi:<https://doi.org/10.1016/j.stemcr.2018.03.017> (2018).
- 184 Lin, H., Du, Q., Li, Q. *et al.* Manufacturing human pluripotent stem cell derived endothelial cells in scalable and cell-friendly microenvironments. *Biomaterials science* **7**, 373-388 (2019).
- 185 Olmer, R., Engels, L., Usman, A. *et al.* Differentiation of human pluripotent stem cells into functional endothelial cells in scalable suspension culture. *Stem cell reports* **10**, 1657-1672 (2018).
- 186 Bao, X., Lian, X., Dunn, K. K. *et al.* Chemically-defined albumin-free differentiation of human pluripotent stem cells to endothelial progenitor cells. *Stem cell research* **15**, 122-129 (2015).
- 187 Jiang, B., Yan, L., Wang, X. *et al.* Concise Review: Mesenchymal Stem Cells Derived from Human Pluripotent Cells, an Unlimited and Quality-Controllable Source for Therapeutic Applications. *Stem cells* **37**, 572-581 (2019).
- 188 Wang, H., Li, D., Zhai, Z. *et al.* Characterization and therapeutic application of mesenchymal stem cells with neuromesodermal origin from human pluripotent stem cells. *Theranostics* **9**, 1683 (2019).
- 189 Abdal Dayem, A., Lee, S. B., Kim, K. *et al.* Production of Mesenchymal Stem Cells through Stem Cell Reprogramming. *International journal of molecular sciences* **20**, 1922 (2019).
- 190 Jossen, V., van den Bos, C., Eibl, R. *et al.* Manufacturing human mesenchymal stem cells at clinical scale: process and regulatory challenges. *Applied microbiology and biotechnology* **102**, 3981-3994 (2018).
- 191 Mizukami, A. & Swiech, K. Mesenchymal stromal cells: from discovery to manufacturing and commercialization. *Stem cells international* **2018** (2018).
- 192 Yan, L., Jiang, B., Li, E. *et al.* Scalable generation of mesenchymal stem cells from human embryonic stem cells in 3D. *International journal of biological sciences* **14**, 1196 (2018).
- 193 Takahashi, T. Organoids for drug discovery and personalized medicine. *Annual review of pharmacology and toxicology* **59**, 447-462 (2019).
- 194 Pettinato, G., Lehoux, S., Ramanathan, R. *et al.* Generation of fully functional hepatocyte-like organoids from human induced pluripotent stem cells mixed with Endothelial Cells. *Sci Rep* **9**, 8920, doi:10.1038/s41598-019-45514-3 (2019).
- 195 Liu, H., Wang, Y., Wang, H. *et al.* A Droplet Microfluidic System to Fabricate Hybrid Capsules Enabling Stem Cell Organoid Engineering. *Advanced Science*, 1903739 (2020).
- 196 Samuelson, L. C. & Lynch, J. P. Organoids and Engineered Organ Systems. *Cellular and molecular gastroenterology and hepatology* **7**, 679 (2019).
- 197 Gjorevski, N., Sachs, N., Manfrin, A. *et al.* Designer matrices for intestinal stem cell and organoid culture. *Nature* **539**, 560-564 (2016).
- 198 Garreta, E., Prado, P., Tarantino, C. *et al.* Fine tuning the extracellular environment accelerates the derivation of kidney organoids from human pluripotent stem cells. *Nature materials* **18**, 397-405 (2019).
- 199 Candiello, J., Grandhi, T. S. P., Goh, S. K. *et al.* 3D heterogeneous islet organoid generation from human embryonic stem cells using a novel engineered hydrogel platform. *Biomaterials* **177**, 27-39 (2018).

- 200 Ng, S. S., Saeb-Parsy, K., Blackford, S. J. *et al.* Human iPS derived progenitors  
bioengineered into liver organoids using an inverted colloidal crystal poly (ethylene  
glycol) scaffold. *Biomaterials* **182**, 299-311 (2018).
- 201 Zhao, S., Agarwal, P., Rao, W. *et al.* Coaxial electrospray of liquid core–hydrogel shell  
microcapsules for encapsulation and miniaturized 3D culture of pluripotent stem cells.  
*Integrative Biology* **6**, 874-884 (2014).
- 202 Wang, H., Liu, H., Liu, H. *et al.* One-Step Generation of Core–Shell Gelatin  
Methacrylate (GelMA) Microgels Using a Droplet Microfluidic System. *Advanced  
Materials Technologies* **4**, 1800632 (2019).
- 203 Chen, C., Mehl, B. T., Munshi, A. S. *et al.* 3D-printed microfluidic devices: fabrication,  
advantages and limitations—a mini review. *Analytical Methods* **8**, 6005-6012 (2016).
- 204 Jing, Y., Zhang, C., Fu, T. *et al.* Combination of dextran sulfate and recombinant trypsin  
on aggregation of Chinese hamster ovary cells. *Cytotechnology* **68**, 241-248 (2016).
- 205 Lei, Y., Jeong, D., Xiao, J. *et al.* Developing defined and scalable 3D culture systems  
for culturing human pluripotent stem cells at high densities. *Cellular and molecular  
bioengineering* **7**, 172-183 (2014).
- 206 Li, Q., Lin, H., Wang, O. *et al.* Scalable production of glioblastoma tumor-initiating cells  
in 3 dimension thermoreversible hydrogels. *Scientific reports* **6**, 31915 (2016).
- 207 Adil, M. M., Rodrigues, G. M., Kulkarni, R. U. *et al.* Efficient generation of hPSC-  
derived midbrain dopaminergic neurons in a fully defined, scalable, 3D biomaterial  
platform. *Scientific reports* **7**, 1-11 (2017).
- 208 Andersen, T., Auk-Emblem, P. & Dornish, M. 3D cell culture in alginate hydrogels.  
*Microarrays* **4**, 133-161 (2015).
- 209 Wang, H., Mehta, J. L., Chen, K. *et al.* Human urotensin II modulates collagen  
synthesis and the expression of MMP-1 in human endothelial cells. *Journal of  
cardiovascular pharmacology* **44**, 577-581 (2004).
- 210 Masckauchán, T. N. H., Agalliu, D., Vorontchikhina, M. *et al.* Wnt5a signaling induces  
proliferation and survival of endothelial cells in vitro and expression of MMP-1 and Tie-  
2. *Molecular biology of the cell* **17**, 5163-5172 (2006).
- 211 Ranga, A. & Grebenyuk, S. Engineering organoid vascularization. *Frontiers in  
bioengineering and biotechnology* **7**, 39 (2019).
- 212 Silva, T. P., Cotovio, J. P., Bekman, E. *et al.* Design principles for pluripotent stem cell-  
derived organoid engineering. *Stem cells international* **2019** (2019).
- 213 Calabro, S. R., Maczurek, A. E., Morgan, A. J. *et al.* Hepatocyte produced matrix  
metalloproteinases are regulated by CD147 in liver fibrogenesis. *PLoS one* **9** (2014).
- 214 Stetler-Stevenson, W. G. Matrix metalloproteinases in angiogenesis: a moving target  
for therapeutic intervention. *The Journal of clinical investigation* **103**, 1237-1241  
(1999).
- 215 Kumagai, A., Kondo, F., Sano, K. *et al.* Immunohistochemical study of hepatocyte,  
cholangiocyte and stem cell markers of hepatocellular carcinoma: the second report:  
relationship with tumor size and cell differentiation. *J Hepatobiliary Pancreat Sci* **23**,  
414-421, doi:10.1002/jhbp.356 (2016).
- 216 Patman, G. Solving the conundrum of cholangiocyte differentiation. *Nature Reviews  
Gastroenterology & Hepatology* **12**, 490-490 (2015).
- 217 Takeishi, K., de l'Hortet, A. C., Wang, Y. *et al.* Assembly and Function of a  
Bioengineered Human Liver for Transplantation Generated Solely from Induced  
Pluripotent Stem Cells. *Cell Reports* **31**, 107711 (2020).
- 218 Eisenstein, M. (Nature Publishing Group, 2018).
- 219 Wi niewski, J. R., Vildhede, A., Norén, A. *et al.* In-depth quantitative analysis and  
comparison of the human hepatocyte and hepatoma cell line HepG2 proteomes.  
*Journal of proteomics* **136**, 234-247 (2016).
- 220 Farzaneh, Z., Abassalizadeh, S., Asghari-Vostikolaee, M. H. *et al.* Dissolved oxygen  
concentration regulates human hepatic organoid formation from pluripotent stem cells  
in a fully controlled bioreactor. *Biotechnology and Bioengineering* (2020).

- 221 Siller, R., Greenhough, S., Mathapati, S. *et al.* Future Challenges in the Generation of Hepatocyte-Like Cells From Human Pluripotent Stem Cells. *Current Pathobiology Reports* **5**, 301-314 (2017).
- 222 Zhao, D., Chen, S., Cai, J. *et al.* Derivation and characterization of hepatic progenitor cells from human embryonic stem cells. *PloS one* **4**, e6468 (2009).
- 223 Cai, J., Wu, J., Wang, J. *et al.* Extracellular vesicles derived from different sources of mesenchymal stem cells: therapeutic effects and translational potential. *Cell & Bioscience* **10**, 1-14 (2020).
- 224 Bakopoulou, A., Apatzidou, D., Aggelidou, E. *et al.* Isolation and prolonged expansion of oral mesenchymal stem cells under clinical-grade, GMP-compliant conditions differentially affects “stemness” properties. *Stem cell research & therapy* **8**, 1-21 (2017).
- 225 Hassan, M. N. F. B., Yazid, M. D., Yunus, M. H. M. *et al.* Large-Scale Expansion of Human Mesenchymal Stem Cells. *Stem Cells International* **2020**, 9529465, doi:10.1155/2020/9529465 (2020).
- 226 Rossen, N. S., Anandakumaran, P. N., zur Nieden, R. *et al.* Injectable therapeutic organoids using sacrificial hydrogels. *iScience*, 101052 (2020).
- 227 Vargas-Valderrama, A., Messina, A., Mitjavila-Garcia, M. T. *et al.* The endothelium, a key actor in organ development and hPSC-derived organoid vascularization. *Journal of Biomedical Science* **27**, 1-13 (2020).
- 228 Darakhshan, S., Pour, A. B., Kowsari-Esfahan, R. *et al.* Generation of Scalable Hepatic Micro-Tissues as a Platform for Toxicological Studies. *Tissue Engineering and Regenerative Medicine* **17**, 459-475 (2020).
- 229 He, H., He, Q., Xu, F. *et al.* Dynamic formation of cellular aggregates of chondrocytes and mesenchymal stem cells in spinner flask. *Cell proliferation* **52**, e12587 (2019).
- 230 Enosawa, S., Horikawa, R., Yamamoto, A. *et al.* Hepatocyte transplantation using a living donor reduced graft in a baby with ornithine transcarbamylase deficiency: a novel source of hepatocytes. *Liver Transplantation* **20**, 391-393 (2014).
- 231 Correia, C. R., Bjørge, I. M., Zeng, J. *et al.* Liquefied Microcapsules as Dual-Microcarriers for 3D+ 3D Bottom-Up Tissue Engineering. *Advanced Healthcare Materials* **8**, 1901221 (2019).
- 232 Bochenek, M. A., Veiseh, O., Vegas, A. J. *et al.* Alginate encapsulation as long-term immune protection of allogeneic pancreatic islet cells transplanted into the omental bursa of macaques. *Nature biomedical engineering* **2**, 810-821 (2018).
- 233 Leong, W. Y., Soon, C. F., Wong, S. C. *et al.* In vitro growth of human keratinocytes and oral cancer cells into microtissues: an aerosol-based microencapsulation technique. *Bioengineering* **4**, 43 (2017).
- 234 Correia, C. R., Ghasemzadeh-Hasankolaei, M. & Mano, J. F. Cell encapsulation in liquified compartments: Protocol optimization and challenges. *PloS one* **14**, e0218045 (2019).
- 235 Correia, C. R., Nadine, S. & Mano, J. F. Cell Encapsulation Systems Toward Modular Tissue Regeneration: From Immunoisolation to Multifunctional Devices. *Advanced Functional Materials*, 1908061 (2020).
- 236 Choe, G., Park, J., Park, H. *et al.* Hydrogel biomaterials for stem cell microencapsulation. *Polymers* **10**, 997 (2018).
- 237 Li, F., Levinson, C., Truong, V. X. *et al.* Microencapsulation improves chondrogenesis in vitro and cartilaginous matrix stability in vivo compared to bulk encapsulation. *Biomaterials Science* **8**, 1711-1725 (2020).
- 238 Echaliier, C., Valot, L., Martinez, J. *et al.* Chemical cross-linking methods for cell encapsulation in hydrogels. *Materials Today Communications* **20**, 100536 (2019).
- 239 Tarabozetti, G., D'Ascenzo, S., Borsotti, P. *et al.* Shedding of the matrix metalloproteinases MMP-2, MMP-9, and MT1-MMP as membrane vesicle-associated components by endothelial cells. *The American journal of pathology* **160**, 673-680 (2002).

- 240 Ali, S., Saik, J. E., Gould, D. J. *et al.* Immobilization of cell-adhesive laminin peptides in degradable PEGDA hydrogels influences endothelial cell tubulogenesis. *BioResearch open access* **2**, 241-249 (2013).
- 241 Nooranidoost, M., Haghshenas, M., Muradoglu, M. *et al.* Cell encapsulation modes in a flow-focusing microchannel: Effects of shell fluid viscosity. *Microfluidics and Nanofluidics* **23**, 31 (2019).
- 242 Headen, D. M., García, J. R. & García, A. J. Parallel droplet microfluidics for high throughput cell encapsulation and synthetic microgel generation. *Microsystems & Nanoengineering* **4**, 1-9 (2018).
- 243 Su, S., Jing, G., Zhang, M. *et al.* One-step bonding and hydrophobic surface modification method for rapid fabrication of polycarbonate-based droplet microfluidic chips. *Sensors and Actuators B: Chemical* **282**, 60-68 (2019).
- 244 Nielsen, J. B., Hanson, R. L., Almughamsi, H. M. *et al.* Microfluidics: Innovations in Materials and Their Fabrication and Functionalization. *Analytical Chemistry* **92**, 150-168 (2019).
- 245 Waheed, S., Cabot, J. M., Macdonald, N. P. *et al.* 3D printed microfluidic devices: enablers and barriers. *Lab on a Chip* **16**, 1993-2013 (2016).
- 246 Lashkaripour, A., Rodriguez, C., Ortiz, L. *et al.* Performance tuning of microfluidic flow-focusing droplet generators. *Lab on a Chip* **19**, 1041-1053 (2019).
- 247 Henise, J., Yao, B., Hearn, B. R. *et al.* High-throughput, aseptic production of injectable Tetra-PEG hydrogel microspheres for delivery of releasable covalently bound drugs. *Engineering Reports*, e12213 (2020).
- 248 Pill, K., Hofmann, S., Redl, H. *et al.* Vascularization mediated by mesenchymal stem cells from bone marrow and adipose tissue: a comparison. *Cell Regeneration* **4**, 8 (2015).
- 249 Almalki, S. G. & Agrawal, D. K. Effects of matrix metalloproteinases on the fate of mesenchymal stem cells. *Stem cell research & therapy* **7**, 1-12 (2016).
- 250 Ouyang, L., Dan, Y., Shao, Z. *et al.* MMP-sensitive PEG hydrogel modified with RGD promotes bFGF, VEGF and EPC-mediated angiogenesis. *Experimental and therapeutic medicine* **18**, 2933-2941 (2019).
- 251 Jha, A. K., Tharp, K. M., Browne, S. *et al.* Matrix metalloproteinase-13 mediated degradation of hyaluronic acid-based matrices orchestrates stem cell engraftment through vascular integration. *Biomaterials* **89**, 136-147 (2016).
- 252 Seliktar, D., Zisch, A., Lutolf, M. *et al.* MMP-2 sensitive, VEGF-bearing bioactive hydrogels for promotion of vascular healing. *Journal of Biomedical Materials Research Part A* **68**, 704-716 (2004).
- 253 Amer, L. D. & Bryant, S. J. The in vitro and in vivo response to MMP-sensitive poly (ethylene glycol) hydrogels. *Annals of biomedical engineering* **44**, 1959-1969 (2016).
- 254 Jha, A. K., Tharp, K. M., Ye, J. *et al.* Enhanced survival and engraftment of transplanted stem cells using growth factor sequestering hydrogels. *Biomaterials* **47**, 1-12 (2015).
- 255 Calabro, S. R., Maczurek, A. E., Morgan, A. J. *et al.* Hepatocyte produced matrix metalloproteinases are regulated by CD147 in liver fibrogenesis. *PloS one* **9**, e90571 (2014).
- 256 Duarte, S., Baber, J., Fujii, T. *et al.* Matrix metalloproteinases in liver injury, repair and fibrosis. *Matrix Biology* **44**, 147-156 (2015).
- 257 Nibourg, G. A., Hoekstra, R., van der Hoeven, T. V. *et al.* Increased hepatic functionality of the human hepatoma cell line HepaRG cultured in the AMC bioreactor. *The international journal of biochemistry & cell biology* **45**, 1860-1868 (2013).
- 258 Rebelo, S. P., Costa, R., Silva, M. M. *et al.* Three-dimensional co-culture of human hepatocytes and mesenchymal stem cells: improved functionality in long-term bioreactor cultures. *Journal of tissue engineering and regenerative medicine* **11**, 2034-2045 (2017).

- 259 Bachmann, A., Moll, M., Gottwald, E. *et al.* 3D cultivation techniques for primary human  
hepatocytes. *Microarrays* **4**, 64-83 (2015).
- 260 Ebrahimkhani, M. R., Neiman, J. A. S., Raredon, M. S. B. *et al.* Bioreactor technologies  
to support liver function in vitro. *Advanced drug delivery reviews* **69**, 132-157 (2014).
- 261 Tomlinson, L., Hyndman, L., Firman, J. W. *et al.* In vitro liver zonation of primary rat  
hepatocytes. *Frontiers in bioengineering and biotechnology* **7**, 17 (2019).
- 262 Kukla, D. A., Crampton, A. L., Wood, D. K. *et al.* Microscale collagen and fibroblast  
interactions enhance primary human hepatocyte functions in 3-dimensional models.  
*Gene Expression The Journal of Liver Research* (2019).
- 263 March, S., Ramanan, V., Trehan, K. *et al.* Micropatterned coculture of primary human  
hepatocytes and supportive cells for the study of hepatotropic pathogens. *Nature  
protocols* **10**, 2027 (2015).
- 264 Cui, J., Wang, H., Shi, Q. *et al.* Multicellular co-culture in three-dimensional gelatin  
methacryloyl hydrogels for liver tissue engineering. *Molecules* **24**, 1762 (2019).
- 265 Carmeliet, P. & Jain, R. K. Molecular mechanisms and clinical applications of  
angiogenesis. *Nature* **473**, 298-307 (2011).
- 266 Yu, Y.-D., Kim, K.-H., Lee, S.-G. *et al.* Hepatic differentiation from human embryonic  
stem cells using stromal cells. *Journal of Surgical Research* **170**, e253-e261 (2011).

Supplementary information

Supplementary Table IV-1 List of main materials used in this study.

CAT#	DESCRIPTION
	hPSCs
A18945	Human Episomal iPSC Line
WA09	Human ES H9
A1517001	Essential 8™ Medium
A1413302	Geltrex™ LDEV-Free, hESC-Qualified, Reduced Growth Factor Basement Membrane Matrix
15040066	Versene Solution
A2644501	RevitaCell™ Supplement (100X)
85857	mTeSR™1
A1110501	StemPro™ Accutase™ Cell Dissociation Reagent
7930	CryoStor® CS10
354277	Corning® Matrigel® hESC-Qualified Matrix, *LDEV-free, 5 mL
	Hepatocytes
CC-3198	HCMTM BulletKit™
D4902-100MG	Dexamethasone
295-OM-010	Recombinant Human Oncostatin M (OSM) Protein
C-64532	HGF, human, recombinant (HEK)
11875085	RPMI 1640 Medium
17504044	B-27™ Supplement (50X), serum free
338-AC-050	Recombinant Human/Mouse/Rat Activin A Protein
4423	CHIR 99021
A3311-50G	Bovine Serum Albumin
SCM151	PLTMax® Human Platelet Lysate
10828010	KnockOut™ Serum Replacement
A1217701	TrypLE™ Select Enzyme (10X), no phenol red
21600010	DPBS, powder, no calcium, no magnesium
T9424-25ML	TRI Reagent®
I2633-25MG	Cardiogreen
J65597-&H	J65597 DiL-Lipoprotein, low density, acetylated, human plasma
E88-129	Human Albumin ELISA Kit, E88-129
V9001	P450-Glo™ CYP3A4 Assay and Screening System
V8771	P450-Gio CYP1A2 Assay kit 10ml
V8891	P450-Gio CYP2D6 Assay kit 10ml
	Mesenchymal stem cells
SCC036	Human Mesenchymal Stem Cells (derived from hES cells)
A1033201	CTS™ StemPro™ MSC SFM
12662011	Fetal Bovine Serum, mesenchymal stem cell-qualified, One Shot™
12634010	Advanced DMEM/F-12
3781	Corning® Low Concentration Synthemax™ II Microcarriers, 10g Vial
	Endothelial
CC-5035	EGMTM-Plus Endothelial Cell Growth Media-Plus BulletKit™
F3917-10MG	Forskolin

<b>314-BP-010</b>	Recombinant Human BMP-4 Protein
<b>293-VE-010</b>	Recombinant Human VEGF 165 Protein
<b>10639011</b>	StemPro™-34 SFM (1X)
<b>A8960-5G</b>	L-Ascorbic acid 2-phosphate sesquimagnesium salt hydrate
<b>11965084</b>	DMEM, high glucose
4979	Corning® Denatured Collagen Dissolvable Microcarriers, 1g Vial
4987	Corning® Synthemax™ II Dissolvable Microcarriers, 1g Vial
ab204726	In Vitro Angiogenesis Assay Kit (ab204726)
3784	Corning Synthemax High concentration
	CHIP MATERIAL
<b>T1162-100MG</b>	Tetramethylrhodamine isothiocyanate–Dextran
<b>PG2-FCTH-1k</b>	Fluorescein PEG Thiol, FITC-PEG-SH
<b>PG2-RBTH-5k</b>	Rhodamine PEG Thiol, RB-PEG-SH
<b>AXS-1114542</b>	OptiPrep
<b>K4002-10X1L</b>	Krebs-Ringer Bicarbonate Buffer
<b>90279-100ML</b>	Triethanolamine
<b>85548</b>	Span 80
<b>D0632</b>	DL-Dithiothreitol
<b>81310-1KG</b>	Peg 35000 KD
<b>A7018-1/4RM-MAL-10k</b>	4arm PEG maleimide
<b>A7029-1/4RM-MAL-20k</b>	4arm PEG maleimide
<b>A7067-1/4RM-MAL-40k</b>	4arm PEG maleimide
<b>MBG-PMW20-5001-COS</b>	Mebiol® Gel PNIPAAm-PEG 3D Thermoreversible Hydrogel
<b>M1180-500ML</b>	Mineral oil
<b>C4830-100G</b>	Calcium carbonate
<b>P2611-50ML</b>	Pectinase
<b>46-034-CI</b>	Corning® 100 mL 0.5M EDTA, pH 8.0
<b>81325-50G</b>	Polygalacturonic acid

**Supplementary Table IV.2 List of antibodies used in this study.**

Excitation	Cat no.	
421	653712	Brilliant Violet 421™ anti-Oct4 (Oct3) Antibody
647	562594	Alexa Fluor® 647 Mouse Anti-Human Sox17
488		Human HNF-3 beta /FoxA2 Alexa Fluor® 488-conjugated Antibody
421	653712	Brilliant Violet 421™ anti-Oct4 (Oct3) Antibody
488		alpha-Fetoprotein Monoclonal Antibody (AFP3), Alexa Fluor 488, eBioscience™
647	IC1455R-100UG	Human Serum Albumin Alexa Fluor® 647-conjugated Antibody
790	sc-374229 AF790	HNF-4 Antibody (H-1) Alexa Fluor® 790
421	653712	Brilliant Violet 421™ anti-Oct4 (Oct3) Antibody
488	ab99302	Anti-Tbx3 antibody
		Goat anti-Rabbit IgG (H+L) Superclonal™ Secondary Antibody, Alexa Fluor 488
594	324228	Alexa Fluor® 594 anti-human CD326 (EpCAM) Antibody
647	MAB1368	Human/Mouse alpha -Fetoprotein/AFP Antibody
488		alpha-1b Adrenergic Receptor Monoclonal Antibody (471802)
561	555689	PE Mouse Anti-Human CD99 Clone TÛ12 (RUO)
647	562903	Alexa Fluor® 647 Rat anti-Human Lgr5 (N-Terminal)
488	53-3249-82	CD324 (E-Cadherin) Monoclonal Antibody (DECMA-1), Alexa Fluor 488, eBioscience™
555	ab212002	Anti-Cytochrome P450 2D6 antibody [EPR17868] (Alexa Fluor® 555)
488	PA1-340	CYP1A1 Polyclonal Antibody
	A27034	Goat anti-Rabbit IgG (H+L) Superclonal™ Secondary Antibody, Alexa Fluor 488
546	sc-53850 AF546	CYP3A4 Antibody (HL3) Alexa Fluor®546
488	HPA003595	Anti-ARG1 antibody produced in rabbit
594	628504	Alexa Fluor® 594 anti-Cytokeratin 19 Antibody
647	ab209599	Recombinant Anti-Cytokeratin 7 antibody [EPR17078]
	A28175	Goat anti-Mouse IgG (H+L) Superclonal™ Secondary Antibody, Alexa Fluor 488
555	ab202511	Anti-CD90 / Thy1 antibody [EPR3133] (Alexa Fluor® 555) (ab202511)
		alpha-1b Adrenergic Receptor Monoclonal Antibody (471802)
	sc-9989	VE-Cadherin
	sc-130616	-SMA
	sc-101060	HNF-3β
	sc-136257	Integrin 2 Antibody (2)
	sc-376764	PECAM-1 Antibody (H-3)

	ab2413	Anti-Fibronectin antibody
	ab14106	SM22A
	555661	Purified Mouse Anti-Human CD144 Clone 55-7H1 (RUO)
	550314	Purified Mouse Anti-Human CD146
	555849	Purified Mouse Anti-Human vWF
	555444	Purified Mouse Anti-Human CD31
	553892	FITC Mouse Anti-Rat IgG1
	550083	PE Rat Anti-Mouse IgG1 Clone A85-1 (RUO)
488	558068	Alexa Fluor® 488 Mouse Anti-Human CD31 Clone M89D3 (RUO)
647	560495	Alexa Fluor® 647 Mouse Anti-Human CD309 (VEGFR-2) Clone 89106 (RUO)
700	343525	Alexa Fluor® 700 anti-human CD34 Antibody

**Supplementary Table IV.3 List of primers used in this study.**

Gene	Primer	DESCRIPTION
<b>TBX3</b>	Forward	TTA CCA AGT CGG GAA GGC GAA T
	Reverse	CAT CCT CTT TGG CAT TTC GGG G
<b>AFP</b>	Forward	CTT TGG GCT GCT CGC TAT GA
	Reverse	GCA TGT TGA TTT AAC AAG CTG CT
<b>PROX1</b>	Forward	GGG CTC TCC TTG TCG CTC ATA AA
	Reverse	GGT AAT GCA TCT GTT GAA CTT TAC GTC
<b>HNF1B</b>	Forward	TGG TAA AAT GAT CTC AGT CTC AGG AGG
	Reverse	GAT GAC AGG GAC ACT CTG TGC T
<b>HNF6</b>	Forward	CCC ACC GAC AAG ATG CTC AC
	Reverse	GCC CTG AAT TAC TTC CAT TGC TG
<b>CEBPA</b>	Forward	AGA AGT CGG TGG ACA AGA ACA GCA
	Reverse	ATT GTC ACT GGT CAG CTC CAG CA
<b>HNF4A</b>	Forward	GAG CGA TCC AGG GAA GAT CA
	Reverse	CAT ACT GGC GGT CGT TGA TG
<b>ALB</b>	Forward	ACC CCA CAC GCC TTT GGC ACA A
	Reverse	CAC ACC CCT GGA ATA AGC CGA GCT
<b>CYP3A4</b>	Forward	AAG TGT GGG GCT TTT ATG ATG GT
	Reverse	GGT GAA GGT TGG AGA CAG CAA TG
<b>CYP3A7</b>	Forward	ATC TCA TCC CAA ACT TGG CCG T
	Reverse	AAC GTC CAA TAG CCC TTA CGG A
<b>SOX9</b>	Forward	CGT CAA CGG CTC CGC AAG AAC AA
	Reverse	GCC GCT TCT CGC TCT CGT TCA GAA GT
<b>SOX17</b>	Forward	CGC ACG GAA TTT GAA CAG TA
	Reverse	GGA TCA GGG ACC TGT CAC AC
<b>CK19</b>	Forward	GAT CCT GAG TGA CAT GCG AAG C
	Reverse	GTA ACC TCG GAC CTG CTC ATC T
<b>ALBUMIN</b>	Forward	CTT CCT GGG CAT GTT TTT GT
	Reverse	TGG CAT AGC ATT CAT GAG GA
<b>TAT</b>	Forward	ATG CTG ATC TCT GTT ATG GG
	Reverse	CAC ATC GTT CTC AAA TTC TGG
<b>PEPCK</b>	Forward	GGCTGAAGAAGTATGACAACCTG

	Reverse	AAATCCTCCTCTGACATCCA
<b>GAPDH</b>	Forward	CTC ATT TCC TGG TAT GAC AAC GA
	Reverse	CTT CCT CTT GTG CTC TTG CT
<b>TDO</b>	Forward	GGT TTA GAG CCA CAT GGA TT
	Reverse	ACA GTT GAT CGC AGG TAG TG
<b>TTR</b>	Forward	GAGGAGGAATTTGTAGAAGGGA
	Reverse	CGTGGTGAATAGGAGTAGG
<b>PDX1</b>	Forward	GCG TTG TTT GTG GCT GTT GCG CA
	Reverse	AGC TTC CCC GCT GTG TGT GTT AGG

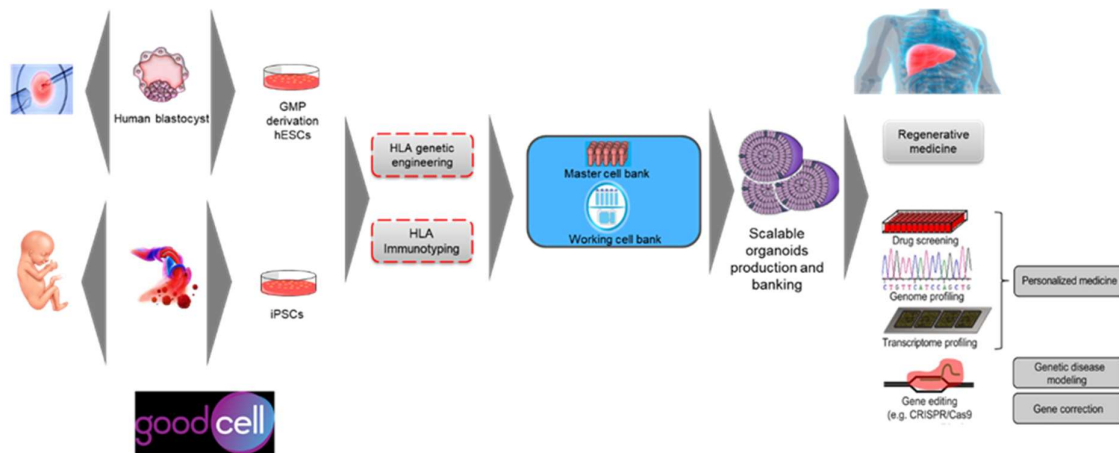
## VI. Chapter 5. Conclusions and Future Directions

## **Future perspective**

Organoid technology advances during past 10 years has opened new era in the field of regenerative medicine that introducing a new class of products offering organ-like functionality in small/tiny scale. These unique components/products have showed great potential for treating diseases considered as unmet medical need including chronic liver diseases through emergence of “organoid medicine” filed along with introducing a new powerful and personalized/patient derived models for studying mechanism of disease that facilitate the development of innovative drugs with improved safety and efficacy.

Despite these great advances, translating established protocols and fabrication techniques for liver organoid generation to robust manufacturing processing technologies capable of producing high quality clinical grade products still need developing advanced biological, bioengineering, and medical approaches and tremendous global effort to address current critical challenges. Three main liver organoid technology categories that facing challenges comprising proper cell source selection, scalable cGMP manufacturing process development while maintaining key important functional properties, and finally developing a viable transplantation strategy.

Currently, adult liver tissue derived progenitors (e.g LGR5<sup>+</sup> cells), directly reprogrammed somatic cells such as iHep cells, and self-renewing pluripotent stem cells has considered as most proper choices for liver organoids generation. However, widespread clinical application of product require massive production of organoids using a readily available cell source as GMP-grade HLA haplotype/HLA matched bank that include most of the HLA diversity to have the best HLA compatibility with different patients as allogeneic cell-based product (e.g. goodcell company platform for hPSCs banking, US) .



Potential platform for commercial use of VHOs using hPSCs as cell source

The best cell types that can meet these criteria are hiPSCs and hESCs since hPSC-derived organoids with components of all three germ layers have been generated that can be employed to create a new human model system for studying disease mechanisms, drug development and therapeutic application. It has been showed that hPSC-derived organoids have remarkable cell type complexity, architecture, and function similar to their *in vivo* counterparts. However, establishing universal differentiation protocols for different cell ingredients including hepatic differentiation process under chemically defined culture condition that can be adopted for all the baked cell lines is the most critical challenge with hPSCs use as cell source. Low reproducibility of the most established protocols is another issue that should be addressed before commercial use of these cells as source.

A robust and fully scalable manufacturing process for production of clinical grade organoids is also an essential prerequisite for realizing the potential of “Organoid Medicine”. However, the biological complexity of cells and with more extent organoids has hampered the translation of laboratory-scale experiments into industrial processes for reliable, cost-effective manufacturing of cell-based/ organoid based therapies. In this project, we showed that multicellular functional hepatic organoids comprising red blood cells generated form hPSCs as 3D aggregates by just regulating dissolved oxygen (DO) concentration in stirred tank bioreactor during dynamic suspension culture. However, the final fetal like hepatic organoid

product was not homogeneously functional and hepatic organoids with different diameter sizes and morphology showed different metabolic activities and functional properties. We identified dissolved oxygen as critical bioprocess parameter that regulated hPSCs fate including final product nature. Accordingly, we emphasized that key bioprocess parameters including dissolved oxygen should be carefully optimized during hepatic differentiation protocol scale-up to generate functional organoids. In fact, nearly all protocols established for generation of hepatic organoids have not explored the protocol efficacy and outcome under fully controlled culture condition to demonstrate the scalability. Thus, translation trials of lab scale protocols to a fully scalable process under fully controlled condition may result in final product with different that can not meet predefined quality attributes for clinical application.

In the next project, we succeeded to establish a continuous and scalable process for production of complex and self-organized vascularized hepatobiliary organoids with high functionality under dynamic suspension culture condition. However, employing fully controlled culture conditions for required cell ingredients production and then during organoids self-organization and maturation may change the process outcome that need to be explored and optimized accordingly. In addition, we realized that production and preparing a uniform mixture of cells from different cell types for coculturing in defined ratio and total density that optimized for self-condensation is a tricky and multivariable process that need to consider very precise controls over the process to have satisfactory outcome in reproducible manner. Thus, we believe that developing a differentiation strategy for generating complex and highly functional organoids by spatiotemporal control of process and taking advantage from unique hPSCs capability in organ bud/organ development would be an optimal strategy for future clinical application. Combining organoid technology and bioengineering will provide a great advantage in precise control of input (morphogens, nutrients, oxygen, pH, 3D microenvironment) and outputs as organoids quality attributes to better recapitulate the liver function better.

Finally developing an effective transplantation strategy for direct clinical application of liver organoids is a highly important translational aspect that should be carefully considered. One of the main considerations is the proliferative capacity of liver organoids because of their fetal nature and potential for in vivo expansion and maturation to create a liver tissue like structure. This proliferative ability will also overcome the difficulty with current hepatocellular transplantation models such as poor supply of human primary hepatocytes. Vascularized hepatobiliary organoids generated in this study could be considered for ectopic transplantation because of their self-supporting, proliferation, and further maturation ability (mesenchymal support and vascular integration) to offer a “bridge” to liver transplantation. Another transplantation approach is mesentery transplanting of vascularized hepatobiliary liver organoids into the mesentery as a “second” liver to support a failing liver. However, transplanting large number of organoids into mesentery and fix them using a layer of mesentery may require an open surgery that is considered as an invasive procedure for the patient. To achieve a non-invasive approach for transplantation, we designed a foldable and biodegradable device made from medical grade oxidized cellulose and 4-arm-10 K PEG-MMP sensitive peptide for delivering the generated vascularized hepatobiliary organoids using a surgical tube to mesentery and then attach the devices to mesentery using surgical glue and laparoscopic instrument (Following figure). Devices can also attach to either a non-fibrotic liver section that can support integration and proliferation of organoids. We hypothesized that organoids could degrade the device mesh and attach to mesentery for vascular integration because of their vascularized nature for facilitated proliferation, future maturation, and creation of liver bud like structure. This part of study defined as new project and will be continued in near future.

Lastly, the safety of organoids transplantation should be fully demonstrated in relevant animal models since malignant transformation of the stem cell-derived organoids after transplantation is a major concern that require extensive investigations to address this concern.

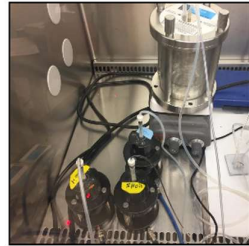
A



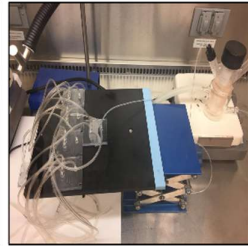
B



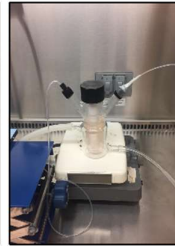
C



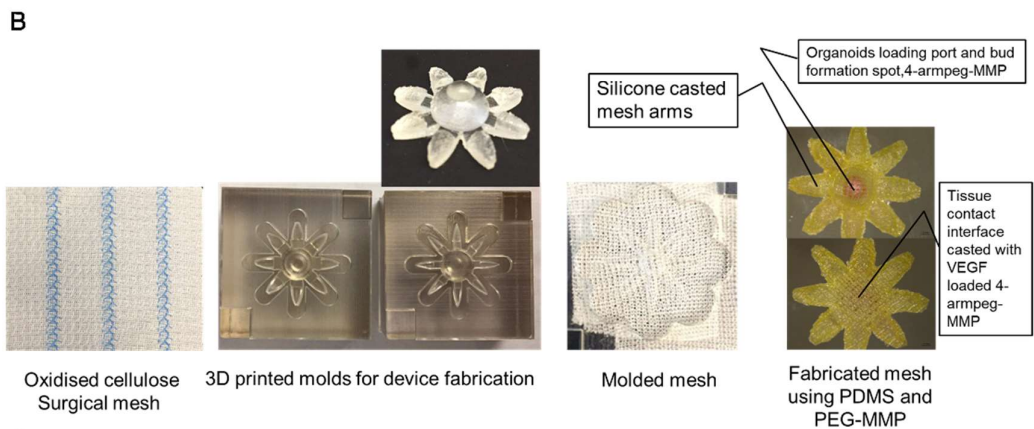
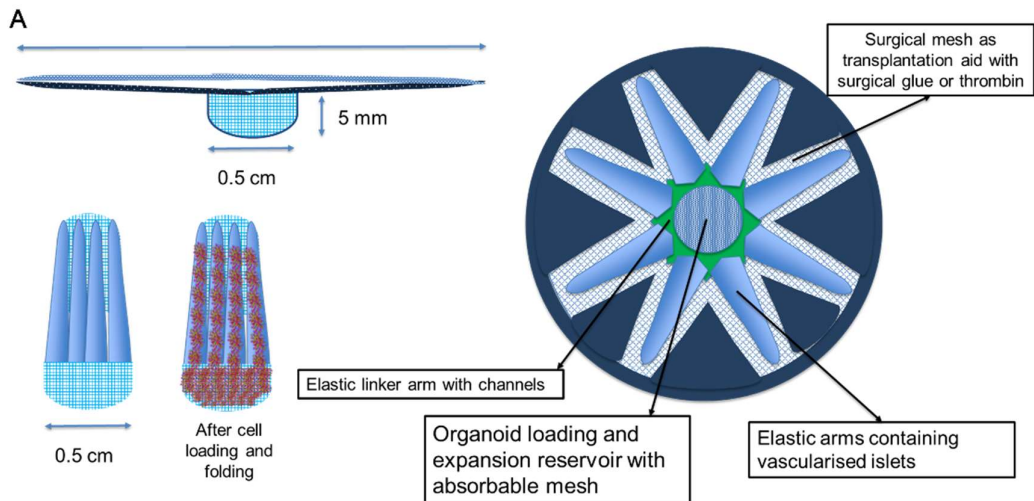
D



E



The high-throughput microfluidic platform for scalable production of complex liver organoids under aseptic culture condition. Whole set up of the microfluidic platform (A) 400 ml pressurized remote chamber containing cell mixing spinner (B) Other remote pressure vessels, Parallel microfluid chips connected to a fluid divider as well as microcapsules collector (C) multiple parallel microfluidic chips with inlet divider and microcapsules collector (D). Jacketed spinner flask for collecting produced microcapsules (E).



**A foldable and biodegradable device for transplantation of vascularized hepatobiliary organoids.** Schematic design of the device (A) B fabrication steps using 3D printed mold, transplantation of device loaded with hepatobiliary organoids in Mesentery of Rat.